Aus der Kinderklinik und Kinderpoliklinik
im Dr. von Haunerschen Kinderspital
Ludwig-Maximilians-Universität München
Direktor: Prof. Dr. med. Dr. sci. nat. Christoph Klein

Neue Aspekte der Mikrozirkulation im Rahmen von Entzündung, Entwicklung und Erkrankung

Kumulative Habilitationsschrift
zur Erlangung der Venia Legendi
im Fach Pädiatrie

vorgelegt von
Dr. med. Claudia Nußbaum
München 2017

Fachmentorat

Prof. Dr. med. Dr. sci. nat. Christoph Klein

Prof. Dr. med. Markus Sperandio

Prof. Dr. med. Orsolya Genzel-Boroviczény

Inhaltsverzeichnis

I) Einführung in das Thema

Im Jahre 1661 bestätigte Malpighi bei mikroskopischen Studien der Froschlunge erstmalig die Existenz von Kapillaren, welche er als Netzwerk, bestehend aus feinsten Gefäßen zwischen Arteriolen und Venolen beschrieb (Young 1929). Während für Malpighi die Funktion dieses Netzwerkes noch unklar war, ist die zentrale Bedeutung der Mikrozirkulation für den Erhalt der Zellfunktionen und somit den gesamten Organismus heute unumstritten.

Die Mikrozirkulation beschreibt die Vorgänge in den kleinsten Gefäßen (< 100 µm Durchmesser) und umfasst Arteriolen, Kapillaren, Venolen und Lymphgefäße (Miranda et al. 2016) (Abb. 1). Die wesentliche Aufgabe besteht in der Versorgung des Gewebes mit Sauerstoff und Nährstoffen, sowie dem Abtransport von Kohlendioxid und Stoffwechselprodukten (Pittman 2005). Darüber hinaus ist die Mikrozirkulation entscheidend für eine adäquate immunologische Funktion und ermöglicht den Transport von Wirkstoffen und Mediatoren zum jeweiligen Zielorgan (Ince 2005).

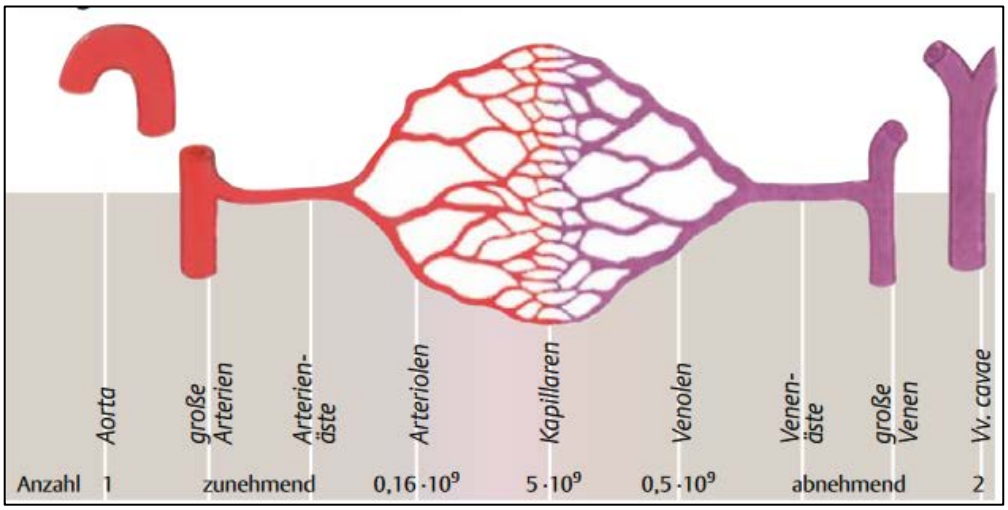

Abb. 1) Schematische Darstellung der Mikrozirkulation (Silbernagl 2012)

Ia) Grundlagen der Mikrozirkulation

Um eine optimale Versorgung des Gewebes zu gewährleisten, bilden die Kapillaren wie bereits von Malpighi beschrieben über multiple Anastomosen ein dreidimensionales Netzwerk. Die Kapillardurchblutung ist dabei an die Funktion und die aktuellen Bedürfnisse des jeweiligen Organs angepasst. So beträgt beispielsweise im ruhenden Skelettmuskel die funktionelle Gefäßdichte (functional vessel density, FVD), d.h. die Anzahl perfundierter Gefäße pro Gewebeeinheit, nur ca. 25% der totalen Gefäßdichte (total vessel density, TVD). Unter körperlicher Arbeit wird die

funktionelle Gefäßdichte durch Erweiterung vorgeschalteter terminaler Arteriolen rasch erhöht, bis schließlich alle zur Verfügung stehenden Kapillaren perfundiert sind (sog. „capillary recruitment“) (Moore et al. 2015; Honig, Odoroff, and Frierson 1982). Durch die Steigerung der funktionellen Kapillardichte erhöht sich einerseits die zum Stoffaustausch zur Verfügung stehende Gefäßoberfläche, zum anderen reduziert sich der maximale Abstand zwischen zwei Kapillaren und damit die maximale Diffusionsstrecke, die überwunden werden muss (Lewick 2010). Darüber hinaus wird der kapilläre Blutfluss gesteigert. Diese Maßnahmen stellen sicher, dass der steigende Sauerstoff- und Nährstoffbedarf der arbeitenden Muskulatur gedeckt wird.

Die zuvor dargestellten Anpassungsvorgänge der Mikrozirkulation werden durch intrinsische und extrinsische Mechanismen gesteuert, wobei der lokale Blutfluss im Gewebe vor allem durch intrinsische Faktoren reguliert wird, während extrinsische Faktoren eine übergeordnete Rolle bei der Regulation des Gesamtblutflusses in der Mikrozirkulation spielen (Moore et al. 2015; Lewick 2010). Zu den intrinsischen Mechanismen zählt die myogene Gefäßantwort, bei der Veränderungen des intraluminalen Drucks mit einer unmittelbaren Kontraktion (Vasokonstriktion) bzw. Relaxation (Vasodilatation) der glatten Muskulatur in der Arteriolenwand beantwortet werden (Davis 2012). Dieser als Autoregulation oder Bayliss-Effekt bezeichnete Mechanismus dient dazu den kapillären Blutfluss über ein großes Blutdruckspektrum konstant zu halten. Weiterhin führt eine Beschleunigung des Blutflusses zu erhöhter Schubspannung an der Gefäßwand, was über Freisetzung von Stickstoffmonoxid (NO) eine Vasodilatation verursacht (sog. shear stress response) (Chien 2007). Neben der myogenen Regulation spielen metabolische Faktoren eine wesentliche Rolle bei der Steuerung der Durchblutung in der Mikrozirkulation, wobei hierzu verschiedene Theorien existieren. Nach der klassischen metabolischen Theorie führt eine lokale Hypoxie zur gesteigerten Freisetzung vasodilatatorisch wirksamer Substanzen (z.B. NO, ATP, Prostaglandine) und bewirkt so eine Zunahme des lokalen Blutflusses um den erhöhten Sauerstoffbedarf zu decken. Anfallende Metabolite wie Laktat, Wasserstoffionen, Kalium und Adenosin unterhalten diesen Effekt (Moore et al. 2015). Dem gegenüber steht die Theorie, dass unter Ruhebedingungen ein relatives Überangebot an Sauerstoff und Nährstoffen besteht, was zu einer Hemmung der Freisetzung von Stickstoffmonoxid und anderer gefäßerweiternder Substanzen führt und so den lokalen Blutfluss drosselt solange kein gesteigerter Bedarf vorliegt (Golub and Pittman 2013). Diese intrinsischen Mechanismen werden durch extrinsische Mechanismen wie die Wirkung des vegetativen Nervensystems und vasoaktiver Hormone (z.B. Adrenalin, Vasopressin, Angiotensin u.a.) an den Widerstandsgefäßen moduliert (Lewick 2010).

Ib) Die Rolle des Endothels in der Mikrozirkulation

Die Mikrozirkulation umfasst verschiedene Zelltypen. Hierzu zählen Endothelzellen, glatte Muskelzellen (hauptsächlich in Arteriolen), Erythrozyten, Leukozyten und Thrombozyten (Miranda et al. 2016). Das Endothel, welches das Lumen des gesamten Gefäßsystems auskleidet, hat eine Gesamtfläche entsprechend der Größe von ca. sechs Fußballfeldern und stellt somit das größte „Organ“ des menschlichen Organismus dar (Cooke 2000). Es bildet eine Permeabilitätsbarriere zwischen dem Gefäßlumen und dem Interstitium und kontrolliert so den Gas-, Substrat- und Flüssigkeitsaustausch zwischen Blut und Gewebe. Zudem kommt dem Endothel eine zentrale Rolle bei der Steuerung des Gefäßtonus zu. Endothelzellen produzieren mithilfe der endothelialen Stickstoffmonoxid-Synthase (eNOS) konstitutiv Stickstoffmonoxid, welches neben einer stark gefäßerweiternden Wirkung auch antiadhäsive Eigenschaften aufweist. Auch die zuvor dargestellte Gefäßantwort auf Veränderungen der Schubspannung wird über das Endothel und die endotheliale Produktion von NO vermittelt (Hsieh et al. 2014; Ait-Oufella et al. 2010). Neben NO liefert das Endothel weitere vasoaktive Substanzen wie z.B. Prostazyklin, Endothelin und EDHF (edothelium-derived hyperpolarizing factor). Die Endothelzellen kommunizieren über Gap Junctions miteinander und mit umliegenden glatten Muskelzellen der Gefäßwand. Über diese Verbindungen können elektrische Signale rasch entlang der Gefäßwand weitergeleitet werden. Dies ermöglicht die Übermittlung lokaler vasoaktiver Impulse an übergeordnete Gefäßabschnitte (sog. conducted vasomotor response) und somit die Anpassung des regionalen Blutflusses an die aktuellen metabolischen Bedürfnisse (de Wit, Hoepfl, and Wolfle 2006; Bagher and Segal 2011) Weitere wesentliche Aufgaben des Endothels sind die Vermittlung der Leukozytenrekrutierung im Rahmen von inflammatorischen Prozessen (s. Abschnitt II, S. 8/9) sowie die Regulation der Thrombozytenadhäsion und –aggregation (s. Abschnitt III, S. 18/19) und die Thrombolyse (Ait-Oufella et al. 2010; Cooke 2000). Auf die Bedeutung der endothelialen Glykokalyx für die vaskuläre Homöostase wird im wissenschaftlichen Hintergrund zu Punkt IV (s. S. 28-30) näher eingegangen.

Ic) Zielsetzung

Aus der zentralen Bedeutung der Mikrozirkulation für die Versorgung aller Organe lässt sich ableiten, dass Störungen derselbigen zu Organdysfunktion und letztlich zu Organversagen führen. Pathologische Veränderungen der Mikrozirkulation sind ein häufiges Merkmal sowohl akuter (z.B. Sepsis, Trauma) als auch chronischer Krankheitszustände (z.B. Diabetes mellitus, Bluthochdruck) und führen zu erheblicher Morbidität und Mortalität der Patienten. Da insbesondere chronische Veränderungen oft schleichend verlaufen und sich daher häufig erst im Erwachsenenalter klinisch

manifestieren, befassen sich die meisten Studien zu diesem Thema mit Untersuchungen von adulten Patienten. Es ist aber davon auszugehen, dass viele Veränderungen der Mikrozirkulation ihren Ausgang bereits im Kindesalter nehmen. Aus diesem Grund ist es notwendig, dass diese Patientengruppe stärker in den Fokus wissenschaftlicher Untersuchungen rückt. Ein besseres Verständnis der physiologischen Grundlagen sowie der Faktoren, welche zu einer Schädigung der Mikrozirkulation führen, stellte eine Grundvoraussetzung für die Entwicklung neuer Strategien zur Prävention und Therapie mikrovaskulärer Komplikationen dar.

Ziel des Habilitationsprojektes war es daher neue Erkenntnisse über Grundlagen und Veränderungen der Mikrozirkulation und deren Rolle bei der Krankheitsentstehung im Kindesalter zu gewinnen.

Die vorliegende Habilitationsschrift beschreibt Forschungsarbeiten aus dem Gebiet der Grundlagenforschung sowie klinisch-experimentelle Studien, die sich mit der Untersuchung der Mikrozirkulation im Rahmen von Entzündung, Entwicklung und Erkrankung befassen.
Im Detail wurden folgende Themenschwerpunkten bearbeitet:

Teil 1: Mechanismen der Leukozytenrekrutierung bei inflammatorischen Prozessen *in vivo*

Teil 2: Regulation der Rekrutierung von Leukozyten und Thrombozyten im Rahmen der fetalen Entwicklung

Teil 3: Veränderungen der Mikrozirkulation bei Kindern im Rahmen ausgewählter Erkrankungen

II) Teil 1: Mechanismen der Leukozytenrekrutierung bei inflammatorischen Prozessen *in vivo*

Wissenschaftlicher Hintergrund

Wie einführend erwähnt, ist eine wesentliche Aufgabe der Mikrozirkulation die Gewährleistung einer adäquaten immunologischen Funktion. Im Rahmen von Entzündung und Infektion müssen Leukozyten aus dem Blutstrom in das betroffene Gewebe auswandern, um dort ihre jeweilige Rolle im Rahmen der Immunantwort zu erfüllen (sog. Leukozytenrekrutierung). Neutrophile Granulozyten stellen beim Menschen die quantitativ größte Population der Leukozyten dar und sind ein zentraler Bestandteil der angeborenen Immunantwort gegen eine Vielzahl verschiedener Pathogene (Nussbaum and Sperandio 2011; Mocsai 2013). Die Auswanderung von Granulozyten in umliegendes Gewebe findet v.a. in postkapillären Venolen der Mikrozirkulation statt und benötigt ein streng reguliertes Zusammenspiel von Adhäsionsmolekülen auf den Granulozyten und dem Endothel der Blutgefäße (Ley et al. 2007) (Abb. 1).

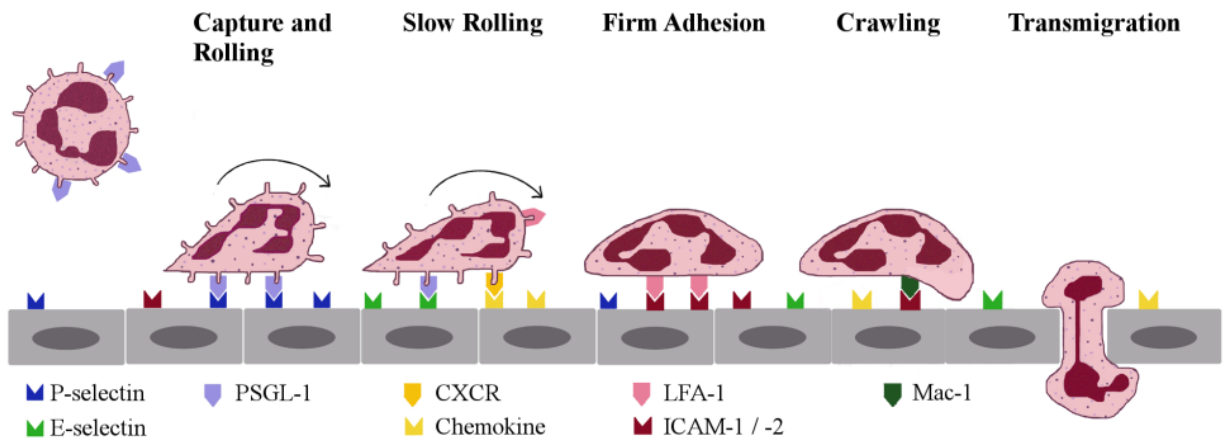

Abb. 1): Schematische Darstellung der Leukozytenrekrutierung (Nussbaum and Sperandio 2011)

Hierbei werden die ersten Schritte, das Einfangen der Zellen aus dem Blutstrom und das nachfolgende Rollen entlang des Endothels, durch Interaktion von Selektinen mit Selektinliganden (v.a. PSGL-1, CD162) vermittelt (Yang et al. 2012; Sperandio et al. 2006). Entzündlich aktivierte Endothelzellen präsentieren P-Selektin (CD62P) und E-Selektin (CD62E) auf ihrer Oberfläche, wobei P-Selektin konstitutiv exprimiert und in Weibel-Palade-Körperchen gespeichert wird, während E-Selektin durch de-novo Synthese entsteht (McEver et al. 1989; Bevilacqua et al. 1987).

Verschiedene Stimuli wie z.B. Trauma führen zu einer raschen Freisetzung von gespeichertem P-Selektin aus den Weibel-Palade-Körperchen, was innerhalb weniger Minuten zu Leukozytenrollen führt (Kubes and Kanwar 1994).

Die nachfolgenden Schritte der Leukozytenrekrutierung benötigen eine Aktivierung der β2-Integrine LFA-1 (αLβ2-integrin; CD11a/CD18) und Mac-1 (αMβ2-integrin; CD11b/CD18) auf neutrophilen Granulozyten (Zarbock and Ley 2009; Jakob et al. 2013). Durch die Interaktion von PSGL-1 mit endothelialen Selektinen gelangen β2-Integrine in einen intermediären Aktivierungszustand, was ein Abbremsen der rollenden Zellen zur Folge hat (Pruenster et al. 2015; Zarbock et al. 2011). Zudem ermöglicht das Rollen eine Bindung von Chemokinen, welche auf dem Endothel präsentiert werden, an ihre jeweiligen Rezeptoren auf den Granulozyten. Dies führt zusammen mit E-Selektin/PSGL-1-Interaktionen zu einer vollständigen Aktivierung der β2-Integrine und ermöglicht über Bindung von endothelialen Integrinliganden (z.B. ICAM-1, CD54) die feste Adhäsion der Zellen am Endothel (Jakob et al. 2013; Zarbock and Ley 2009). Integrin-vermittelte Signale festigen die Zelladhäsion und führen zu einer Ausbreitung der Zellen auf dem Endothel (sog. Spreading). Durch Kriechbewegungen (sog. Crawling) entlang der Gefäßwand gelangen die Granulozyten schließlich zu geeigneten Pforten für die Transmigration in das umliegende Gewebe (Phillipson et al. 2006).

Dank intensiver internationaler Forschungsaktivitäten in den letzten Jahrzehnten ist unser Verständnis über die Abläufe der Leukozytenrekrutierung wesentlich gesteigert worden. Dennoch sind die genauen Vorgänge und die molekularen Akteure dieses komplexen Prozesses weiterhin nur unvollständig bekannt. Die im Folgenden dargestellten Arbeiten des Habilitationsprojektes identifizieren neue Mechanismen, welche zur Leukozytenrekrutierung bei inflammatorischen Prozessen *in vivo* beitragen und diese regulieren.

IIa) *Myeloperoxidase attracts neutrophils by physical forces.*

(Klinke A., Nussbaum C.* et al., Blood 2011;117(4):1350-8, *gleichberechtigte Erstautorschaft)*

Einleitung und Zielsetzung

Das Hämenzym Myeloperoxidase (MPO) wird in großer Menge in den azurophilen Granula neutrophiler Granulozyten gespeichert und nach Phagozytose von Pathogenen in das Phagosom freigesetzt, wo es seine mikrobizide Wirkung entfaltet (Klebanoff 2005). Darüber hinaus wird MPO von aktivierten Granulozyten sezerniert und kann bei verschiedenen inflammatorischen Prozessen im Blut und Gewebe der Patienten nachgewiesen werden, wo es mit der Krankheitsaktivität korreliert (Askari et al. 2003; Rudolph et al. 2009). In den letzten Jahren gibt es zunehmende Hinweise darauf, dass MPO neben seiner Eigenschaft als Oxigenase auch immunmodulatorische Funktionen ausübt, die unabhängig von seiner katalytischen Aktivität sind (Nussbaum et al. 2013). So stimulierte inaktives MPO die Produktion von Interleukin-6 und -8 in Endothelzellen und die Freisetzung reaktiver Sauerstoffspezies wirksamer als aktives MPO (Lefkowitz et al. 2000). Interleukin-8 ist ein Chemokin, das maßgeblich an der Aktivierung und Chemotaxis von Granulozyten beteiligt ist und somit eine wichtige Rolle bei der Leukozytenrekrutierung spielt (Ley et al. 2007). Lau und Kollegen konnten zudem zeigen, dass extrazelluläres MPO neutrophile Granulozyten in auto- und parakriner Weise aktiviert, was zu Degranulation, erhöhter NADPH-Oxidase Aktivität und vermehrter Oberflächenexpression des β2-Integrins Mac-1 (CD11b/CD18) führte (Lau et al. 2005). Darüber hinaus vermittelte MPO die Adhäsion von neutrophilen Granulozyten *in vitro* (Johansson et al. 1997) und verzögerte deren Apoptose (El Kebir et al. 2008). Diese Effekte waren nicht an die oxidative Wirkung von MPO gebunden, sondern verliefen über eine Signalkaskade, welche Mac-1 und die MAP-Kinasen p38, ERK1/2 und Akt involvierte (El Kebir et al. 2008; Lau et al. 2005). Der genaue Wirkmechanismus von inaktivem MPO ist nicht geklärt, es wurde aber schon früher postuliert, dass MPO nach extrazellulärer Freisetzung rasch inaktiviert wird und in dieser Form eine wichtige physiologische Rolle spielen könnte (King, Jefferson, and Thomas 1997). Als stark kationisches Protein reichert sich extrazelluläres MPO entlang des Endothels und im subendothelialen Raum an, wo es an anionische Bestandteile der Glykokalyx (s. Abschnitt IV, S. 28/29) bindet (Baldus et al. 2001). Im Hinblick auf die hohe Affinität von MPO sowohl gegenüber dem Endothel als auch gegenüber neutrophilen Granulozyten und seine aktivierende Wirkung auf Granulozyten war es Ziel der Studie zu untersuchen, ob MPO die Rekrutierung von Granulozyten beeinflusst.

Ergebnisse

Die wichtigsten Ergebnisse der Studie werden im Folgenden zusammengefasst:

1) MPO führt konzentrationsabhängig zur gerichteten Migration von Granulozyten *in vitro* (Abb. 2).

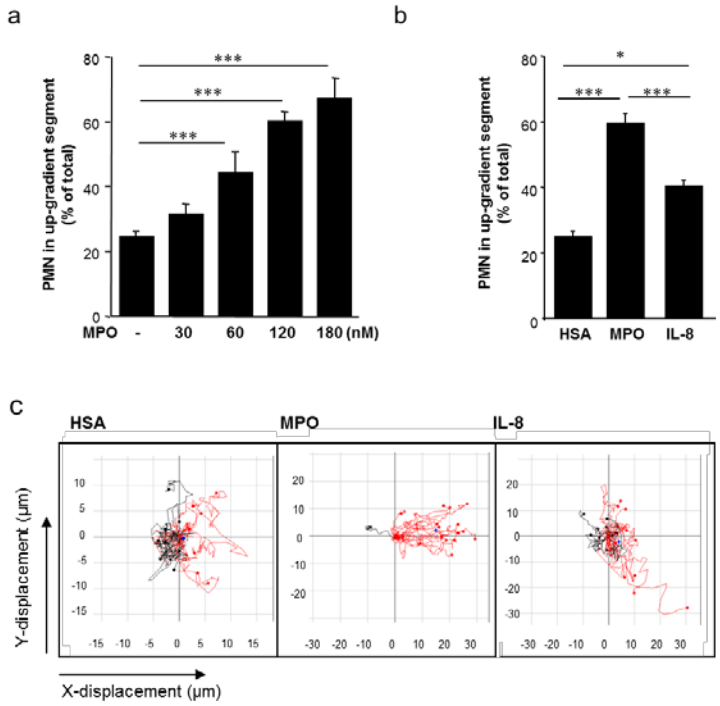

Abb. 2): Gerichtete Migration humaner Granulozyten in Mikrokammern.
Durch Einbringen der jeweiligen Substanz auf einer Seite der Kammer wurde ein Konzentrationsgradient hergestellt. Die Anzahl migrierender Zellen wurde im Segment mit dem steilsten Gradienten quantifiziert.

a) MPO bewirkt eine konzentrationsabhängige Migration von Granulozyten.
b) Die Wirkung von MPO auf die Migration von Granulozyten ist stärker als die von IL-8 (= Positivkontrolle).
c) Graphische Darstellung der Migrationswege von Granulozyten in der Mikrokammer. Die roten Linien zeigt eine Bewegung der Zellen in Richtung des jeweiligen Stimulus an. HSA (Humanes Serumalbumin = neg. Kontrolle); IL-8 (= pos. Kontrolle)

2) Der Effekt von MPO ist unabhängig von dessen katalytischer Aktivität und benötigt keine Beteiligung des Zytoskeletts. So hatte eine Vorbehandlung mit dem MPO-Inhibitor 4-ABAH keine Auswirkung auf die Migration der Zellen in Richtung MPO Gradient. Ebenso zeigten zwei inaktive MPO-Varianten einen vergleichbaren Effekt auf die Migration von Granulozyten wie aktives MPO. Darüber hinaus wurde die Migration nicht durch pharmakologische Inhibitoren des zytoskelettalen Umbaus (z.B. Cytochalasin D) beeinflusst.
3) Der Effekt von MPO auf die Migration von Granulozyten ist abhängig von elektrostatischen Interaktionen. Die Migration der Zellen wurde durch ein Anheben des pH-Wertes in der Kammer auf 9,2 (isoelektrischer Punkt von MPO) oder ein Zusetzen der polykationischen Substanzen Poly-L-Arginin, Protamin und Histon A2 (Egalisierung des elektrischen Gradienten) vollständig aufgehoben.
4) MPO ist an der Rekrutierung von Granulozyten in verschiedenen *in vivo*-Modellen beteiligt (Abb. 3).

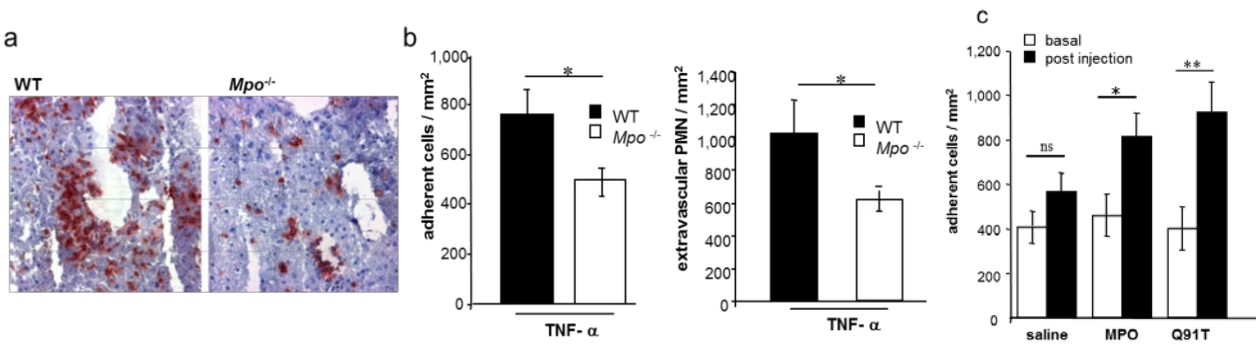

Abb. 3): Rekrutierung neutrophiler Granulozyten *in vivo*. a) Repräsentative Leberschnitte von Wildtyp (WT) und MPO-defizienten (*MPO-/-*) Tieren 24h nach Ischämie/Reperfusion (braune Färbung = Granulozyten). b) Adhärente und extravasierte Granulozyten im TNFα -behandelten Mauscremaster-muskel in WT und *MPO-/-* Tieren. c) Adhäsion von Granulozyten in postkapillären Venolen des Mauscremastermuskels vor und nach Injektion von Kochsalz (Träger), aktivem MPO und inaktivem Q91T MPO.

Diskussion

Die hier dargestellten Untersuchungen demonstrieren eine Rolle der Myeloperoxidase bei der Rekrutierung neutrophiler Granulozyten *in vitro* und *in vivo*. Die Ergebnisse bestätigen damit die Vorstellung, dass MPO neben seiner Funktion im antimikrobiellen Arsenal von Granulozyten weitere wichtige Aufgaben im Rahmen der Immunantwort übernimmt (Nussbaum et al. 2013). Interessanterweise war die enzymatische Aktivität von MPO hierbei nicht von Bedeutung. Vielmehr scheint MPO über elektrostatische Interaktion die Bindung von Granulozyten an das Endothel zu vermitteln. Ein vergleichbarer Effekt auf die Adhäsion von Immunzellen wurde auch für andere kationische Proteine aus Granulozyten wie z.B. Azurodizin und Proteinase 3 beschrieben (Soehnlein, Lindbom, and Weber 2009; Soehnlein et al. 2005). Bereits vor über 50 Jahren berichteten Janoff und Zweifach, dass eine kationische Proteinfraktion isoliert aus neutrophilen Granulozyten in der Lage ist, eine inflammatorische Reaktion in Gefäßen des Rattenmesenteriums auszulösen, die mit der Adhäsion und Emigration von Leukozyten einherging (Janoff and Zweifach 1964). Als möglicher Mechanismus wurde dabei eine Veränderung der Oberflächenladung diskutiert. Das Konzept der elektrostatisch vermittelten Interaktion durch kationische Granulozytenbestandteile wird durch mehrere Studien unterstützt (Gallin 1980; Schaack et al. 1980). Unter physiologischen Bedingungen übt die endotheliale Glykokalyx antiadhäsive Eigenschaften aus, die zum Teil auf repulsive Kräfte zwischen negativ geladenen Bausteinen der Glykokalyx (z.B. Heparansulfat) und den ebenfalls negativ geladenen Leukozyten zurückgeführt werden (Constantinescu, Vink, and Spaan 2003; Reitsma et al. 2007). Extrazelluläres MPO bindet als stark kationisches Protein mit hoher Affinität an Heparansulfat und andere Bestandteile der

extrazellulären Matrix (Baldus et al. 2001; Baldus et al. 2006) und könnte so durch Abschwächung der negativen Oberflächenladung den Kontakt von Leukozyten mit der Gefäßoberfläche erleichtern. Dieser enge Kontakt ist für die weiteren Schritte der Rekrutierungskaskade, welche die Bindung von spezifischen endothelialen Liganden und Chemokinen voraussetzen, von hoher Bedeutung. Darüber hinaus könnte die Freisetzung von MPO aus bereits adhärenten und migrierenden Granulozyten dazu dienen, nachfolgende Zellen zu den Austrittspforten für die Transmigration in das umliegende Gewebe zu geleiten. Die Vorstellung, dass MPO eher die etablierten Mechanismen der Leukozytenrekrutierung unterstützt, als wahllos die Adhäsion von Zellen an das Endothel zu vermitteln, wird durch die Beobachtung gestützt, dass MPO nur in postkapillären Venolen, dem üblichen Ort der Leukozytenrekrutierung, nicht aber in Arteriolen effektiv war. Während dieser Mechanismus im Rahmen der primären Immunantwort gegen pathogene Keime durchaus sinnvoll erscheint, ist er bei entzündlichen Erkrankungen, die mit einer überschießenden Aktivierung von Granulozyten einhergehen, möglicherweise problematisch, da er die Inflammation unterhält. Zusammenfassend identifizieren die Untersuchungsergebnisse eine bislang unbekannte Rolle von MPO und demonstrieren einen neuartigen Mechanismus, wie MPO die Motilität und Rekrutierung neutrophiler Granulozyten *in vitro* und *in vivo* begünstigt. Die Ergebnisse tragen somit zum besseren Verständnis grundlegender Mechanismen der Leukozytenrekrutierung bei und identifizieren MPO als mögliches Ziel neuer anti-inflammatorischer Therapien.

IIb) *Sphingosine-1-phosphate receptor 3 promotes leukocyte rolling by mobilizing endothelial P-selectin.*

(Nussbaum C. et al., Nat Commun 2015 Apr 2;6:6416)

Einleitung und Zielsetzung

Spingosin-1-Phospat (S1P) ist ein bioaktives Lysophospholipid mit Bedeutung für die Funktion des Immunsystems und des kardiovaskulären Systems (Aoki et al. 2016; Rivera, Proia, and Olivera 2008). Es entsteht durch Phosphorylierung von Sphingosin durch Spingosinkinasen. Die Wirkung von S1P wird über Bindung spezifischer, G-Protein gekoppelter Rezeptoren ($S1P_{1-5}$ Rezeptor) vermittelt (Spiegel and Milstien 2011).

Die Rolle von S1P und seinen Rezeptoren bei der Leukozytenrekrutierung im Rahmen der angeborenen Immunität wird derzeit kontrovers diskutiert. Einerseits belegen mehrere Studien, dass exogenes S1P die Expression der Adhäsionsmoleküle VCAM-1 und E-Selektin auf dem Endothel induzieren kann (Kimura et al. 2006; Krump-Konvalinkova et al. 2005). Zudem steigert eine chronische Überexpression der Sphingosinkinase-1 (Produzent von endogenem S1P) die TNF-α induzierte Expression von VCAM-1 und E-Selektin (Limaye et al. 2009). Andere Studien zeigen dagegen, dass S1P und $S1P_1$-Rezeptor-Agonisten eine inhibitorische Wirkung auf die durch TNF-α stimulierte Expression endothelialer Adhäsionsmoleküle und die Adhäsion von Immunzellen haben (Bolick et al. 2005; Whetzel et al. 2006). Mögliche Erklärung für diese diskrepanten Ergebnisse sind eine unterschiedliche S1P-Rezeptor-Besetzung in verschiedenen Endothelien sowie stark variierende S1P Konzentrationen in den jeweiligen Studien. Eine Beteiligung von endogenem S1P bei der Vermittlung von P-Selektin abhängigem Leukozytenrollen legte kürzlich eine Arbeit von Sun und Kollegen nahe. Die Autoren konnten zeigen, dass Histamin-induziertes Rollen von Leukozyten durch eine Blockade oder den genetischen Verlust der Shingosinkinase-1 aufgehoben wurde (Sun et al. 2012). Weder die Zugabe von exogenem S1P noch eine pharmakologische S1P-Rezeptorblockade zeigte Auswirkungen auf das Histamin-induzierte Rollen, was zur Schlussfolgerung führte, dass es sich hierbei um einen S1P-Rezeptor-unabhängigen Prozess handelt.

Während sich die meisten Untersuchungen zur Funktion von S1P im Rahmen der angeborenen und adaptiven Immunität auf dessen Wirkung am $S1P_1$-Rezeptor konzentrieren, ist bislang wenig über die Rolle des $S1P_3$-Rezeptors bekannt. In einer vorausgegangenen Studie wurden bei $S1P_3$-Rezeptor defizienten Mäusen Defekte bei der Rekrutierung von Leukozyten im Rahmen von Arteriosklerose und peritonealer Inflammation identifiziert (Keul et al. 2011). Inwiefern hiervon auch das Leukozytenrollen betroffen ist, blieb dabei unklar. Ziel war es daher, die Bedeutung von S1P und

insbesondere des $S1P_3$-Rezeptors für das Leukozytenrollen im Rahmen einer akuten Inflammation näher zu untersuchen.

Ergebnisse

Die wesentlichen Ergebnisse der Arbeit werden in Abb. 4. schematisch zusammengefasst.

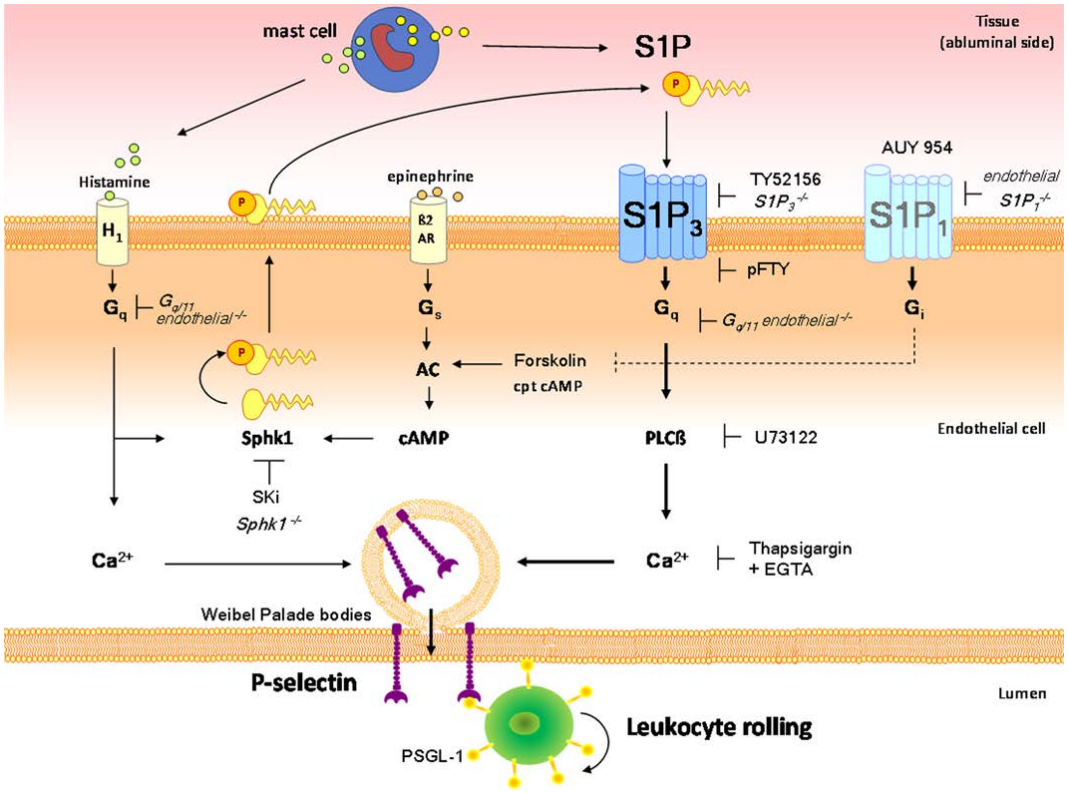

Abb. 4): Schematische Darstellung der Effekte von S1P und seiner Rezeptoren $S1P_3$ und $S1P_1$ auf die endotheliale P-Selektin Mobilisierung und das P-Selektin-vermittelte Rollen.

Anhand statischer und dynamischer *in vitro* Assays (u.a. Zellkultur, Durchflusszytometrie, Flusskammern) sowie intravitalmikroskopischer Untersuchungen am Modell des Mauscremaster-muskels (Trauma-induzierte Inflammation) wurden folgende neue Erkenntnisse zur Rolle von S1P und seinen Rezeptoren bei der Vermittlung von P-Selektin abhängigem Leukozytenrollen gewonnen:

1) S1P bewirkt als direkter Agonist die rasche endotheliale Mobilisierung von P-Selektin und P-Selektin-abhängiges Leukozytenrollen.

2) S1P-abhängiges Leukozytenrollen wird maßgeblich über den $S1P_3$-Rezeptor vermittelt und verläuft über eine Signalkaskade, welche die G-Protein Untereinheit Gq, Phospholipase C (PLC) und intrazelluläres Calcium involviert.
3) Der P-Selektin-mobilisierende Effekt verschiedener anderer Mediatoren wie z.B. Histamin oder Epinephrin wird durch Aktivierung der Spingosinkinase-1 zum Teil indirekt über S1P und den $S1P_3$-Rezeptor vermittelt.
4) Die Mobilisierung von P-Selektin kann durch einen neu identifizierten cAMP-abhängigen Signalweg, welcher die Sphingosinkinase 1 aktiviert, induziert werden.
5) Der S1P- Rezeptor Typ 1 ($S1P_1$) hemmt das Leukozytenrollen und ist somit eine Gegenspieler von $S1P_3$.
6) Die pharmakologische Blockade oder Herunterregulierung von $S1P_3$ setzt das Leukozytenrollen unter physiologischen *in vivo*-Bedingungen herab.

Diskussion

Die Arbeit identifiziert S1P als einen wesentlichen Akteur bei der raschen Mobilisierung von präformiertem P-Selektin an die Endotheloberfläche und die Vermittlung von P-Selektin-abhängigem Rollen *in vitro* und *in vivo*. S1P wirkt hierbei über den $S1P_3$-Rezeptor als direkter Agonist auf das Leukozytenrollen, wie auch indirekt als Mediator anderer P-Selektin-mobilisierender Substanzen, wie z.B. Histamin oder Epinephrin (Cleator et al. 2006). Leukozytenrollen in dem hier verwendeten *in vivo*-Modell der Trauma-induzierten Entzündung ist komplett P-Selektin abhängig und wird durch Degranulation von Mastzellen getriggert, wobei die Freisetzung von Histamin ca. 50% des Effekts ausmacht (Kubes and Kanwar 1994). Die Freisetzung von S1P aus Mastzellen wurde bislang für allergisch-aktivierte Mastzellen beschrieben (Olivera and Rivera 2011). Unsere Versuche zeigen, dass Mastzellen *in vitro* innerhalb von Minuten S1P freisetzen und zur raschen Mobilisierung von P-Selektin in HUVEC führen. Inwiefern die Freisetzung von S1P die andere Hälfte des Mastzelleffekts auf das Trauma-induzierte Leukozytenrollen *in vivo* ausmacht, muss durch weiterführende Untersuchungen geklärt werden.

Die Beobachtung, dass S1P an verschiedenen Rezeptoren unterschiedliche und sogar gegensätzliche Wirkung entfaltet, wie hier für den $S1P_1$- und $S1P_3$-Rezeptor demonstriert, greift frühere Befunde zu anderen S1P-regulierten Prozessen auf. So zeigten beispielsweise die S1P-Rezeptoren Typ 1 und 2 entgegengesetzte Effekte auf die Migration von Endothelzellen (Skoura and Hla 2009) und die Gefäßpermeabilität (Camerer et al. 2009; Sanchez et al. 2007). Matsushita und Kollegen konnten zudem zeigen, dass S1P eine duale Rolle bei der Exozytose von Weibel-Palade-Körperchen hat,

indem es diese über unterschiedliche intrazelluläre Signalwege sowohl fördert als auch hemmt (Matsushita, Morrell, and Lowenstein 2004). Interessanterweise waren für die fördernde Wirkung Phospholipase C und Calcium notwendig, zwei der intrazellulären Signalmoleküle, die auch bei der $S1P_3$-Rezeptor-vermittelten P-Selektin-Freisetzung von Bedeutung waren.

Die unterschiedliche Aktion von S1P an seinen verschiedenen Rezeptoren zusammen mit einer dosisabhängigen Wirkung von S1P könnte eine mögliche Erklärung für die bislang kontroversen Befunde zur Rolle von S1P bei der Leukozytenrekrutierung liefern. Zudem wird deutlich, warum der geringe Effekt einer pharmakologischen S1P-Rezeptor Blockade auf die P-Selektin-Freisetzung, wie er von Sun und Kollegen beobachtet wurde (Sun et al. 2012), nicht unbedingt gleichbedeutend mit einer fehlenden Beteiligung dieser Rezeptoren sein muss. Da die meisten pharmakologischen Inhibitoren nicht komplett selektiv für einen S1P-Rezeptor Subtyp sind, führt die gleichzeitige Blockade von aktivierenden und hemmenden Rezeptoren nur zu einem geringen Nettoeffekt. Der Sinn einer solchen differentiellen Wirkweise *in vivo* ist möglicherweise das „fine tuning“ der Immunantwort in Rahmen inflammatorischer Prozesse.

Zusammenfassend erweitert die Arbeit das Wissen über die komplexe Rolle von S1P im Rahmen der Immunfunktion und liefert wichtige neue Erkenntnisse zur Regulation von P-Selektin-abhängigem Leukozytenrollen *in vitro* und *in vivo*.

III) Teil 2: Regulation der Rekrutierung von Leukozyten und Thrombozyten im Rahmen der fetalen Entwicklung

Wissenschaftlicher Hintergrund

Wie bereits im ersten Teil ausgeführt, stellt die Rekrutierung von Leukozyten aus dem Gefäßsystem in das umliegende Gewebe einen komplexen und streng regulierten Prozess dar (s. Abschnitt II, S. 8/9). Gleichermaßen ist auch die Rekrutierung von Thrombozyten im Rahmen der primären Hämostase ein vielschichtiger Vorgang, der das funktionelle Zusammenspiel einer Vielzahl spezifischer Oberflächenrezeptoren mit ihren jeweiligen Liganden voraussetzt (Clemetson 2012; Sachs and Nieswandt 2007). Abb. 5 skizziert die einzelnen Schritte der Rekrutierung von Thrombozyten an die Gefäßwand.

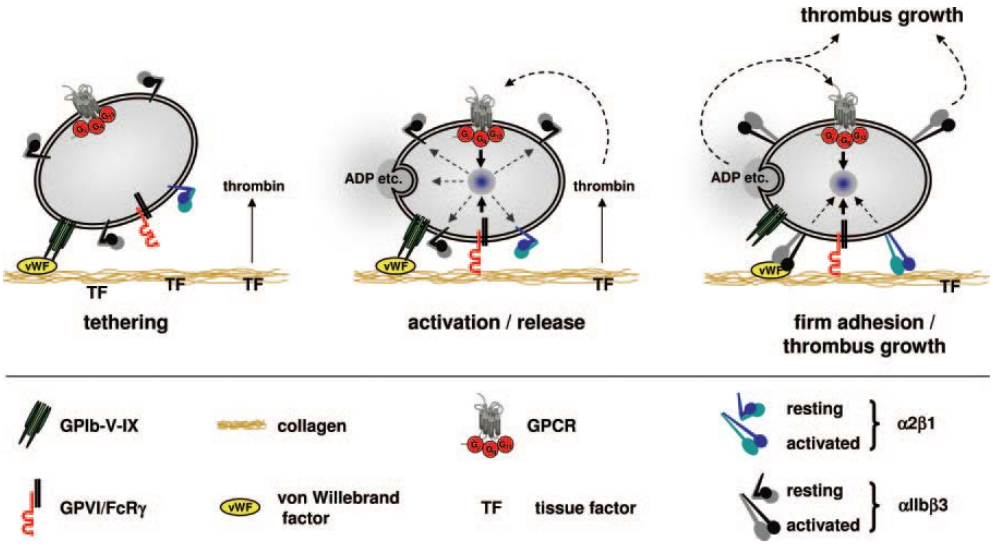

Abb. 5): Schematische Darstellung der Thrombozytenrekrutierung (Sachs and Nieswandt 2007)

Im Rahmen von Gefäßverletzungen werden Komponenten der subendothelialen Matrix exponiert, welche den initialen Schritt der Rekrutierungskaskade, das sog. Tethering unter hoher Schubspannung vermitteln. Hierbei spielt die Interaktion zwischen von-Willebrand-Faktor (vWF) und dem Glykoprotein Ib (GPIb, CD42)-Komplex auf Thrombozyten eine entscheidende Rolle (Moroi and Jung 1997). Durch die vWF-GPIb Verbindung werden die Thrombozyten abgebremst, was eine Interaktion von Glykoprotein VI (GPVI) auf den Plättchen mit Kollagen der extrazellulären Matrix ermöglicht. Die Bindung von GPVI führt zu einer starken Aktivierung der

Thrombozyten mit Freisetzung diverser Agonisten (u.a. ADP, ATP und Thromboxan A_2), welche die Thrombozyten zusätzlich in auto- und parakriner Weise aktivieren und die Rekrutierung weiterer Plättchen unterstützen (Moroi and Jung 1997). Gleichzeitig trägt auch Thrombin, das unter der Wirkung von Gewebefaktor (tissue factor) lokal gebildet wird, zur Plättchenaktivierung bei (Sachs and Nieswandt 2007). Infolge der Aktivierung kommt es vermittelt durch die Integrin-Adaptermoleküle Kindlin-3 und Talin-1 sowie die GTPase Rap1 zu einer Konformationsänderung des β_3-Integrins GPIIb/IIIa ($\alpha_{2b}\beta_3$; CD41/CD61) in einen Zustand hoher Affinität (Moser et al. 2008). In diesem ist eine Bindung an Fibrinogen (und über vWF auch an Kollagen) möglich, was zur festen Adhäsion und zur Ausbreitung der Plättchen (sog. Spreading) an der Gefäßwand führt. Daneben unterhalten β_1-Integrin-vermittelte Signale den Aktivierungszustand der Plättchen (Petzold et al. 2013). Adhärente Thrombozyten bilden so eine proadhäsive Oberfläche, an welche sich weitere Thrombozyten anheften können, was letztlich zur Bildung eines primären Thrombus führt. Die Interaktion und Vernetzung zwischen den Plättchen wird dabei v.a. über Bindung von Fibrinogen und vWF an aktiviertes GPIIb/IIIa vermittelt. Hierdurch werden das Thrombuswachstum und die -stabilität unterstützt (Bennett 2005). Zusätzlich spielt auch die Interaktion von Thrombozyten mit Leukozyten eine Rolle bei der primären Hämostase (McEver 2001). Aktivierte Plättchen setzten in großer Menge P-Selektin (CD62P) frei, welches an PSGL-1, den wesentlichen Roll-Liganden auf Leukozyten, binden kann (s. Abschnitt II, S. 9). Darüber hinaus bewirken Thrombozyten über CD40-CD40 Liganden- und GPIbα-Mac-1-Interaktionen eine Aktivierung von Leukozyten (Lindmark, Tenno, and Siegbahn 2000; Wang et al. 2005). Diese können wiederum durch Freisetzung von Chemokinen und anderen vasoaktiven Substanzen die Thrombusbildung verstärken.

Unser Verständnis über die Vorgänge der Leukozyten- und Thrombozytenrekrutierung basiert vornehmlich auf Studien, die am adulten Organismus durchgeführt wurden. Vergleichende Untersuchungen deuten jedoch darauf hin, dass es erhebliche Unterschiede zwischen dem erwachsenen Organismus und Neugeborenen gibt (Nussbaum and Sperandio 2011; Sola-Visner 2012). Diese Unterschiede beruhen vermutlich auf einer differentiellen Regulation der Prozesse im Fetus, wobei bislang nur wenige Daten zu diesem Thema existieren. Im Nachfolgenden werden Arbeiten des Habilitationsprojektes vorgestellt, die sich mit der Regulation der Rekrutierung von Leukozyten und Thrombozyten im Rahmen der fetalen Entwicklung befassen.

IIIa) ***Neutrophil and endothelial adhesive function during human fetal ontogeny.***

(Nussbaum C. et al., J Leukoc Biol 2013; 93(2):175-84)

Einleitung und Zielsetzung

Schwere Infektionen stellen trotz großer Fortschritte in der intensivmedizinischen Versorgung von Neugeborenen weiterhin eine führende Ursache von neonataler Morbidität und Mortalität dar. Schätzungen zu Folge sterben jährlich über 1,4 Millionen Neugeborene weltweit infolge von invasiven Infektionen (Shane and Stoll 2014). Die Sepsisinzidenz korreliert dabei invers mit dem Gestationsalter der Kinder und erreicht bei extrem frühgeborenen Kindern Raten von bis zu 62% (Stoll et al. 2010; Genzel-Boroviczeny et al. 2006). Neben extrinsischen Faktoren wie häufige invasive Prozeduren und lange Krankenhausaufenthalte scheint im Hinblick auf die inverse Korrelation schwerer Infektionen mit dem Gestationsalter auch eine Unreife des Immunsystems ursächlich für die hohe Infektanfälligkeit zu sein (Levy 2007).

Neutrophile Granulozyten spielen bei der angeborenen Immunantwort v.a. gegen bakterielle Pathogene eine zentrale Rolle und werden als erste Zellen aus dem Blutstrom an der Ort der Infektion rekrutiert (Kantari, Pederzoli-Ribeil, and Witko-Sarsat 2008). Schon seit längerem ist bekannt, dass Granulozyten von Neugeborenen im Vergleich zu Erwachsenen Unterschiede im Adhäsions- und Migrationsverhalten aufweisen (Nussbaum and Sperandio 2011). Über die Steuerung der Leukozytenrekrutierung im Verlauf der fetalen Entwicklung ist jedoch nur wenig bekannt. Tierversuche, die sich mit dieser Fragestellung beschäftigen, sind limitiert und beschränken sich überwiegend auf Untersuchungen an Nichtsäugern (Rouwet et al. 2000; Le Guyader et al. 2008). Die Ergebnisse dieser Studien deuten auf eine ontogenetische Regulation der Leukozytenrekrutierung mit „Reifung“ im Verlauf der fetalen Entwicklung hin. Inwiefern ein solcher Reifungsprozess aber auch bei der humanen Entwicklung stattfindet ist unklar.

Ziel dieser klinisch-experimentellen Studie war es daher das Rekrutierungspotential neutrophiler Granulozyten und Endothelzellen von Reifgeborenen und Frühgeborenen verschiedener Gestationsaltersstufen zu untersuchen, um genaueren Aufschluss über die Regulation der Leukozytenrekrutierung im humanen Fetus zu erlangen.

Ergebnisse

Zur Klärung der Fragestellung wurden neutrophile Granulozyten und Endothelzellen aus dem Nabelschnurblut von früh- und reifgeborenen Neonaten isoliert und in Mikroflusskammersystemen sowie mittels Durchflusszytometrie und Immunhistochemie untersucht.

Die Untersuchungen zeigten, dass die Fähigkeit zur Leukozytenrekrutierung signifikant mit dem Gestationsalter korreliert und sowohl die Funktion von Granulozyten als auch Endothelzellen betrifft.

1) Rollen und Adhäsion von Granulozyten sind bei extremen Frühgeborenen < 30 Schwangerschaftswochen (SSW) massiv herabgesetzt gegenüber späteren Entwicklungszeitpunkten, wobei auch Reifgeborene nicht das Niveau von Erwachsenen erreichten (Abb. 6A,B). Gleichermaßen ist die Fähigkeit von Nabelschnur-Endothelzellen (HUVEC) eine Leukozytenrekrutierung zu induzieren abhängig vom Gestationsalter und steigt im Verlauf der fetalen Entwicklung schrittweise an. HUVEC von extremen Frühgeborenen zeigten dabei ein signifikant reduziertes Potential Rollen und Adhäsion von adulten Granulozyten zu vermitteln (Abb. 6C).

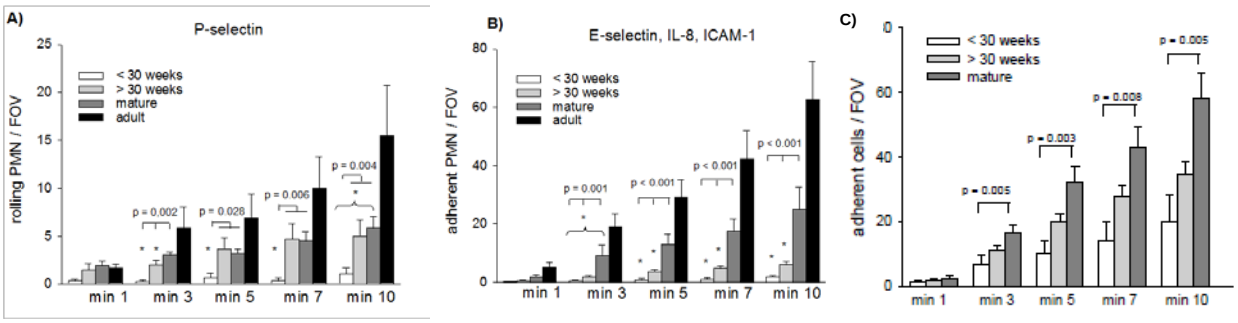

Abb. 6): Leukozytenrekrutierung in Abhängigkeit vom Gestationsalter. Anzahl rollender (A) und adhärenter (B) Granulozyten von früh- und reifgeborenen Neonaten sowie adulten Kontrollen in Mikroflusskammern, welche mit Adhäsionsmolekülen wie angegeben beschichtet wurden. C) Anzahl adhärenter adulter Granulozyten (immunkompetent) auf LPS-stimulierten HUVEC von früh- und reifgeborenen Neonaten.

2) Die Expression von Adhäsionsmolekülen mit Bedeutung für die Leukozytenrekrutierung korreliert mit dem Gestationsalter. Die Expression von E- Selektin und ICAM auf LPS-stimulierten HUVEC (Abb. 7A) sowie von PSGL-1 (Selektinligand) und dem β2-Integrin Mac-1 auf Granulozyten (Abb. 7B) war bei extrem Frühgeborenen signifikant herabgesetzt gegenüber späteren Entwicklungszeitpunkten und adulten Kontrollen.

3) Der altersabhängige Reifungsprozess der Leukozytenrekrutierung findet auch *ex utero* statt und unterscheidet sich nicht von der Entwicklung *in utero* (Abb. 7C).
4) Die Leukozytenrekrutierung und die Expression von Adhäsionsmolekülen werden durch eine Vorbehandlung mit Betamethason nicht beeinflusst.

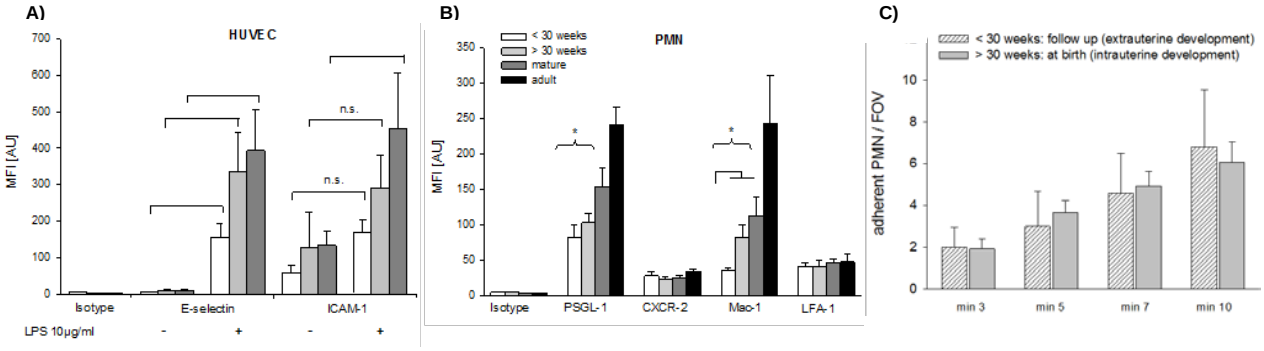

Abb. 7): Expression von Adhäsionsmolekülen in Abhängigkeit vom Gestationsalter. A) Durchflusszytometrische Analyse von E-Selektin und ICAM-1 auf HUVEC und B) PSGL-1 (Selektin-Ligand), CXCR2 (Chemokinrezeptor) und β_2-Integrinen auf Granulozyten (PMN). C) Vergleich zw. extrauteriner Entwicklung (< 30 SSW bei Geburt, Messung mit korrigiert > 30 SSW) und intrauteriner Entwicklung (> 30 SSW bei Geburt, Messung bei Geburt)

Diskussion

Die vorliegende Arbeit identifiziert einen Reifungsprozess der Leukozytenrekrutierung im Verlauf der fetalen Entwicklung, welcher die Funktion von Granulozyten und Endothelzellen umfasst. Die Ergebnisse bestätigen die Befunde früherer Studien, die eine Verminderung der Granulozytenrekrutierung bei reifgeborenen Neonaten im Vergleich zu Erwachsenen demonstrieren (Mariscalco, Tcharmtchi, and Smith 1998; Anderson et al. 1991; Abbassi et al. 1993) und erweitern diese auf die Gruppe Frühgeborener. Dabei zeigte sich, dass Granulozyten extrem frühgeborener Neonaten kaum in der Lage sind unter Flussbedingungen zu rollen oder zu adhärieren.

Als Ursache für die verminderte Rollbereitschaft der Granulozyten von Reifegeborenen wurde eine Reduktion des Selektinliganden PSGL-1 diskutiert (Tcharmtchi, Smith, and Mariscalco 2000). Unsere Analysen offenbaren eine darüber hinausgehende Verminderung von PSGL-1 auf Granulozyten von Frühgeborenen, welche die stark verminderte Anzahl rollender Zellen in dieser Untersuchungsgruppe wiederspiegelt. Diese trägt sicherlich zu der signifikanten Reduktion adhärenter Zellen bei, da Rollen eine Voraussetzung für die Adhäsion unter Fluss darstellt (Lawrence and Springer 1991). Zusätzlich scheinen Unterschiede von β_2-Integrinen für die reduzierte Rekrutierung neonataler Granulozyten verantwortlich zu sein (McEvoy, Zakem-Cloud,

and Tosi 1996; Anderson et al. 1987). Dementsprechend zeigte sich eine Korrelation der Mac-1 Expression mit dem Gestationsalter. Bei der Leukozytenrekrutierung spielt auch das Endothel eine entscheidende Rolle. Die vorliegende Arbeit identifiziert ein funktionelles Defizit neonataler Endothelzellen, welches v.a. bei extremen Frühgeborenen zum Vorschein kommt. Um Rollen und Adhäsion zu induzieren, müssen Endothelzellen in der Lage sein Adhäsionsmoleküle auf ihrer Oberfläche hochzuregulieren. In einer früheren Studie konnte demonstriert werden, dass die Expression von P-Selektin auf Endothelzellen vom Gestationsalter abhängt (Lorant et al. 1999). Unsere Ergebnisse zeigen zudem, dass auch die endotheliale Expression von E-Selektin und ICAM-1 bei Frühgeborenen signifikant reduziert ist im Vergleich zu Reifgeborenen und mit zunehmender Reife ansteigt.

Überraschenderweise offenbarten Folgeuntersuchungen von extremen Frühgeborenen, dass der altersabhängige Reifungsprozess durch extrinsische Faktoren kaum beeinflusst wird und sich nicht signifikant von der intrauterinen Entwicklung unterscheidet. Zudem wurde ausgeschlossen, dass die Unterschiede zwischen früh- und reifgeborenen Neonaten auf einer Behandlung mit Steroiden, wie sie zur Induktion der Lungenreife standardmäßig stattfindet, beruhen (Msan et al. 2015). Zusammengefasst deuten diese Ergebnisse auf eine ontogenetische Regulation der Leukozytenrekrutierung hin als physiologische Anpassung an die besonderen Bedürfnisse im Verlauf der fetalen Entwicklung. Die Befunde konnten parallel hierzu anhand eines neuartigen Modells zur Observation der Mikrozirkulation bei murinen Feten *in vivo* bestätigt werden (Sperandio et al. 2013).

Die massiv herabgesetzte Fähigkeit zur funktionellen Leukozytenrekrutierung bei Frühgeborenen disponiert diese in besonderem Maße für invasive Infektionen. Für die Entwicklung neuer Strategien zur Prävention und Therapie neonataler Infektionen sind weiterführende Studien notwendig, um die Mechanismen zu entschlüsseln, welche dieser ontogenetischen Regulation zugrunde liegen.

IIIb) ***Maturation of platelet function during murine fetal development in vivo.***

(Margraf A., Nussbaum C. et al,. Arterioscler Thromb Vasc Biol 2017 Apr 20, * gleichberechtigte Erstautorenschaft)*

Einleitung und Zielsetzung

Wie im wissenschaftlichen Hintergrund ausgeführt (s. Abschnitt III, S. 18/19) sind Thrombozyten die wesentlichen Akteure bei der primären Hämostase und verhindern größere Blutverluste bei Gefäßverletzungen durch rasche Rekrutierung an die verletzte Gefäßwand mit nachfolgender Ausbildung einen Thrombus. Während es ausführliche Untersuchungen zur Funktion von Thrombozyten im adulten Organismus gibt, ist die Datenlage zu den Vorgängen im sich entwickelnden Fetus limitiert und z.T. widersprüchlich.
Einerseits haben vorausgegangene Studien demonstriert, dass Plättchen von Neugeborenen eine Hyporeaktivität gegenüber verschiedenen Agonisten besitzen (Sola-Visner 2012; Israels et al. 1999). Andererseits zeigen Neugeborene im Vergleich zu Erwachsenen eine verkürzte Blutungszeit und eine verstärkte Ristocetin-induzierte Agglutination, was auf höhere Spiegel und eine verstärkte Aktivität des plasmatischen von Willebrand-Faktor (vWF) zurückgeführt wurde (Israels, Rand, and Michelson 2003). Mehrere Arbeitsgruppen haben eine Korrelation der Thromboyztenzahl und -aktivität mit dem Gestationsalter beschrieben (Levy-Shraga et al. 2006; Bednarek et al. 2009; Wiedmeier et al. 2009). Dies könnte v.a. bei Frühgeborenen zu Komplikationen führen. So wurde beispielsweise gezeigt, dass der postnatale Verschluss des Ductus arteriosus mit der Bildung eines Thrombus einhergeht und bei Thrombozytopenie gestört ist (Echtler et al. 2010).

Die bisherigen Erkenntnisse zur fetalen Plättchenfunktion stammen fast ausschließlich aus *in vitro*-Untersuchungen, während systematische *in vivo*-Untersuchungen der primären Hämostase sicherlich auch aufgrund der schwierigen experimentellen Untersuchungsbedingungen fehlen. Ziel dieser Studie war es daher ein intravitalmikroskopisches Modell zu entwickeln, welches eine Untersuchung der Thrombusbildung im lebenden Fetus ermöglicht, um so die Vorgänge bei der primären Hämostase im Verlauf der fetalen Entwicklung zu analysieren. Zusätzlich erfolgte eine retrospektive Datenanalyse einer neonatalen Kohorte aus einem Level 1 Perinatalzentrum, um die Auswirkung einer Thrombozytentransfusion bei thrombozytopenen Neonaten auf die pharmakologische Verschlussrate eines persistierenden Ductus arteriosus (PDA) zu untersuchen.

Ergebnisse:

Für die *in vivo* Untersuchung der fetalen Thrombozytenfunktion wurden ein zuvor etabliertes Modell der fetalen Mikrozirkulation verwendet und entsprechend adaptiert (Sperandio et al. 2013). Die Thrombozytenrekrutierung in Dottersackgefäßen wurde dabei durch phototoxischen Endothelschaden nach Mikroinjektion von FITC-Dextran induziert (Abb. 8). Die Untersuchungen erfolgten an den Entwicklungstagen E13.5 bis E17.5 von insgesamt 21 Tagen Gestationsdauer.

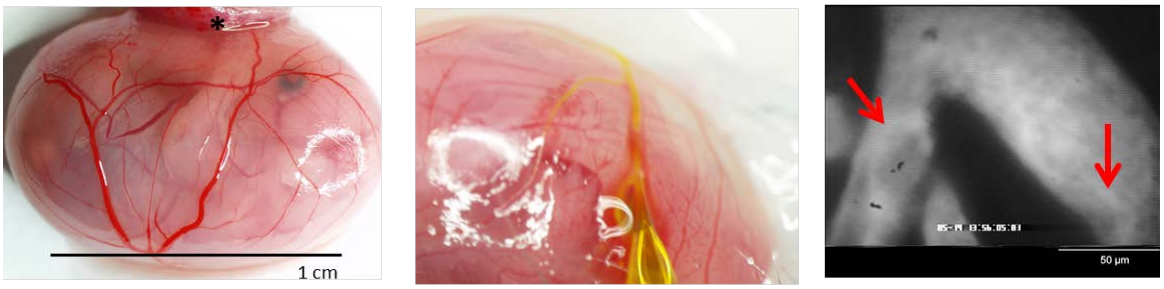

Abb. 8): *In vivo* Modell zur Untersuchung der fetalen Thrombozytenfunktion. Links: Präparation des Feten im intakten Dottersack (* Verbindung zur Plazenta). Mitte: Injektion von 10% FITC-Dextran in ein Dottersackgefäß. Rechts: intravitale Fluoreszenzmikroskopie der Dottersackgefäße. Die Pfeile markieren wandständige Thromben.

Die Untersuchungen ergaben zusammengefasst folgende Ergebnisse:

1) Die Fähigkeit zur funktionellen Thrombusbildung *in vivo* korreliert mit dem Gestationsalter. So zeigten E13.5 Feten im Vergleich zu späteren Entwicklungszeitpunkten eine signifikant geringere Rate an Thrombozytenadhäsion (Abb. 9A), eine Thrombusinstabilität mit 100% Wiedereröffnungsrate primär okkludierter Gefäße (Abb. 9B) und weniger Rekrutierung von Thrombozyten in den wachsenden Thrombus (Abb. 9C)

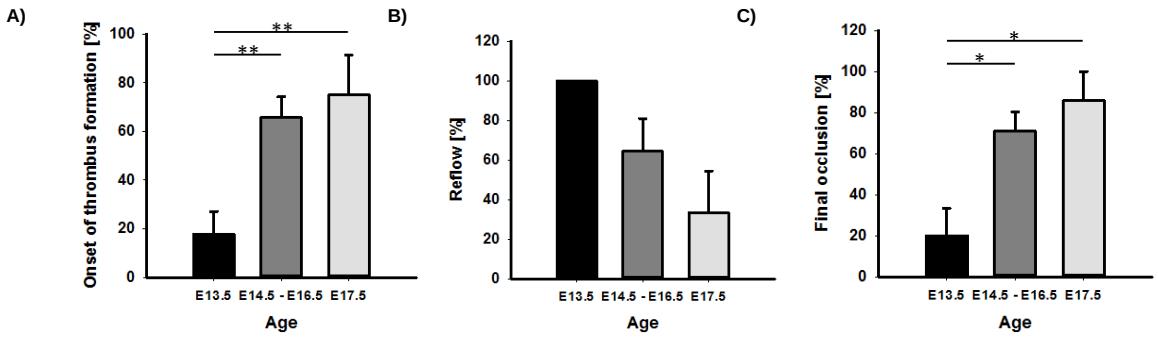

Abb. 9): Funktionelle Thrombusbildung in Abhängigkeit vom Gestationsalter. A) Rate der primären Thrombozytenadhäsion an der Gefäßwand (onset). B) Prozentualer Anteil an wiedereröffneten Gefäßen nach primärem Verschluss (reflow). C) Rate endgültiger gefäßokkludierender Thromben (final occlusion).

2) Die Thrombozytenzahl hängt vom Gestationsalter ab und war bei E13.5 Feten massiv herabgesetzt, wobei das Plättchenvolumen und der prozentuale Anteil großer Plättchen invers mit dem Gestationsalter korrelieren.
3) Der Gesamtgehalt und die Oberflächenexpression von P-Selektin sowie von Glykoprotein Ib- sind in fetalen Thrombozyten im Vergleich zu adulten Kontrollen signifikant reduziert.
4) Fetale Thrombozyten besitzen im Vergleich zu adulten Kontrollen signifikant geringere Proteinspiegel der Integrin-Adaptermoleküle Kindlin-3, Talin-1 und der GTPase Rap1 und zeigen eine gestörte Aktivierung des α2bβ3-Integrins (GPIIb/IIIa) nach Stimulation mit Thrombin (Abb. 10). Dies resultiert in einer signifikant verminderten Fähigkeit fetaler Plättchen zum „Spreading“ auf Fibrinogen.

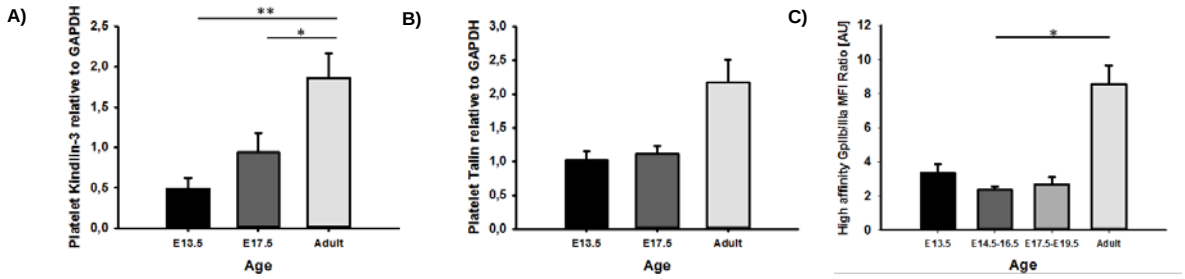

Abb. 10): Integrin-Adaptermoleküle und -Aktivierung in Abhängigkeit vom Gestationsalter

5) Die verminderte Fähigkeit zur Thrombozytenrekrutierung in Feten kann durch Transfusion adulter Plättchen kompensiert werden. So resultierte eine Transfusion adulter Thrombozyten in E14.5 Feten in einer prompten Plättchenaggregation, wohingegen die Transfusion altersadaptierter Thrombozyten (E14.5 Spender in E14.5 Empfänger) nur in einem Drittel der Fälle zur Ausbildung eines Thrombus führte.
6) Die Transfusion adulter Thrombozyten bei thrombozytopenen Frühgeborenen scheint keinen wesentlichen Einfluss auf den Verschluss eines hämodynamisch relevanten PDA zu haben.

Diskussion

Wie zuvor für die Leukozytenrekrutierung demonstriert, offenbart sich ein Reifungsprozess der Thrombozytenrekrutierung im Verlauf der fetalen Entwicklung. Dabei zeigte sich, dass murine Feten an frühen Zeitpunkten der Gestation (E13.5) kaum in der Lage sind einen stabilen Thrombus zu bilden. Die Ergebnisse bestätigen die *in vivo*-Relevanz früherer *in vitro*-Untersuchungen, welche eine Abhängigkeit der Thrombozytenfunktion vom Gestationsalter darstellten (Del Vecchio et al. 2008; Levy-Shraga et al. 2006; Bednarek et al. 2009). Interessanterweise ist nicht nur die Fähigkeit zur Ausbildung eines primären Thrombus betroffen, sondern auch die Thrombusstabilität, wie an

dem „Reflow“-Phänomen in E13.5 Feten sichtbar wird. Eine Korrelation der Thrombusstabilität mit dem Gestationsalter wurde zuvor für humane Plättchen *in vitro* demonstriert (Strauss et al. 2010). Im Hinblick auf die essentielle Bedeutung von GPIb und dem $\alpha_{2b}\beta_3$-Integrin für die Adhäsion und Vernetzung von Thrombozyten (Clemetson 2012) erscheint es plausibel, dass die Reduktion von GPIb und die herabgesetzte Fähigkeit zur Integrinaktivierung an der verminderten Thrombusbildung und –stabilität in E13.5 Feten beteiligt sind. Als mögliche Ursache für die verminderte Integrinaktivierung konnte erstmals eine altersabhängige Expression von Kindlin-3, Talin-1 und Rap1 demonstriert werden. Die funktionelle Relevanz dieses Befundes zeigt sich im verminderten „Spreading“ fetaler Thrombozyten *in vitro*, einem Prozess, der entscheidend von β_3-Integrin-vermittelten Signalen nach deren Aktivierung abhängt (Shattil 1999). Darüber hinaus spielen sicherlich die ausgeprägten Unterschiede in der Thrombozytenzahl und möglicherweise auch in Faktoren der plasmatischen Gerinnung eine Rolle. Unter Berücksichtigung der Ergebnisse der Transfusionsexperimente ist es aber wahrscheinlich, dass neben der reduzierten Anzahl an Plättchen auch funktionelle Defizite für die Verminderung der Thrombusbildung bei jungen Feten verantwortlich sind. So resultierte eine Transfusion mit adulten Thrombozyten, nicht jedoch mit Thrombozyten von E14.5 Spendern (trotz gleicher Anzahl) in einer spontanen Thrombusbildung in der fetalen Zirkulation. Interessanterweise wurden nach Transfusion adulter Thrombozyten in adulte Spendertiere (Kontrollversuche) keine spontane Adhäsion und Aggregation der Plättchen gesehen. Diese Beobachtungen sprechen für das Vorliegen von „prokoagulatorischen“ Faktoren im fetalen Plasma (z.B. erhöhte Spiegel an vWF und übergroße vWF-Multimere) möglicherweise als Kompensation für die reduzierte Anzahl und Funktionalität fetaler Thrombozyten, wie es bereits von Sola Visner und Kollegen postuliert wurde (Ferrer-Marin et al. 2011). Unter diesem Aspekt sollte die Indikation zur Transfusion adulter Thrombozyten bei extremen Frühgeborenen besonders kritisch hinterfragt werden.

Zusammengefasst weist die Arbeit eine ontogenetische Regulation der Plättchenfunktion nach. Diese erscheint unter physiologischen Bedingungen sinnvoll, da Verletzungen in der geschützten Umgebung des Uterus unwahrscheinlich sind, wohingegen eine Thrombose im sich entwickelnden Fetus fatale Konsequenzen haben könnte. Im Falle einer Frühgeburt trägt die Unreife von Thrombozyten dagegen möglicherweise zu Komplikationen wie intrakranieller Blutung und PDA bei (Kuperman, Brenner, and Kenet 2013; Echtler et al. 2010). Eine retrospektive Datenanalyse ergab zwar keinen Hinweis auf einen Vorteil einer Thrombozytentransfusion zum PDA-Verschluss, allerdings könnten die Ergebnisse durch Faktoren wie Ductusgröße, Komorbiditäten und Behandlungszeitpunkt beeinflusst worden sein und müssen daher durch größere, prospektive Studien bestätigt werden.

IV) Teil 3: Veränderungen der Mikrozirkulation bei Kindern im Rahmen ausgewählter Erkrankungen

Wissenschaftlicher Hintergrund

Aufgrund der Bedeutung der Mikrozirkulation für die Funktion aller Organe und Gewebe des menschlichen Organismus können Veränderungen derselben zu schwerwiegenden gesundheitlichen Schäden führen. Dabei sind Mikrozirkulationsstörungen oftmals Erkrankungsfolge und -ursache zugleich (Wiernsperger and Rapin 2012). So führen z.B. bei einer unkontrollierten bakteriellen Infektion Veränderungen der Mikrozirkulation wie eine Verminderung der funktionellen Gefäßdichte, ein heterogener Blutfluss, eine gestörte Endothelfunktion und eine überschießende Leukozyten- und Thrombozytenrekrutierung erst zum klinischen Vollbild einer Sepsis (Colbert and Schmidt 2016; Ince 2005). Auch verschiedene chronische Krankheitsbilder wie z.B. Diabetes mellitus, Bluthochdruck und metabolisches Syndrom gehen mit strukturellen und funktionellen Veränderungen der Mikrozirkulation einher (Gartner and Eigentler 2008; Wiernsperger and Rapin 2012). Diese liegen Krankheits-assoziierten Komplikationen wie z.B. Retinopathie oder Nephropathie zugrunde und tragen wesentlich zur Morbidität und Mortalität der Patienten bei.

Die Mechanismen, welche zu Mikrozirkulationsstörung und Mikroangiopathie führen, sind weiterhin nicht vollständig geklärt. Ein wichtiger Faktor scheint dabei die Entwicklung einer endothelialen Dysfunktion darzustellen (Colbert and Schmidt 2016; Schalkwijk and Stehouwer 2005). Diese geht strukturellen Gefäßveränderungen voraus und lässt sich bereits im Kindesalter bei Patienten mit Diabetes mellitus und Adipositas nachweisen (Khan et al. 2000; Mahmud et al. 2008). Bei der Pathogenese scheinen Faktoren wie Hyperlipidämie, Hyperglykämie, arterielle Hypertension und chronische Inflammation eine wichtige Rolle zu spielen. Diese begünstigen die Entwicklung einer endothelialen Dysfunktion u.a. durch vermehrte Produktion von Sauerstoffradikalen, vasoaktiven Substanzen und pro-inflammatorischen Mediatoren wie Tumornekrosefaktor oder sog. advanced glycation endproducts (AGEs) (Hink et al. 2001). Zudem ist in den letzten Jahren die endotheliale Glykokalyx als Ausgangspunkt einer endothelialen Dysfunktion in den Fokus wissenschaftlicher Untersuchungen gerückt (Rabelink and de Zeeuw 2015; Salmon and Satchell 2012).

Die Glykokalyx ist eine kohlenhydratreiche Schicht, welche das Lumen des gesamten Gefäßsystems auskleidet und von entscheidender Bedeutung für die vaskuläre Integrität ist (Abb.11) (Reitsma et al. 2007). Der endothelnahe Anteil wird von Proteoglykanen (z.B. Syndecan, Glypican) und Glykoproteinen (diverse Zelladhäsionsmoleküle) gebildet, welche fest im Endothel

verankert sind und das „Rückgrat“ der Glykokalyx formen. Die Glykoproteine besitzen lange Glykosaminoglykan (GAG)-Seitenketten (z.B. Heparansulfat) und bilden zusammen mit den Glykoproteinen ein dreidimensionales Netzwerk, an welches sich lösliche Plasmaproteine und GAGs anlagern (Abb. 11). Diese weiter luminal befindliche Schicht steht in einem dynamischen Gleichgewicht mit dem Blutfluss und ist ständigen Auf-und Abbauprozessen unterworfen, wodurch sich die Dicke und Zusammensetzung ändern (Reitsma et al. 2007).

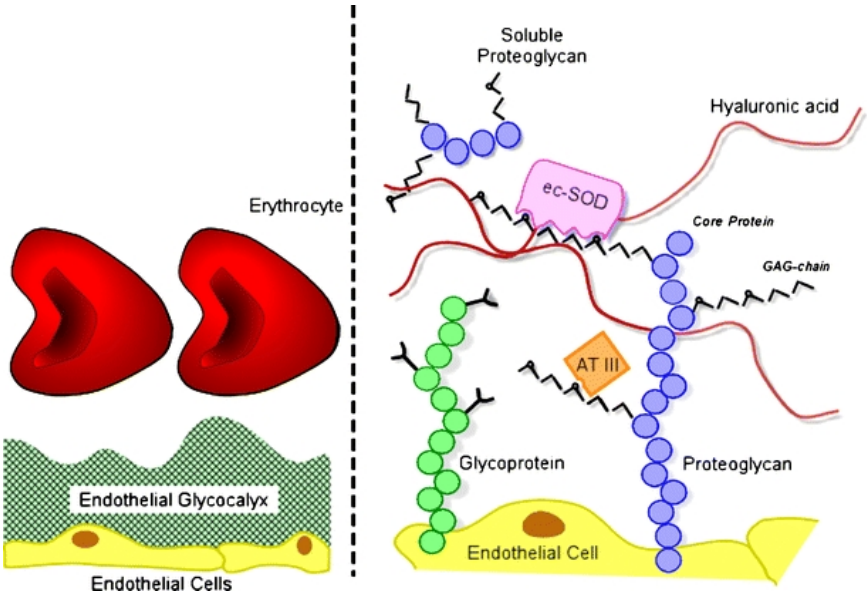

Abb. 11): Schematische Darstellung der endothelialen Glykokalyx (Reitsma et al. 2007)

Die Glykokalyx und assoziierte lösliche Plasmaproteine bilden zusammen den sog. endothelial surface layer (ESL), eine Oberflächenschicht, die eine Dicke von mehreren Mikrometern erreichen kann. An der Grenze zwischen dem Blut und dem Endothel ist sie ein wichtiger Regulator verschiedener Gefäßfunktionen. So bestimmt sie die Permeabilität der Gefäßwand, beeinflusst die rheologischen Eigenschaften der Mikrozirkulation, fungiert als Sensor für Schubspannung und übt antiadhäsive und vaskuloprotektive Effekte aus (Nieuwdorp et al. 2005). Strukturelle Veränderungen bzw. ein Abbau (sog. shedding) der Glykokalyx führen zu einer erhöhten Gefäßpermeabilität mit Durchlässigkeit für Makromoleküle, einer gestörten Endothel-abhängigen Reaktion auf Veränderungen des Blutflusses, sowie einer vermehrten Adhäsion von Leukozyten und Thrombozyten (Chappell, Westphal, and Jacob 2009; Nieuwdorp, van Haeften, et al. 2006; Perrin, Harper, and Bates 2007). Bei kritisch kranken Patienten wurde gezeigt, dass das Ausmaß der

Glykokalyxschädigung mit der Schwere der Erkrankung und der Mortalität korreliert (Donati et al. 2013; Nelson et al. 2008).

Dank neuer Videomikroskopie-Techniken wie z.B. OPS (Orthogonal Polarization Spectral) oder SDF (Sidestream Dark Field) -Imaging ist eine bessere Visualisierung der Mikrozirkulation *in vivo* möglich geworden (De Backer et al. 2010). Während bei Erwachsenen eine ausreichende Bildqualität nur an nicht-epithelialisierten Geweben (z.B. sublinguale Mikrozirkulation) erreicht werden kann, sind bei Kindern im Säuglingsalter und insbesondere bei früh- und reifgeborenen Neonaten auch Messungen der Hautmikrozirkulation möglich (Genzel-Boroviczeny et al. 2002; Kroth et al. 2008). Mit Hilfe dieser Techniken können pathologische Veränderungen der Mikrozirkulation im Rahmen von Erkrankungen unmittelbar sichtbar gemacht und quantifiziert werden. Sie eignen sich damit auch zur Überwachung und Evaluation von Therapien (Boerma et al. 2010; den Uil et al. 2009; Koopmans et al. 2015) und für ein mögliches Monitoring zur frühzeitigen Detektion von Erkrankungen (Weidlich et al. 2009) oder zur Abschätzung der Prognose (De Backer et al. 2013; Sakr et al. 2004; Trzeciak et al. 2007).

Die meisten der hier angeführten Studien wurden an Erwachsenen durchgeführt. Da der kindliche Organismus jedoch eine eigene (Patho-)Physiologie besitzt, welche sich meist deutlich von der des Erwachsenen unterscheidet, können Studienergebnisse, die an adulten Probanden bzw. Patienten erhoben wurden, nicht ohne weiteres auf Kinder übertragen werden. Zudem ist bekannt, dass chronische vaskuläre Veränderungen häufig schon im Kindesalter ihren Ausgang nehmen (Kavey et al. 2006). Um ein genaueres Verständnis der Prozesse zu erlagen, welche bei Kindern zur Entstehung von akuten und chronischen Störungen der Mikrozirkulation führen, ist es daher notwendig entsprechende Untersuchungen in diesem Patientengut durchzuführen. Im Folgenden werden Arbeiten des Habilitationsprojektes vorgestellt, die sich mit solchen Untersuchungen bei pädiatrischen Patientengruppen mit erhöhtem Risiko für das Auftreten von Mikrozirkulations-störungen befassen.

IVa) ***Early microvascular changes with loss of the glycocalyx in children with type 1 diabetes.***

(Nussbaum C. et al., J Pediatr 2014; 164(3):584-9)

Einleitung und Zielsetzung

Typ 1 Diabetes mellitus (T1DM) gehört zu den häufigsten chronischen Erkrankungen im Kindesalter und zeigt eine steigende Inzidenz. Schätzungen zufolge wird sich die Anzahl an T1DM Fällen bei Kindern unter 5 Jahren zwischen 2005 und 2020 verdoppeln (Patterson et al. 2009). Die Prognose von Patienten mit T1DM hängt von der Entwicklung vaskulärer Folgeerkrankungen wie Nephropathie, Retinopathie und kardiovaskulären Erkrankungen ab, welche zu erheblicher Morbidität und frühzeitiger Mortalität führen (Daneman 2006). Folglich stellen die Prävention und die frühzeitige Detektion vaskulärer Komplikationen einen zentralen Aspekt bei der medizinischen Versorgung der Patienten dar.

Die Pathogenese der diabetischen Mikroangiopathie ist weiterhin nur unvollständig geklärt, wie aber im wissenschaftlichen Hintergrund dargestellt, scheint die Entwicklung einer endothelialen Dysfunktion eine wesentliche Rolle zu spielen (Schalkwijk and Stehouwer 2005) (s. Abschnitt IV, S. 29). Einige Arbeiten konnten zeigen, dass endothelabhängige Gefäßfunktionen bei Kindern und Jugendlichen mit T1DM bereits gestört sind, wenn es noch keine klinischen Anzeichen für vaskuläre Komplikationen gibt (Babar et al. 2011; Khan et al. 2000). Dementsprechend wurden erhöhte Spiegel von ICAM-1, E-Selektin und vWF als Marker für eine Beeinträchtigung des Endothels bei Kindern mit T1DM nachgewiesen (Elhadd et al. 1999). Wie bereits erwähnt, sind die Mechanismen, die zu endothelialer Dysfunktion führen, multifaktoriell (Hink et al. 2001), wobei im Falle von Diabetes mellitus Hyperglykämie sicherlich ein zentraler Faktor ist (The Diabetes Control and Complications Trial Research Group 1993). In den letzten Jahren wurde die endotheliale Glykokalyx als mögliches Ziel einer hyperglykämischen vaskulären Schädigung identifiziert (Salmon and Satchell 2012). So verursachten erhöhte Blutzuckerspiegel eine Störung der Glykokalyx, die zu endothelialer Dysfunktion bei Erwachsenen und zu einer erhöhten Permeabilität der Mikrozirkulation führte (Brower et al. 2010; Nieuwdorp, van Haeften, et al. 2006). Zudem wurden bei adulten Patienten mit T1DM erhöhte zirkulierende Spiegel von Hyaluronsäure, einem wesentlichen Bestandteil der Glykokalyx, im Blut gemessen, was mit einem höheren Risiko für präarteriosklerotische Gefäßveränderungen einherging (Nieuwdorp et al. 2007). Mittels neuer Videomikroskopie-Techniken (s. Abschnitt IV, S. 31) ist es sogar möglich, Veränderungen der

Glykokalyxdicke bei Diabetespatienten auf mikrovaskulärer Ebene zu quantifizieren (Nieuwdorp, Mooij, et al. 2006).

Bislang ist unklar, ob derartige Veränderungen der Glykokalyx bei Patienten mit T1DM bereits im Kindesalter auftreten. Ziel der vorliegenden Studie war es daher, die Mikrozirkulation und die mikrovaskuläre Glykokalyx bei Kindern mit T1DM und bei gesunden Kontrollkindern zu untersuchen.

Ergebnisse:

Die sublinguale Mikrozirkulation wurde bei 14 Kindern mit T1DM und 14 gesunden Kontrollen mittels Sidestream Dark Field (SDF)-Imaging untersucht. Patienten und Kontrollen unterschieden sich nicht signifikant hinsichtlich Geschlecht, Alter, Blutdruck, Body Mass Index (BMI) und Hämatokrit. Die Blutzuckerspiegel und die Leukozytenzahl waren bei Kindern mit T1DM signifikant erhöht gegenüber der Kontrollgruppe. Bei keinem der Patienten lag in den Routineuntersuchungen eine Mikroalbuminurie oder eine Retinopathie vor.

Die Messungen ergaben folgende Ergebnisse:

1) Kinder mit T1DM zeigen Veränderungen der Gefäßarchitektur in der sublingualen Mikrozirkulation. Während die Gefäßdichte und der mikrozirkulatorische Blutfluss zwischen den Gruppen vergleichbar waren, zeigte sich bei Kindern mit T1DM ein signifikant erhöhter Anteil großer Gefäße (> 20 µm Durchmesser) auf Kosten der Kapillaren (< 10 µm) (Abb. 12A). Hieraus resultierte eine signifikant höhere Gefäßabdeckung pro Bildausschnitt (vessel surface coverage) bei diabetischen Kindern im Vergleich zu Kontrollen (Abb. 12B).
2) Kinder mit T1DM zeigen eine Störung der mikrovaskulären Glykokalyx. So war die Glykokalyxdicke bei diabetischen Kindern signifikant reduziert gegenüber Kontrollen (Abb. 12C). Zudem wurde eine inverse Korrelation der Glykokalyxdicke mit dem Blutzuckerspiegel beobachtet (Abb. 12D). Es bestand keine Korrelation der Glykokalyxdicke mit dem HbA1c-Wert, der BMI, der Diabetesdauer, dem Alter und dem Blutdruck.

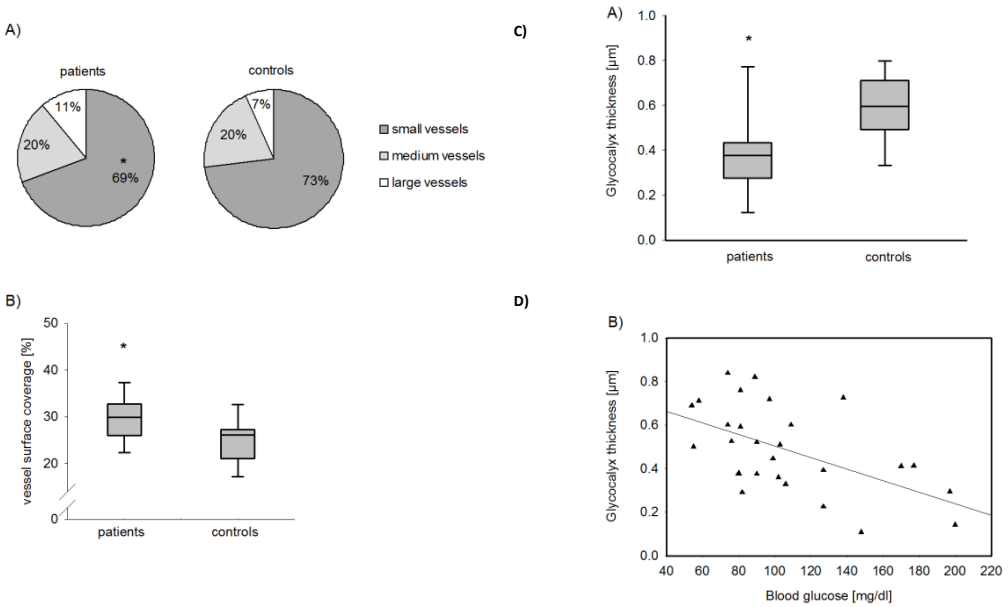

Abb. 12): Veränderung der sublingualen Mikrozirkulation und der Glykokalyx bei Kindern mit T1DM. A) Prozentuale Verteilung der Gefäßdurchmesser. B) Prozentuale Gefäßabdeckung (= Anteil des Bildausschnitts, der mit Gefäßen bedeckt ist). C) Dicke der Glykokalyx in sublingualen Gefäßen < 10 µm. D) Korrelation der Glykokalyxdicke mit den Blutzuckerspiegeln (Pearson Korrelation: r = -0.55, p = 0.003)

Diskussion:

Die Studie liefert Einsicht in mikrovaskuläre Veränderungen bei Kindern mit Diabetes mellitus. Ein wesentlicher Befund war hierbei der Nachweis einer Glykokalyxschädigung mit einer Reduktion der mikrovaskulären Glykokalyxdicke um 36% gegenüber gesunden Kindern. Diese Beobachtung stimmt mit früheren Berichten zu erwachsenen Diabetikern überein, welche einen Verlust der sublingualen Glykokalyx von 18-44% beobachteten (Broekhuizen et al. 2010; Nieuwdorp, Mooij, et al. 2006). Interessanterweise korrelierte die Glykokalyxdicke invers mit dem Blutzuckerspiegel. Experimentelle Untersuchungen konnten zeigen, dass selbst eine kurzfristige Erhöhung der Blutzuckerspiegel in pathologische Bereiche zu einem akuten Abbau der Glykokalyx führt (Nieuwdorp, van Haeften, et al. 2006; Zuurbier et al. 2005). Die Ergebnisse stützten somit die Idee, dass die endotheliale Glykokalyx direktes Ziel einer hyperglykämischen vaskulären Schädigung ist. Dies könnte schwerwiegende Konsequenzen nach sich ziehen, da eine Schädigung der Glykokalyx in direkten Zusammenhang mit der Entstehung einer Mikroalbuminurie als Marker für eine diabetische Nephropathie gebracht wurde (Nieuwdorp, Mooij, et al. 2006; Rabelink and de Zeeuw 2015).

Mögliche Mechanismen der Glykokalyxschädigung im Rahmen von Hyperglykämie sind u.a. eine gesteigerte Produktion reaktiver Sauerstoffspezies (ROS) sowie die Aktivierung von Enzymen,

welche die Glykokalyx abbauen (z.B. Hyaluronidase) (Brownlee 2001; Nieuwdorp, Mooij, et al. 2006). Hyperglykämie und oxidativer Stress induzieren auch die Produktion sog. advanced glycation endproducts (AGEs) und anderer inflammatorisch wirksamer Mediatoren (Pahwa, Nallasamy, and Jialal 2016) im Sinne der Vorstellung, dass Diabetes einen Zustand chronischer Inflammation darstellt (Llaurado et al. 2012). Dies könnte möglicherweise die erhöhte Leukozytenzahl bei Kindern mit T1DM erklären.

Ein weiteres Untersuchungsergebnis ist der Nachweis einer Veränderung der Gefäßarchitektur in der sublingualen Mikrozirkulation mit einer Umverteilung der Gefäßdurchmesser zugunsten größerer Gefäße. Eine tierexperimentelle Studie an diabetischen Mäusen hat bereits in einem frühen Krankheitsstadium ähnliche Veränderungen mit einer Zunahme größerer Gefäße und einer signifikanten Abnahme der Kapillaren gezeigt (sog. capillary rarefication) (Algenstaedt et al. 2003). Diese Veränderungen sind insofern relevant, da der Gas- und Nährstoffaustausch im Gewebe in den Kapillaren stattfindet (s. Abschnitt I, S.4). Eine fortschreitende Reduktion der Kapillaren führt somit letztlich zur Gewebshypoxie (Pittman 2005).

Zusammenfassend belegen die Untersuchungen, dass Kinder mit T1DM bereits vor Auftreten sichtbarer vaskulärer Komplikationen wie Nephropathie oder Retinopathie strukturelle Veränderungen der Mikrozirkulation aufweisen, welche mit der Entstehung von endothelialer Dysfunktion und Mikroangiopathie in Verbindung gebracht wurden. Obwohl sich die Untersuchungen auf die sublingualen Gefäße beschränken, erscheint es plausibel, dass die Ergebnisse auf andere Organe übertragbar sind, da sich erhöhte Blutzuckerspiegel auf den gesamten Organismus auswirken sollten. Die sublinguale Mikrozirkulation könnte sich daher als Monitoringparameter eignen zur Identifikation von Patienten mit erhöhtem Risiko für die Entwicklung einer Vaskulopathie. Die Glykokalyx als frühes Ziel einer Diabetes-induzierten Schädigung stellt einen möglichen Ansatzpunkt für die Entwicklung neuer Therapiestrategien zur Prävention vaskulärer Komplikationen dar. So wurde z.B. ein positiver Effekt einer Therapie mit Sulodexid, einem natürlich vorkommenden Glykosaminoglykan, auf den Grad der Mikroalbuminurie als Ausdruck einer Glykokalyxschädigung in den Glomerula bei Erwachsenen mit Diabetes mellitus beschrieben (Broekhuizen et al. 2010; Gambaro et al. 2002). Inwieweit und unter welchen Umständen derartige Strategien, welche auf eine Protektion bzw. eine Regeneration der Glykokalyx abzielen, eine wirklichen therapeutischen Nutzen haben und ob dies auch bei Kindern zutrifft, ist jedoch derzeit noch unklar und bedarf weiterer, groß angelegter klinischer Studien.

IVb) *Perturbation of the microvascular glycocalyx and perfusion in infants after cardiopulmonary bypass.*

(Nussbaum C. et al., J Thorac Cardiovasc Surg 2015; 150(6):1474-81)

Einleitung und Zielsetzung:

Die Bedeutung der endothelialen Glykokalyx für die vaskuläre Integrität und Homöostase wurden bereits im wissenschaftlichen Hintergrund dargelegt (s. Abschnitt VI, S. 28-30). Interessanterweise werden bei Kindern mit angeborenen Herzfehlern nach Operationen an der Herz-Lungen-Maschine (HLM) Veränderungen beobachtet, welche auch nach einer Schädigung bzw. einem Verlust der Glykokalyx auftreten. Hierzu zählt z.B. eine gestörte Permeabilitätsbarriere mit Entstehung generalisierter Ödeme (Kapillarlecksyndrom) sowie eine systemische inflammatorische Reaktion mit Aktivierung des Endothels und vermehrter Rekrutierung von Leukozyten und Thrombozyten (Ignjatovic et al. 2012; Kubicki et al. 2013; Stiller et al. 2001). Diese Veränderungen können zu Organdysfunktion führen und den postoperativen Verlauf und das Outcome der Patienten negativ beeinflussen. So wurde beispielsweise gezeigt, dass Kinder mit ausgeprägtem Kapillarlecksyndrom einen längeren Katecholaminbedarf haben als Kinder, die nur eine geringe Ödembildung aufweisen (Neuhof et al. 2003). Bei der Entstehung HLM-assoziierter Komplikationen könnte also eine Beeinträchtigung der Glykokalyx eine kausale Rolle spielen. In diesem Sinn konnte in einer Vorarbeit gezeigt werden, dass Kinder, die sich einer Herzoperation an der HLM unterziehen, erhöhte Spiegel von Hyaluronsäure und Syndecan-1, zwei wesentlichen Bestandteilen der Glykokalyx, im Blut aufweisen, welche mit dem Ausmaß der ischämischen Belastung korrelierten (Bruegger et al. 2015). Diese Studie und vergleichbare Studien an erwachsenen Patienten (Rehm et al. 2007) sind ein indirekter Beleg dafür, dass es im Rahmen der Herz-Lungen-Maschine zu einem Shedding der Glykokalyx kommt. Inwiefern es sich hierbei um ein lokal begrenztes Phänomen handelt, welches sich primär auf die Organe beschränkt, die während der HLM einer Ischämie ausgesetzt waren, oder um globale Veränderungen kann anhand der Studien nicht hinreichend beantwortet werden. Ebenso wenig erlauben die Untersuchungen einen Rückschluss auf den Zustand der Glykokalyx auf Einzelgefäßbasis.

Aus diesem Grund war es das Ziel dieser Studie zu untersuchen, wie sich Operationen an der HLM bei Kindern mit angeborenen Herzfehlern auf die Mikrozirkulation und die mikrovaskuläre Glykokalyx auswirken und inwieweit mögliche Veränderungen mit dem postoperativen Outcome der Kinder korrelieren.

Ergebnisse:

Die Messungen erfolgten an der Ohrmuschel mittels SDF-Imaging und speziellen Softwareprogrammen zur Quantifizierung von Parametern der Mikrozirkulation sowie der mikrovaskulären Glykokalyx. Insgesamt wurden 36 Kinder mit angeborenem Herzfehler und Operation an der HLM an vier Zeitpunkten untersucht (T0: präoperativ, T1: unmittelbar postoperativ, T2: 24h postoperativ und T3: 7d postoperativ). Als Kontrollen dienten Kinder, die sich kleineren herzchirurgischen Eingriffen ohne HLM unterzogen (n = 4), Kinder vor und nach diagnostischem Herzkatheter (n = 6) und Kinder vor und nach operativem Verschluss einer Lippen-Kiefer-Gaumenspalte (n = 9). Die Gruppen unterschieden sich nicht signifikant in Alter, Gewicht und Geschlecht. Das postoperative Outcome wurde anhand der Entwicklung eines Kapillarlecksyndroms sowie dem postoperativem Beatmungs- und Katecholaminbedarf beurteilt. Die Messungen lieferten zusammengefasst folgende Ergebnisse:

1) Nach Operation an der HLM kommt es vorübergehend zu einer signifikanten Zunahme der sog. Perfused Boundary Region (PBR) als Surrogat für die Glykokalyxdicke, entsprechend einem Glykokalyxverlust von ~190 nm. Im Gegensatz dazu zeigten die Kontrollgruppen keine Veränderung der PBR (Abb. 13 A,B)
2) Der Glykokalyxverlust besteht auch bei Kindern, die einen Eingriff an der HLM ohne Unterbrechung des Kreislaufs erhielten (sog. heart beating Kondition) und somit keiner Organischämie ausgesetzt waren (Abb. 13 C)

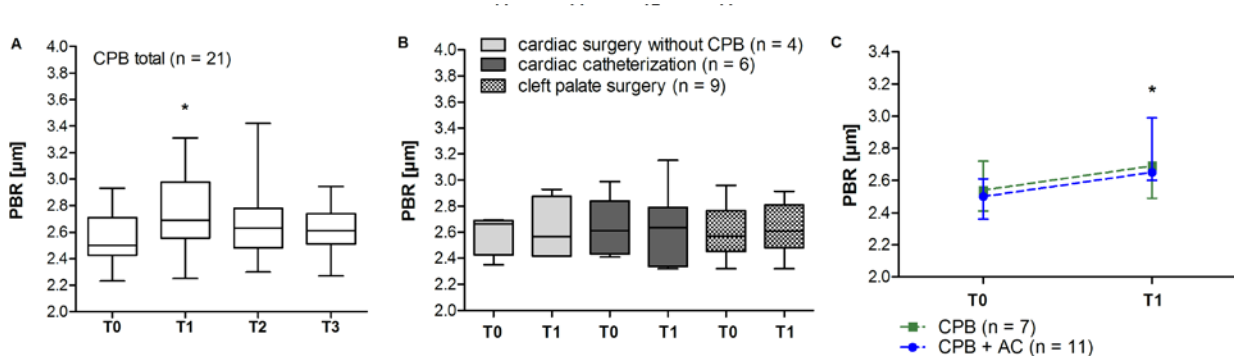

Abb. 13): Auswirkung der Herz-Lungen-Maschine auf die Glykokalyx. Als Surrogat für die Glykokalyxdicke wurde die Perfused Boundary Region (PBR) gemessen. Eine Zunahme der PBR entspricht einem Abbau der funktionellen Glykokalyx. A) PBR-Verlauf bei allen Kindern mit Operationen an der HLM (= CPB; cardiopulmonary bypass). B) prä- und postoperative PBR in den Kontrollgruppen. C) HLM-Subgruppenanalyse. In grün sind Kinder mit HLM ohne Kreislaufunterbrechung (CPB), in blau Kinder mit HLM und Abklemmen der Aorta (CPB + AC) dargestellt. * $p < 0.05$

3) Nach Operationen an der HLM kommt es zu einer akuten, signifikanten Reduktion des mikrozirkulatorischen Flussindex und der Dichte perfundierter Gefäße, welche invers mit der HLM-Dauer und dem Ausmaß der Ischämie korreliert. Kinder mit herzchirurgischen Eingriffen ohne HLM wiesen eine ähnliche Tendenz auf, während in den anderen Kontrollgruppen keine Veränderungen beobachtet wurden.
4) Der postoperative Beatmungs- und Katecholaminbedarf korreliert mit der HLM-Dauer, es besteht aber kein signifikanter Zusammenhang mit der Perfused Boundary Region oder Parametern der mikrozirkulatorischen Perfusion. Bei insgesamt geringer Rate eines relevanten Kapillarlecksyndroms (n = 4) war eine diesbezügliche Stratifizierung der experimentellen Daten nicht möglich.

Diskussion:

Die Arbeit zeigt erstmalig eine akute Reduktion der endothelialen Glykokalyx und der mikrozirkulatorischen Perfusion auf Einzelgefäßbasis bei Kindern nach Operationen an der Herz-Lungen-Maschine. Die Ergebnisse bestätigen und erweitern frühere Studien, welche indirekte Hinweise auf eine HLM-assoziierte Schädigung der Glykokalyx lieferten (Bruegger et al. 2015; Rehm et al. 2007). Bisherige Daten deuteten darauf hin, dass Ischämie/Reperfusion die wesentliche Ursache für die HLM-assoziierte Glykokalyxschädigung ist (Bruegger et al. 2015). Dagegen demonstrieren die aktuellen Messungen, dass es auch in Regionen (Ohrmuschel), die nicht unmittelbar einer Ischämie während der HLM ausgesetzt sind, zu einem Abbau der Glykokalyx kommt. Somit scheint es sich -zumindest teilweise- um ein systemisches Phänomen zu handeln, das nicht alleine durch Ischämie/Reperfusion erklärt werden kann. Mögliche Faktoren, die zur Glykokalyxschädigung beitragen, sind der Kontakt mit Fremdoberflächen, veränderte Blutflussbedingungen und die Manipulation der großen Gefäße während der HLM (Bruegger et al. 2011; Murphy and Angelini 2004). Zudem zeigt der Vergleich von Erwachsenen, die eine Bypass-Operation mit und ohne HLM erhielten, dass der Eingriff selbst zu einer Schädigung der Glykokalyx führen kann (Bruegger et al. 2011; Svennevig et al. 2008; Bruegger et al. 2009). Ein solcher Vergleich ist bei Kindern unmöglich, da die operative Versorgung angeborener Herzfehler fast immer den Einsatz einer HLM benötigt. Die Analyse von vier Kindern mit kleineren herzchirurgischen Eingriffen ohne HLM zeigte keine signifikante Beeinträchtigung der Glykokalyx, allerdings ist die Aussagekraft der Daten aufgrund der kleinen Fallzahl und der unterschiedlichen Operationstechniken deutlich eingeschränkt.

Der Nachweis einer akuten Verminderung der mikrozirkulatorischen Perfusion nach HLM stimmt mit Berichten von erwachsenen Patienten überein, welche eine transiente Reduktion der

Durchblutung in der sublingualen Mikrozirkulation während und nach der HLM darstellten (De Backer et al. 2013; Koning et al. 2014). Interessanterweise war in der vorliegenden Arbeit das Ausmaß der Perfusionsminderung abhängig vom HLM-Protokoll, wobei Kinder mit HLM und hypothermem Kreislaufstillstand die stärkste Beeinträchtigung zeigten und Kinder mit HLM unter sog. heart beating Konditionen die geringste. Hierfür könnten neben der unterschiedlichen ischämischen Belastung und Temperaturunterschieden auch veränderte Blutflussbedingungen verantwortlich sein. So bleibt bei „heart beating“ Konditionen ein pulsatiler Fluss erhalten, während bei Operationen, in denen die Aorta abgeklemmt wird, ein kontinuierliches Flussmuster von der HLM erzeugt wird. Studien, welche eine pulsatile vs. kontinuierliche HLM verglichen, zeigten, dass die mikrovaskuläre Perfusion unter pulsatilem Fluss signifikant und nachhaltig verbessert war (Koning et al. 2012; O'Neil et al. 2012).

Die Relevanz dieser Ergebnisse zeigt sich bei Patienten mit Sepsis und kardiogenem Schock, bei denen eine gestörte Perfusion der Mikrozirkulation mit dem Auftreten von Organdysfunktion und Mortalität korrelierte (De Backer et al. 2004; Trzeciak et al. 2007). Obwohl in der vorliegenden Arbeit keine Korrelation der experimentellen Daten mit Parametern des klinischen Outcome wie Katecholamin- oder Beatmungsbedarf bestand, ist ein Zusammenhang nicht ausgeschlossen, da die Rate von Komplikationen in der untersuchten Kohorte insgesamt niedrig war und somit für diese Fragestellung keine ausreichende statistische Teststärke bestand. Zur Klärung eines kausalen Zusammenhangs zwischen Veränderungen der Mikrozirkulation und der Entstehung postoperativer Komplikationen sind daher größer angelegte Studien notwendig.

Zusammenfassend zeigen die Untersuchungen, dass ein Nachweis akuter HLM-assoziierter Veränderungen der Mikrozirkulation und der mikrovaskulären Glykokalyx mittels SDF-Imaging ohne wesentliche Belastung der Kinder möglich ist. Erst kürzlich wurden diese Ergebnisse auch für erwachsene Patienten reproduziert (Koning et al. 2016). Ein Monitoring der Mikrozirkulation könnte somit einen vielversprechenden Ansatz darstellen zur postoperativen Überwachung und zur Evaluation von Therapiestrategien, welche auf die Reduktion von Komplikationen nach HLM abzielen.

V) Zusammenfassung und Ausblick

Das vorliegende Habilitationsprojekt beschäftigt sich mit Studien zu verschiedenen Aspekten der Mikrozirkulation im Rahmen von Entzündung, Entwicklung und Erkrankung. Hierbei wurden drei Themenkomplexe bearbeitet: i) grundlegende Mechanismen, welche die Rekrutierung von Leukozyten im Rahmen inflammatorischer Prozesse steuern ii) Regulation der Rekrutierung von Leukozyten und Thrombozyten im Verlauf der fetalen Entwicklung und iii) Veränderungen der Mikrozirkulation bei Kindern im Rahmen ausgewählter Krankheiten. Grundlage für die Arbeit ist das zunehmende Wissen um die essentielle Bedeutung der Mikrozirkulation für die Funktion des gesamten Organismus und damit einhergehend die Rolle von Störungen der Mikrozirkulation bei der Krankheitsentstehung.

Eine wesentliche Funktion der Mikrozirkulation ist die Gewährleistung einer adäquaten Immunantwort. Hierzu ist es notwendig, dass Zellen des Immunsystems aus dem Gefäßsystem in entzündlich verändertes Gewebe auswandern, um dort ihrer jeweiligen Funktion nachzugehen. Dieser als Leukozytenrekrutierung bezeichnete Prozess ist hoch komplex und wird durch unzählige Faktoren beeinflusst und reguliert, die nach wie vor nur unvollständig verstanden werden. Ziel der Untersuchungen im ersten Themenkomplex war es daher weitere Erkenntnisse über die Regulation der Leukozytenrekrutierung *in vivo* zu erlangen. Zu diesem Zweck wurden die einzelnen Schritte der Rekrutierungskaskade im murinen Modell unter Einsatz genveränderter Tiere sowie verschiedener pharmakologischer Substanzen untersucht und durch *in vitro* Analysen ergänzt. Anhand dieser Untersuchungen konnte eine bislang unbekannte Funktion des Enzyms Myeloperoxidase (MPO) bei der Rekrutierung neutrophiler Granulozyten nachgewiesen werden. So zeigte sich, dass MPO die Adhäsion von Granulozyten an der Gefäßwand und die gerichtete (Trans-) Migration fördert, indem es die repulsiven Kräfte zwischen Endothel und Zelloberfläche vermindert. Dieser Effekt konnte auf die stark kationische Ladung von MPO zurückgeführt werden und war unabhängig von dessen katalytischer Aktivität. Die Ergebnisse verleihen MPO eine neue Bedeutung im Rahmen der angeborenen Immunantworten, indem es die Rekrutierung von Granulozyten und vermutlich auch anderer Immunzellen erleichtert und potenziert. Während dieser Mechanismus bei der Abwehr pathogener Erreger sinnvoll erscheint, könnte er durch Unterhaltung einer inflammatorischen Reaktion auch zur Pathogenese entzündlicher Erkrankungen beitragen. Somit liefern die Ergebnisse Impulse für die Entwicklung neuer anti-inflammatorischer Therapiestrategien. In einer weiteren Studie wurde die Bedeutung des Lipidmediators Sphingosin-1-Phosphat (S1P) für das Leukozytenrollen genauer untersucht. Bislang war bekannt, dass S1P ein wichtiger Regulator des Immunsystems ist und dieses auf vielfache Weise beeinflusst. Die Daten

zur Rolle von S1P und seinen Rezeptoren im Rahmen der Rekrutierung von Zellen der angeborenen Immunität sind jedoch widersprüchlich. Die vorliegende Arbeit konnte zeigen, dass S1P das P-Selektin abhängige Rollen von neutrophilen Granulozyten *in vivo* über verschiedene Rezeptoren differentiell reguliert. Hierbei bewirkt es sowohl direkt als auch indirekt als Mediator anderer Roll-Agonisten über den S1P-Rezeptor Typ 3 eine rasche P-Selektin Mobilisation aus Endothelzellen und induziert so Rollen. In diesem Zusammenhang wurde ein neuer cAMP-abhängiger Signalweg identifiziert, welcher über Aktivierung der Sphingosinkinase 1 und Bildung von S1P zur raschen Freisetzung von P-Selektin führt. Im Gegensatz dazu entfaltet S1P über den S1P-Rezeptor Typ 1 eine hemmende Wirkung auf das Rollen. Diese Befunde verdeutlichen die Komplexität der Immunregulation durch S1P und bieten eine mögliche Erklärung für die kontroversen Ergebnisse früherer Studien. Zusammengefasst liefern die dargestellten Arbeiten somit neue Erkenntnisse zu den vielschichtigen Mechanismen und Regulatoren der Leukozytenrekrutierung *in vivo*.

Der zweite Teil des Habilitationsprojektes beschäftigt sich mit der Rekrutierung von Leukozyten und Thrombozyten im Rahmen der fetalen Entwicklung. Anlass für die Untersuchungen ist die Tatsache, dass das bisherige Wissen über diese Prozesse fast ausschließlich aus Untersuchungen am adulten Organismus stammt, während bislang nur sehr wenig über die Situation im sich entwickelnden Fetus und Neugeborenen bekannt ist. Um dieser Frage nachzugehen wurden statische und dynamische Untersuchungen humaner Granulozyten und Endothelzellen aus dem Nabelschnurblut von früh- und reifgeborenen Neonaten, sowie *in vivo* Untersuchungen an einem neuartigen Modell zur intravitalmikroskopischen Analyse der murinen fetalen Mikrozirkulation durchgeführt. Anhand dieser Untersuchungen wurde demonstriert, dass die Fähigkeit zur Rekrutierung neutrophiler Granulozyten bei humanen Neonaten einem ontogenetischen Reifungsprozess unterliegt und bei extrem Frühgeborenen massiv herabgesetzt ist, wobei selbst Reifgeborene nicht das Niveau von Erwachsenen erreichen. Hierbei konnten sowohl funktionelle Defizite der Granulozyten als auch der Endothelzellen aufgezeigt werden. Die *in vivo*-Gültigkeit dieser Ergebnisse wurde im murinen fetalen Modell bestätig. Die Arbeit trägt somit zum besseren Verständnis der ontogenetischen Regulation angeborener Immunfunktionen bei als Grundlage für die Entwicklung innovativer Therapieansätze zur Behandlung und Prävention neonataler Infektionen. Dies ist insbesondere im Hinblick auf die steigenden Überlebenschancen immer unreiferer Frühgeborener, welche in höchstem Maße von lebensbedrohlichen Infektionen gefährdet sind, von großer klinischer Bedeutung. Neben der funktionellen Reifung der Leukozytenrekrutierung im Verlauf der fetalen Entwicklung konnte in einer nachfolgenden Studie auch ein ontogenetischer Reifungsprozess der Thrombozytenrekrutierung aufgezeigt werden. Hierbei wurde erstmalig *in vivo* gezeigt, dass die adhäsive und aggregatorische Kapazität fetaler

Thrombozyten vom Gestationsalter abhängt, wobei die Fähigkeit zur Ausbildung eines stabilen Thrombus erst gegen Ende der Gestation erworben wird. Ursächlich hierfür scheinen sowohl quantitative als auch qualitative Veränderungen fetaler Thrombozyten zu sein. Zusätzliche Transfusionsexperimente weisen darauf hin, dass diese Veränderungen durch Einbringen adulter Thrombozyten in den fetalen Kreislauf kompensiert werden können. Die Indikation zur Transfusion adulter Thrombozyten, insbesondere bei extremen Frühgeborenen, sollte jedoch kritisch geprüft werden, da es Hinweise auf eine vermehrte Aktivierung und Aggregation adulter Thrombozyten durch fetales Plasma gibt.

Wie auch bei der Leukozytenrekrutierung erlangen diese Ergebnisse insbesondere im Rahmen von Frühgeburtlichkeit klinische Relevanz. In diesem Zusammenhang wurde berichtet, dass Thrombozyten eine funktionelle Rolle beim postnatalen Verschluss des Ductus arteriosus spielen. Die Persistenz des Ductus arteriosus (PDA) ist eine typische Komplikation bei Frühgeborenen und korreliert invers mit dem Gestationsalter. Basierend auf den Ergebnissen der Transfusionsexperimente wurde daher in einer retrospektiven Datenanalyse die Auswirkung einer Thrombozytentransfusion bei Frühgeborenen mit Thrombozytopenie und PDA untersucht. Diese ergab jedoch keinen Hinweis auf einen positiven Effekt einer Thrombozytentransfusion auf die medikamentöse Verschlussrate eines PDA, so dass die Rolle von Plättchen in diesem Prozess kontrovers bleibt. Die Ergebnisse müssen aber aufgrund einer möglichen Beeinflussung durch Faktoren wie die Größe des PDA, der Zeitpunkt des Therapiebeginns sowie Unterschiede im Hämatokrit und möglicherweise in plasmatischen Gerinnungsfaktoren mit Vorsicht interpretiert werden. Zur weiteren Klärung der Nutzen und Risiken von Thrombozytentransfusionen bei Frühgeborenen sind daher größer angelegte, prospektive Studien notwendig.

Im dritten Teil des Habilitationsprojektes wurden mithilfe von Videomikroskopie-Technik und spezieller Computerprogramme Veränderungen der Mikrozirkulation bei Kindern mit ausgewählten Krankheitsbildern analysiert. Diesen klinisch-experimentellen Untersuchungen liegt die Beobachtung zugrunde, dass viele Krankheitsbilder oder Folgeerkrankungen derselben auf Störungen der Mikrozirkulation beruhen. Dabei wird davon ausgegangen, dass vaskuläre Veränderungen im Rahmen chronischer Erkrankungen häufig schon im Kindesalter ihren Ausgang nehmen. Studien, die dieser Hypothese nachgehen, sind jedoch selten. Aus diesem Grund wurde in einer ersten Arbeit die Mikrozirkulation von Kindern mit Typ 1 Diabetes mellitus (T1DM) untersucht, da hier vaskuläre Folgeerkrankungen im Erwachsenenalter typisch sind. Die Untersuchungen belegen, dass bereits im Kindesalter bei Patienten mit T1DM messbare Veränderungen der Mikrozirkulation mit Verlust der endothelialen Glykokalyx und relativer Verminderung der Anzahl von Kapillaren bestehen. Diese mikroskopischen Veränderungen waren

bereits zu einem Zeitpunkt nachweisbar, an dem bei den Routine-Screeninguntersuchungen zum Nachweis einer Mikroangiopathie noch keine auffälligen Befunde vorlagen. Ein mikrozirkulatorisches Monitoring eignet sich somit möglicherweise zur frühzeitigeren Identifikation von Patienten mit hohem Risiko für vaskuläre Komplikationen. Zudem zeigten die Untersuchungen eine inverse Korrelation der Glykokalyxdicke mit dem Blutzuckerspiegel und weisen so auf die pathogenetische Rolle erhöhter Blutzuckerspiegel hin. Die Ergebnisse betonen somit die Bedeutung von Maßnahmen zur Blutzuckerkontrolle bei Kindern mit T1DM und identifizieren die endotheliale Glykokalyx als mögliches Ziel präventiver Therapieansätze.

Veränderungen der Mikrozirkulation treten aber nicht nur bei chronischen Erkrankungen auf, sondern kennzeichnen auch akute Krankheitszustände wie z.B. eine Sepsis oder einen kardiogenen Schock. Von Studien an Erwachsenen ist bekannt, dass das Ausmaß von Mikrozirkulationsstörungen direkt mit der Prognose dieser Patienten korreliert. Operationen an der Herz-Lungen-Maschine (HLM) führen ebenfalls zu einer akuten Beeinträchtigung der Mikrozirkulation, wobei vorausgegangene Arbeiten indirekte Hinweise auf eine HLM-assoziierte Schädigung der endothelialen Glykokalyx ergaben. Um diesem Befund nachzugehen wurden daher in einer weiteren Studie die Mikrozirkulation und die mikrovaskuläre Glykokalyx von Kindern nach herzchirurgischen Eingriffen an der HLM untersucht. Hierbei konnten erstmalig auf mikrovaskulärer Ebene ein passagerer Abbau der endothelialen Glykokalyx sowie eine Reduktion der Perfusion bei Kindern nach Operationen an der HLM nachgewiesen werden. Diese Veränderungen scheinen zumindest zum Teil unabhängig von der ischämischen Belastung während der Operation zu sein und beruhen möglicherweise auf Faktoren wie dem Kontakt mit Fremdoberflächen und veränderten Blutflussbedingungen während der HLM. Zukünftige Forschungsprojekte sollten klären, inwiefern sich ein Monitoring der Mikrozirkulation eignet zur Vorhersage postoperativer Komplikationen und zur Überwachung von Interventionen, welche eine Reduktion solcher Komplikationen zum Ziel haben.

VI) Übersicht der themenrelevanten Publikationen

VIa) Originalarbeiten als Erstautor

Teil 1 des Habilitationsprojektes:

Nussbaum C et al.: Sphingosine-1-phosphate receptor 3 promotes leukocyte rolling by mobilizing endothelial P-selectin. Nat Commun 2015; 6:6416. **(IF 11,47)**

Klinke A, **Nussbaum C** (both authors contributed equally) et al.: Myeloperoxidase attracts neutrophils by physical forces. Blood 2011; 117(4):1350-8. **(IF 9,898)**

Teil 2 des Habilitationsprojektes:

Margraf A, **Nussbaum C** (both authors contributed equally) et al.: Maturation of Platelet Function During Murine Fetal Development In Vivo. Arterioscler Thromb Vasc Biol. 2017; Apr 20. Epub ahead of print. **(IF 5,96)**

Nussbaum C et al.: Neutrophil and endothelial adhesive function during human fetal ontogeny. J Leukoc Biol 2013; 93(2):175-84. **(IF 4,304)**

Teil 3 des Habilitationsprojektes:

Nussbaum C et al.: Early microvascular changes with loss of the glycocalyx in children with type 1 diabetes. J Pediatr 2014; 164(3):584-9. **(IF 3,79)**

Nussbaum C et al.: Perturbation of the microvascular glycocalyx and perfusion in infants after cardiopulmonary bypass. J Thorac Cardiovasc Surg 2015; 150(6):1474-81. **(IF 4,168)**

VIb) Originalarbeiten als Koautor

Teil 1 des Habilitationsprojektes:

Kurz AR, Pruenster M, Rohwedder I, Ramadass M, Schäfer K, Harrison U, Gouveia G, **Nussbaum C** et al.: MST1-dependent vesicle trafficking regulates neutrophil transmigration through the vascular basement membrane. J Clin Invest 2016; 126(11):4125-4139. **(IF 12,575)**

Pruenster M, Kurz AR, Chung KJ, Cao-Ehlker X, Bieber S, **Nussbaum CF** et al.: Extracellular MRP8/14 is a regulator of β2 integrin-dependent neutrophil slow rolling and adhesion. Nat Commun 2015; 6:6915. **(IF 11,47)**

Jakob SM, Pick R, Brechtefeld D, **Nussbaum C** et al: Hematopoietic progenitor kinase 1 (HPK1) is required for LFA-1-mediated neutrophil recruitment during the acute inflammatory response. Blood 2013; 121(20):4184-94. **(IF 9,775)**

Yang WH, **Nussbaum C** et al.: Coordinated roles of ST3Gal-VI and ST3Gal-IV sialyltransferases in the synthesis of selectin ligands. M. Blood 2012; 120(5):1015-26. **(IF 9,06)**

Gambardella L, Anderson KE, **Nussbaum C** et al.: The GTPase-activating protein ARAP3 regulates chemotaxis and adhesion-dependent processes in neutrophils. Blood 2011; 118(4):1087-98. **(IF 9,898)**

Teil 2 des Habilitationsprojektes:

Sperandio M, Quackenbush EJ, Sushkova N, Altstätter J, **Nussbaum C** et al.: Ontogenetic regulation of leukocyte recruitment in mouse yolk sac vessels. Blood 2013; 121(21):e118-28. **(IF 9,775)**

Marcos V, **Nussbaum C** et al.: Delayed but functional neutrophil extracellular trap formation in neonates. Blood 2009; 114(23):4908-11. **(IF 10,555)**

Teil 3 des Habilitationsprojektes:

Bruegger D, Brettner F, Rossberg I, **Nussbaum C** et al.: Acute degradation of the endothelial glycocalyx in infants undergoing cardiac surgical procedures. Ann Thorac Surg 2015; 99(3):926-31. IF **(IF 3,849)**

Weidlich K, Kroth J, **Nussbaum C** et al.: Changes in microcirculation as early markers for infection in preterm infants--an observational prospective study. Pediatr Res 2009; 66(4):461-5. **(IF 2,607)**

Kroth J, Weidlich K, Hiedl S, **Nussbaum C** et al.: Functional vessel density in the first month of life in preterm neonates. Pediatr Res 2008; 64(5):567-71. **(IF 2,604)**

VIc) Übersichtsarbeiten

Nussbaum C et al.: Myeloperoxidase: a leukocyte-derived protagonist of inflammation and cardiovascular disease. Antioxid Redox Signal 2013; 18(6):692-713. **(IF 7,667)**

Nussbaum C, Sperandio M.: Innate immune cell recruitment in the fetus and neonate. J Reprod Immunol 2011; 90(1):74-81. **(IF 2,966)**

VII) Abkürzungsverzeichnis

AC: Aortic clamping

ABAH: Aminobenzoic acid hydrazide

ADP: Adenosindiphosphat

AGEs: Advanced glycation end products

ATP: Adenosintriphosphat

BMI: Body-Mass-Index

cAMP: Cyklisches Adenosinmonophosphat

CD: Cluster of differentiation

CPB: Cardiopulmonary bypass

CXCR1: CXC-Motiv-Chemokinrezeptor 1

eNOS: endotheliale NO-Synthase

ESL: Endothelial surface layer

FITC: Fluoresceinisothiocyanat

FVD: Functional vessel density

GP: Glykoprotein

GTP: Guanosintriphosphat

HLM: Herz-Lungen-Maschine

HUVEC: Human umbilical vein endothelial cells

HSA: Humanes Serumalbumin

ICAM-1: Intercellular adhesion molecule 1

IL-8: Interleukin-8

LFA-1: Lymphocyte function-associated antigen 1

LPS: Lipopolysaccharid

Mac-1: Macrophage-1 antigen

MPO: Myeloperoxidase

NO: Stickstoffmonoxid

OPS: Orthogonal Polarization Spectral

PBR: Perfused Boundary Region

PDA: Persistierender Ductus arteriosus

PLC: Phospholipase C

PMN: Polymorphkernige Neutrophile

PSGL-1: P-selectin glycoprotein ligand-1

SDF: Sidestream Dark Field

S1P: Sphingosin-1-Phosphat

SSW: Schwangerschaftswochen

T1DM: Typ 1 Diabetes mellitus

TNF: Tumornekrosefaktor

TVD: Total vessel density

VCAM-1: Vascular cell adhesion protein 1

vWF: von-Willebrand-Faktor

VIII) Literaturverzeichnis

Abbassi, O., T. K. Kishimoto, L. V. McIntire, D. C. Anderson, and C. W. Smith. 1993. 'E-selectin supports neutrophil rolling in vitro under conditions of flow', *J Clin Invest*, 92: 2719-30.

Ait-Oufella, H., E. Maury, S. Lehoux, B. Guidet, and G. Offenstadt. 2010. 'The endothelium: physiological functions and role in microcirculatory failure during severe sepsis', *Intensive Care Med*, 36: 1286-98.

Algenstaedt, P., C. Schaefer, T. Biermann, A. Hamann, B. Schwarzloh, H. Greten, W. Ruther, and N. Hansen-Algenstaedt. 2003. 'Microvascular alterations in diabetic mice correlate with level of hyperglycemia', *Diabetes*, 52: 542-9.

Anderson, D. C., O. Abbassi, T. K. Kishimoto, J. M. Koenig, L. V. McIntire, and C. W. Smith. 1991. 'Diminished lectin-, epidermal growth factor-, complement binding domain-cell adhesion molecule-1 on neonatal neutrophils underlies their impaired CD18-independent adhesion to endothelial cells in vitro', *J Immunol*, 146: 3372-9.

Anderson, D. C., K. L. Freeman, B. Heerdt, B. J. Hughes, R. M. Jack, and C. W. Smith. 1987. 'Abnormal stimulated adherence of neonatal granulocytes: impaired induction of surface Mac-1 by chemotactic factors or secretagogues', *Blood*, 70: 740-50.

Aoki, M., H. Aoki, R. Ramanathan, N. C. Hait, and K. Takabe. 2016. 'Sphingosine-1-Phosphate Signaling in Immune Cells and Inflammation: Roles and Therapeutic Potential', *Mediators Inflamm*, 2016: 8606878.

Askari, A. T., M. L. Brennan, X. Zhou, J. Drinko, A. Morehead, J. D. Thomas, E. J. Topol, S. L. Hazen, and M. S. Penn. 2003. 'Myeloperoxidase and plasminogen activator inhibitor 1 play a central role in ventricular remodeling after myocardial infarction', *J Exp Med*, 197: 615-24.

Babar, G. S., H. Zidan, M. E. Widlansky, E. Das, R. G. Hoffmann, M. Daoud, and R. Alemzadeh. 2011. 'Impaired endothelial function in preadolescent children with type 1 diabetes', *Diabetes Care*, 34: 681-5.

Bagher, P., and S. S. Segal. 2011. 'Regulation of blood flow in the microcirculation: role of conducted vasodilation', *Acta Physiol (Oxf)*, 202: 271-84.

Baldus, S., J. P. Eiserich, A. Mani, L. Castro, M. Figueroa, P. Chumley, W. Ma, A. Tousson, C. R. White, D. C. Bullard, M. L. Brennan, A. J. Lusis, K. P. Moore, and B. A. Freeman. 2001. 'Endothelial transcytosis of myeloperoxidase confers specificity to vascular ECM proteins as targets of tyrosine nitration', *J Clin Invest*, 108: 1759-70.

Baldus, S., V. Rudolph, M. Roiss, W. D. Ito, T. K. Rudolph, J. P. Eiserich, K. Sydow, D. Lau, K. Szocs, A. Klinke, L. Kubala, L. Berglund, S. Schrepfer, T. Deuse, M. Haddad, T. Risius, H. Klemm, H. C. Reichenspurner, T. Meinertz, and T. Heitzer. 2006. 'Heparins increase endothelial nitric oxide bioavailability by liberating vessel-immobilized myeloperoxidase', *Circulation*, 113: 1871-8.

Bednarek, F. J., S. Bean, M. R. Barnard, A. L. Frelinger, and A. D. Michelson. 2009. 'The platelet hyporeactivity of extremely low birth weight neonates is age-dependent', *Thromb Res*, 124: 42-5.

Bennett, J. S. 2005. 'Structure and function of the platelet integrin alphaIIbbeta3', *J Clin Invest*, 115: 3363-9.

Bevilacqua, M. P., J. S. Pober, D. L. Mendrick, R. S. Cotran, and M. A. Gimbrone, Jr. 1987. 'Identification of an inducible endothelial-leukocyte adhesion molecule', *Proc Natl Acad Sci U S A*, 84: 9238-42.

Boerma, E. C., M. Koopmans, A. Konijn, K. Kaiferova, A. J. Bakker, E. N. van Roon, H. Buter, N. Bruins, P. H. Egbers, R. T. Gerritsen, P. M. Koetsier, W. P. Kingma, M. A. Kuiper, and C. Ince. 2010. 'Effects of nitroglycerin on sublingual microcirculatory blood flow in patients with severe sepsis/septic shock after a strict resuscitation protocol: a double-blind randomized placebo controlled trial', *Crit Care Med*, 38: 93-100.

Bolick, D. T., S. Srinivasan, K. W. Kim, M. E. Hatley, J. J. Clemens, A. Whetzel, N. Ferger, T. L. Macdonald, M. D. Davis, P. S. Tsao, K. R. Lynch, and C. C. Hedrick. 2005. 'Sphingosine-1-phosphate prevents tumor necrosis factor-{alpha}-mediated monocyte adhesion to aortic endothelium in mice', *Arterioscler Thromb Vasc Biol*, 25: 976-81.

Broekhuizen, L. N., B. A. Lemkes, H. L. Mooij, M. C. Meuwese, H. Verberne, F. Holleman, R. O. Schlingemann, M. Nieuwdorp, E. S. Stroes, and H. Vink. 2010. 'Effect of sulodexide on endothelial glycocalyx and vascular permeability in patients with type 2 diabetes mellitus', *Diabetologia*, 53: 2646-55.

Brower, J. B., J. H. Targovnik, M. R. Caplan, and S. P. Massia. 2010. 'High glucose-mediated loss of cell surface heparan sulfate proteoglycan impairs the endothelial shear stress response', *Cytoskeleton (Hoboken)*, 67: 135-41.

Brownlee, M. 2001. 'Biochemistry and molecular cell biology of diabetic complications', *Nature*, 414: 813-20.

Bruegger, D., F. Brettner, I. Rossberg, C. Nussbaum, C. Kowalski, K. Januszewska, B. F. Becker, and D. Chappell. 2015. 'Acute degradation of the endothelial glycocalyx in infants undergoing cardiac surgical procedures', *Ann Thorac Surg*, 99: 926-31.

Bruegger, D., M. Rehm, J. Abicht, J. O. Paul, M. Stoeckelhuber, M. Pfirrmann, B. Reichart, B. F. Becker, and F. Christ. 2009. 'Shedding of the endothelial glycocalyx during cardiac surgery: on-pump versus off-pump coronary artery bypass graft surgery', *J Thorac Cardiovasc Surg*, 138: 1445-7.

Bruegger, D., L. Schwartz, D. Chappell, M. Jacob, M. Rehm, M. Vogeser, F. Christ, B. Reichart, and B. F. Becker. 2011. 'Release of atrial natriuretic peptide precedes shedding of the endothelial glycocalyx equally in patients undergoing on- and off-pump coronary artery bypass surgery', *Basic Res Cardiol*, 106: 1111-21.

Camerer, E., J. B. Regard, I. Cornelissen, Y. Srinivasan, D. N. Duong, D. Palmer, T. H. Pham, J. S. Wong, R. Pappu, and S. R. Coughlin. 2009. 'Sphingosine-1-phosphate in the plasma compartment regulates basal and inflammation-induced vascular leak in mice', *J Clin Invest*, 119: 1871-9.

Chappell, D., M. Westphal, and M. Jacob. 2009. 'The impact of the glycocalyx on microcirculatory oxygen distribution in critical illness', *Curr Opin Anaesthesiol*, 22: 155-62.

Chien, S. 2007. 'Mechanotransduction and endothelial cell homeostasis: the wisdom of the cell', *Am J Physiol Heart Circ Physiol*, 292: H1209-24.

Cleator, J. H., W. Q. Zhu, D. E. Vaughan, and H. E. Hamm. 2006. 'Differential regulation of endothelial exocytosis of P-selectin and von Willebrand factor by protease-activated receptors and cAMP', *Blood*, 107: 2736-44.

Clemetson, K. J. 2012. 'Platelets and primary haemostasis', *Thromb Res*, 129: 220-4.

Colbert, J. F., and E. P. Schmidt. 2016. 'Endothelial and Microcirculatory Function and Dysfunction in Sepsis', *Clin Chest Med*, 37: 263-75.

Constantinescu, A. A., H. Vink, and J. A. Spaan. 2003. 'Endothelial cell glycocalyx modulates immobilization of leukocytes at the endothelial surface', *Arterioscler Thromb Vasc Biol*, 23: 1541-7.

Cooke, J. P. 2000. 'The endothelium: a new target for therapy', *Vasc Med*, 5: 49-53.

Daneman, D. 2006. 'Type 1 diabetes', *Lancet*, 367: 847-58.

Davis, M. J. 2012. 'Perspective: physiological role(s) of the vascular myogenic response', *Microcirculation*, 19: 99-114.

De Backer, D., J. Creteur, M. J. Dubois, Y. Sakr, and J. L. Vincent. 2004. 'Microvascular alterations in patients with acute severe heart failure and cardiogenic shock', *Am Heart J*, 147: 91-9.

De Backer, D., K. Donadello, Y. Sakr, G. Ospina-Tascon, D. Salgado, S. Scolletta, and J. L. Vincent. 2013. 'Microcirculatory alterations in patients with severe sepsis: impact of time of assessment and relationship with outcome', *Crit Care Med*, 41: 791-9.

De Backer, D., G. Ospina-Tascon, D. Salgado, R. Favory, J. Creteur, and J. L. Vincent. 2010. 'Monitoring the microcirculation in the critically ill patient: current methods and future approaches', *Intensive Care Med*, 36: 1813-25.

de Wit, C., B. Hoepfl, and S. E. Wolfle. 2006. 'Endothelial mediators and communication through vascular gap junctions', *Biol Chem*, 387: 3-9.

Del Vecchio, A., G. Latini, E. Henry, and R. D. Christensen. 2008. 'Template bleeding times of 240 neonates born at 24 to 41 weeks gestation', *J Perinatol*, 28: 427-31.

den Uil, C. A., K. Caliskan, W. K. Lagrand, M. van der Ent, L. S. Jewbali, J. P. van Kuijk, P. E. Spronk, and M. L. Simoons. 2009. 'Dose-dependent benefit of nitroglycerin on microcirculation of patients with severe heart failure', *Intensive Care Med*, 35: 1893-9.

Donati, A., E. Damiani, R. Domizi, R. Romano, E. Adrario, P. Pelaia, C. Ince, and M. Singer. 2013. 'Alteration of the sublingual microvascular glycocalyx in critically ill patients', *Microvasc Res*, 90: 86-9.

Echtler, K., K. Stark, M. Lorenz, S. Kerstan, A. Walch, L. Jennen, M. Rudelius, S. Seidl, E. Kremmer, N. R. Emambokus, M. L. von Bruehl, J. Frampton, B. Isermann, O. Genzel-Boroviczeny, C. Schreiber, J. Mehilli, A. Kastrati, M. Schwaiger, R. A. Shivdasani, and S. Massberg. 2010. 'Platelets contribute to postnatal occlusion of the ductus arteriosus', *Nat Med*, 16: 75-82.

El Kebir, D., L. Jozsef, W. Pan, and J. G. Filep. 2008. 'Myeloperoxidase delays neutrophil apoptosis through CD11b/CD18 integrins and prolongs inflammation', *Circ Res*, 103: 352-9.

Elhadd, T. A., G. Kennedy, A. Hill, M. McLaren, R. W. Newton, S. A. Greene, and J. J. Belch. 1999. 'Abnormal markers of endothelial cell activation and oxidative stress in children, adolescents and young adults with type 1 diabetes with no clinical vascular disease', *Diabetes Metab Res Rev*, 15: 405-11.

Ferrer-Marin, F., C. Chavda, M. Lampa, A. D. Michelson, A. L. Frelinger, 3rd, and M. Sola-Visner. 2011. 'Effects of in vitro adult platelet transfusions on neonatal hemostasis', *J Thromb Haemost*, 9: 1020-8.

Gallin, J. I. 1980. 'Degranulating stimuli decrease the neagative surface charge and increase the adhesiveness of human neutrophils', *J Clin Invest*, 65: 298-306.

Gambaro, G., I. Kinalska, A. Oksa, P. Pont'uch, M. Hertlova, J. Olsovsky, J. Manitius, D. Fedele, S. Czekalski, J. Perusicova, J. Skrha, J. Taton, W. Grzeszczak, and G. Crepaldi. 2002. 'Oral sulodexide reduces albuminuria in microalbuminuric and macroalbuminuric type 1 and type 2 diabetic patients: the Di.N.A.S. randomized trial', *J Am Soc Nephrol*, 13: 1615-25.

Gartner, V., and T. K. Eigentler. 2008. 'Pathogenesis of diabetic macro- and microangiopathy', *Clin Nephrol*, 70: 1-9.

Genzel-Boroviczeny, O., S. MacWilliams, M. Von Poblotzki, and L. Zoppelli. 2006. 'Mortality and major morbidity in premature infants less than 31 weeks gestational age in the decade after introduction of surfactant', *Acta Obstet Gynecol Scand*, 85: 68-73.

Genzel-Boroviczeny, O., J. Strotgen, A. G. Harris, K. Messmer, and F. Christ. 2002. 'Orthogonal polarization spectral imaging (OPS): a novel method to measure the microcirculation in term and preterm infants transcutaneously', *Pediatr Res*, 51: 386-91.

Golub, A. S., and R. N. Pittman. 2013. 'Bang-bang model for regulation of local blood flow', *Microcirculation*, 20: 455-83.

Hink, U., H. Li, H. Mollnau, M. Oelze, E. Matheis, M. Hartmann, M. Skatchkov, F. Thaiss, R. A. Stahl, A. Warnholtz, T. Meinertz, K. Griendling, D. G. Harrison, U. Forstermann, and T. Munzel. 2001. 'Mechanisms underlying endothelial dysfunction in diabetes mellitus', *Circ Res*, 88: E14-22.

Honig, C. R., C. L. Odoroff, and J. L. Frierson. 1982. 'Active and passive capillary control in red muscle at rest and in exercise', *Am J Physiol*, 243: H196-206.

Hsieh, H. J., C. A. Liu, B. Huang, A. H. Tseng, and D. L. Wang. 2014. 'Shear-induced endothelial mechanotransduction: the interplay between reactive oxygen species (ROS) and nitric oxide (NO) and the pathophysiological implications', *J Biomed Sci*, 21: 3.

Ignjatovic, V., J. Than, R. Summerhayes, F. Newall, S. Horton, A. Cochrane, and P. Monagle. 2012. 'The quantitative and qualitative responses of platelets in pediatric patients undergoing cardiopulmonary bypass surgery', *Pediatr Cardiol*, 33: 55-9.

Ince, C. 2005. 'The microcirculation is the motor of sepsis', *Crit Care*, 9 Suppl 4: S13-9.

Israels, S. J., T. Cheang, C. Roberston, E. M. McMillan-Ward, and A. McNicol. 1999. 'Impaired signal transduction in neonatal platelets', *Pediatr Res*, 45: 687-91.

Israels, S. J., M. L. Rand, and A. D. Michelson. 2003. 'Neonatal platelet function', *Semin Thromb Hemost*, 29: 363-72.

Jakob, S. M., R. Pick, D. Brechtefeld, C. Nussbaum, F. Kiefer, M. Sperandio, and B. Walzog. 2013. 'Hematopoietic progenitor kinase 1 (HPK1) is required for LFA-1-mediated neutrophil recruitment during the acute inflammatory response', *Blood*, 121: 4184-94.

Janoff, A., and B. W. Zweifach. 1964. 'Adhesion and Emigration of Leukocytes Produced by Cationic Proteins of Lysosomes', *Science*, 144: 1456-8.

Johansson, M. W., M. Patarroyo, F. Oberg, A. Siegbahn, and K. Nilsson. 1997. 'Myeloperoxidase mediates cell adhesion via the alpha M beta 2 integrin (Mac-1, CD11b/CD18)', *J Cell Sci*, 110 (Pt 9): 1133-9.

Kantari, C., M. Pederzoli-Ribeil, and V. Witko-Sarsat. 2008. 'The role of neutrophils and monocytes in innate immunity', *Contrib Microbiol*, 15: 118-46.

Kavey, R. E., V. Allada, S. R. Daniels, L. L. Hayman, B. W. McCrindle, J. W. Newburger, R. S. Parekh, and J. Steinberger. 2006. 'Cardiovascular risk reduction in high-risk pediatric patients', *Circulation*, 114: 2710-38.

Keul, P., S. Lucke, K. von Wnuck Lipinski, C. Bode, M. Graler, G. Heusch, and B. Levkau. 2011. 'Sphingosine-1-phosphate receptor 3 promotes recruitment of monocyte/macrophages in inflammation and atherosclerosis', *Circ Res*, 108: 314-23.

Khan, F., T. A. Elhadd, S. A. Greene, and J. J. Belch. 2000. 'Impaired skin microvascular function in children, adolescents, and young adults with type 1 diabetes', *Diabetes Care*, 23: 215-20.

Kimura, T., H. Tomura, C. Mogi, A. Kuwabara, M. Ishiwara, K. Shibasawa, K. Sato, S. Ohwada, D. S. Im, H. Kurose, T. Ishizuka, M. Murakami, and F. Okajima. 2006. 'Sphingosine 1-phosphate receptors mediate stimulatory and inhibitory signalings for expression of adhesion molecules in endothelial cells', *Cell Signal*, 18: 841-50.

King, C. C., M. M. Jefferson, and E. L. Thomas. 1997. 'Secretion and inactivation of myeloperoxidase by isolated neutrophils', *J Leukoc Biol*, 61: 293-302.

Klebanoff, S. J. 2005. 'Myeloperoxidase: friend and foe', *J Leukoc Biol*, 77: 598-625.

Koning, N. J., A. B. Vonk, M. I. Meesters, T. Oomens, M. Verkaik, E. K. Jansen, C. Baufreton, and C. Boer. 2014. 'Microcirculatory perfusion is preserved during off-pump but not on-pump cardiac surgery', *J Cardiothorac Vasc Anesth*, 28: 336-41.

Koning, N. J., A. B. Vonk, L. J. van Barneveld, A. Beishuizen, B. Atasever, C. E. van den Brom, and C. Boer. 2012. 'Pulsatile flow during cardiopulmonary bypass preserves postoperative microcirculatory perfusion irrespective of systemic hemodynamics', *J Appl Physiol (1985)*, 112: 1727-34.

Koning, N. J., A. B. Vonk, H. Vink, and C. Boer. 2016. 'Side-by-Side Alterations in Glycocalyx Thickness and Perfused Microvascular Density During Acute Microcirculatory Alterations in Cardiac Surgery', *Microcirculation*, 23: 69-74.

Koopmans, M., M. A. Kuiper, H. Endeman, G. Veenstra, N. A. Vellinga, R. de Vos, and E. C. Boerma. 2015. 'Microcirculatory perfusion and vascular reactivity are altered in post cardiac arrest patients, irrespective of target temperature management to 33 degrees C vs 36 degrees C', *Resuscitation*, 86: 14-8.

Kroth, J., K. Weidlich, S. Hiedl, C. Nussbaum, F. Christ, and O. Genzel-boroviczeny. 2008. 'Functional vessel density in the first month of life in preterm neonates', *Pediatr Res*, 64: 567-71.

Krump-Konvalinkova, V., S. Yasuda, T. Rubic, N. Makarova, J. Mages, W. Erl, C. Vosseler, C. J. Kirkpatrick, G. Tigyi, and W. Siess. 2005. 'Stable knock-down of the sphingosine 1-phosphate receptor S1P1 influences multiple functions of human endothelial cells', *Arterioscler Thromb Vasc Biol*, 25: 546-52.

Kubes, P., and S. Kanwar. 1994. 'Histamine induces leukocyte rolling in post-capillary venules. A P-selectin-mediated event', *J Immunol*, 152: 3570-7.

Kubicki, R., J. Grohmann, M. Siepe, C. Benk, F. Humburger, A. Rensing-Ehl, and B. Stiller. 2013. 'Early prediction of capillary leak syndrome in infants after cardiopulmonary bypass', *Eur J Cardiothorac Surg*, 44: 275-81.

Kuperman, A. A., B. Brenner, and G. Kenet. 2013. 'Intraventricular hemorrhage in preterm infants and coagulation--ambivalent perspectives?', *Thromb Res*, 131 Suppl 1: S35-8.

Lau, D., H. Mollnau, J. P. Eiserich, B. A. Freeman, A. Daiber, U. M. Gehling, J. Brummer, V. Rudolph, T. Munzel, T. Heitzer, T. Meinertz, and S. Baldus. 2005. 'Myeloperoxidase mediates neutrophil activation by association with CD11b/CD18 integrins', *Proc Natl Acad Sci U S A*, 102: 431-6.

Lawrence, M. B., and T. A. Springer. 1991. 'Leukocytes roll on a selectin at physiologic flow rates: distinction from and prerequisite for adhesion through integrins', *Cell*, 65: 859-73.

Le Guyader, D., M. J. Redd, E. Colucci-Guyon, E. Murayama, K. Kissa, V. Briolat, E. Mordelet, A. Zapata, H. Shinomiya, and P. Herbomel. 2008. 'Origins and unconventional behavior of neutrophils in developing zebrafish', *Blood*, 111: 132-41.

Lefkowitz, D. L., E. Roberts, K. Grattendick, C. Schwab, R. Stuart, J. Lincoln, R. C. Allen, N. Moguilevsky, A. Bollen, and S. S. Lefkowitz. 2000. 'The endothelium and cytokine secretion: the role of peroxidases as immunoregulators', *Cell Immunol*, 202: 23-30.

Levy-Shraga, Y., A. Maayan-Metzger, A. Lubetsky, B. Shenkman, J. Kuint, U. Martinowitz, and G. Kenet. 2006. 'Platelet function of newborns as tested by cone and plate(let) analyzer correlates with gestational Age', *Acta Haematol*, 115: 152-6.

Levy, O. 2007. 'Innate immunity of the newborn: basic mechanisms and clinical correlates', *Nat Rev Immunol*, 7: 379-90.

Lewick, J.R. 2010. *An Introction to Cardiovascular Physiology* (Taylor & Francis).

Ley, K., C. Laudanna, M. I. Cybulsky, and S. Nourshargh. 2007. 'Getting to the site of inflammation: the leukocyte adhesion cascade updated', *Nat Rev Immunol*, 7: 678-89.

Limaye, V., P. Xia, C. Hahn, M. Smith, M. A. Vadas, S. M. Pitson, and J. R. Gamble. 2009. 'Chronic increases in sphingosine kinase-1 activity induce a pro-inflammatory, pro-angiogenic phenotype in endothelial cells', *Cell Mol Biol Lett*, 14: 424-41.

Lindmark, E., T. Tenno, and A. Siegbahn. 2000. 'Role of platelet P-selectin and CD40 ligand in the induction of monocytic tissue factor expression', *Arterioscler Thromb Vasc Biol*, 20: 2322-8.

Llaurado, G., V. Ceperuelo-Mallafre, C. Vilardell, R. Simo, N. Freixenet, J. Vendrell, and J. M. Gonzalez-Clemente. 2012. 'Arterial stiffness is increased in patients with type 1 diabetes without cardiovascular disease: a potential role of low-grade inflammation', *Diabetes Care*, 35: 1083-9.

Lorant, D. E., W. Li, N. Tabatabaei, M. K. Garver, and K. H. Albertine. 1999. 'P-selectin expression by endothelial cells is decreased in neonatal rats and human premature infants', *Blood*, 94: 600-9.

Mahmud, F. H., S. Van Uum, N. Kanji, H. Thiessen-Philbrook, and C. L. Clarson. 2008. 'Impaired endothelial function in adolescents with type 1 diabetes mellitus', *J Pediatr*, 152: 557-62.

Mariscalco, M. M., M. H. Tcharmtchi, and C. W. Smith. 1998. 'P-Selectin support of neonatal neutrophil adherence under flow: contribution of L-selectin, LFA-1, and ligand(s) for P-selectin', *Blood*, 91: 4776-85.

Matsushita, K., C. N. Morrell, and C. J. Lowenstein. 2004. 'Sphingosine 1-phosphate activates Weibel-Palade body exocytosis', *Proc Natl Acad Sci U S A*, 101: 11483-7.

McEver, R. P. 2001. 'Adhesive interactions of leukocytes, platelets, and the vessel wall during hemostasis and inflammation', *Thromb Haemost*, 86: 746-56.

McEver, R. P., J. H. Beckstead, K. L. Moore, L. Marshall-Carlson, and D. F. Bainton. 1989. 'GMP-140, a platelet alpha-granule membrane protein, is also synthesized by vascular endothelial cells and is localized in Weibel-Palade bodies', *J Clin Invest*, 84: 92-9.

McEvoy, L. T., H. Zakem-Cloud, and M. F. Tosi. 1996. 'Total cell content of CR3 (CD11b/CD18) and LFA-1 (CD11a/CD18) in neonatal neutrophils: relationship to gestational age', *Blood*, 87: 3929-33.

Miranda, M., M. Balarini, D. Caixeta, and E. Bouskela. 2016. 'Microcirculatory dysfunction in sepsis: pathophysiology, clinical monitoring, and potential therapies', *Am J Physiol Heart Circ Physiol*, 311: H24-35.

Mocsai, A. 2013. 'Diverse novel functions of neutrophils in immunity, inflammation, and beyond', *J Exp Med*, 210: 1283-99.

Moore, J. P., A. Dyson, M. Singer, and J. Fraser. 2015. 'Microcirculatory dysfunction and resuscitation: why, when, and how', *Br J Anaesth*, 115: 366-75.

Moroi, M., and S. M. Jung. 1997. 'Platelet receptors for collagen', *Thromb Haemost*, 78: 439-44.

Moser, M., B. Nieswandt, S. Ussar, M. Pozgajova, and R. Fassler. 2008. 'Kindlin-3 is essential for integrin activation and platelet aggregation', *Nat Med*, 14: 325-30.

Msan, A. K., I. M. Usta, F. G. Mirza, and A. H. Nassar. 2015. 'Use of antenatal corticosteroids in the management of preterm delivery', *Am J Perinatol*, 32: 417-26.

Murphy, G. J., and G. D. Angelini. 2004. 'Side effects of cardiopulmonary bypass: what is the reality?', *J Card Surg*, 19: 481-8.

Nelson, A., I. Berkestedt, A. Schmidtchen, L. Ljunggren, and M. Bodelsson. 2008. 'Increased levels of glycosaminoglycans during septic shock: relation to mortality and the antibacterial actions of plasma', *Shock*, 30: 623-7.

Neuhof, C., O. Walter, F. Dapper, J. Bauer, B. Zickmann, E. Fink, H. Tillmanns, and H. Neuhof. 2003. 'Bradykinin and histamine generation with generalized enhancement of microvascular permeability in neonates, infants, and children undergoing cardiopulmonary bypass surgery', *Pediatr Crit Care Med*, 4: 299-304.

Nieuwdorp, M., F. Holleman, E. de Groot, H. Vink, J. Gort, A. Kontush, M. J. Chapman, B. A. Hutten, C. B. Brouwer, J. B. Hoekstra, J. J. Kastelein, and E. S. Stroes. 2007. 'Perturbation of hyaluronan metabolism predisposes patients with type 1 diabetes mellitus to atherosclerosis', *Diabetologia*, 50: 1288-93.

Nieuwdorp, M., M. C. Meuwese, H. Vink, J. B. Hoekstra, J. J. Kastelein, and E. S. Stroes. 2005. 'The endothelial glycocalyx: a potential barrier between health and vascular disease', *Curr Opin Lipidol*, 16: 507-11.

Nieuwdorp, M., H. L. Mooij, J. Kroon, B. Atasever, J. A. Spaan, C. Ince, F. Holleman, M. Diamant, R. J. Heine, J. B. Hoekstra, J. J. Kastelein, E. S. Stroes, and H. Vink. 2006. 'Endothelial glycocalyx damage coincides with microalbuminuria in type 1 diabetes', *Diabetes*, 55: 1127-32.

Nieuwdorp, M., T. W. van Haeften, M. C. Gouverneur, H. L. Mooij, M. H. van Lieshout, M. Levi, J. C. Meijers, F. Holleman, J. B. Hoekstra, H. Vink, J. J. Kastelein, and E. S. Stroes. 2006. 'Loss of endothelial glycocalyx during acute hyperglycemia coincides with endothelial dysfunction and coagulation activation in vivo', *Diabetes*, 55: 480-6.

Nussbaum, C., A. Gloning, M. Pruenster, D. Frommhold, S. Bierschenk, O. Genzel-Boroviczeny, U. H. von Andrian, E. Quackenbush, and M. Sperandio. 2013. 'Neutrophil and endothelial adhesive function during human fetal ontogeny', *J Leukoc Biol*, 93: 175-84.

Nussbaum, C., and M. Sperandio. 2011. 'Innate immune cell recruitment in the fetus and neonate', *J Reprod Immunol*, 90: 74-81.

O'Neil, M. P., J. C. Fleming, A. Badhwar, and L. R. Guo. 2012. 'Pulsatile versus nonpulsatile flow during cardiopulmonary bypass: microcirculatory and systemic effects', *Ann Thorac Surg*, 94: 2046-53.

Olivera, A., and J. Rivera. 2011. 'An emerging role for the lipid mediator sphingosine-1-phosphate in mast cell effector function and allergic disease', *Adv Exp Med Biol*, 716: 123-42.

Pahwa, R., P. Nallasamy, and I. Jialal. 2016. 'Toll-like receptors 2 and 4 mediate hyperglycemia induced macrovascular aortic endothelial cell inflammation and perturbation of the endothelial glycocalyx', *J Diabetes Complications*, 30: 563-72.

Patterson, C. C., G. G. Dahlquist, E. Gyurus, A. Green, G. Soltesz, and Eurodiab Study Group. 2009. 'Incidence trends for childhood type 1 diabetes in Europe during 1989-2003 and predicted new cases 2005-20: a multicentre prospective registration study', *Lancet*, 373: 2027-33.

Perrin, R. M., S. J. Harper, and D. O. Bates. 2007. 'A role for the endothelial glycocalyx in regulating microvascular permeability in diabetes mellitus', *Cell Biochem Biophys*, 49: 65-72.

Petzold, T., R. Ruppert, D. Pandey, V. Barocke, H. Meyer, M. Lorenz, L. Zhang, W. Siess, S. Massberg, and M. Moser. 2013. 'beta1 integrin-mediated signals are required for platelet granule secretion and hemostasis in mouse', *Blood*, 122: 2723-31.

Phillipson, M., B. Heit, P. Colarusso, L. Liu, C. M. Ballantyne, and P. Kubes. 2006. 'Intraluminal crawling of neutrophils to emigration sites: a molecularly distinct process from adhesion in the recruitment cascade', *J Exp Med*, 203: 2569-75.

Pittman, R. N. 2005. 'Oxygen transport and exchange in the microcirculation', *Microcirculation*, 12: 59-70.

Pruenster, M., A. R. Kurz, K. J. Chung, X. Cao-Ehlker, S. Bieber, C. F. Nussbaum, S. Bierschenk, T. K. Eggersmann, I. Rohwedder, K. Heinig, R. Immler, M. Moser, U. Koedel, S. Gran, R. P. McEver, D. Vestweber, A. Verschoor, T. Leanderson, T. Chavakis, J. Roth, T. Vogl, and M. Sperandio. 2015.

'Extracellular MRP8/14 is a regulator of beta2 integrin-dependent neutrophil slow rolling and adhesion', *Nat Commun*, 6: 6915.

Rabelink, T. J., and D. de Zeeuw. 2015. 'The glycocalyx--linking albuminuria with renal and cardiovascular disease', *Nat Rev Nephrol*, 11: 667-76.

Rehm, M., D. Bruegger, F. Christ, P. Conzen, M. Thiel, M. Jacob, D. Chappell, M. Stoeckelhuber, U. Welsch, B. Reichart, K. Peter, and B. F. Becker. 2007. 'Shedding of the endothelial glycocalyx in patients undergoing major vascular surgery with global and regional ischemia', *Circulation*, 116: 1896-906.

Reitsma, S., D. W. Slaaf, H. Vink, M. A. van Zandvoort, and M. G. oude Egbrink. 2007. 'The endothelial glycocalyx: composition, functions, and visualization', *Pflugers Arch*, 454: 345-59.

Rivera, J., R. L. Proia, and A. Olivera. 2008. 'The alliance of sphingosine-1-phosphate and its receptors in immunity', *Nat Rev Immunol*, 8: 753-63.

Rouwet, E. V., R. J. Beuk, E. Heineman, D. W. Slaaf, and M. G. oude Egbrink. 2000. 'Effect of repetitive asphyxia on leukocyte-vessel wall interactions in the developing chick intestine', *J Pediatr Surg*, 35: 49-55.

Rudolph, V., T. K. Rudolph, L. Kubala, N. Clauberg, R. Maas, M. Pekarova, A. Klinke, D. Lau, K. Szocs, T. Meinertz, R. H. Boger, and S. Baldus. 2009. 'A myeloperoxidase promoter polymorphism is independently associated with mortality in patients with impaired left ventricular function', *Free Radic Biol Med*, 47: 1584-90.

Sachs, U. J., and B. Nieswandt. 2007. 'In vivo thrombus formation in murine models', *Circ Res*, 100: 979-91.

Sakr, Y., M. J. Dubois, D. De Backer, J. Creteur, and J. L. Vincent. 2004. 'Persistent microcirculatory alterations are associated with organ failure and death in patients with septic shock', *Crit Care Med*, 32: 1825-31.

Salmon, A. H., and S. C. Satchell. 2012. 'Endothelial glycocalyx dysfunction in disease: albuminuria and increased microvascular permeability', *J Pathol*, 226: 562-74.

Sanchez, T., A. Skoura, M. T. Wu, B. Casserly, E. O. Harrington, and T. Hla. 2007. 'Induction of vascular permeability by the sphingosine-1-phosphate receptor-2 (S1P2R) and its downstream effectors ROCK and PTEN', *Arterioscler Thromb Vasc Biol*, 27: 1312-8.

Schaack, T. M., A. Takeuchi, I. Spilberg, and R. H. Persellin. 1980. 'Alteration of polymorphonuclear leukocyte surface charge by endogenous and exogenous chemotactic factors', *Inflammation*, 4: 37-44.

Schalkwijk, C. G., and C. D. Stehouwer. 2005. 'Vascular complications in diabetes mellitus: the role of endothelial dysfunction', *Clin Sci (Lond)*, 109: 143-59.

Shane, A. L., and B. J. Stoll. 2014. 'Neonatal sepsis: progress towards improved outcomes', *J Infect*, 68 Suppl 1: S24-32.

Shattil, S. J. 1999. 'Signaling through platelet integrin alpha IIb beta 3: inside-out, outside-in, and sideways', *Thromb Haemost*, 82: 318-25.

Silbernagl, S. 2012. *Taschenatlas Physiologie* (Thieme).

Skoura, A., and T. Hla. 2009. 'Regulation of vascular physiology and pathology by the S1P2 receptor subtype', *Cardiovasc Res*, 82: 221-8.

Soehnlein, O., L. Lindbom, and C. Weber. 2009. 'Mechanisms underlying neutrophil-mediated monocyte recruitment', *Blood*, 114: 4613-23.

Soehnlein, O., X. Xie, H. Ulbrich, E. Kenne, P. Rotzius, H. Flodgaard, E. E. Eriksson, and L. Lindbom. 2005. 'Neutrophil-derived heparin-binding protein (HBP/CAP37) deposited on endothelium enhances monocyte arrest under flow conditions', *J Immunol*, 174: 6399-405.

Sola-Visner, M. 2012. 'Platelets in the neonatal period: developmental differences in platelet production, function, and hemostasis and the potential impact of therapies', *Hematology Am Soc Hematol Educ Program*, 2012: 506-11.

Sperandio, M., J. Pickard, S. Unnikrishnan, S. T. Acton, and K. Ley. 2006. 'Analysis of leukocyte rolling in vivo and in vitro', *Methods Enzymol*, 416: 346-71.

Sperandio, M., E. J. Quackenbush, N. Sushkova, J. Altstatter, C. Nussbaum, S. Schmid, M. Pruenster, A. Kurz, A. Margraf, A. Steppner, N. Schweiger, L. Borsig, I. Boros, N. Krajewski, O. Genzel-Boroviczeny, U. Jeschke, D. Frommhold, and U. H. von Andrian. 2013. 'Ontogenetic regulation of leukocyte recruitment in mouse yolk sac vessels', *Blood*, 121: e118-28.

Spiegel, S., and S. Milstien. 2011. 'The outs and the ins of sphingosine-1-phosphate in immunity', *Nat Rev Immunol*, 11: 403-15.

Stiller, B., J. Sonntag, I. Dahnert, V. Alexi-Meskishvili, R. Hetzer, T. Fischer, and P. E. Lange. 2001. 'Capillary leak syndrome in children who undergo cardiopulmonary bypass: clinical outcome in comparison with complement activation and C1 inhibitor', *Intensive Care Med*, 27: 193-200.

Stoll, B. J., N. I. Hansen, E. F. Bell, S. Shankaran, A. R. Laptook, M. C. Walsh, E. C. Hale, N. S. Newman, K. Schibler, W. A. Carlo, K. A. Kennedy, B. B. Poindexter, N. N. Finer, R. A. Ehrenkranz, S. Duara, P. J. Sanchez, T. M. O'Shea, R. N. Goldberg, K. P. Van Meurs, R. G. Faix, D. L. Phelps, I. D. Frantz, 3rd, K. L. Watterberg, S. Saha, A. Das, R. D. Higgins, Health Eunice Kennedy Shriver National Institute of Child, and Network Human Development Neonatal Research. 2010. 'Neonatal outcomes of extremely preterm infants from the NICHD Neonatal Research Network', *Pediatrics*, 126: 443-56.

Strauss, T., Y. Levy-Shraga, B. Ravid, I. Schushan-Eisen, A. Maayan-Metzger, J. Kuint, and G. Kenet. 2010. 'Clot formation of neonates tested by thromboelastography correlates with gestational age', *Thromb Haemost*, 103: 344-50.

Sun, W. Y., L. D. Abeynaike, S. Escarbe, C. D. Smith, S. M. Pitson, M. J. Hickey, and C. S. Bonder. 2012. 'Rapid histamine-induced neutrophil recruitment is sphingosine kinase-1 dependent', *Am J Pathol*, 180: 1740-50.

Svennevig, K., T. Hoel, A. Thiara, S. Kolset, A. Castelheim, T. Mollnes, F. Brosstad, E. Fosse, and J. Svennevig. 2008. 'Syndecan-1 plasma levels during coronary artery bypass surgery with and without cardiopulmonary bypass', *Perfusion*, 23: 165-71.

Tcharmtchi, M. H., C. W. Smith, and M. M. Mariscalco. 2000. 'Neonatal neutrophil interaction with P-selectin: contribution of P-selectin glycoprotein ligand-1 and sialic acid', *J Leukoc Biol*, 67: 73-80.

The Diabetes Control and Complications Trial Research Group. 1993. 'The effect of intensive treatment of diabetes on the development and progression of long-term complications in insulin-dependent diabetes mellitus. ', *N Engl J Med*, 329: 977-86.

Trzeciak, S., R. P. Dellinger, J. E. Parrillo, M. Guglielmi, J. Bajaj, N. L. Abate, R. C. Arnold, S. Colilla, S. Zanotti, S. M. Hollenberg, Resuscitation Microcirculatory Alterations in, and Investigators Shock. 2007. 'Early microcirculatory perfusion derangements in patients with severe sepsis and septic shock: relationship to hemodynamics, oxygen transport, and survival', *Ann Emerg Med*, 49: 88-98, 98 e1-2.

Wang, Y., M. Sakuma, Z. Chen, V. Ustinov, C. Shi, K. Croce, A. C. Zago, J. Lopez, P. Andre, E. Plow, and D. I. Simon. 2005. 'Leukocyte engagement of platelet glycoprotein Ibalpha via the integrin Mac-1 is critical for the biological response to vascular injury', *Circulation*, 112: 2993-3000.

Weidlich, K., J. Kroth, C. Nussbaum, S. Hiedl, A. Bauer, F. Christ, and O. Genzel-Boroviczeny. 2009. 'Changes in microcirculation as early markers for infection in preterm infants--an observational prospective study', *Pediatr Res*, 66: 461-5.

Whetzel, A. M., D. T. Bolick, S. Srinivasan, T. L. Macdonald, M. A. Morris, K. Ley, and C. C. Hedrick. 2006. 'Sphingosine-1 phosphate prevents monocyte/endothelial interactions in type 1 diabetic NOD mice through activation of the S1P1 receptor', *Circ Res*, 99: 731-9.

Wiedmeier, S. E., E. Henry, M. C. Sola-Visner, and R. D. Christensen. 2009. 'Platelet reference ranges for neonates, defined using data from over 47,000 patients in a multihospital healthcare system', *J Perinatol*, 29: 130-6.

Wiernsperger, N., and J. R. Rapin. 2012. 'Microvascular diseases: is a new era coming?', *Cardiovasc Hematol Agents Med Chem*, 10: 167-83.

Yang, W. H., C. Nussbaum, P. K. Grewal, J. D. Marth, and M. Sperandio. 2012. 'Coordinated roles of ST3Gal-VI and ST3Gal-IV sialyltransferases in the synthesis of selectin ligands', *Blood*, 120: 1015-26.

Young, J. 1929. 'Malpighi's "De Pulmonibus"', *Proc R Soc Med*, 23: 1-11.

Zarbock, A., and K. Ley. 2009. 'Neutrophil adhesion and activation under flow', *Microcirculation*, 16: 31-42.

Zarbock, A., K. Ley, R. P. McEver, and A. Hidalgo. 2011. 'Leukocyte ligands for endothelial selectins: specialized glycoconjugates that mediate rolling and signaling under flow', *Blood*, 118: 6743-51.

Zuurbier, C. J., C. Demirci, A. Koeman, H. Vink, and C. Ince. 2005. 'Short-term hyperglycemia increases endothelial glycocalyx permeability and acutely decreases lineal density of capillaries with flowing red blood cells', *J Appl Physiol (1985)*, 99: 1471-6.

IX) Lebenslauf

Persönliche Angaben

Name	Dr. med. Claudia Franziska Nußbaum
Geburtsdatum/-ort	31.03.1979, Kaufbeuren
Nationalität	deutsch
Familienstand	verheiratet, ein Kind (* 31.10.2014)

Ausbildung

05/2006	3. Abschnitt der Ärztlichen Prüfung (Note 1,0)
03/2004	2. Abschnitt der Ärztlichen Prüfung (Note 1,0)
03/2003	1. Abschnitt der Ärztlichen Prüfung (Note 1,0)
08/2001	Ärztliche Vorprüfung (Note 1,3)
1999 – 2006	Studium der Humanmedizin, LMU München
1989 – 1998	Marien-Gymnasium, Kaufbeuren
1986 – 1989	Konradin-Grundschule, Kaufbeuren

Ärztliche Weiterbildung

04/2016	Qualifikation zur fachgebundenen Genetischen Beratung
Seit 07/2015	Weiterbildung im Schwerpunktbereich Neonatologie
07/2014	Anerkennung zur Fachärztin für Kinder- und Jugendmedizin

Ärztliche Tätigkeit

Seit 06/2016	Funktionsoberärztin (50%), Abteilung für Neonatologie, Campus Innenstadt, Dr. von Haunersches Kinderspital, LMU
10/2012 - 06/2016	Assistenzärztin am Dr. von Haunerschen Kinderspital, LMU (09/2014 - 06/2015 Mutterschutz und Elternzeit)
08/2011 - 09/2012	Assistenzärztin, Abt. für Kinderkardiologie u. Pädiatrische Intensivmedizin, Dr. von Haunersches Kinderspital, LMU
03/2007 - 2/2008	Assistenzärztin, Abteilung für Neonatologie, Campus Innenstadt, Dr. von Haunersches Kinderspital, LMU

Wissenschaftliche Tätigkeit

Seit 02/2017	DFG-Rotationsstelle (50%) innerhalb des SFB 914, Biomedizinisches Centrum der LMU
10/2015 - 09/2016	Habilitations-Stipendiatin der BGF (50%), AG Prof. Dr. M. Sperandio, Walter-Brendel-Zentrum für experimentelle Medizin, LMU
12/2008 - 07/2011	Post-Doktorandin, AG Prof. Dr. M. Sperandio Walter-Brendel-Zentrum für experimentelle Medizin, LMU
Seit 2008	Grundlagenforschung und klinisch-experimentelle Studien zur Regulation der Leukozyten- und Thrombozytenrekrutierung sowie zu Veränderungen der Mikrozirkulation im Kindesalter bei verschiedenen Krankheitsentitäten
09/2006 - 02/2007	Wissenschaftliche Mitarbeiterin, Schwerpunkt Medizindidaktik (Leitung: Prof. Dr. M. Fischer), Med. Klinik Innenstadt, LMU

Dissertation

2004 - 2008	„Funktion von Thrombozyten bei antivaskulärer Therapie solider Tumore durch Paclitaxel enkapsuliert in kationische Liposomen“ (summa cum laude) Institut für Chirurgische Forschung der LMU München, PD. Dr. M. Dellian

Betreuung von Promotionsarbeiten

Seit 2016	Cand. med. Marie Kreis und cand. med. Eveline Anzinger: „Evaluation der Mikrozirkulation als Monitoringparameter zur Steuerung des peri- und postoperativen Flüssigkeitsmanagement bei Kindern“ (in Arbeit)
Seit 2013	Stefanie Artmann: „Etablierung von Normwerten der endothelialen Glykokalyx bei gesunden Neugeborenen“ (in Arbeit) Lea Rajwich: „Longitudinale Untersuchung der endothelialen Glykokalyx bei Frühgeborenen“ (in Arbeit)
2011 - 2016	Andreas Margraf: „Regulation der Thromboyztenfunktion im Mausfetus in vivo“ (experimenteller Teil abgeschlossen, Daten publiziert)
2011 - 2015	Amelie Haberer: „Veränderungen der Mikrozirkulation und der mikrovaskulären Glykokalyx bei Kindern nach Operationen an der Herz-Lungen-Maschine“ (experimenteller Teil abgeschlossen, Daten publiziert)
2010 - 2014	Dr. med. Ana Cavalcanti-Fernandes-Hering: „Frühzeitige Veränderungen der Mikrozirkulation und Verlust der endothelialen Glykokalyx bei Kindern mit Diabetes mellitus Typ I“ (Dissertation abgeschlossen, Daten publiziert)
2009 - 2013	Dr. med. Anna Gloning: „Ontogenese der Rekrutierung neutrophiler Granulozyten bei humanen Neonaten in Abhängigkeit vom Gestationsalter“ (Dissertation abgeschlossen, Daten publiziert)

Lehrtätigkeit

Seit 2007	Dozentin im MeCuM Modul 5 (Seminar, Blockpraktikum und Tutorial Pädiatrie, E-Learning)
SoSe 2010 und 2011	Dozentin im MeCuM Seminar und Praktikum „Vegetative Physiologie“
WiSe 06/07 - WiSe 08/09	Organisation und Dozentin im MeCuM Longitudinalkurs (Untersuchungskurs, Kurs „Ambulante Medizin“, E-Learning)

Stipendien/Förderungen/Preise

Seit 02/2017	Rotationsstelle der Deutschen Forschungsgemeinschaft (SFB914)
2015/2016	Habilitations-Stipendium der Bayerischen Gleichstellungsförderung (50%)
2015	Servier Award der Europäischen Gesellschaft für Mikrozirkulation
2013	Young Investigator Award der Dt. Gesellschaft für Pädiatrische Kardiologie
2012	Forschungsförderung Dt. Gesellschaft für Pädiatrische Kardiologie
2010	Projektförderung FöFoLe-Promotionsstudiengang
2009	Forschungsförderung B.Braun Stiftung Forschungsförderung Friedrich-Baur Stiftung
2008/2009	Post-Doktoranden Stipendium der Bayerischen Gleichstellungsförderung
2007 - 2012	Mentee im Mentoringprogramm der LMU Exzellenzinitiative
2005	PJ-Stipendium der München-Harvard Allianz

Sonstige akademische Positionen

2013/2014	Assistentensprecherin am Dr. von Haunerschen Kinderspital
Seit 2010	Mentorin im MeCuM Mentoring Programm

Reviewertätigkeit

Plos One, Resucitation, Journal of Endocrinology and Diabetes Research, Innate Immunity

X) Danksagung

An dieser Stelle möchte ich ganz herzlich allen Personen danken, die mich auf dem Weg zur Habilitation unterstützt haben.

Herrn Professor Dr. med. Dr. sci. nat. Christoph Klein, der als Direktor der Kinderklinik und geschäftsführender Fachmentor meine klinische und wissenschaftliche Karriere stets gefördert hat.

Frau Professor Dr. med. Orsolya Genzel-Boroviczény und Herrn Professor Dr. med. Markus Sperandio, die mir - weit über die Bedeutung des Fachmentorates hinaus - echte Mentoren in allen Lebenslagen waren und sind. Ihr habt mein Verständnis von Klinik und Forschung geprägt und meinen Werdegang wesentlich beeinflusst. Ohne eure Unterstützung wäre diese Arbeit nicht möglich gewesen. Vielen Dank!

Frau Professor Dr. med. Ania Muntau, die mich auch in schwierigen Zeiten immer wieder dazu ermutigt und mir geholfen hat diesen Weg zu gehen.

Meinen Kolleginnen und Kollegen am Dr. von Haunerschen Kinderspital für ihre beständige Kollegialität und das gute Arbeitsklima. Selbst unter der steigenden Arbeitsbelastung, der wir alle ausgesetzt sind, macht ihr es möglich, dass ich auch nach vielen Jahren noch gerne diesem wunderbaren Beruf nachgehe.

Meinen Mitstreitern und Freunden aus der AG Sperandio für euren Ratschlag in wissenschaftlichen wie zwischenmenschlichen Fragen. Ohne euch wäre so manches Projekt sicherlich gescheitert und die Forschung nur halb so lustig. Daher herzlichen Dank an Moni, Roland, Ina, Myri, Angi, Krisi, Verena, Suse und Nadine.

Danken möchte ich auch allen Doktorandinnen und Doktoranden, die zur Entstehung dieser Arbeit beigetragen haben.

Zuletzt möchte ich meiner Familie von ganzem Herzen danken. Meinen Eltern, Heidi und Thomas, für ihre Liebe und immerwährende Unterstützung bei allen kleinen und großen Belangen des Lebens. Ihr habt immer an mich geglaubt und mir die Möglichkeiten und Chancen geboten, mich zu dem Menschen zu entwickeln, der ich heute bin. Auch meiner Schwester Sandra möchte ich für den guten familiären Zusammenhalt danken und dass sie immer ein offenes Ohr für mich hat. Großer Dank gilt auch meinen Schwiegereltern, Doris und Günter, ohne deren Unterstützung der tägliche Spagat zwischen Klinik, Forschung und Familie nicht möglich wäre.

Last, but not least gilt mein größter Dank und meine Liebe meinem Ehemann. Frank, Du bist meine wichtigste Stütze und hältst mir den Rücken frei, wann immer nötig. Der Weg bis hierher war oft nicht einfach und hat mich und uns zum Teil an unsere Grenzen gebracht, aber am Ende auch gestärkt. Ich freue mich auf unseren weiteren Lebensweg gemeinsam mit unserem wunderbaren Sohn Karl und dem kleinen Wunder, das sich angekündigt hat.

XI) Faksimile der themenrelevanten Publikationen

Klinke A, **Nussbaum C** (both authors contributed equally) et al.: Myeloperoxidase attracts neutrophils by physical forces. Blood 2011; 117(4):1350-8.

Nussbaum C et al.: Sphingosine-1-phosphate receptor 3 promotes leukocyte rolling by mobilizing endothelial P-selectin. Nat Commun 2015; 6:6416.

Nussbaum C et al.: Neutrophil and endothelial adhesive function during human fetal ontogeny. J Leukoc Biol 2013; 93(2):175-84.

Margraf A, **Nussbaum C** (both authors contributed equally) et al.: Maturation of Platelet Function During Murine Fetal Development In Vivo. Arterioscler Thromb Vasc Biol. 2017; Apr 20. Epub ahead of print.

Nussbaum C et al.: Early microvascular changes with loss of the glycocalyx in children with type 1 diabetes. J Pediatr 2014; 164(3):584-9.

Nussbaum C et al.: Perturbation of the microvascular glycocalyx and perfusion in infants after cardiopulmonary bypass. J Thorac Cardiovasc Surg 2015; 150(6):1474-81

Nussbaum C et al.: Myeloperoxidase: a leukocyte-derived protagonist of inflammation and cardiovascular disease. Antioxid Redox Signal 2013; 18(6):692-713.

Nussbaum C, Sperandio M.: Innate immune cell recruitment in the fetus and neonate. J Reprod Immunol 2011; 90(1):74-81.

Myeloperoxidase attracts neutrophils by physical forces

*Anna Klinke,[1] *Claudia Nussbaum,[2] Lukas Kubala,[3] Kai Friedrichs,[1] Tanja K. Rudolph,[1] Volker Rudolph,[1] Hans-Joachim Paust,[4] Christine Schröder,[5] Daniel Benten,[6] Denise Lau,[1] Katalin Szocs,[1] Paul G. Furtmüller,[7] Peter Heeringa,[8] Karsten Sydow,[1] Hans-Jürgen Duchstein,[9] Heimo Ehmke,[10] Udo Schumacher,[5] Thomas Meinertz,[1] Markus Sperandio,[2] and Stephan Baldus[1]

[1]Department of Cardiology, University Heart Center, Hamburg, Germany; [2]Walter Brendel Centre of Experimental Medicine, Ludwig-Maximilians-University, Munich, Germany; [3]Institute of Biophysics, Academy of Sciences of the Czech Republic, Brno, Czech Republic; Departments of [4]Nephrology and Rheumatology, [5]Anatomy II, and [6]Gastroenterology, University Hospital Eppendorf, Hamburg, Germany; [7]Department of Chemistry, University of Natural Resources and Applied Life Sciences, Vienna, Austria; [8]Department of Pathology and Medical Biology, University Medical Center Groningen, Groningen, The Netherlands; [9]Department of Chemistry, University of Hamburg, Hamburg, Germany; and [10]Department of Physiology, University Hospital Eppendorf, Hamburg, Germany

Recruitment of polymorphonuclear neutrophils (PMNs) remains a paramount prerequisite in innate immune defense and a critical cofounder in inflammatory vascular disease. Neutrophil recruitment comprises a cascade of concerted events allowing for capture, adhesion and extravasation of the leukocyte. Whereas PMN rolling, binding, and diapedesis are well characterized, receptor-mediated processes, mechanisms attenuating the electrostatic repulsion between the negatively charged glycocalyx of leukocyte and endothelium remain poorly understood. We provide evidence for myeloperoxidase (MPO), an abundant PMN-derived heme protein, facilitating PMN recruitment by its positive surface charge. In vitro, MPO evoked highly directed PMN motility, which was solely dependent on electrostatic interactions with the leukocyte's surface. In vivo, PMN recruitment was shown to be MPO-dependent in a model of hepatic ischemia and reperfusion, upon intraportal delivery of MPO and in the cremaster muscle exposed to local inflammation or to intraarterial MPO application. Given MPO's affinity to both the endothelial and the leukocyte's surface, MPO evolves as a mediator of PMN recruitment because of its positive surface charge. This electrostatic MPO effect not only displays a so far unrecognized, catalysis-independent function of the enzyme, but also highlights a principal mechanism of PMN attraction driven by physical forces. (*Blood*. 2011; 117(4):1350-1358)

Introduction

Recruitment of polymorphonuclear neutrophils (PMNs) is considered a hallmark in host defense.[1] With vessel- and tissue-infiltrating PMNs also being mechanistically linked to a broad range of vascular inflammatory diseases including coronary artery disease, heart failure and ischemia/reperfusion injury, the pathophysiologic significance of PMN motility reaches far beyond innate immunity.[2-4] So far, PMN migration is primarily viewed to be energy-dependent and cytoskeleton-dependent with G-protein coupled receptors and integrins initiating and orchestrating signaling pathways obligatory for neutrophil adhesion, spreading, diapedesis and chemotactic agitation.[5-7] On activation, PMN releases myeloperoxidase (MPO), an abundant heme protein in PMN with potent bactericidal and vascular-inflammatory properties. The enzyme accumulates along the endothelium and in the subendothelial space,[8] where it binds to anionic glycocalyx residues such as heparan sulfate glycosaminoglycans. Given the affinity of MPO to both PMN and endothelial cells, we evaluated whether MPO affects PMN locomotion and recruitment.

Methods

Isolation of PMN

Peripheral blood was drawn from healthy human volunteers and heparinized, and isolation of PMN was performed as previously described.[9] In brief, after sedimentation in dextran solution (45 mg/mL), the supernatant was placed over Histopaque 1077 (Sigma-Aldrich) for density gradient centrifugation. Remaining red blood cells were eliminated by hypotonic lysis and the pellet was resuspended in Hanks balanced salt solution (HBSS; Invitrogen) containing 0.25% bovine serum albumin (BSA) (*cell buffer*) and stored on ice until use.

Microslide motility experiments

Microslides (Ibidi μ-slide I, ibitreat; IBIDI) were coated with fibrinogen (250 μg/mL). PMN or red blood cells (RBCs; 1×10^6/mL in cell buffer or plasma, where indicated) were incubated with 4-amino-benzoic acid hydrazide (ABAH; 50μM, Calbiochem) and H_2O_2 (50μM, 30 minutes, Merck), (-)-Blebbistatin (100μM, 30 minutes, Sigma-Aldrich), Cytochalasin D (1μM, 30 minutes, Sigma-Aldrich), LY 294002 (200μM, 2 hours, Calbiochem), or with sodium azide and 2-deoyxglucose (50mM, 1 hour, Sigma-Aldrich). 100 μg of poly-L-arginine (PLA, Sigma-Aldrich), protamine (Protamin Valeant, MEDA Pharma), or histone H2A (Millipore) was added directly before application to microslides, where indicated. For experiments in pH 9.2, PMN were resuspended and lyophilized MPO was reconstituted in cell buffer of pH 9.2. 100 μL of PMN suspension was applied into the microslide channel; cells were allowed to attach for 5 minutes. Subsequently, 30 μL of MPO (120nM unless otherwise indicated, Planta Natural Products), recombinant, mutant MPO Q91T or M243T (120nM), IL-8 (25nM, PeproTech), or human serum albumin (120nM, Sigma-Aldrich) in cell buffer or plasma, optionally supplemented with inhibitors, PLA, protamine, or histone, respectively, was added from one side into the channel. Where indicated, Sepharose beads with anionic

Submitted May 10, 2010; accepted October 13, 2010. Prepublished online as *Blood* First Edition paper, October 27, 2010; DOI 10.1182/blood-2010-05-284513.

*A.K. and C.M. contributed equally to this study.

An Inside *Blood* analysis of this article appears at the front of this issue.

The online version of this article contains a data supplement.

The publication costs of this article were defrayed in part by page charge payment. Therefore, and solely to indicate this fact, this article is hereby marked "advertisement" in accordance with 18 USC section 1734.

(HiTrap SP HP, GE Healthcare/Amersham) or cationic (HiTrap Q HP, GE Healthcare) coating were used instead of PMN. The area of the steepest gradient was calculated as before (www.ibidi.com) and captured for 20 minutes with a light microscope (CK 2, Olympus)–mounted charge-coupled device (CCD) camera (Retiga 1300, QImaging).

Image acquisition and processing of in vitro experiments

During leukocyte or Sepharose-bead motility experiments, pictures were captured at 0 minutes and 20 minutes, and time-lapse imaging was used to create a stack of images (iVision version 4.0, BioVision). The percentage of cells oriented in an angle of less than 180° toward the segment of upward gradient was evaluated (PMN in up-gradient segment). Twenty PMNs per stack were tracked and transformed to 2-dimensional plots, with the x-direction indicating the upward gradient orientation (manual tracking and chemotaxis-tool, created for ImageJ by IBIDI). The mean accumulated distance and the x-forward-migration index (x-displacement × accumulated distance^{-1}) were calculated.

Quantification of f-actin with flow cytometry

PMN (1×10^6/mL cell buffer) were incubated with MPO (120nM) or IL-8 (25nM). After indicated times, cells were fixed, permeabilized, and incubated with Alexa Fluor 488–Phalloidin (20 minutes, 5 U/mL in phosphate buffer solution [PBS] with 1% BSA, Molecular Probes). Flow cytometric analysis was performed using a FACSCalibur flow cytometer and CellQuest Pro 5.1 software (BD Biosciences).

Mouse liver experimental protocols

Male C57BL/6J (wild-type; WT) and MPO_tm1lus (*Mpo*$^{-/-}$) mice aged 12-15 weeks were treated either to occlude the blood supply to the median and left hepatic lobes with an atraumatic vascular clamp for 90 minutes, and reperfusion then initiated; or, their inferior mesenteric veins were injected with recombinant human serum albumin (Prospec); recombinant active MPO (R&D Systems); inactive MPO M243T, Q91T MPO, or recombinant MPO preincubated with 50μM ABAH and H_2O_2 (4 μg in 200 μL of physiologic saline), respectively. Two hours after intraportal injection or 20 hours after initiation of reperfusion, mice were again anaesthetized. The liver was flushed by intraportal injection of 1 mL of PBS and excised. All animal experiments were approved by the local ethics committees (Hamburg, Germany, G100/06) and in accordance with the US National Research Council's "Guide for the Care and Use of Laboratory Animals."

Quantitative assessment of hepatic PMN infiltration by immunohistochemistry

Frozen liver specimens were fixed with acetone. Sections were incubated with anti-mouse Ly6G primary antibody (ratio of 1:40; Hycult Biodiagnostics), and endogenous peroxidase activity was blocked. The secondary antibody was horseradish peroxidase (hrp)–labeled rabbit IgG to rat IgG (1:100, Dako), and the tertiary antibody was hrp-labeled goat anti–rabbit IgG (1:500, Vector Laboratories) in 3% normal mouse serum. PMNs were stained with 3-amino-9-ethylcarbazol (AEC) solution and tissue was counterstained with hematoxyline. The number of neutrophils attached to sinusoids or extravasated into hepatic parenchyma was counted in 30 high-power fields per animal (original magnification ×600) under a light microscope (Olympus).

Mouse cremaster muscle experimental protocols

Recombinant murine tumor necrosis factor (TNF)-α (500 ng per mouse, R&D) in sterile saline was injected into the scrotum of male C57BL/6J (WT) mice and MPO_tm1lus (*Mpo*$^{-/-}$) mice aged 12-15 weeks. Two hours after injection, the carotid artery was cannulated and the cremaster muscle surgically prepared for intravital microscopy as previously described.[10] During intravital microscopy, the cremaster muscle preparation was continuously superfused with a 37°C warm buffer solution. In separate experiments, the cremaster muscle was surgically prepared without prior treatment (trauma induced inflammation). Twenty minutes after surgical preparation of the cremaster muscle, the animals received a bolus injection of active MPO (20 μg per mouse) or recombinant, inactive MPO Q91T (20 μg per mouse) in a volume of 0.2 mL of sterile saline, or an injection of saline alone, into the carotid artery. During all experiments systemic blood samples were obtained (10 μL in 90 μL of Tuerk solution; Merck) for quantification of systemic white blood cell count. All animal experiments were approved by the local ethics committees (Regierung von Oberbayern, Az. 55.2-1-54-2531-80-07) and in accordance with the "Guide for the Care and Use of Laboratory Animals."

Intravital microscopy and data analysis

Intravital microscopy was performed on an upright microscope (Olympus BX51) with a saline immersion objective (original magnification 40×, 0.8 numerical aperture) as described.[10] Experiments were recorded on an S-VHS recorder using a CCD camera (model CF8/1, Kappa) for later offline analysis. Vessel diameter, segment length of postcapillary cremaster muscle venules, and PMN diameter were measured with a digital image processing system.[11] Centerline red blood cell velocity was determined by a dual photodiode and a digital online cross-correlation program (Circusoft Instrumentation) and used for offline calculation of mean blood flow velocity and wall shear rates as previously reported.[12] Supplemental Tables 1 and 2 (available on the *Blood* Web site; see the Supplemental Materials link at the top of the online article) give an overview of microvascular parameters observed during intravital microscopy experiments. PMN adherence was quantified by counting the number of leukocytes per mm^2 of vessel surface that remained stationary for more than 30 seconds.

Whole-mount histology

To assess leukocyte extravasation on intrascrotal injection of TNF-α, whole mounts of cremaster muscles were prepared as previously described.[13] Leukocyte extravasation was quantified by counting the number of extravascular cells per mm^2 of cremaster muscle tissue using a Zeiss upright microscope with an oil immersion objective (original magnification 100×, 1.3 numerical aperture).

MPO and Alcian blue staining

For hepatic MPO staining, human MPO (4 μg, Planta Natural Products) or human serum albumin (4 μg, Sigma-Aldrich) was injected to the mesenteric vein of C57Bl/6J mice as described. Hepatic sections were incubated with the primary antibody to human MPO (rabbit, Calbiochem). For cremasteric MPO staining, human MPO (20 μg) was injected into the carotid artery of WT mice, and after 10 minutes an antibody to human MPO (40 μg, rabbit, Calbiochem) was injected. After another 10 minutes, the vena cava inferior was incised and 3 mL of PBS were flushed via the carotid catheter. Where indicated, Alcian blue 8 GX (1 mL, 0.1% solution, Sigma-Aldrich) was injected into the artery and flushed with 1 mL of PBS and 1 mL of 4% formaldehyde. The cremaster muscle was excised as described, placed on a microslide, and fixed with 4% formaldehyde. All samples were treated with secondary antibody Alexa 488 to rabbit IgG (Molecular Probes) and tissue was counterstained with DAPI. Images were acquired with a Leica microscope (DMLB) and IVision software.

Statistical analysis

Data were tested for normal distribution using the Kolmogorov-Smirnov test. When normality was shown, Student unpaired *t* test was used for pairwise comparison; otherwise, the Mann-Whitney rank sum test was used. A before-after comparison was performed with the Student paired *t* test. For multiple comparison, one-way ANOVA followed by a Bonferroni post hoc test, or Kruskal-Wallis ANOVA on ranks test followed by Dunn post hoc test, was used as appropriate. A P value $< .05$ was considered statistically significant. All statistical analyses were carried out with SPSS Version 13 (SPSS). Data are presented as mean ± SEM.

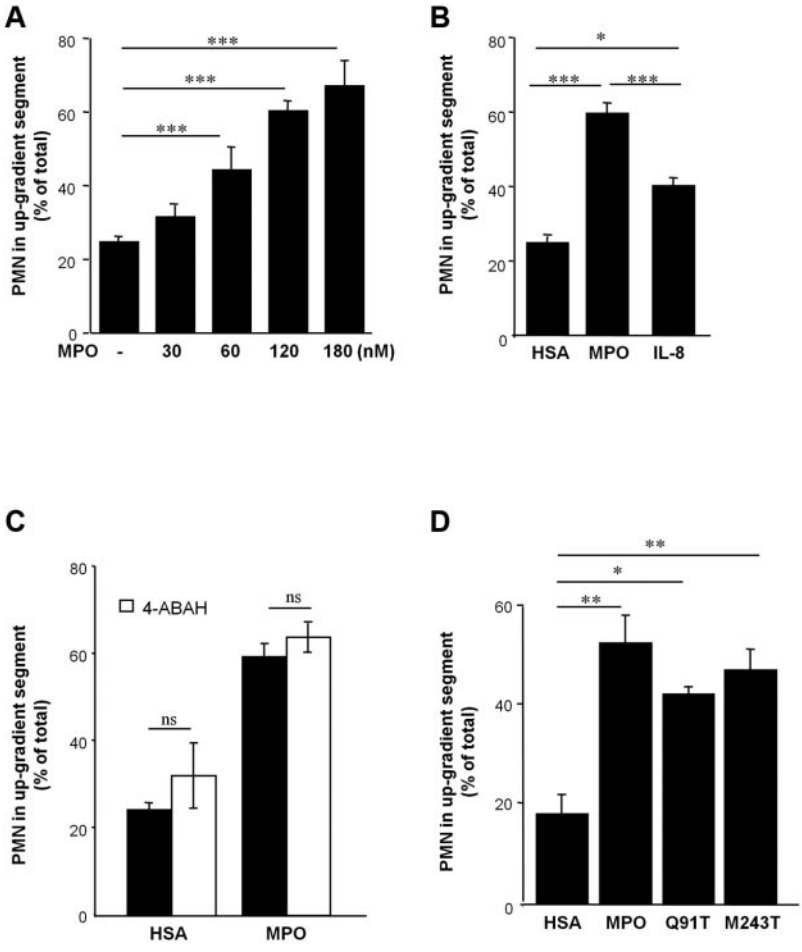

Figure 1. MPO-dependent PMN motility in vitro. PMN motility was evaluated at the steepest gradient of a chemotactic factor or control in Ibidi microslides. (A) MPO provoked directed locomotion of PMN in a concentration-dependent manner (n = 4, one-way ANOVA; $P < .0001$). (B) Directed PMN motility after application of human serum albumin (HSA, n = 21), MPO (n = 34), and interleukin-8 (IL-8, n = 9) was investigated (one-way ANOVA; $P < .0001$). (C) Directed motility toward HSA or MPO was evaluated on preincubation with the MPO-inhibitor 4-amino-benzoic acid hydrazide (ABAH; white bars, n = 3-4). (D) MPO-variants Q91T (n = 4) and M243T (n = 9) devoid of catalytic activity also yielded increased directed PMN motility (one-way ANOVA $P < .003$). Number of independent experiments denoted by n; number of donors of PMN ≥ 3. Bars represent means; error bars, standard error of the mean (SEM). *$P < .05$, **$P < .01$, ***$P < .001$.

Results

To test PMN motility in response to MPO, isolated human PMN added to microslides were challenged with MPO administered to one pole of the chamber. The resulting gradient of MPO provoked PMN motility in a concentration-dependent manner (Figure 1A). The presence of human plasma did not affect MPO-directed motility (Suppl. Figure 1A). The extent of directed PMN locomotion toward MPO was significantly elevated compared with human serum albumin (HSA) and the chemokine interleukin-8 (IL-8, Figure 1B), with eosinophil peroxidase (EPO) attracting PMN to a similar extent as MPO (supplemental Figure 1B). Interestingly, inactivation of MPO by the inhibitor 4-amino-benzoic acid hydrazide (ABHA) did not attenuate MPO-dependent PMN motility. Furthermore, 2 MPO variants, which lack either total enzymatic activity (Q91T) or the chlorinating, brominating, NO-oxidizing and NO-nitrating activity of the enzyme (M243T[14]), provoked PMN attraction to a similar extent as active MPO, thus indicating a mechanism that operates irrespective of the enzyme's catalytic activity (Figure 1C, D).

Remarkably, although MPO-exposed PMN traveled a shorter distance compared with IL-8, MPO-dependent motility was strikingly more vectored (as expressed by the x-forward-migration index[15]; Figure 2A-C, supplemental Figure 2). These differences between MPO-evoked compared with IL-8–evoked motility were accompanied by a discrepancy in cell morphology: PMN exposed to MPO lacked the morphologic characteristics observed on migration in response to IL-8, that is, polarization and formation of lamellipodia[16] (Figure 2D). Given these directional and morphologic peculiarities in PMN motility toward MPO, characterization of central intracellular signaling cascades involved in mediating leukocyte migration were explored. Whereas inhibition of nonmuscle myosin II by blebbistatin, phosphatidylinositol 3-kinase activity by LY 294002, and actin filament polymerization using cytochalasin D impaired IL-8-induced migration,[17-19] MPO-induced PMN motility remained unaffected. The rise in filamentous actin content (f-actin), which is a prerequisite of active PMN migration and observed in IL-8 treated cells, was blunted in MPO-exposed cells. This indicates that PMN motility on MPO exposure is independent of cytoskeletal rearrangements (Figure 2E, F). Instead, MPO provoked passive PMN locomotion irrespective of energy consumption, as evidenced by preserved cell motility in the presence of respiratory chain and glycolysis-inhibiting sodium azide and 2-deoxyglucose, respectively (Figure 2G). Moreover, PMN movement toward MPO was retained after fixation of the cells using methanol (Figure 3A).

Given that MPO-dependent PMN motility was revealed to be independent of energy-consuming cytoskeletal modifications, electrostatic interactions between the cationic MPO and the negatively charged PMN-surface were explored. In support of electrostatic interactions as a prerequisite for MPO-evoked PMN motility, alkalization of the assay buffer to the isoelectric point of MPO (p*I* 9.2) entirely prevented motility of methanol-fixed PMN (Figure

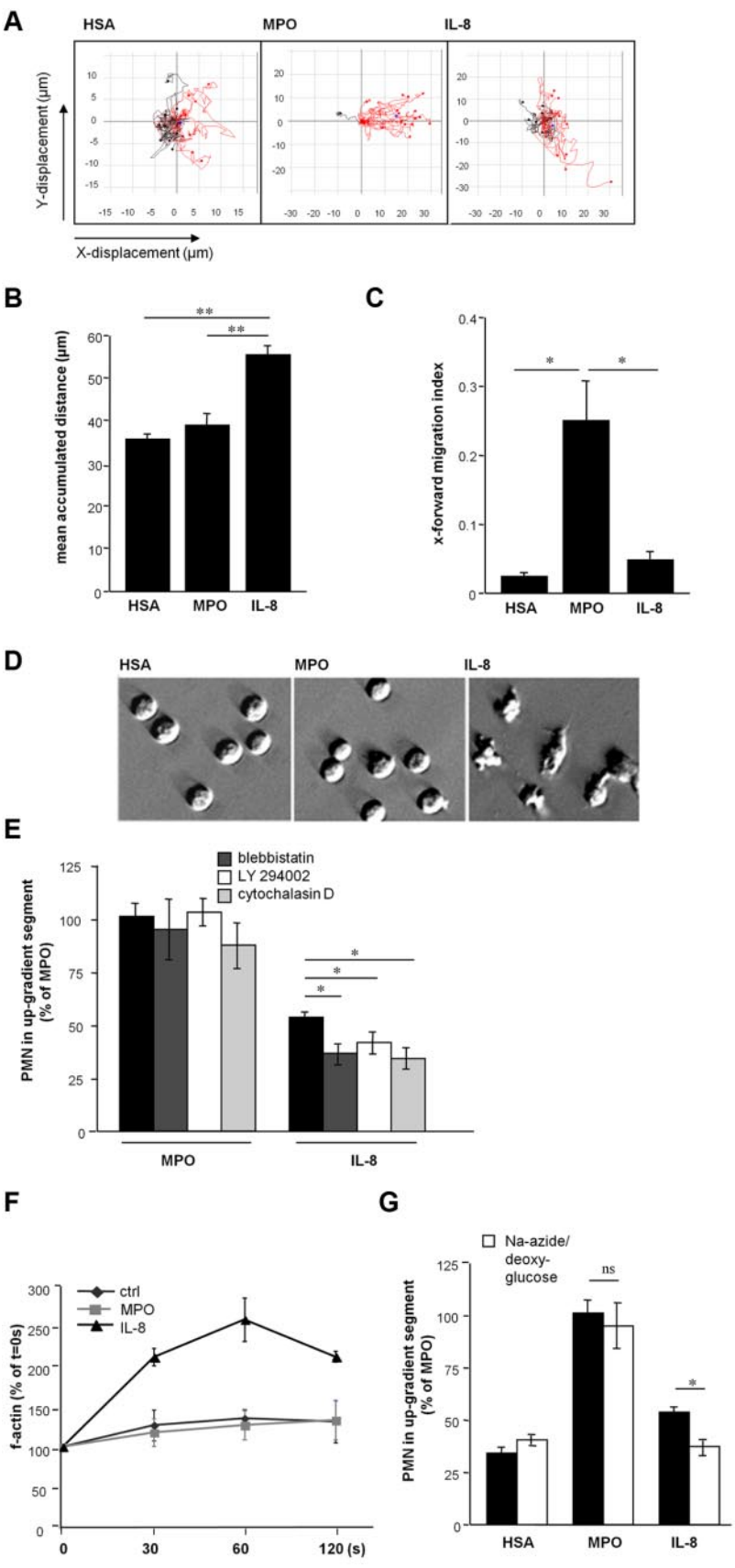

Figure 2. MPO-mediated PMN motility is highly directed and independent of cytoskeletal rearrangements. (A) Plots of PMN locomotion in microslides are depicted, red lines represent tracks of cells moving toward the up-gradient segment. Cell motility was followed under an Olympus CK2 inverted microscope with a mounted CCD camera (Retiga 1300, QImaging). Time-lapse microscopy was performed with iVision version 4.0 (Biovision) software and tracks created with ImageJ. (B) The mean accumulated distance of plotted tracks was calculated (n = 3-4 plots including 20 tracks, respectively, one-way ANOVA $P < .002$). (C) The x-forward–migration index (x-displacement × accumulated distance^{-1}) of plotted tracks (n = 3-4 plots including 20 tracks) represents the extent of vectored PMN movement (one-way ANOVA $P < .01$). (D) PMN administered to microslides in HSA-, MPO-, and IL-8–gradients were visualized with relief contrast microscopy (magnification ×400, digital interference contrast (DIC) microscopy, Olympus CKX31). (E) Motility toward MPO or IL-8 after preincubation of PMN with blebbistatin (dark gray), LY294002 (white), or cytochalasin D (light gray) was tested (n = 3-4, one-way ANOVA $P < .0001$). (F) Intracellular f-actin content of PMN after exposure to HSA, MPO, or IL-8 for indicated times was assessed by flow cytometry (n = 3-4). (G) Chemotaxis experiments in microslides were performed after preincubation of PMN with sodium azide and 2-deoxyglucose (white bars) to deplete energy metabolism. (n = 3-6, one-way ANOVA $P < .0001$). In this case, n denotes number of independent experiments, number of donors of PMN ≥ 3. Bars represent means; error bars, SEM. $^*P < .05$, $^{**}P < .01$, $^{***}P < .001$.

3A). The profound effect of the monomeric MPO mutants on PMN motility (Figure 1D) suggests that cleavage of MPO to hemi-myeloperoxidase, which occurs on alkalization, is not responsible for attenuation of PMN motility under alkaline conditions.[20] The significance of electrostatic interactions for MPO-directed cell motility was further stressed by the observation, that addition of

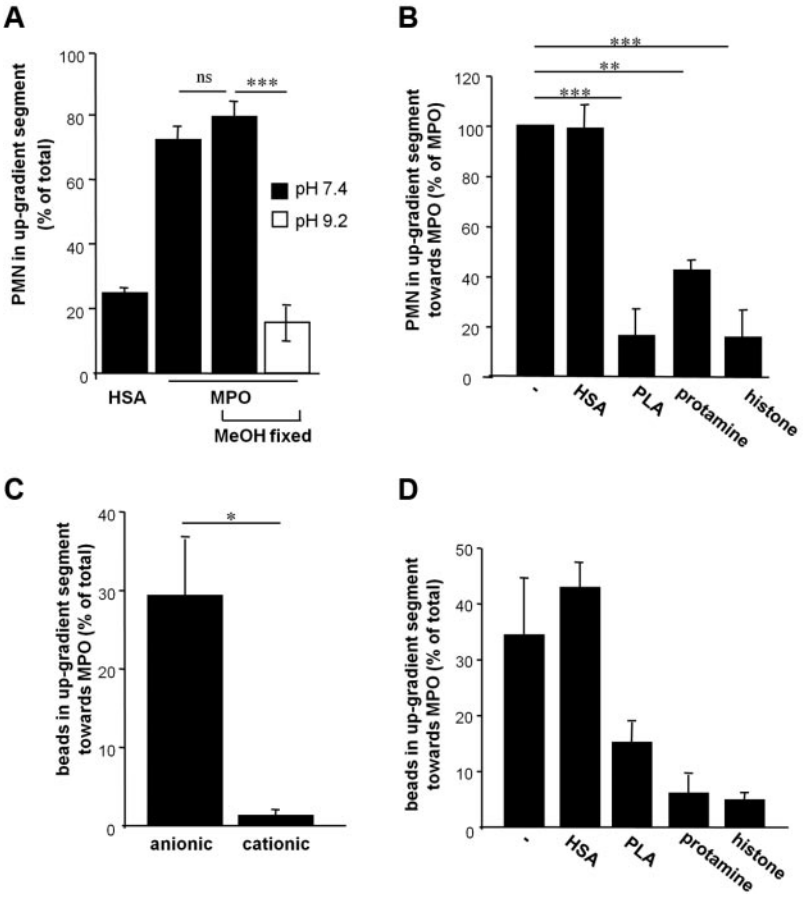

Figure 3. MPO-mediated PMN-motility is dependent on electrostatic interactions. (A) Methanol (MeOH) treatment of PMN did not impair MPO-induced motility, while directed movement of MeOH-fixed PMN toward MPO was blunted in buffer with the pH raised to the isoelectric point of MPO (p*I* 9.2, white bar, n = 3–4, one-way ANOVA $P < .0001$). (B) Poly-L-arginine (PLA), protamine and histone H2A were coadministered to PMN-suspension and MPO to equalize the cationic gradient. HSA was coadministered as a control protein (n = 3, one-way ANOVA $P < .0001$). (C) MPO-directed locomotion of sepharose beads with anionic or cationic coating was tested (n = 3-6). (D) Coadministration of PLA, protamine, and histone H2A impaired the motility of anionic beads toward MPO. In this case, n denotes number of independent experiments, number of donors of PMN ≥ 3. Bars represent means; error bars, SEM. $^*P < .05$, $^{**}P < .01$, $^{***}P < .001$.

highly polycationic molecules such as protamine, poly-L-arginine (PLA), and histone H2A coadministered to blunt the cationic gradient indeed abrogated the MPO-effect (Figure 3B). Along these lines, sepharose particles carrying a negative surface charge displayed a highly directed motility toward MPO, whereas cationic particles hardly did. In accordance with experiments performed with PMN, PLA, protamine, and histone H2A diminished MPO-directed locomotion of negatively charged particles (Figure 3C-D), underscoring the necessity of a cationic gradient as a prerequisite for cell motility. Moreover, and in support of MPO-mediated cell attraction, coating of microslides with MPO caused increased leukocyte adhesion under flow conditions compared with BSA (supplemental Figure 3).

To test whether these observations translate into MPO-dependent changes in PMN accumulation in vivo, we applied different mouse models using WT and MPO-deficient ($Mpo^{-/-}$) animals. In a first set of experiments, WT and $Mpo^{-/-}$ mice were subjected to 90 minutes of hepatic ischemia, followed by 20 hours of reperfusion. This resulted in systemic and hepatic accumulation of endogenous MPO in WT mice (supplemental Figure 4A-C), accompanied by a profound increase in PMN-infiltration compared with sham-operated animals. In $Mpo^{-/-}$ mice, the extent of PMN infiltration was markedly reduced (Figure 4A-B), reconfirming observations previously made in myocardial ischemia and renal ischemia and reperfusion.[3,21] Likewise, TNF-α–treated $Mpo^{-/-}$ mice revealed significantly reduced endothelial PMN adhesion and extravasation compared with WT mice (Figure 4C-D), as monitored by intravital microscopy and histologic evaluation of cremaster muscle postcapillary venules. Endothelial deposition of MPO on intrascrotal TNF-α injection in WT mice was confirmed immunohistochemically (supplemental Figure 5). Importantly, basal systemic leukocyte numbers and PMN surface expression of Mac-1 integrins did not differ between the mouse strains (supplemental Figure 6A-C).

To assess the direct contribution of MPO for PMN recruitment in vivo, MPO was injected into the superior mesenteric vein of WT mice. Accumulation of MPO in hepatic tissue was confirmed by immunofluorescence staining (Figure 4E). Administration of active MPO and the catalytically inactive MPO variants M243T and Q91T, as well as ABAH-inactivated MPO, resulted in significantly increased hepatic PMN accumulation compared with HSA, implying that the effect of MPO on PMN recruitment remains independent of the enzyme′s catalytic activity (Figure 4F). In line with these observations, injection of active MPO and inactive Q91T MPO into the carotid artery of WT and $Mpo^{-/-}$ mice provoked rapid PMN adhesion in cremaster muscle postcapillary venules (Figure 4G, supplemental Figure 7A, supplemental Video 1A-B). Microcirculatory parameters remained similar between the experimental groups (supplemental Tables 1-2). Of note, determination of cell diameters perpendicular to the endothelium[22] revealed that vessel-adherent PMN in MPO-treated mice was characterized by less spreading compared with PMN in animals challenged with TNF-α (Figure 4H). This observation recalls the in vitro findings and demonstrates distinctions between mechanisms evoked by established inflammatory cytokines. Importantly, MPO application did not affect PMN recruitment in arterioles of the cremaster muscle (supplemental Figure 7B-C, supplemental Video 1C). This underscores that MPO does not replace but rather supports the multiple mechanisms responsible for PMN recruitment, which hardly occurs in arterioles. In support of this MPO-dependent, charge-mediated PMN recruitment in vivo, MPO indeed profoundly

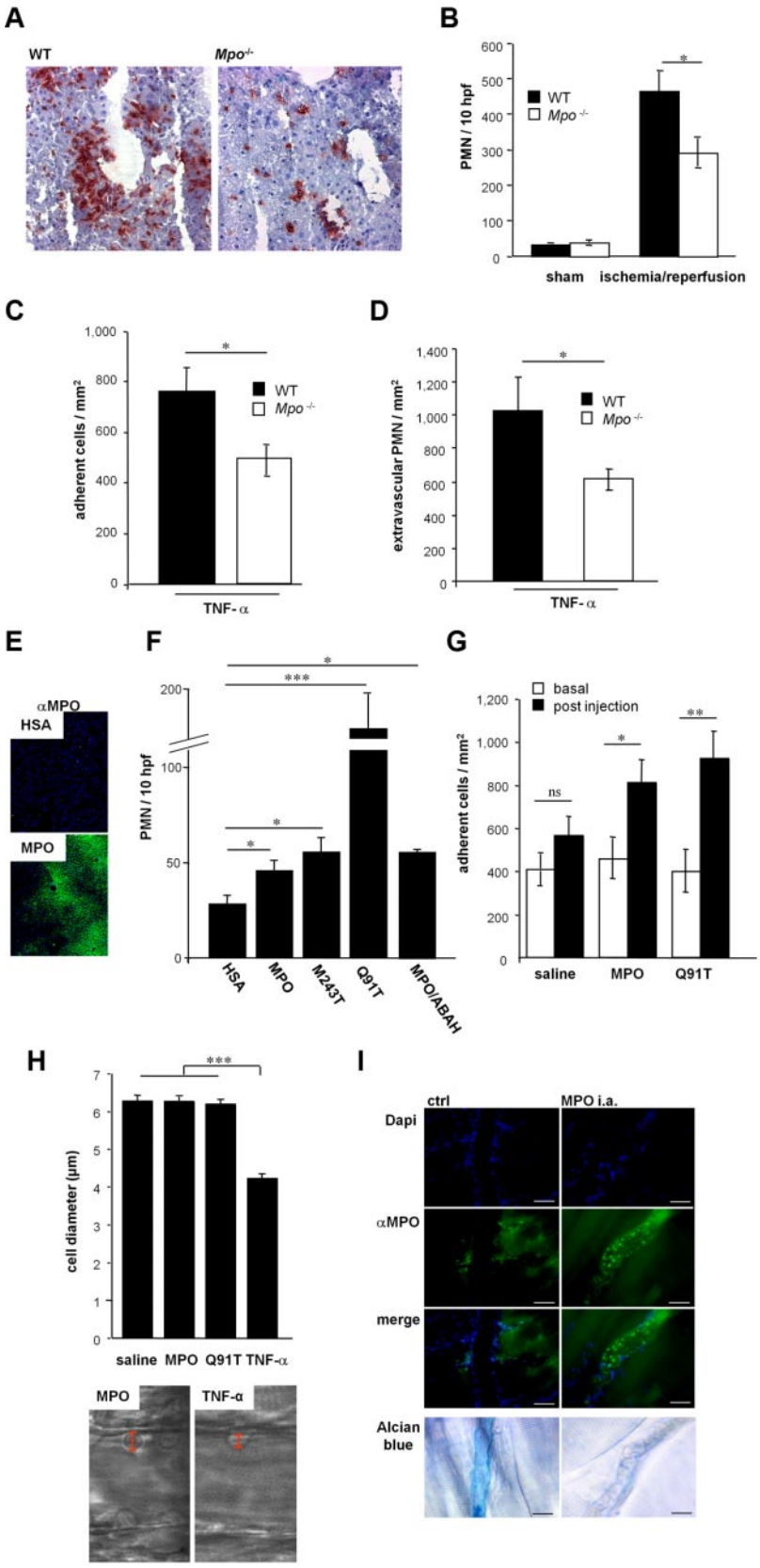

Figure 4. MPO provokes neutrophil recruitment in vivo. (A) Representative liver sections of WT and *Mpo*$^{-/-}$ mice after 90 minutes of hepatic ischemia with subsequent 20 hours of reperfusion are shown (PMN = red-brown; ×200, captured with Zeiss AxioCam HRc mounted on a Zeiss Axioskop with AxioVision 3.1. Tonal value correction, brightness, and contrast were adjusted with Adobe Photoshop CS3 extended 10.0). (B) PMN were quantified in liver sections of WT or *Mpo*$^{-/-}$ mice on hepatic ischemia and reperfusion (hpf = high-power field; magnification ×600; sham n = 5-8, treated n = 9-10, one-way ANOVA $P < .0001$). (C) Number of adherent leukocytes in postcapillary venules of the cremaster muscle of WT (19 vessels in 4 mice) and *Mpo*$^{-/-}$ mice (18 vessels in 4 mice) stimulated with TNF-α was assessed by intravital microscopy. (D) Number of perivascular PMN in TNF-α stimulated cremaster muscle of WT (n = 4) and *Mpo*$^{-/-}$ mice (n = 4) was evaluated in Giemsa-stained whole mounts. (E) MPO-immunoreactivity (αMPO, green, Alexa Fluor 488) on intraportal injection of HSA or human MPO is shown in hepatic sections of WT mice (blue = Dapi, original magnification ×100, captured with Retiga 1300 CCD camera mounted on Leica DMLB fluorescence microscope by iVision version 4.0, processed as described in panel A). (F) Hepatic PMN-infiltration was quantified on intraportal injection of HSA, active MPO (MPO), inactive MPO M243T and Q91T, or ABAH-inactivated MPO (n = 3-8, hpf = high-power field, magnification ×600, one-way ANOVA $P < .01$). (G) Number of adherent leukocytes in cremaster muscle postcapillary venules was assessed before (basal, white bars) and after (post injection, black bars) injection of saline solution (16 vessels in 5 mice), active (15 vessels in 3 mice) or inactive MPO Q91T (12 vessels in 3 mice) into the carotid artery of WT mice. (H) Mean diameter of PMN adherent to the endothelium of cremaster muscle venules in mice on injection of saline, MPO, or Q91T MPO to the carotid artery or intrascrotal TNF-α application (500 ng) and a representative image of vessel-adherent PMN in MPO and TNF-α–treated mice are shown (magnification ×400; intravital microscopy was performed with an Olympus BX51 microscope with a CF8/1 CCD-camera [Kappa]), recorded on S-VHS recorder and digitalized with MetaMorph software [Molecular Devices]). (I) Intraluminal staining of MPO (green) and negatively charged glycocalyx residues (Alcian blue) in WT mice on MPO injection of the carotid artery (MPO i.a.) or control (ctrl). Scale bars, 30 μm; fluorescence images captured and processed as described in panel E and bright-field images as described in panel A. Bars represent means; error bars, SEM. *$P < .05$, **$P < .01$, ***$P < .001$.

attenuated the anionic endothelial surface charge in cremaster muscle venules, illustrated by diminished deposition of the cationic dye Alcian blue, which binds to the glycocalyx in a charge-dependent fashion[23-25] (Figure 4I).

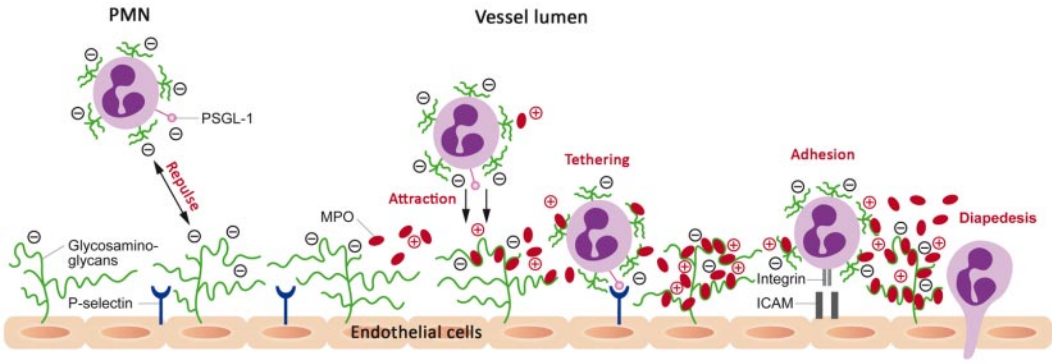

Figure 5. Scheme of the suggested mechanism of MPO-mediated PMN recruitment. Electrostatic repulsion between the negatively charged glycocalyx of PMN and the vessel wall prevents the interactions of PMN with the endothelium. Given the difference in height, the glycocalyx (~ 500 nm) shields selectins (~ 40 nm), which communicate the definite contact of PMN to the vessel wall (for instance, binding of constitutively expressed P-selectin glycoprotein ligand-1 [PSGL-1] on the PMN membrane with P-selectins on the endothelial surface). Thus binding of MPO to glycosaminoglycans reduces the negative surface charge and allows for electrostatic attraction of PMN to the endothelium, which then mediates receptor-ligand interactions, resulting in PMN tethering and rolling, adhesion, and diapedesis.

Discussion

Recruitment of PMN during inflammation implies a complex multistep process, which is initiated by capture, tethering, and rolling of leukocytes followed by leukocyte adhesion, spreading, and crawling on the inflamed vessel wall, and finally diapedesis into tissue. We herein propose a central role of MPO during the early steps of PMN interaction with the endothelium, this role being mediated by electrostatic forces between the cationic MPO surface and the anionic PMN surface.

Whereas the initial steps of the migration cascade are primarily considered to be selectin-dependent, nonselective physical forces have been suggested as alternative and potentially preceding mechanisms allowing PMN interaction with the vessel wall. Previous reports speculated on cationic proteins being responsible for the initiation of leukocyte emigration by alteration of the surface charge.[26] The attenuation of electrostatic repulsive forces has been hypothesized to permit short-range forces like Van der Waals and hydrophobic forces between leukocytes and the endothelium to act, and thereby facilitate leukocyte adhesion.[27] In fact, reports in the 1970s and early 1980s suggested that PMN-derived proteins enhance PMN margination and aggregation by decreasing negative surface charge, but these reports failed to identify the underlying effector molecules.[28-30] In accordance with these observations, sulfated glycosaminoglycans became established epitopes mediating the repulsion of blood cells and attenuating adhesion of circulating leukocytes, in part because of their negative charge, and by shielding endothelial adhesion molecules. Depletion of heparan sulfate chains has been shown to increase leukocyte adhesion in postcapillary venules,[31] whereas the negative charge of the leukocyte surface protein leukosialin (CD 43) appears to exert antiadhesive properties.[32]

The current data now expand on these findings and introduce MPO as a powerful inducer of PMN recruitment. In fact, as the enzyme is capable of attracting PMN in vitro independently of cytoskeletal-dependent and energy-dependent rearrangements of the leukocyte, electrostatic forces may indeed account for essential steps of PMN migration in vivo. Given its high affinity to glycosaminoglycans and matrix proteins such as collagen, fibronectin,[8,33] and fibrinogen (data not shown), MPO, released at and covering sites of inflammation, attenuates the antiadhesive properties of the vessel wall. This cationic "coat" may ease the interplay of PMN with the endothelium and allow PMN to interact with adhesion molecules harbored within the glycocalyx.[34] Furthermore, MPO deposition by adherent and crawling leukocytes on the endothelial surface layer may even help to guide upcoming PMN to the exit point into tissue (Figure 5). This concept of MPO supporting established mechanisms of PMN recruitment rather than unselectively promoting firm PMN adhesion is underscored by the fact that the enzyme did not provoke PMN recruitment in arterioles, where leukocyte interaction with the endothelium remains restricted because of high shear forces and a limited expression of adhesion molecules.

Alternative mechanisms apart from electrostatic interactions may be responsible for the current observations. For example, one could speculate that MPO increases vascular permeability as shown for other cationic molecules.[35,36] Vascular permeability is mainly regulated by the adhesion molecule vascular endothelial (VE)–cadherin, with its blockade resulting in increased permeability and enhanced PMN emigration.[37] However, research does not confirm that MPO affects vascular permeability.[8] Moreover, MPO binding to the neutrophil integrin Mac-1[38,39] may facilitate PMN adhesion and thus support electrostatically driven cell recruitment, as previously described for elastase and proteinase 3.[40,41]

It is possible to deduce from the current study that other cationic granular proteins should exhibit similar effects as MPO. However, electrostatically driven PMN recruitment does not only depend on the p*I* of the affecting protein: For example, lactoferrin, α-chymotrypsinogen A, and histone, despite a similar p*I*, promote endothelial leukocyte adhesion in varying degrees.[42] In fact, the different binding affinities of the proteins to the endothelium appear to be of critical importance as well.[43] MPO is characterized by its high affinity to heparan sulfate glycosaminoglycans,[8,44] the major components of the endothelial surface layer. In conjunction with its abundant granular expression, this results in profound deposition on the endothelial surface and might account for the enzyme's profound effects on PMN recruitment.

Of note, the proposed mechanism might also affect the affinity of other blood corpuscles toward the vessel wall as shown, for example, for red blood cells in vitro (supplemental Figure 8). However, MPO-mediated affinity of leukocytes to the vessel wall might be of particular significance, given that leukocytes subsequently adhere to endothelial cells and extravasate in an MPO-independent fashion.

In conclusion, these findings describe a novel mechanism underlying neutrophil motility and highlight a so-far unrecognized role for MPO in the recruitment of PMN, which is independent of

the enzyme's catalytic activity. Instead, PMN attraction is communicated by MPO's positive charge, an observation that calls for revisiting the role of MPO in innate immunity and the impact of physical forces on the recruitment of neutrophils.

Acknowledgments

The authors thank Klaus Ley, Barbara Walzog, Jürgen Schymeinsky, and Henry Bourne for insightful discussions, and Hartwig Wieboldt and Susanne Bierschenk for expert technical assistance.

This work was supported by the Deutsche Forschungsgemeinschaft (S.B. and T.K.R.), the Deutsche Herzstiftung (V.R.), the Werner Otto Stiftung (S.B.) and the Academy of Science Czech Republic (grant M200040908, L.K.). P.H. is supported by the Netherlands Organization for Scientific Research (VIDI 91766341).

Authorship

Contribution: A.K. designed the project, performed experiments, and wrote the manuscript; C.N. designed and performed the intravital microscopy experiments and wrote the manuscript; L.K., K.F., D.B., D.L., and K. Szocs provided suggestions on the project and performed experiments; H.-J.P. performed flow cytometric experiments; C.S. and U.S. were responsible for flow chamber experiments; P.H. designed animal experiments; P.G.F. synthesized MPO variants and made suggestions on the in vitro experiments; T.K.R., V.R., K. Sydow, H.-J.D., H.E., and T.M. provided suggestions on the project and revised the manuscript; and M.S. and S.B. supervised the project and wrote the manuscript.

Conflict-of-interest disclosure: The authors declare no competing financial interests.

Correspondence: Anna Klinke, PhD, Cardiovascular Research Center, University Hospital Hamburg Eppendorf and University Heart Center Hamburg, Department of Cardiology, Martinistr 52, Hamburg, Germany, 20246; e-mail: aklinke@uke.uni-hamburg.de; or Stephan Baldus, MD, Cardiovascular Research Center, University Hospital Hamburg Eppendorf and University Heart Center Hamburg, Department of Cardiology, Martinistr 52, Hamburg, Germany, 20246; e-mail: baldus@uke.uni-hamburg.de.

References

1. Nathan C. Neutrophils and immunity: challenges and opportunities. *Nat Rev Immunol.* 2006;6(3):173-182.
2. Naruko T, Ueda M, Haze K, van der Wal AC, et al. Neutrophil infiltration of culprit lesions in acute coronary syndromes. *Circulation.* 2002;106(23):2894-2900.
3. Askari AT, Brennan ML, Zhou X, et al. Myeloperoxidase and plasminogen activator inhibitor 1 play a central role in ventricular remodeling after myocardial infarction. *J Exp Med.* 2003;197(5):615-624.
4. Litt MR, Jeremy RW, Weisman HF, Winkelstein JA, Becker LC. Neutrophil depletion limited to reperfusion reduces myocardial infarct size after 90 minutes of ischemia. Evidence for neutrophil-mediated reperfusion injury. *Circulation.* 1989;80(6):1816-1827.
5. Ley K, Laudanna C, Cybulsky MI, Nourshargh S. Getting to the site of inflammation: the leukocyte adhesion cascade updated. *Nat Rev Immunol.* 2007;7(9):678-689.
6. Ridley AJ, Schwartz MA, Burridge K, et al. Cell migration: integrating signals from front to back. *Science.* 2003;302(5651):1704-1709.
7. Phillipson M, Heit B, Colarusso P, Liu L, Ballantyne CM, Kubes P. Intraluminal crawling of neutrophils to emigration sites: a molecularly distinct process from adhesion in the recruitment cascade. *J Exp Med.* 2006;203(12):2569-2575.
8. Baldus S, Eiserich JP, Mani A, et al. Endothelial transcytosis of myeloperoxidase confers specificity to vascular ECM proteins as targets of tyrosine nitration. *J Clin Invest.* 2001;108(12):1759-1770.
9. Eiserich JP, Baldus S, Brennan ML, et al. Myeloperoxidase, a leukocyte-derived vascular NO oxidase. *Science.* 2002;296(5577):2391-2394.
10. Sperandio M, Frommhold D, Babushkina I, et al. Alpha 2,3-sialyltransferase-IV is essential for L-selectin ligand function in inflammation. *Eur J Immunol.* 2006;36(12):3207-3215.
11. Pries AR. A versatile video image analysis system for microcirculatory research. *Int J Microcirc Clin Exp.* 1988;7(4):327-345.
12. Long DS, Smith ML, Pries AR, Ley K, Damiano ER. Microviscometry reveals reduced blood viscosity and altered shear rate and shear stress profiles in microvessels after hemodilution. *Proc Natl Acad Sci U S A.* 2004;101(27):10060-10065.
13. Frommhold D, Ludwig A, Bixel MG, et al. Sialyltransferase ST3Gal-IV controls CXCR2-mediated firm leukocyte arrest during inflammation. *J Exp Med.* 2008;205(6):1435-1446.
14. Zederbauer M, Furtmüller PG, Ganster B, Moguilevsky N, Obinger C. The vinyl-sulfonium bond in human myeloperoxidase: impact on compound I formation and reduction by halides and thiocyanate. *Biochem Biophys Res Commun.* 2007;356(2):450-456.
15. Kessenbrock K, Frohlich L, Sixt M, et al. Proteinase 3 and neutrophil elastase enhance inflammation in mice by inactivating antiinflammatory progranulin. *J Clin Invest.* 2008;118(7):2438-2447.
16. Mitchison TJ, Cramer LP. Actin-based cell motility and cell locomotion. *Cell.* 1996;84(3):371-379.
17. Xu J, Wang F, Van Keymeulen A, et al. Divergent signals and cytoskeletal assemblies regulate self-organizing polarity in neutrophils. *Cell.* 2003;114(2):201-214.
18. Zaslaver A, Feniger-Barish R, Ben-Baruch A. Actin filaments are involved in the regulation of trafficking of two closely related chemokine receptors, CXCR1 and CXCR2. *J Immunol.* 2001;166(2):1272-1284.
19. Willeke T, Scharffetter-Kochanek K, Gaehtgens P, Walzog B. A role for beta2 integrin CD11/CD18-mediated tyrosine signaling in extravasation of human polymorphonuclear neutrophils. *Biorheology.* 2001;38(2-3):89-100.
20. Andrews PC, Krinsky NI. The reductive cleavage of myeloperoxidase in half, producing enzymically active hemi-myeloperoxidase. *J Biol Chem.* 1981;256(9):4211-4218.
21. Matthijsen RA, Huugen D, Hoebers NT, et al. Myeloperoxidase is critically involved in the induction of organ damage after renal ischemia reperfusion. *Am J Pathol.* 2007;171(6):1743-1752.
22. Frommhold D, Mannigel I, Schymeinsky J, et al. Spleen tyrosine kinase Syk is critical for sustained leukocyte adhesion during inflammation in vivo. *BMC Immunol.* 2007;8:31.
23. Ghitescu L, Fixman A. Surface charge distribution on the endothelial cell of liver sinusoids. *J Cell Biol.* 1984;99(2):639-647.
24. Haldenby KA, Chappell DC, Winlove CP, Parker KH, Firth JA. Focal and regional variations in the composition of the glycocalyx of large vessel endothelium. *J Vasc Res.* 1994;31(1):2-9
25. Klinger M, Kramarz S, Wendycz D, Kopec W. Different erythrocyte and platelet surface electric charge in various types of glomerulonephritis. *Nephrol Dial Transplant.* 1997;12(4):707-712.
26. Janoff A, Zweifach BW. Adhesion and Emigration of Leukocytes Produced by Cationic Proteins of Lysosomes. *Science.* 1964;144:1456-1458.
27. Fehr J, Jacob HS. In vitro granulocyte adherence and in vivo margination: two associated complement-dependent functions. Studies based on the acute neutropenia of filtration leukophoresis. *J Exp Med.* 1977;146(3):641-652.
28. Gallin JI, Durocher JR, Kaplan AP. Interaction of leukocyte chemotactic factors with the cell surface. I. Chemotactic factor-induced changes in human granulocyte surface charge. *J Clin Invest.* 1975;55(5):967-974.
29. Gallin JI. Degranulating stimuli decrease the neagative surface charge and increase the adhesiveness of human neutrophils. *J Clin Invest.* 1980;65(2):298-306.
30. Schaack TM, Takeuchi A, Spilberg I, Persellin RH. Alteration of polymorphonuclear leukocyte surface charge by endogenous and exogenous chemotactic factors. *Inflammation.* 1980;4(1):37-44.
31. Constantinescu AA, Vink H, Spaan JA. Endothelial cell glycocalyx modulates immobilization of leukocytes at the endothelial surface. *Arterioscler Thromb Vasc Biol.* 2003;23(9):1541-1547.
32. Woodman RC, Johnston B, Hickey MJ, Teoh D, Reinhardt P, et al. The functional paradox of CD43 in leukocyte recruitment: a study using CD43-deficient mice. *J Exp Med.* 1998;188(11):2181-2186.
33. Baldus S, Rudolph V, Roiss M, Ito WD, Rudolph TK, et al. Heparins increase endothelial nitric oxide bioavailability by liberating vessel-immobilized myeloperoxidase. *Circulation.* 2006;113(15):1871-1878.
34. Reitsma S, Slaaf DW, Vink H, van Zandvoort MA, oude Egbrink MG. The endothelial glycocalyx: composition, functions, and visualization. *Pflugers Arch.* 2007;454(3):345-359.
35. Peterson MW, Stone P, Shasby DM. Cationic neutrophil proteins increase transendothelial albumin movement. *J Appl Physiol.* 1987;62(4):1521-1530.
36. Dull RO, Dinavahi R, Schwartz L, Humphries DE, Berry D, et al. Lung endothelial heparan sulfates

mediate cationic peptide-induced barrier dysfunction: a new role for the glycocalyx. *Am J Physiol Lung Cell Mol Physiol.* 2003;285(5):L986-L995.

37. Engelhardt B, Wolburg H. Mini-review: Transendothelial migration of leukocytes: through the front door or around the side of the house? *Eur J Immunol.* 2004;34(11):2955-2963.
38. Johansson MW, Patarroyo M, Oberg F, Siegbahn A, Nilsson K. Myeloperoxidase mediates cell adhesion via the alpha M beta 2 integrin Mac-1, CD11b/CD18. *J Cell Sci.* 1997;110 (Pt 9):1133-1139.
39. Lau D, Mollnau H, Eiserich JP, et al. Myeloperoxidase mediates neutrophil activation by association with CD11b/CD18 integrins. *Proc Natl Acad Sci U S A.* 2005;102(2):431-436.
40. Cai TQ, Wright SD. Human leukocyte elastase is an endogenous ligand for the integrin CR3 CD11b/CD18, Mac-1, alpha M beta 2 and modulates polymorphonuclear leukocyte adhesion. *J Exp Med.* 1996;184(4):1213-1223.
41. David A, Kacher Y, Specks U, Aviram I. Interaction of proteinase 3 with CD11b/CD18 beta2 integrin on the cell membrane of human neutrophils. *J Leukoc Biol.* 2003;74(4):551-557.
42. Asako H, Kurose I, Wolf RE, Granger DN. Mechanisms of lactoferrin-induced leukocyte-endothelial cell adhesion in postcapillary venules. *Microcirculation.* 1994;1(1):27-34.
43. Morgan DM, Larvin VL, Pearson JD. Biochemical characterisation of polycation-induced cytotoxicity to human vascular endothelial cells. *J Cell Sci.* 1989;94(Pt 3):553-559.
44. Daphna EM, Michaela S, Eynat P, Irit A, Rimon S. Association of myeloperoxidase with heparin: oxidative inactivation of proteins on the surface of endothelial cells by the bound enzyme. *Mol Cell Biochem.* 1998;183(1-2):55-61.

nature COMMUNICATIONS

ARTICLE

Received 15 Sep 2014 | Accepted 27 Jan 2015 | Published 2 Apr 2015

DOI: 10.1038/ncomms7416 OPEN

Sphingosine-1-phosphate receptor 3 promotes leukocyte rolling by mobilizing endothelial P-selectin

Claudia Nussbaum[1,2,*], Sarah Bannenberg[3,*], Petra Keul[3], Markus H. Gräler[4], Cassiano F. Gonçalves-de-Albuquerque[1,5], Hanna Korhonen[6], Karin von Wnuck Lipinski[3], Gerd Heusch[3], Hugo C. de Castro Faria Neto[5], Ina Rohwedder[1], Joachim R. Göthert[7], Vysakh Pushpa Prasad[8], Günter Haufe[8], Baerbel Lange-Sperandio[2], Stefan Offermanns[6], Markus Sperandio[1,*] & Bodo Levkau[3,*]

Sphingosine-1-phosphate (S1P) participates in inflammation; however, its role in leukocyte rolling is still unclear. Here we use intravital microscopy in inflamed mouse cremaster muscle venules and human endothelial cells to show that S1P contributes to P-selectin-dependent leukocyte rolling through endothelial S1P receptor 3 ($S1P_3$) and $G\alpha_q$, PLCβ and Ca^{2+}. Intra-arterial S1P administration increases leukocyte rolling, while $S1P_3$ deficiency or inhibition dramatically reduces it. Mast cells involved in triggering rolling also release S1P that mobilizes P-selectin through $S1P_3$. Histamine and epinephrine require $S1P_3$ for full-scale effect accomplishing it by stimulating sphingosine kinase 1 (Sphk1). In a counter-regulatory manner, $S1P_1$ inhibits cAMP-stimulated Sphk1 and blocks rolling as observed in endothelial-specific $S1P_1^{-/-}$ mice. In agreement with a dominant pro-rolling effect of $S1P_3$, FTY720 inhibits rolling in control and $S1P_1^{-/-}$ but not in $S1P_3^{-/-}$ mice. Our findings identify S1P as a direct and indirect contributor to leukocyte rolling and characterize the receptors mediating its action.

[1] Walter Brendel Center, Ludwig Maximilians Universität München, 81377 München, Germany. [2] Dr v. Haunersches Children's Hospital, Ludwig Maximilians University München, 80337 München, Germany. [3] Institute of Pathophysiology, West German Heart and Vascular Center, University Hospital Essen, University of Duisburg-Essen, 45122 Essen, Germany. [4] Department of Anesthesiology and Intensive Care Medicine, Center for Sepsis Control and Care, Center for Molecular Biomedicine, University Hospital Jena, 07745 Jena, Germany. [5] Laboratorio de Imunofarmacologia, Instituto Oswaldo Cruz, Fiocruz, Rio de Janeiro 21040900, Brazil. [6] Max Planck Institute for Heart and Lung Research, 61231 Bad Nauheim, Germany. [7] Department of Hematology, University Hospital Essen, University of Duisburg-Essen, 45122 Essen, Germany. [8] Organisch-Chemisches Institut, Westfälische Wilhelms-Universität Münster, 48149 Münster, Germany. * These authors contributed equally to this work. Correspondence and requests for materials should be addressed to M.S. (email: markus.sperandio@lmu.de) or to B.L. (email: bodo.levkau@uni-due.de).

Sphingosine-1-phospate (S1P) is a bioactive lysophospholipid with important functions in the immune and cardiovascular systems and has been implicated in different aspects of inflammatory disorders[1]. High S1P concentrations have been measured locally at inflammatory sites[2,3], where it is generated by sphingosine kinases activated through inflammatory cytokines, lipopolysaccharide (LPS) or thrombin. This suggests a role for S1P in the propagation of the inflammatory response[4]. In contrast, S1P opposes the pathologically increased endothelial permeability common to all inflammatory processes and prevents vascular leakage caused by LPS, thrombin or platelet-activating factor[5–7]. There is also evidence both for stimulatory and inhibitory effects of S1P on leukocyte recruitment in inflammation. In favour of a pro-inflammatory role, exogenous S1P induces endothelial vascular cell adhesion molecule 1 (VCAM-1) and E-selectin, while endogenous S1P mediates the stimulatory effect of tumor-necrosis factor (TNF)-α and LPS on adhesion molecules, which is suppressed by $S1P_1$ short interfering RNA[8–10]. In support, chronic overexpression of sphingosine kinase 1 augments VCAM-1 and E-selectin expression and enhances neutrophil adhesion after TNF-α[11]. In contrast, both S1P and $S1P_1$ agonists have been demonstrated to inhibit TNF-α-induced endothelial adhesion molecule expression and adherence of inflammatory cells by interfering with endothelial NF-κB and stimulating nitric oxide production[12–14]. Several explanations have been put forward for these apparent discrepancies such as the assumption that S1P receptors may be differentially expressed among endothelial beds, and that the wide range of S1P concentrations employed in the individual studies may have led to contrary effects as observed for S1P in other systems[15]. However, in all these studies the focus has been on $S1P_1$, while any involvement of S1P receptor 3 ($S1P_3$) has not been addressed.

In contrast to the effects of S1P on firm leukocyte adhesion, its role on leukocyte rolling—the crucial initial step of inflammatory cell recruitment—has not been investigated in detail. Recently, sphingosine kinase-1 has been shown to contribute to histamine-induced leukocyte rolling, but the mechanism of action has remained elusive[16]. In general, leukocyte capture and rolling is mediated by the selectin family of adhesion molecules consisting of three selectins: L-, E- and P-selectin[17,18]. L-selectin is expressed on most leukocytes and mediates leukocyte capture and rolling through binding to selectin ligands found on high endothelial venules of lymphoid organs. E-selectin and P-selectin are expressed on the activated vascular endothelium during inflammation and mediate rolling through binding to carbohydrate moieties of selectin ligands on leukocytes[17,18]. Among the selectins, P-selectin contributes to disease pathology in many experimental models including myocardial and renal infarction, thrombosis, stroke, atherosclerosis, cerebral malaria and sickle cell disease[19], as has been shown using P-selectin-blocking antibodies and knockout strategies in mouse, feline and baboon models[20–23].

We have recently identified leukocyte recruitment defects in $S1P_3^{-/-}$ mice in atherosclerosis and peritoneal inflammation that were caused by both haematopoietic and non-haematopoietic $S1P_3$ deficiency[3]. In addition, treatment with the S1P analogue FTY720 severely reduced leukocyte recruitment into the inflamed peritoneum[3]. Currently, it is controversial if S1P in general and $S1P_3$ in particular affect leukocyte rolling.

In this study, we address this issue by studying P-selectin-dependent leukocyte rolling in surgically prepared post-capillary venules of the mouse cremaster muscle *in vivo*. These studies are complemented by experiments in a novel *in vitro* system to investigate the mechanisms of the rapid P-selectin mobilization that occurs within minutes in endothelial cells and stems from the exocytosis of Weibel–Palade bodies. Our results demonstrate a unique role of S1P and $S1P_3$ in P-selectin-dependent rolling both by direct action as well as by contributing to P-selectin mobilization by other agonists.

Results

$S1P_3$ deficiency and inhibition reduce leukocyte rolling. To examine whether $S1P_3$ plays a role in P-selectin-dependent leukocyte rolling *in vivo*, we employed intravital microscopy to monitor rolling in post-capillary venules of the surgically exteriorized mouse cremaster muscle[24,25]. In this model, profound spontaneous leukocyte rolling is induced by the surgical preparation of the cremaster (hence termed trauma), which exclusively depends on the rapid mobilization of P-selectin from endothelial Weibel–Palade bodies to the luminal surface in its initial phase (<45 min after exteriorization of the cremaster muscle)[17,26–28]. Elegant studies from the 1990s have shown that the endothelial P-selectin mobilization is in large part caused by activation products of tissue mast cells released upon mechanical manipulation during surgery[29]. Here we employed this model to study leukocyte rolling in $S1P_3^{-/-}$ mice and observed that their rolling flux fraction (as a measure of rolling) was greatly diminished compared with C57Bl6 controls (Fig. 1a). Neither microvascular/haemodynamic conditions nor leukocyte rolling velocities differed between groups excluding any bias by these variables (Table 1 and Supplementary Fig. 1). Systemic application of a P-selectin-blocking antibody completely abrogated leukocyte rolling in both genotypes (Fig. 1a) confirming the dependence of rolling on P-selectin in this model and both genotypes, respectively. In addition, whole-mount immunohistochemistry for intravascular P-selectin clearly showed the appearance of luminal P-selectin in controls but not in $S1P_3^{-/-}$ mice (Fig. 1a). Of note, $S1P_3$-deficient leukocytes had no intrinsic defect in rolling as we determined in an *ex vivo* flow chamber system[30], where blood was diverted from the carotid artery into microflow chambers coated with immobilized murine P-selectin[31] (Fig. 1b). We also assessed cell surface expression of P-selectin glycoprotein ligand-1 as the main, if not only, functional P-selectin ligand on neutrophils, and found no differences between $S1P_3^{-/-}$ and *C57Bl6* mice (Supplementary Table 1).

We next tested the effect of TY-52156, a highly specific $S1P_3$ inhibitor[32], on leukocyte rolling in C57Bl6 mice. As TY-52156 is not commercially available, we synthesized it according to published protocols[32] and confirmed its specificity for $S1P_3$ in comparison to $S1P_1$ (Supplementary Figs 2,3). Intraperitoneal administration of TY-52156 (1.25 mg per kg body weight) 30 min before the experiment leads to a dramatic reduction in leukocyte rolling (Fig. 1c). To test whether the opposite–stimulation of the vasculature by exogenous S1P–would increase rolling, we injected S1P directly into the carotid artery (30 μg per kg body weight) in *C57Bl6* mice and measured leukocyte rolling immediately thereafter. Indeed, we observed that rolling was dramatically enhanced by S1P (Fig. 1d).

$S1P_3$ induces P-selectin and rolling via G_q, PLC and Ca^{2+}. Exposure of cell surface P-selectin on luminal endothelial cells is the prerequisite for trauma-induced leukocyte rolling in the experimental model we have used here[17,26–28]. To pursue the mechanism by which S1P and $S1P_3$ affect P-selectin mobilization, we established an assay for quantitative assessment of cell surface P-selectin using flow cytometry in human umbilical endothelial cells (HUVECs) as the only system applicable for such studies. Nevertheless, HUVECs are still extremely difficult to work with in respect to studying P-selectin as they express it only under certain culture conditions and lose ability for mobilizing it already after one to two passages. Nevertheless, we successfully established the

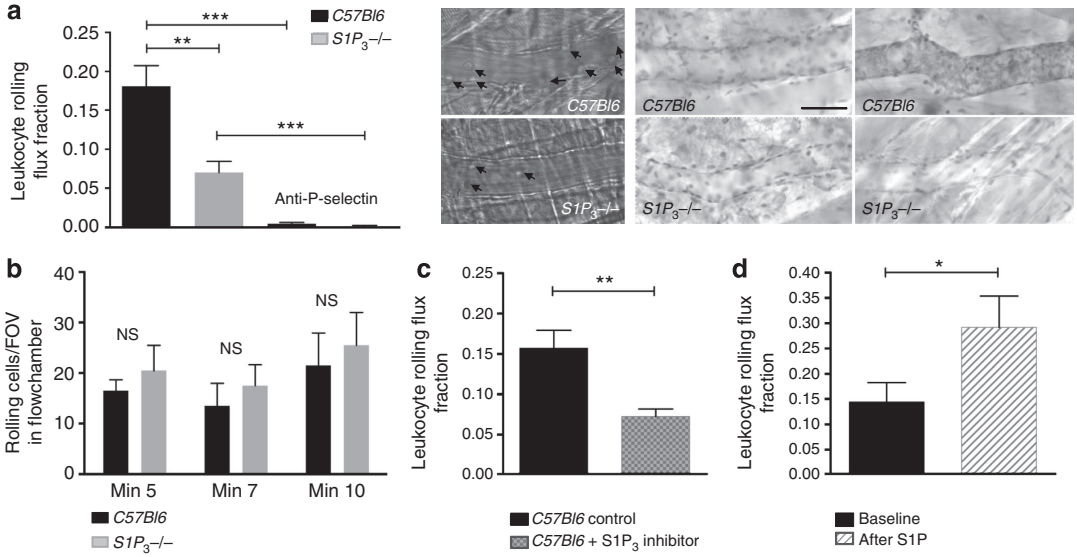

Figure 1 | Leukocyte rolling is reduced in $S1P_3^{-/-}$ mice and after $S1P_3$ blockade, respectively, and is enhanced by S1P administration. Leukocyte rolling was quantified in postcapillary venules of the cremaster muscle of (**a**) $S1P_3^{-/-}$ mice ($n=5$) and *C57Bl6* controls ($n=6$). Rolling was abolished by systemic injection of a P-selectin-blocking antibody in both groups. Middle: representative snap shot images of rolling leukocytes (arrows) are shown. Right: representative whole-mount immunohistochemistry for P-Selectin after *in vivo* injection of an anti-P-selectin antibody (left: no staining in uninjured cremaster, right: luminal P-selectin staining in the contralateral exteriorized cremaster). Scale bar, 40 μm. (**b**) Unaltered rolling of $S1P_3^{-/-}$ leukocytes on immobilized P-selectin. Microflow chambers were coated with recombinant murine P-selectin and perfused with arterial blood diverted from the carotid artery of *C57Bl6* and $S1P_3^{-/-}$ mice ($n=3$ each) for the indicated times. The number of rolling cells was quantified per field of view (FOV). (**c**) Rolling in *C57Bl6* mice with ($n=4$) and without ($n=5$) the $S1P_3$ inhibitor TY-52156 (1.25 mg kg^{-1} intraperitoneally (i.p.) 30 min before experiment). (**d**) Rolling in *C57Bl6* mice at baseline and immediately after S1P injection into the carotid artery (30 μg kg^{-1}, $n=5$). Quantitative data are presented as mean ± s.e.m. Significance was established using a Wilcoxon rank sum test or a paired two-tailed Student's *t*-test. In all experiments: $^*P<0.05$; $^{**}P<0.01$; $^{***}P<0.001$.

assay and validated it extensively using histamine and H1 and H2 receptor antagonists (Supplementary Fig. 4). Using this assay, we observed that stimulation of HUVEC with 1 μM S1P resulted in an extremely rapid (within 5 min) appearance of P-selectin on the cell surface (Fig. 2a). In contrast, the agonist of the $S1P_1$ receptor SEW2871 was ineffective (Fig. 2a). In agreement with a role of $S1P_3$ in the process, preincubation with 10 μM TY-52156 for 30 min substantially diminished P-selectin mobilization by S1P (Fig. 2a).

We then addressed the signalling pathways downstream of $S1P/S1P_3$ responsible for P-selectin mobilization. Phospholipase C (PLC) and Ca^{2+} are known to play a role in the exocytosis of Weibel–Palade bodies[33], and S1P has been shown to activate PLC in CHO cells overexpressing $S1P_3$ (ref. 34,35). Thus, we added the PLC inhibitor U73122 (3 μM) 2 min before S1P stimulation and observed a clear reduction in P-selectin mobilization (Fig. 2b). To address the role of Ca^{2+}, we depleted internal Ca^{2+} pools by adding thapsigargin (3 μM) for 5 min before stimulation with S1P, while simultaneously preventing the extracellular Ca^{2+} influx by EGTA (3 mM) added for the last minute. This treatment substantially suppressed P-selectin mobilization (Fig. 2b).

Although $S1P_3$ couples to three G proteins (G_q, G_i and $G_{12/13}$), the predominant signalling pathway it exercises is through G_q (ref. 36). To test for an involvement of G_q in leukocyte rolling in our model in general, we employed mice deficient for G_q in endothelial cells on a global G_{11}-deficient background ($G_{q/11}-/-$ mice)[37]. We observed them to have a substantial reduction in leukocyte rolling (Fig. 2c). Administration of TY-52156 did not reduce rolling any further in $G_{q/11}-/-$ mice (Fig. 2c), suggesting that under normal circumstances $S1P_3$ enhances rolling through G_q.

FTY720 and S1P lyase blockade suppress rolling by impacting on $S1P_3$. On the basis of our results so far, we hypothesized that downregulation of $S1P_3$ by FTY720 would inhibit leukocyte rolling to a similar extent as does $S1P_3$ deficiency or a $S1P_3$ inhibitor. Furthermore, if $S1P_3$ were the only receptor inducing P-selectin mobilization by S1P, FTY720 should not decrease rolling any further in $S1P_3^{-/-}$ mice. Indeed, administration of 1.25 mg per kg FTY720 either 30 min or 24 h before the experiment dramatically attenuated leukocyte rolling (Fig. 3a). In agreement with our second hypothesis, we observed no additional inhibition of rolling by FTY720 in $S1P_3^{-/-}$ mice (Fig. 3b). Finally, treatment with the S1P lyase inhibitor 4-deoxypyridoxine (DOP) that elevates plasma and tissue S1P and downregulates all S1P receptors[38] also inhibited rolling (Fig. 3c). Rolling velocities did not differ significantly between the experimental groups (Supplementary Fig. 1), and P-selectin-mediated rolling was independent of putative DOP effects on plasma or leukocytes as no differences in rolling were observed on immobilized P-selectin (Supplementary Fig. 5).

We then went further to examine the effect of FTY720 on P-selectin mobilization *in vitro*. Pretreatment of HUVEC with the active, phosphorylated form of FTY720 (pFTY720, 10 μM for 30 min) almost completely abolished S1P-induced mobilization of P-selectin (Fig. 3d). PhosphoFTY720 itself (1 μM) had only a minor, almost negligible effect on P-selectin compared with 1 μM S1P after 5 min and no effect at all after 30 min (a time when the S1P effect was still clearly visible; Fig. 3d). This may seem surprising in light of the agonistic effect of pFTY720 known for all S1P receptors except $S1P_2$ before their subsequent cell surface downregulation. However, we have previously shown that pFTY720 activates only the G_i and not the G_q signalling pathway of $S1P_3$ and also inhibits G_q-transmitted $S1P_3$ signalling by native S1P[39]. Here we observed something very similar in respect to P-selectin: addition of a 10-fold higher concentration of pFTY720 simultaneously with S1P resulted in a clear inhibition of S1P-induced P-selectin mobilization (Fig. 3d). In agreement, addition of S1P or pFTY720 for 30 min to another cellular system

Table 1 | Haemodynamic parameters of mouse cremaster muscle experiments.

Mouse strain	Treatment	Fig.	Mice (*n*)	Venules	Diameter (μm)	Centreline velocity (μm s^{-1})	Shear rate (s^{-1})	WBC ($\times 10^3$ μl^{-1})
C57Bl6	*None*	1a	6	21	30.0 ± 1.1	1,876 ± 215	1,562 ± 160	5,704 ± 622
S1P$_3^{-/-}$			5	20	28.8 ± 1.4	1,885 ± 182	1,449 ± 203	8,060 ± 983
C57Bl6	*None*	1c	5	16	33.6 ± 1.6	2,181 ± 324	1,693 ± 319	6,659 ± 192
C57B6	*S1P$_3$i*		4	17	29.9 ± 1.0	1,861 ± 183	1,614 ± 138	5,808 ± 633
C57Bl6	*None*	1d	5	5	34.9 ± 1.6	1,638 ± 406	1,150 ± 270	5,032 ± 613
	S1P		5	5	34.0 ± 1.8	1,427 ± 408	1,006 ± 248	4,144 ± 367
C57Bl6	*None*	2c	4	17	29.3 ± 1.9	2,635 ± 195	2,303 ± 188	5,633 ± 254
$G_{q/11}^{-/-}$	*None*		5	22	30.8 ± 1.3	2,973 ± 162	2,445 ± 160	6,405 ± 163
$G_{q/11}^{-/-}$	*S1P$_3$i*		4	22	29.7 ± 1.2	1,623 ± 113*	1,367 ± 93*	3,348 ± 1,076
C57Bl6	*None*	3a	5	26	33.4 ± 1.1	2,017 ± 163	1,524 ± 131	7,043 ± 899
	FTY 30 min		6	36	34.3 ± 0.8	1,857 ± 127	1,380 ± 94	4,270 ± 203
	FTY 24 h		6	35	32.5 ± 1.0	1,540 ± 100	1,178 ± 71	1,110 ± 152*
C57Bl6	*None*†	3b	6	21	30.0 ± 1.1	1,876 ± 215	1,562 ± 160	5,704 ± 622
	FTY 30 min		8	32	29.4 ± 0.6	2,419 ± 203	2,033 ± 175	7,147 ± 343
S1P$_3^{-/-}$	*None*†		5	20	28.8 ± 1.4	1,885 ± 182	1,449 ± 203	8,060 ± 983
	FTY 30 min		5	19	29.2 ± 0.6	2,384 ± 196	2,014 ± 185*	6,998 ± 937
C57Bl6	*Normal diet*	3c	4	17	30.3 ± 0.7	1,894 ± 185	1,510 ± 132	4,819 ± 1,090
	DOP diet		5	23	30.3 ± 0.9	1,839 ± 186	1,476 ± 125	2,415 ± 297
C57Bl6	*None*	4c	4	16	33.6 ± 1.0	1,613 ± 145	1,178 ± 101	8,143 ± 548
Sphk1$^{-/-}$			4	15	33.7 ± 1.7	1,709 ± 217	1,420 ± 241	7,760 ± 299
C57Bl6	*None*‡	5e	5	26	33.4 ± 1.1	2,017 ± 163	1,524 ± 131	7,043 ± 899
	Forskolin		5	21	30.4 ± 1.2	2,143 ± 163	1,768 ± 147	3,382 ± 579*
$S1P_1^{SCL\text{-}Cre\text{-}ERT}$ Cre$^-$	*None*	7a	9	32	30.1 ± 0.8	1,778 ± 153	1,465 ± 127	3,250 ± 567
$S1P_1^{SCL\text{-}Cre\text{-}ERT}$ Cre$^+$			9	35	29.1 ± 0.6	1,849 ± 172	1,546 ± 136	2,238 ± 289
$S1P_1^{SCL\text{-}Cre\text{-}ERT}$ Cre$^-$	*None*§	7b	9	32	30.1 ± 0.8	1,778 ± 153	1,465 ± 127	3,250 ± 567
	FTY720		3	12	27.7 ± 0.9	1,675 ± 209	1,488 ± 184	2,280 ± 742
$S1P_1^{SCL\text{-}Cre\text{-}ERT}$ Cre$^+$	*None*§		9	35	29.1 ± 0.6	1,849 ± 172	1,546 ± 136	2,238 ± 289
	FTY720		4	16	27.8 ± 0.9	2,237 ± 232	1,999 ± 213	3,015 ± 459

DOP, 4-deoxypyridoxine; S1P, sphingosine-1-phosphate; SCL, stem cell leukaemia; WBC, white blood cell.
*$P<0.05$ versus respective control ('none').
†Data are identical to Fig. 1a ('none').
‡Data are identical to Fig. 3a ('none').
§Data are identical to Fig. 7a ('none').

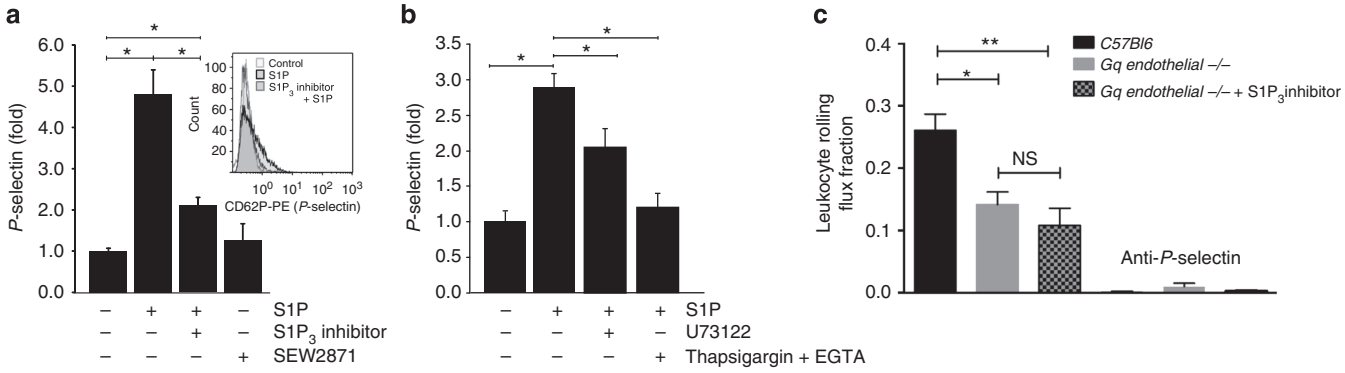

Figure 2 | S1P mobilizes P-selectin in endothelial cells and induces rolling through a S1P$_3$/G$_q$/PLC/Ca^{2+} pathway. (**a**) HUVECs were stimulated with S1P (1 μM) for 5 min in the presence or absence of the S1P$_3$ inhibitor TY-52156 (10 μM) or stimulated with the S1P$_1$ agonist SEW2871 (1 μM). P-selectin surface expression was analysed using flow cytometry. Data shown are from at least three independent experiments. Representative histogram is shown as inset. (**b**) HUVECs were stimulated with S1P (1 μM) in the presence or absence of U73122 (3 μM for 2 min) or thapsigargin (3 μM for 5 min) in combination with EGTA (3 mM for the last 1 min). P-selectin was analysed using flow cytometry 5 min after the addition of S1P. Data shown are from at least three independent experiments. (**c**) Leukocyte rolling was quantified in postcapillary venules of the cremaster muscle of $G_{q/11}-/-$ mice (Gq endothelial $-/-$) in the presence ($n=4$) or absence ($n=5$) of the S1P$_3$ inhibitor TY-52156 (1.25 mg kg^{-1} i.p. 30 min before the experiment) and in controls ($n=4$). P-selectin-blocking antibody was injected to confirm complete dependence of rolling on P-selectin. Quantitative data are presented as mean ± s.e.m. Significance was established using a paired two-tailed Student's *t*-test or a Kruskal–Wallis analysis of variance (ANOVA) on ranks. *$P<0.05$; **$P<0.01$.

— S1P$_3$-overexpressing CHO cells — followed by removal and subsequent (30 min later) S1P stimulation abolished S1P$_3$-dependent signalling such as Erk MAPK activation (Supplementary Fig. 6).

S1P$_3$ conveys part of the P-selectin mobilization by histamine. P-selectin mobilization and consecutive leukocyte rolling in the trauma-stimulated cremaster muscle venules that we have examined here are known to be predominantly mediated by

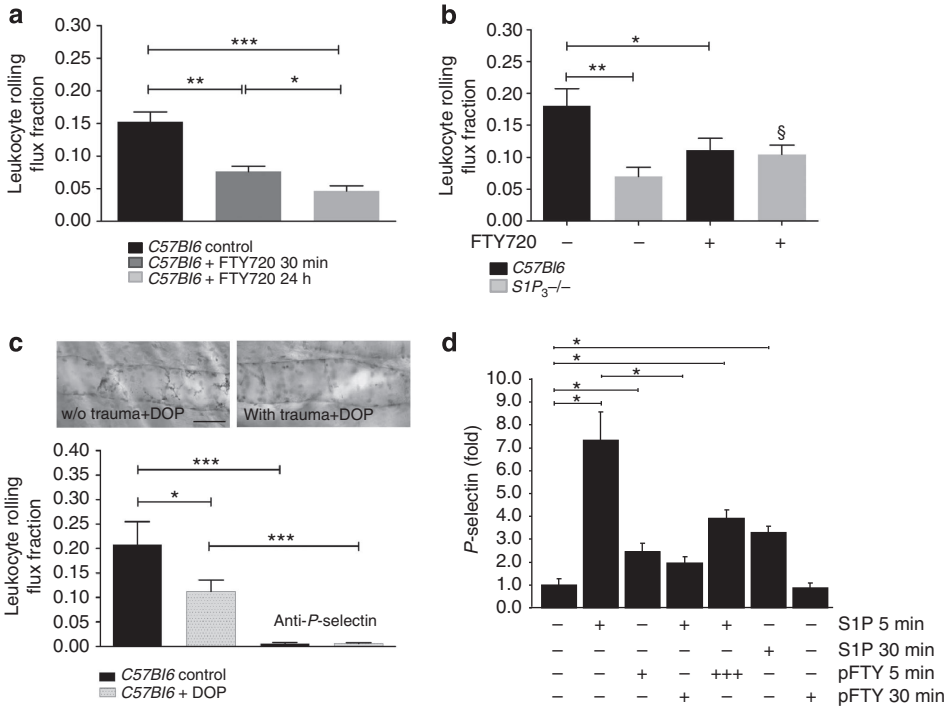

Figure 3 | FTY720 inhibit leukocyte rolling and P-selectin mobilization by S1P by interfering with $S1P_3$. Reduced rolling after S1P lyase inhibition. (**a**) Leukocyte rolling in *C57Bl6* mice treated without ($n=5$) or with 1.25 mg kg^{-1} FTY720 i.p. either 30 min or 24 h ($n=6$ each) before experiment. (**b**) Leukocyte rolling in *C57Bl6* ($n=8$) and $S1P_3^{-/-}$ mice ($n=5$) treated with 1.25 mg kg^{-1} i.p. FTY720 30 min before experiment. Untreated *C57Bl6* and $S1P_3^{-/-}$ mice served for comparison ($n=6$ and 5). (**c**) Leukocyte rolling in *C57Bl6* mice treated with ($n=5$) and without the S1P lyase inhibitor DOP ($n=4$). Top: whole-mount immunohistochemistry for P-Selectin after *in vivo* injection of an anti-P-selectin antibody shows the lack of P-selectin mobilization in the exteriorized traumatized cremaster (right) compared with the contralateral uninjured one (left). Scale bar, 40 μm. (**d**) HUVECs were stimulated with S1P (1 μM) or pFTY720 (1 μM) for 5 and 30 min with and without pFTY720 preincubation (1 μM) for 30 min. In some experiments, pFTY720 (10 μM) and S1P (1 μM) were added simultaneously for 5 min. '+ + +' indicates the 10-fold higher pFTY720 concentration that was added simultaneously with S1P in this case. P-selectin surface expression was analysed by flow cytometry. Data are from three independent experiments. Quantitative data are presented as mean ± s.e.m. Significance was established using a Kruskal–Wallis ANOVA on ranks or a Wilcoxon rank sum test, or a paired two-tailed Student's *t*-test (**d**). $P<0.05$; $^{**}P<0.01$; $^{***}P<0.001$; §<0.05 between $S1P_3^{-/-}$ and $S1P_3^{-/-}$ with FTY720 in (**b**).

products of tissue mast cells activated upon mechanical manipulation during surgery[29]. Of these products, histamine accounts for approximately half of the effect on rolling as elegantly shown using H1 and H2 histamine receptor antagonists[29]. Recently, Sun *et al.*[16] demonstrated that histamine superfusion of the cremaster muscle induces leukocyte rolling dependent on sphingosine kinase 1 (Sphk1), but the mechanism has remained unidentified. We asked the question whether $S1P_3$ might be involved in histamine-induced P-selectin mobilization. To tackle this, we first titrated down the histamine concentration from 25 μM (routinely used in the vast majority of the literature) to a 100-fold lower concentration of 0.25 μM (Fig. 4a). This much lower histamine concentration still leads to a substantial P-selectin mobilization in HUVEC within 5 min (Fig. 4a). The well-characterized sphingosine kinase inhibitor 4-[[4-(4-chlorophenyl)-2-thiazolyl]amino]-phenol (SKi, 25 μM (ref. 40)) suppressed P-selectin mobilization at both histamine concentrations, but was particularly effective at the lower one (Fig. 4a). Remarkably, administration of exogenous S1P in addition to SKi partially restored P-selectin mobilization by histamine (Fig. 4a), arguing for a S1P receptor conveying Sphk1-mediated, histamine-dependent P-selectin mobilization. We then tested whether the responsible S1P receptor may be $S1P_3$. Indeed, preincubation with the $S1P_3$ inhibitor TY-52156 for 30 min dramatically reduced P-selectin mobilization by 0.25 μM histamine (Fig. 4b). Thus, the reduction of histamine to lower and presumably more physiological concentrations in our model allowed us to assign part of its P-selectin-mobilizing effect to the engagement of $S1P_3$ through endogenous Sphk1-generated S1P. Finally, we observed that leukocyte rolling was substantially reduced in cremaster muscle venules of $Sphk1^{-/-}$ mice *in vivo* compared with *C57Bl6* controls (Fig. 4c). Altogether, our data suggest that part of the histamine effect on P-selectin-mediated rolling is mediated by its activation of Sphk1, production of endogenous S1P and subsequent stimulation of P-selectin mobilization by endothelial $S1P_3$.

cAMP induces P-selectin and rolling through Sphk1 and $S1P_3$. Several other agents besides histamine such as thrombin, vasopressin receptor agonists, purine nucleotides and epinephrine are well known to induce rapid P-selectin mobilization[41]. Many of them elevate intracellular cAMP through activation of the G_s/adenylate cyclase (AC) pathway; however, the exact mechanisms leading to subsequent P-selectin mobilization are not entirely clear. In our hands, epinephrine (9 μM) potently induced P-selectin mobilization in HUVEC (Fig. 5a). Remarkably, the $S1P_3$ inhibitor TY-52156 substantially albeit not entirely suppressed epinephrine-induced P-selectin mobilization (Fig. 5a). Assuming that the cAMP/AC pathway is involved, we applied forskolin (10 μM) as an established tool to directly stimulate AC. Indeed, forskolin potently mobilized P-selectin mobilization in HUVEC (Fig. 5b). Interestingly, this was clearly inhibited by $S1P_3$ inhibitor TY-52156 (Fig. 5b). These

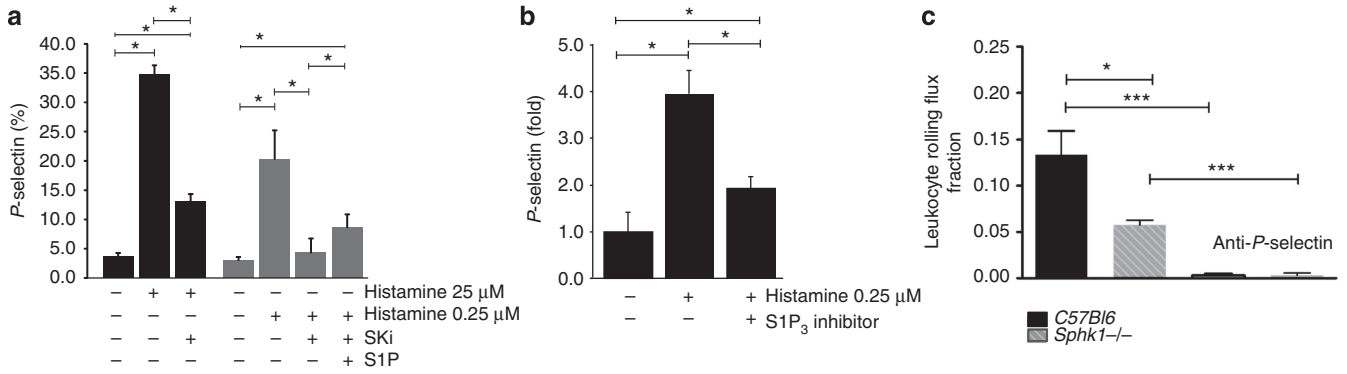

Figure 4 | $S1P_3$ and Sphk1 mediate in part the effect of histamine on P-selectin mobilization and leukocyte rolling. (**a**) HUVECs were stimulated with two histamine concentrations (0.25 and 25 µM) in the presence or absence of SKi (25 µM) or SKi + S1P (1 µM) for 5 min as indicated, and cell surface P-selectin was measured by flow cytometry. Data shown are from three independent experiments. (**b**) HUVECs were stimulated with histamine (0.25 µM) in the presence or absence of the $S1P_3$ inhibitor TY-52156 (10 µM) and P-selectin was analysed by flow cytometry. Data are from five independent experiments. (**c**) Leukocyte rolling was quantified in postcapillary venules of the cremaster muscle of $Sphk1^{-/-}$ mice and controls ($n = 4$ per group). P-selectin-blocking antibody was injected to confirm rolling dependence on P-selectin. Quantitative data are presented as mean ± s.e.m. Significance was established using a paired two-tailed Student's *t*-test or a Wilcoxon rank sum test.*$P < 0.05$; *$P < 0.05$; ***$P < 0.001$.

data suggested that a mechanism involving AC activation and relying on $S1P_3$ is in part responsible for P-selectin mobilization by cAMP-generating agents such as epinephrine and forskolin. Forskolin has been shown to activate Sphk1 in pheochromocytoma cells[42]. We thus hypothesized that this may be the case in endothelial cells as well. Thus, we determined enzymatic Sphk1 activity after forskolin stimulation by measuring the conversion of C17-sphingosine to C17-S1P using mass spectrometry. Indeed, C17-S1P production was clearly increased after forskolin (10 µM) treatment of HUVEC for 30 min (Fig. 5c). To explore the consequences for P-selectin mobilization, we employed forskolin and the nondegradable cAMP analogue cpt-cAMP, respectively, to activate Sphk and added the Sphk inhibitor SKi. Indeed, both forskolin (10 µM) and cpt-cAMP (0.3 mM) induced P-selectin mobilization, and in both cases SKi treatment substantially reduced it (Fig. 5d). Finally, we sought to reproduce these findings at the level of leukocyte rolling *in vivo* and applied forskolin ($1.3\ mg\ kg^{-1}$) intraperitoneally in our cremaster model. In agreement with its induction of P-selectin *in vitro*, forskolin clearly stimulated leukocyte rolling *in vivo* (Fig. 5e). In summary, these data have identified a novel cAMP-dependent mechanism of P-selectin mobilization that acts through Sphk1 activation and employs subsequent $S1P_3$ signalling.

Mast cell-derived S1P induces P-selectin in HUVEC via $S1P_3$. According to previous studies, histamine release from mast cells accounts for half of the leukocyte rolling in the cremaster model that by itself is completely mast cell-dependent[29]. Although S1P is not contained in mast cell granules, mast cell can release large amounts of S1P when allergically stimulated[43–45]. Thus, we hypothesized that tissue mast cells may be another source of S1P in our model thereby causing P-selectin mobilization and rolling. Physical stimuli such as pressure and temperature are known to induce mast cell activation *in vitro* and *in vivo*[46,47]. As surrogate for the physical stimulus of mechanical mast cell manipulation occurring during cremaster muscle exteriorization, we employed transient exposure of isolated peritoneal mast cells to a temperature of 53 °C for 2 min as commonly employed to activate mast cell without adverse effects on viability[46,47]. We then added the mast cell supernatants immediately to HUVEC and measured P-selectin surface expression (Fig. 6). To exclude effects of histamine released under these conditions, we added diphenhydramine and cimetidine in concentrations sufficient to completely block P-selectin mobilization by 0.25 µM histamine (Supplementary Fig. 4). The mast cell supernatants induced an impressive four- to fivefold increase in cell surface P-selectin expression compared with supernatants of unchallenged mast cells after 10 min (Fig. 6). Remarkably, this increase was suppressed by more than half by the $S1P_3$ inhibitor TY-52156 (Fig. 6). Mass spectrometry of the identical supernatants revealed that S1P had been released (90 ± 41 pmol S1P per 10^6 mast cells) resulting in a 64.73 ± 7.95 nM S1P concentration in the mast cell supernatants that the HUVEC had been exposed to. Another proof of biologically active S1P being present in the mast cell supernatants was their ability to activate Erk MAPK in $S1P_1$-overexpressing CHO cells and the inhibition thereof by a $S1P_1$ antagonist (Supplementary Fig. 7).

Rolling is increased in endothelial $S1P_1$ deficiency. Finally, we examined leukocyte rolling in mice deficient for the endothelial $S1P_1$ receptor ($S1P_1^{SCL\text{-}Cre\text{-}ERT}$) and observed it to be increased compared with respective controls (Fig. 7a). Furthermore, administration of FTY720 reduced rolling in $S1P_1^{SCL\text{-}Cre\text{-}ERT}$ mice to the same lower than basal levels observed with FTY720 in control mice and *C57Bl6* mice, respectively, and $S1P_3^{-/-}$ mice (Fig. 7b). Microvascular and haemodynamic parameters as well as rolling velocities were unaffected (Table 1 and Supplementary Fig. 1). Interestingly, the highly specific $S1P_1$ agonist AUI 954 (ref. 48) inhibited forskolin-induced C17-S1P generation in HUVEC *in vitro* along with inhibiting cAMP generation (Supplementary Fig. 8). These results suggest that $S1P_1$ negatively regulates cAMP-stimulated Sphk1 and by reducing S1P generation possibly inhibits P-selectin-dependent rolling, hence acting as an opponent to $S1P_3$.

Discussion

Our study reveals the following six important and novel findings (Fig. 8): (1) we provide evidence that S1P is a direct agonist of P-selectin mobilization and leukocyte rolling; (2) we identify $S1P_3$ as the major responsible S1P receptor; (3) we show that several P-selectin agonists employ S1P and $S1P_3$ as mediators of their P-selectin-mobilizing effects by activating Sphk1; (4) we

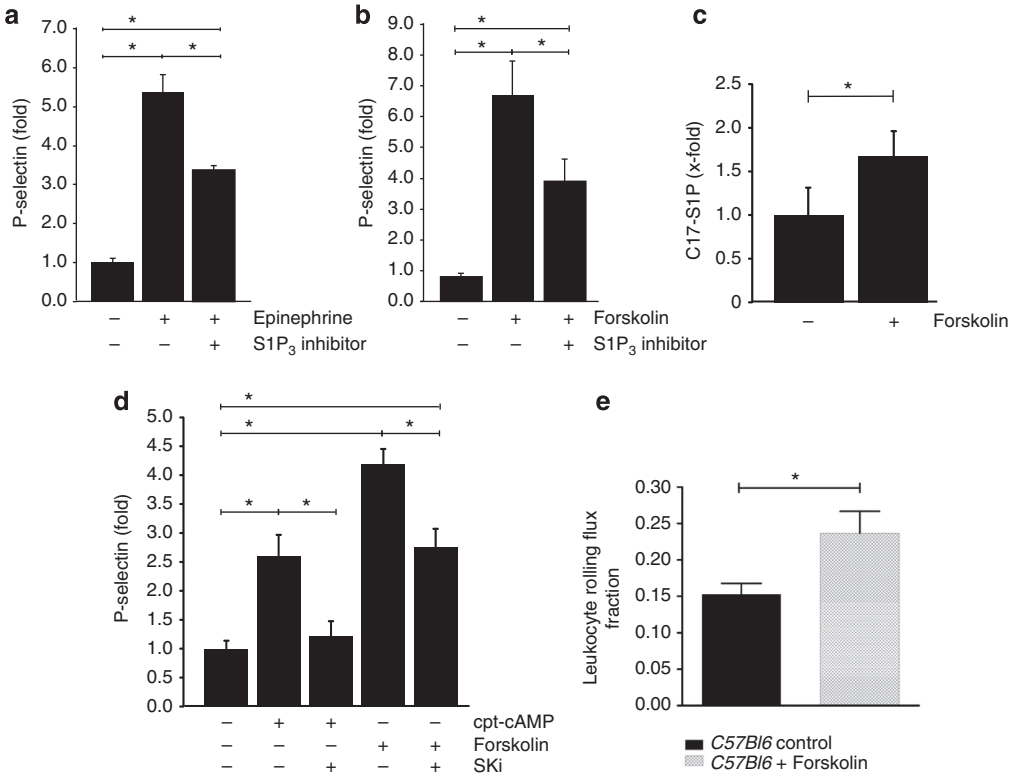

Figure 5 | Epinephrine and forskolin stimulate P-selectin mobilization and leukocyte rolling through adenylate cyclase/cAMP-dependent Sphk1 activation and engagement of $S1P_3$. HUVECs were stimulated with (**a**) epinephrine (9 μM) in the presence of IBMX (100 μM) and (**b**) forskolin (10 μM) with or without the $S1P_3$ inhibitor TY-52156 (10 μM), and P-selectin was analysed by flow cytometry. Data shown are from five independent experiments. (**c**) HUVECs were stimulated with forskolin (10 μM) in the presence of C17-sphingosine for 30 min, washed and analysed for intracellular C17-S1P using mass spectrometry. Data shown are from four independent experiments. (**d**) HUVECs were stimulated with forskolin (10 μM) or cpt-cAMP (0.3 mM) in the presence or absence of SKi (25 μM) for 30 min. P-selectin was analysed by flow cytometry. Data shown are from five independent experiments. (**e**) Leukocyte rolling in *C57Bl6* mice treated with forskolin or vehicle ($n=5$ per group). Quantitative data are presented as mean ± s.e.m. Significance was established using a paired two-tailed Student's *t*-test or a Wilcoxon rank sum test. $^*P<0.05$.

characterize a novel cAMP-dependent mechanism of Sphk1 activation and P-selectin mobilization; (5) we identify a rolling-inhibitory effect of endothelial $S1P_1$; and (6) we show that pharmacological inhibition or downregulation of $S1P_3$ for example by FTY720 attenuates leukocyte rolling in a physiological setting. Only few studies have addressed S1P in the context of processes related to leukocyte rolling: (1) S1P has been demonstrated to both induce and inhibit the exocytosis of von Willebrand factor through different pathways[49]; (2) Sphk1 was suggested to play no role in basal leukocyte rolling but to promote rolling after exogenous histamine administration[16]; (3) although S1P promoted firm neutrophil adhesion *in vitro*[50], neutrophil recruitment was inhibited during acute inflammatory lung injury in S1P lyase-deficient mice[51], with S1P lyase inhibitors[52] and by S1P administration[53], respectively, and (4) FTY720 was shown to suppress neutrophil recruitment in several disease models[3,53,54]. This has made general conclusions on the role of S1P and its receptors in leukocyte rolling or their mode of action rather difficult.

Our findings add some new evidence that helps to better understand the role of S1P in rolling. First, it is crucial to distinguish acute S1P effects on pre-stored P-selectin occurring within minutes from S1P effects on cytokine-induced P-selectin transcription that takes hours. Second, the acute S1P effects on P-selectin are different from those caused by continuous exposure to high S1P levels or the lack of S1P receptors. Third, the effects of S1P analogues such as FTY720 may differ considerably from the effects of genuine S1P at the receptor level[55]. In respect to rapid P-selectin mobilization, we have clearly shown that S1P is a direct P-selectin agonist and leads to increased P-selectin-dependent leukocyte rolling within minutes of its direct administration into the circulation. It is known that despite the high amounts of S1P already present in the blood, intravascular injection of S1P can still cause functional effects on the endothelium such as attenuation of vascular leakage, vasodilatation and protection against reperfusion injury[53,56,57]. Accordingly, the reduced leukocyte rolling we observed after pharmacological $S1P_3$ inhibition and in $S1P_3^{-/-}$ mice, respectively, are strong arguments for the causal and direct positive contribution of endothelial S1P signalling to P-selectin-dependent leukocyte rolling. However, we have also found evidence that endothelial $S1P_1$ plays an opposite role in rolling as its deletion led to a rolling increase. However, the pro-rolling effect of $S1P_3$ appears to be dominant over the anti-rolling effect of $S1P_1$ as the net effect of acute intravascular S1P administration in wild-type mice (where both receptors are being engaged) was an overall increase in rolling. However, in the absence of $S1P_3$, anti-rolling effects of $S1P_1$ may also contribute to the reduction in rolling. In fact, there was a minor but significant increase in rolling with FTY720 in $S1P_3$ deficiency that may have occurred because of $S1P_1$ downregulation by FTY720. Accordingly, in the absence of endothelial $S1P_1$, the increase in rolling may be due to a combination of the loss of anti-rolling $S1P_1$ effects and the still intact and potent pro-rolling $S1P_3$ effects. Indeed, in $S1P_1^{-/-}$ mice, FTY720 inhibited rolling to lower than basal levels.

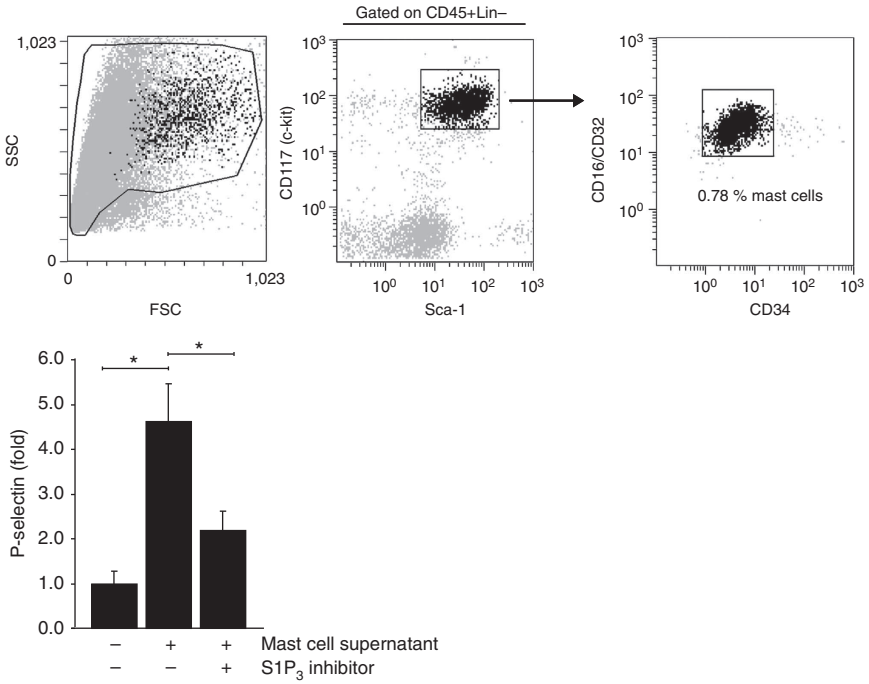

Figure 6 | Supernatants of activated mast cells stimulate P-selectin mobilization in HUVEC in a $S1P_3$-dependent manner. (Top) FACS analysis of mouse peritoneal mast cells ($CD45^+$ Lin^- $CD117^+$ $Sca\text{-}1^+$ $CD16/32^+$ $CD34^+$) used for stimulation. (Bottom) HUVECs were stimulated with supernatants of heat-activated peritoneal mast cells for 10 min in the presence or absence or the $S1P_3$ inhibitor TY-52156 (10 μM). Diphenhydramine and cimetidine (10 μM each) were present in all experiments. P-selectin was measured using flow cytometry. Quantitative data are presented as mean ± s.e.m. for three independent mast cell preparations and three independent HUVEC preparations. Significance was established using a paired two-tailed Student's *t*-test. $P<0.05$.

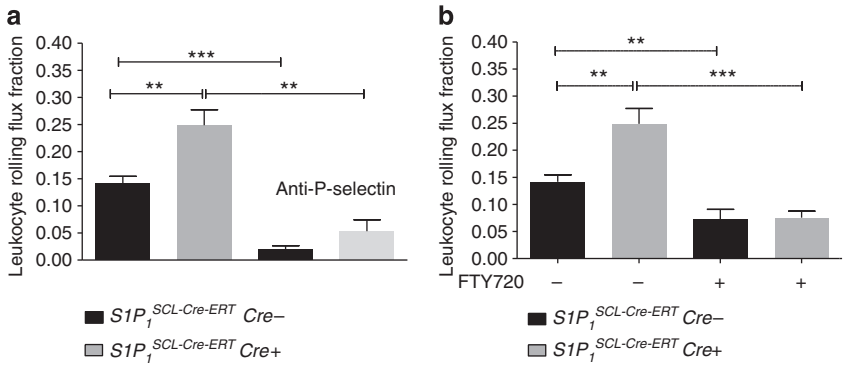

Figure 7 | Leukocyte rolling is increased in endothelial-specific $S1P_1$ knockout mice ($S1P_1^{SCL\text{-}Cre\text{-}ERT}$). (**a**) Leukocyte rolling was quantified in postcapillary venules of the cremaster muscle of $S1P_1^{SCL\text{-}Cre\text{-}ERT}$ mice (Cre+ and Cre−, $n=9$ per group). Rolling was also measured after systemic injection of a P-selectin-blocking antibody ($n=4$ per group). (**b**) Leukocyte rolling after administration of 1.25 mg kg^{-1} i.p. FTY720 30 min before the experiment in both genotypes (Cre+ $n=4$, Cre− $n=3$). Quantitative data are presented as mean ± s.e.m. Significance was established using a Wilcoxon rank sum test. *$P<0.05$; *$P<0.05$; ***$P<0.001$.

We have identified two possible sources of endogenous S1P involved in P-selectin mobilization in our model: interstitial mast cells and endothelial cells (Fig. 8). Interstitial mast cell activation following mechanical cremaster muscle manipulation is entirely responsible for the leukocyte rolling occurring there, and histamine release accounts for ~50% of it (ref. 29). As S1P can be released by allergically activated mast cells[45], and physical stimuli such as pressure and heat can activate mast cells[46,47], we hypothesized that S1P may be another mast cell product contributing to the remaining part of leukocyte rolling. The physical stimulus we employed to test this in mast cells was a short, harmless temperature elevation[46,47]. Indeed, we found them to release S1P within minutes that mobilized P-selectin in HUVEC in part in a $S1P_3$-dependent manner. Whether this occurs *in vivo* and actually contributes to leukocyte rolling in our model should be addressed by future studies. Although platelets are the major source of P-selectin, elaborate studies have shown that platelet P-selectin does not play a role in leukocyte rolling[58,59], and, in our hands, S1P had no effect on basal or thrombin-stimulated P-selectin in platelets; neither was platelet activation altered in $Sphk1^{-/-}$ mice (Supplementary Fig. 9).

We have identified endothelial cells as the second source of endogenous S1P capable of inducing P-Selectin mobilization. Sphk1 activation has been known to occur after stimulation with inflammatory cytokines as well as histamine; however, the pathway

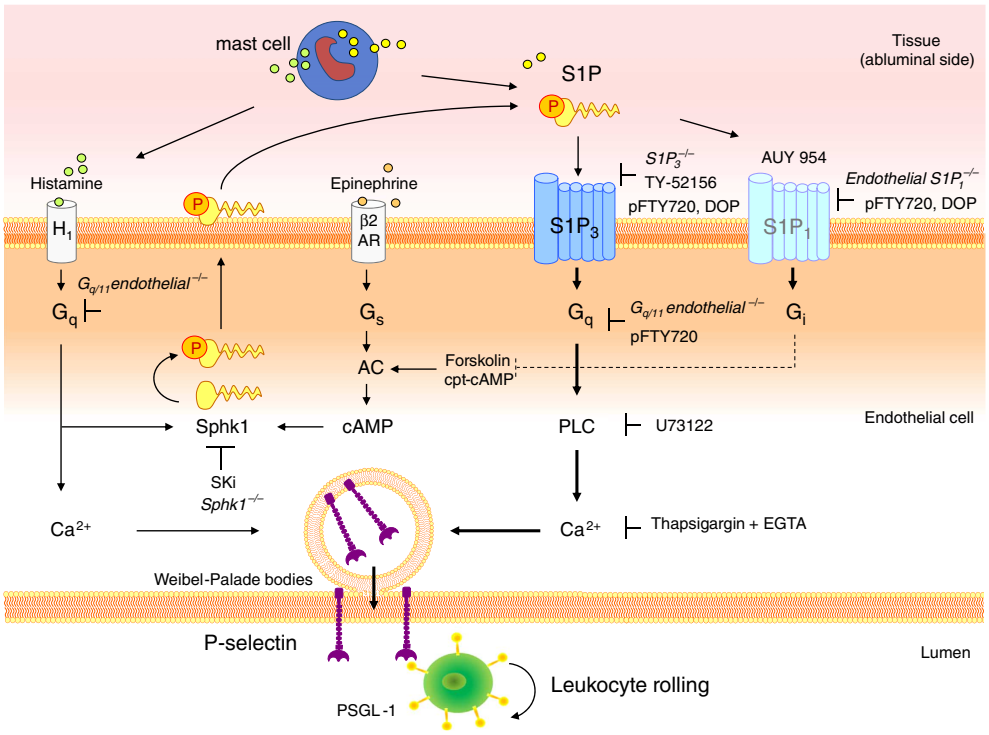

Figure 8 | The role of S1P and its receptors in P-Selectin mobilization. Schematic representation of the direct and indirect roles S1P plays in P-selectin mobilization. Mast cells release both histamine and S1P that can both mobilize P-selectin independently through the H1 and $S1P_3$ receptor, respectively. However, histamine achieves full scale P-selectin mobilization by additional Gq-dependent activation of Sphk1, S1P production/release and subsequent activation of S1P3. Other P-selectin mobilizing agents such as epinephrine that require cAMP for P-selectin mobilization also employ Sphk1 for full-blown effect but do so through a Gs/AC/cAMP-dependent pathway. S1P1 plays an inhibitory effect on P-selectin-dependent rolling by reducing AC-induced Sphk1 activity through Gi. DOP and pFTY720 act in an inhibitory manner on rolling by downregulating S1P1 and S1P3, but in addition, pFTY720 directly inhibits the Gq-dependent part of S1P-incuded S1P3-dependent P-selectin mobilization. In summary, the pro-rolling effect of S1P3 dominates over the anti-rolling of $S1P_1$, and the net effect of acute S1P exposure is an overall increase in P-selectin-dependent leukocyte rolling. AC, adenylate cyclase; AUY 954, S1P1-specific agonist; β2AR, β2 adrenergic receptor; DOP, the S1P lyase inhibitor 4-deoxypyridoxine; H1, H1 histamine receptor; PSGL, P-selectin glycoprotein ligand-1; Sphk1, sphingosine kinase 1; TY-52156, $S1P_3$-specific inhibitor.

by which it contributes to rolling has remained unclear[16]. We provide evidence that S1P produced by histamine-activated Sphk1 contributes to full-blown histamine mobilization of P-selectin through $S1P_3$. The evidence stems from two observations: (1) the partial inhibition of P-selectin mobilization after histamine by the blockade of Sphk1 or $S1P_3$ and (2) the elimination of the inhibitory effect of Sphk1 blockade on P-selectin by exogenous S1P. Coincidently, the $S1P_3$ receptor, the H1 histamine receptor and the thrombin PAR-1 receptor[41] not only all mobilize P-selectin but also couple to G_q; on the other side, pharmacological G_q inhibition has been shown to inhibit P-selectin exocytosis at least in platelets[60]. This offers a plausible explanation of why $S1P_3$ effects have gone unnoticed in experiments employing H1 blockers or G_q inhibitors. Our finding that endothelial-specific $G_{q/11}-/-$ mice have reduced P-selectin-dependent leukocyte rolling can certainly be explained by the blockade of several G_q-coupled receptors including $S1P_3$. Indeed, all these agonists have their own S1P-independent pathways of inducing P-selectin as neither $S1P_3$ nor Sphk1 deletion/inhibition was able to completely inhibit P-selectin mobilization. However, part of the histamine effect can be attributed to $S1P_3$. Our observation that rolling could not be reduced any further by pharmacological $S1P_3$ inhibition in $G_{q/11}-/-$ mice argues that G_q mediates the pro-rolling effect of $S1P_3$. The site of action of S1P released by interstitial mast cells or by endothelial cells exposed to histamine from the same mast cells would primarily be on the abluminal side of the vascular endothelium. This complies with an oriented signalling mode as the abluminal side should be reached first by any locally released interstitial agents. This scenario is in line with the dynamic signalling model proposed by Camerer *et al.*[7] of how abluminal S1P signalling maintains endothelial integrity despite high S1P levels in blood.

We were also intrigued by the observation that not only histamine but another P-selectin-mobilizing agonist such as epinephrine[41] that couples with G_s and not G_q employed Sphk1 and $S1P_3$ for full-scale P-selectin mobilization (Fig. 8). We have demonstrated that epinephrine also activated Sphk1 but through a cAMP-dependent mechanism and — similar to histamine — also employed S1P and $S1P_3$ to help mobilize P-selectin. Indeed, direct stimulation of Sphk1 by forskolin (as measured by the conversion of C17-sphingosine to C17-S1P) mobilized P-selectin through $S1P_3$ *in vitro* and induced leukocyte rolling *in vivo*. In agreement with a role for cAMP, forskolin has been shown to activate Sphk1 in pheochromocytoma cells years ago[42]. However, $S1P_3$ or Sphk1 inhibition did not completely abrogate the effects of epinephrine or forskolin, suggesting that there must be additional pathways of how cAMP mobilizes P-selectin[41]. Interestingly, the pathway of cAMP-stimulated Sphk1 provides a putative mechanism of how $S1P_1$, with its established inhibitory effect on cAMP generation[4], may be exerting its antirolling effect. Indeed, the highly specific $S1P_1$ agonist AUI 954 (ref. 48) inhibited C17-S1P generation after forskolin along with lowering cAMP (Supplementary Fig. 8). This suggests that $S1P_1$ may be attenuating cAMP-induced Sphk1 activation in a negative-feedback manner, thereby restricting the

amounts of S1P available for P-selectin mobilization by $S1P_3$. The reduced leukocyte rolling we have observed in *Sphk1*$^{-/-}$ mice is in line with Sphk1/S1P serving as a general transmission/amplification hub for different incoming P-selectin mobilization signals. While the $S1P_1$ receptor has often been implicated in Sphk1 signalling, there is to our knowledge only scarce evidence for an involvement of $S1P_3$ in conveying Sphk1 signals: only one study has implied $S1P_3$ as a mediator of thrombin-induced Sphk1 effects in dendritic cells[61]. The requirement of $S1P_3$ for full efficiency of several P-selectin agonists may also serve another purpose: $S1P_3$ downregulation or desensitization after engagement by endogenous S1P may help ameliorate excessive P-selectin stimulation and help turn it off.

Acute S1P effects on P-selectin mobilization should be distinguished from those caused by continuous exposure to S1P or S1P analogues. High S1P levels after S1P lyase inhibition or deficiency and administration of FTY720 have been shown to downregulate S1P receptors[1,62,63] including $S1P_3$ (ref. 64) and impair lymphocyte trafficking. Accordingly, the reduced neutrophil recruitment found in S1P lyase-deficient mice[51] or after FTY720 treatment[53,54] may be due to downregulation of $S1P_3$. In line with this, we have observed that FTY720 had no additional inhibitory effect on rolling in *S1P*$_3^{-/-}$ mice. However, another mechanism may also be involved: we have previously shown that pFTY720 is a potent inhibitor of G_q-mediated S1P-induced $S1P_3$ signalling[39]. In the present study, we extended this observation to P-selectin mobilization by $S1P_3$. Thus, both mechanisms could be taking place simultaneously as: (1) preincubation with pFTY720 abolished S1P-induced P-selectin mobilization in endothelial cells as well as $S1P_3$-dependent S1P signalling in $S1P_3$-CHO cells; (2) pFTY720 had a minor and very short-lived positive effect on P-selectin compared with S1P, while (3) its simultaneous application together with S1P abolished P-selectin mobilization by S1P. In line with this interpretation, another P-selectin-dependent process, the recruitment of early thymic progenitors to the thymic endothelium, has been shown to be inhibited by FTY720 (ref. 65), although the responsible receptor was not identified.

In summary, our study suggests an important role for S1P and $S1P_3$ in the induction of rapid endothelial P-selectin mobilization and consecutive P-selectin-dependent leukocyte rolling. S1P acts thereby both directly as an agonist and, indirectly, as a contributor to P-selectin mobilization by other P-selectin agonists.

Methods

Mice. *S1P*$_3^{-/-}$ mice were provided by Jerold Chun, Scripps Research Institute to B.L. and crossbred to *C57Bl6J* for more than six generations. *Sphk1*$^{-/-}$ mice were provided to M.H.G. by Richard Proia (NIH) and Tie2-Cre-ER(T2); *G*$\alpha_q^{flox/flox}$; *G*$\alpha_{11}-/-$ were from S.O. Mice deficient for the endothelial $S1P_1$ receptor were generated by crossbreeding *S1P*$_1^{flox/flox}$ mice[66] with *endothelial-SCL-Cre-ER*^{T} mice, in which the tamoxifen-inducible Cre-ER^T recombinase is driven by the 5′-endothelial enhancer of the stem cell leukaemia (SCL) locus[67] (Supplementary Fig. 11). Cre-negative *S1P*$_1^{SCL\text{-}Cre\text{-}ERT}$ littermates treated with the same tamoxifen regimen were used as controls. Recombination was induced by daily intraperitoneal injections of tamoxifen (40 mg per kg body weight) for five consecutive days, and the experiments were performed 6 weeks later. Successful recombination was shown in lung endothelial cells isolated using CD31-coated magnetic beads (Dynabeads) by site-specific PCR for the excised exon. All mice used in the study were male and at least 10 weeks of age. All procedures were performed in accordance with the institutional guidelines for health and care of experimental animals and were approved by the Regierung von Baden Württemberg and Oberbayern, respectively.

Substances and antibodies. S1P was purchased from Enzo Life Science. The $S1P_3$ inhibitors TY-52156 (Supplementary Fig. 2) and FTY720 were synthesized as described[32]. AUY 954 was a kind gift from Klaus Seuwen (Novartis). *In vivo*, FTY720 and TY-52156 were applied intraperitoneally at 1.25 mg per kg and forskolin at 1.3 mg per kg body weight 30 min or 24 h before the experiment as indicated. S1P was injected via a carotid artery catheter at 30 μg per kg body weight (125 μM S1P solution in 2% BSA per 0.9% NaCl). The S1P lyase inhibitor DOP (Sigma Aldrich) was supplemented in the drinking water (30 mg l^{-1}) for 1 week. W146 and C17 sphingosine were from Avanti polar lipids, the SKi 4-[[4-(4-chlorophenyl)-2-thiazolyl]amino]-phenol (SKi, SKI II and SPHK I2), pFTY720, SEW2871 and U73122 from Cayman Chemical Co; epinephrine from Sanofi Aventis; forskolin from Calbiochem; IBMX, cpt-cAMP, diphenhydramine and cimetidine from Sigma Aldrich; and thapsigargin from AppliChem. $S1P_1$-CHO and $S1P_3$-CHO cells were from Novartis. The following antibodies were used: CD62P-PE (phycoerythrin) anti-mouse (eBioscience, 12-0626-82, 3:100), CD4-PE anti-mouse (eBioscience, 12-0041, 1:100), CD8-PE anti-mouse (eBioscience, 12-0081, 1.4:100), Ter119-PE anti-mouse (Miltenyi, 130-091-783, 3:100), Ly6G&Ly6C-PE anti-mouse (BD Pharmingen, 553128, 1.6:100), CD45R-PE anti-mouse (BD Pharmingen, 553089, 1.6:100), CD34-AlexaFluor700 anti-mouse (BD Pharmingen, 1.6:100), CD16/32-PerCpCy5.5 anti-mouse (BD Pharmingen, 560540, 1.65:100), LyA/E-FITC anti-mouse (BD Pharmingen, 557405, 1.1:100), CD117-PE-Cy7 anti-mouse (BD Pharmingen, 558163, 1.7:100), CD450-V450 anti-mouse (BD Pharmingen, 560697, 1.8:100) and P-selectin glycoprotein ligand-1-PE anti-mouse (BD Pharmingen, 555306, 1:1,000). The P-selectin-blocking rat-anti-mouse monoclonal antibody RB40.34 was a generous gift from Dietmar Vestweber (MPI Münster).

Flow chamber assay for rolling on immobilized P-selectin. Rectangular glass capillaries (0.4 × 0.04 mm, VitroCom) were used for *ex vivo* flow chamber experiments as described[31]. Chambers were coated with recombinant murine (rm)P-selectin (CD62-P, 20 μg ml^{-1}, R&D Systems). Following overnight incubation at 4 °C, flow chambers were blocked with 5% casein (Sigma-Aldrich) in PBS for 2 h. For experiments, one end of the chamber was attached to a carotid artery catheter, while the other was left open to regulate blood flow through the microflow chamber. Microscopy was performed using a modified Olympus BX51 upright microscope (LaVision Biotec) with a saline immersion objective (40/0.8 numerical aperture (NA), Olympus). Leukocyte rolling was recorded over 10 min per microflow chamber with a CCD (charge-coupled device) video camera (model CF8/1; Kappa) connected to a Panasonic S-VHS recorder and analysed offline.

Intravital microscopy of the cremaster muscle. Intravital microscopy of post-capillary venules of the mouse cremaster muscle was used to study leukocyte rolling under different inflammatory conditions[25,27]. Briefly, mice were anaesthetized by intraperitoneal injection of ketamine and xylazine (100 and 20 mg per kg body weight, respectively), after which a tracheal tube was inserted and the carotid artery cannulated for blood sampling and systemic application of substances. Thereafter, the scrotum was opened, the cremaster muscle exteriorized, spread over a cover glass and superfused with warmed (35 °C) bicarbonate-buffered saline. Observation of postcapillary venules was conducted on an upright microscope (Olympus BX51) with a saline immersion objective (× 40/0.8 NA). To abolish P-selectin-dependent rolling, the P-selectin-blocking monoclonal antibody RB40.34 (30 μg per mouse) was diluted in 200 μl saline and injected via the carotid artery catheter. Experiments were recorded via a CCD camera system (model CF8/1; Kappa) on a Panasonic S-VHS recorder. Systemic blood samples (10 μl) were obtained before and during the experiment, stained using Turck's solution and assessed for white blood cell count using a haemocytometer. Data analysis was performed offline using the video tapes from *in vivo* experiments. Diameter, segment length of postcapillary venules and venular centreline blood flow velocity were assessed using a digital image-processing system and a digital online cross-correlation programme, respectively (Circusoft Instrumentation)[24]. Leukocyte rolling flux fraction was calculated from the number of rolling cells that crossed a perpendicular line through a given vessel within 1 min in relation to the total number of circulating leukocytes.

Whole-mount immunohistochemistry. For immunohistochemical detection of luminal endothelial P-selectin expression in cremaster muscle whole mounts, primary monoclonal antibody against P-selectin RB40.34 (30 μg per mouse) was systemically injected after 20-min superfusion of the exteriorized right cremaster muscle ensuring binding to P-selectin on the luminal vessel surface. To remove excess antibody, the inferior vena cava was cut and animals were perfused with 10 ml of 0.9% NaCl. The left cremaster muscle was exteriorized *post mortem* to serve as unstimulated negative control. The cremaster muscles were then mounted on adhesive slides (Superfrost), transferred into −20° acetone over night and stored at −80 °C until further processing. For staining of P-selectin expression, cremaster whole mounts were permeabilized with saponin (0.03% in Tris-buffer) and incubated with 2 μg ml^{-1} biotinylated secondary goat anti-rat IgG (Southern Biotechnology Associates Inc, Cat. No 3030-08). Detection of antigen–antibody complexes was carried out with a commercial biotinylated horseradish peroxidase/avidin complex (Vectastain ABC, Vector Laboratories) according to the manufacturer's instructions. Slides were counterstained using Mayer's Hemalaun and analysed using a Zeiss microscope with a × 100, 1.4 NA oil immersion objective.

P-selectin mobilization in HUVEC. HUVECs (passage 1–4) were cultured in 20% human serum/RPMI. After incubation in serum-free medium for 4 h, cells were stimulated with histamine (0.25 or 25 μM), S1P (1 μM), SEW2871 (1 μM) and

epinephrine (9 μM)/IBMX (100 nM), respectively, for the indicated times. Before histamine or S1P stimulation, the $S1P_3$ inhibitor TY-52156, SKi or phosphorylated FTY720 (10 μM) were added for 30 min; with forskolin, inhibitors were added 10 min before stimulation. Five minutes before the end of the experiment, PE-conjugated anti-P-selectin antibody (eBioscience; 1.6:100) was added directly into the 500 μl of incubation medium after which the cells were washed twice and analysed immediately by flow cytometry.

Stimulation with supernatants of activated mast cells. Mouse peritoneal mast cells were isolated by a Percoll gradient as described[68] and characterized as $CD45^+$, Lin^- (CD45R, Ly6G, Ly6C, Ter119, CD4 and CD8), $CD117^+$, Sca-1^+, $CD16/32^+$ and $CD34^+$ cells by flow cytometry and consecutive toluidine blue staining[68,69]. The yield was 0.05–0.1 × 10^6 mast cells per mouse. All peritoneal cells were incubated with 10 μM sphingosine for 30 min at 37 °C before the Percoll gradient isolation procedure. Stimulation was performed by adding 250 μl warm (53 °C) 2% BSA/alphaMEM to 0.5 × 10^6 mast cells and subsequent incubation for 2 min at 53 °C as described[46,47]. For stimulation of HUVEC, 100 μl of the mast cell supernatant was supplemented with diphenhydramine and cimetidine (10 μM each) and added to confluent HUVEC cultured in 200 μl RPMI for 10 min. PE-conjugated anti-P-selectin antibody was added directly into the 300 μl at the time of stimulation. Cells were washed twice with serum-free medium, trypsinized and analysed by flow cytometry.

Measurements of Sphk1 activity using C17-sphingosine. Five μM C17-sphingosine was added together with 10 μM forskolin to HUVEC in RPMI with 2 mg per ml BSA fraction V (Serva) for 30 min. Cells were washed extensively and lysed in 50 mM Tris/HCl (pH 7.5), 0.5%NP-40, 10% glycerol, 250 mM NaCl, 5 mM EDTA, 0.5 mM phenylmethyl sulphonyl fluoride, 5 μg ml^{-1} leupeptin and aprotinin. Protein concentration was measured using the Pierce BCA Protein Assay Kit (Thermo Scientific). C17-S1P was determined by mass spectrometry as described[70] and expressed per milligram cell protein.

Statistics. For pair-wise comparison between experimental groups, a Wilcoxon rank sum test or paired Student's *t*-test was performed. For multiple comparisons, a Kruskal–Wallis nonparametric analysis of variance on ranks was performed followed by Dunn's *post hoc* test. A P value < 0.05 was considered statistically significant. All statistical analyses were carried out with GraphPad Prism 5.2 (PraphPad Software Inc, La Jolla). Data are presented as mean ± s.e.m. Sample size has been provided for each experiment in the figure legend (no exclusion criteria, randomization or blinding).

References

1. Rivera, J., Proia, R. L. & Olivera, A. The alliance of sphingosine-1-phosphate and its receptors in immunity. *Nat. Rev. Immunol.* **8,** 753–763 (2008).
2. Ledgerwood, L. G. *et al.* The sphingosine 1-phosphate receptor 1 causes tissue retention by inhibiting the entry of peripheral tissue T lymphocytes into afferent lymphatics. *Nat. Immunol.* **9,** 42–53 (2008).
3. Keul, P. *et al.* Sphingosine-1-phosphate receptor 3 promotes recruitment of monocyte/macrophages in inflammation and atherosclerosis. *Circ. Res.* **108,** 314–323 (2010).
4. Rivera, R. & Chun, J. Biological effects of lysophospholipids. *Rev. Physiol. Biochem. Pharmacol.* **160,** 25–46 (2008).
5. McVerry, B. J. & Garcia, J. G. *In vitro* and *in vivo* modulation of vascular barrier integrity by sphingosine 1-phosphate: mechanistic insights. *Cell Signal.* **17,** 131–139 (2005).
6. Tauseef, M. *et al.* Activation of sphingosine kinase-1 reverses the increase in lung vascular permeability through sphingosine-1-phosphate receptor signaling in endothelial cells. *Circ. Res.* **103,** 1164–1172 (2008).
7. Camerer, E. *et al.* Sphingosine-1-phosphate in the plasma compartment regulates basal and inflammation-induced vascular leak in mice. *J. Clin. Invest.* **119,** 1871–1879 (2009).
8. Xia, P. *et al.* Tumor necrosis factor-alpha induces adhesion molecule expression through the sphingosine kinase pathway. *Proc. Natl Acad. Sci. USA* **95,** 14196–14201 (1998).
9. Kimura, T. *et al.* Sphingosine 1-phosphate receptors mediate stimulatory and inhibitory signalings for expression of adhesion molecules in endothelial cells. *Cell Signal.* **18,** 841–850 (2006).
10. Krump-Konvalinkova, V. *et al.* Stable knock-down of the sphingosine 1-phosphate receptor S1P1 influences multiple functions of human endothelial cells. *Arterioscler. Thromb. Vasc. Biol.* **25,** 546–552 (2005).
11. Limaye, V. *et al.* Chronic increases in sphingosine kinase-1 activity induce a pro-inflammatory, pro-angiogenic phenotype in endothelial cells. *Cell Mol. Biol. Lett.* **14,** 424–441 (2009).
12. Kimura, T. *et al.* Role of scavenger receptor class B type I and sphingosine 1-phosphate receptors in high density lipoprotein-induced inhibition of adhesion molecule expression in endothelial cells. *J. Biol. Chem.* **281,** 37457–37467 (2006).
13. Bolick, D. T. *et al.* Sphingosine-1-phosphate prevents tumor necrosis factor-{alpha}-mediated monocyte adhesion to aortic endothelium in mice. *Arterioscler. Thromb. Vasc. Biol.* **25,** 976–981 (2005).
14. Whetzel, A. M. *et al.* Sphingosine-1 phosphate prevents monocyte/endothelial interactions in type 1 diabetic NOD mice through activation of the S1P1 receptor. *Circ. Res.* **99,** 731–739 (2006).
15. Sattler, K. & Levkau, B. Sphingosine-1-phosphate as a mediator of high-density lipoprotein effects in cardiovascular protection. *Cardiovasc. Res.* **82,** 201–211 (2009).
16. Sun, W. Y. *et al.* Rapid histamine-induced neutrophil recruitment is sphingosine kinase-1 dependent. *Am. J. Pathol.* **180,** 1740–1750 (2012).
17. Sperandio, M., Gleissner, C. A. & Ley, K. Glycosylation in immune cell trafficking. *Immunol. Rev.* **230,** 97–113 (2009).
18. Sperandio, M., Pickard, J., Unnikrishnan, S., Acton, S. T. & Ley, K. Analysis of leukocyte rolling *in vivo* and *in vitro*. *Methods Enzymol.* **416,** 346–371 (2006).
19. Ley, K. The role of selectins in inflammation and disease. *Trends Mol. Med.* **9,** 263–268 (2003).
20. Rossi, B. & Constantin, G. Anti-selectin therapy for the treatment of inflammatory diseases. *Inflamm. Allergy Drug Targets* **7,** 85–93 (2008).
21. Impellizzeri, D. & Cuzzocrea, S. Targeting selectins for the treatment of inflammatory diseases. *Expert Opin. Ther. Targets* **18,** 55–67 (2014).
22. Luo, W. *et al.* P-selectin glycoprotein ligand-1 inhibition blocks increased leukocyte-endothelial interactions associated with sickle cell disease in mice. *Blood* **120,** 3862–3864 (2012).
23. Combes, V. *et al.* Pathogenic role of P-selectin in experimental cerebral malaria: importance of the endothelial compartment. *Am. J. Pathol.* **164,** 781–786 (2004).
24. Sperandio, M. *et al.* Alpha 2,3-sialyltransferase-IV is essential for L-selectin ligand function in inflammation. *Eur. J. Immunol.* **36,** 3207–3215 (2006).
25. Klinke, A. *et al.* Myeloperoxidase attracts neutrophils by physical forces. *Blood* **117,** 1350–1358 (2010).
26. Rivera-Nieves, J. *et al.* Critical role of endothelial P-selectin glycoprotein ligand 1 in chronic murine ileitis. *J. Exp. Med.* **203,** 907–917 (2006).
27. Kunkel, E. J. *et al.* Absence of trauma-induced leukocyte rolling in mice deficient in both P-selectin and intercellular adhesion molecule 1. *J. Exp. Med.* **183,** 57–65 (1996).
28. Mayadas, T. N., Johnson, R. C., Rayburn, H., Hynes, R. O. & Wagner, D. D. Leukocyte rolling and extravasation are severely compromised in P selectin-deficient mice. *Cell* **74,** 541–554 (1993).
29. Kubes, P. & Kanwar, S. Histamine induces leukocyte rolling in post-capillary venules. A P-selectin-mediated event. *J. Immunol.* **152,** 3570–3577 (1994).
30. Nussbaum, C. *et al.* Neutrophil and endothelial adhesive function during human fetal ontogeny. *J. Leukoc. Biol.* **93,** 175–184 (2013).
31. Frommhold, D. *et al.* RAGE and ICAM-1 cooperate in mediating leukocyte recruitment during acute inflammation in vivo. *Blood* **116,** 841–849 (2010).
32. Murakami, A. *et al.* Sphingosine 1-phosphate (S1P) regulates vascular contraction via S1P3 receptor: investigation based on a new S1P3 receptor antagonist. *Mol. Pharmacol.* **77,** 704–713 (2010).
33. van Mourik, J. A., Romani de Wit, T. & Voorberg, J. Biogenesis and exocytosis of Weibel-Palade bodies. *Histochem. Cell Biol.* **117,** 113–122 (2002).
34. An, S., Bleu, T. & Zheng, Y. Transduction of intracellular calcium signals through G protein-mediated activation of phospholipase C by recombinant sphingosine 1-phosphate receptors. *Mol. Pharmacol.* **55,** 787–794 (1999).
35. Sato, K. *et al.* Activation of phospholipase C-Ca2 + system by sphingosine 1-phosphate in CHO cells transfected with Edg-3, a putative lipid receptor. *FEBS Lett.* **443,** 25–30 (1999).
36. Chun, J., Hla, T., Lynch, K. R., Spiegel, S. & Moolenaar, W. H. International Union of Basic and Clinical Pharmacology. LXXVIII. Lysophospholipid receptor nomenclature. *Pharmacol. Rev.* **62,** 579–587 (2010).
37. Korhonen, H. *et al.* Anaphylactic shock depends on endothelial Gq/G11. *J. Exp. Med.* **206,** 411–420 (2009).
38. Schwab, S. R. *et al.* Lymphocyte sequestration through S1P lyase inhibition and disruption of S1P gradients. *Science* **309,** 1735–1739 (2005).
39. Sensken, S. C. *et al.* Selective activation of G alpha i mediated signalling of SIP(3) by FTY720-phosphate. *Cell. Signal.* **20,** 1125–1133 (2008).
40. French, K. J. *et al.* Discovery and evaluation of inhibitors of human sphingosine kinase. *Cancer Res.* **63,** 5962–5969 (2003).
41. Cleator, J. H., Zhu, W. Q., Vaughan, D. E. & Hamm, H. E. Differential regulation of endothelial exocytosis of P-selectin and von Willebrand factor by protease-activated receptors and cAMP. *Blood* **107,** 2736–2744 (2006).
42. Rius, R. A., Edsall, L. C. & Spiegel, S. Activation of sphingosine kinase in pheochromocytoma PC12 neuronal cells in response to trophic factors. *FEBS Lett.* **417,** 173–176 (1997).
43. Prieschl, E. E., Csonga, R., Novotny, V., Kikuchi, G. E. & Baumruker, T. The balance between sphingosine and sphingosine-1-phosphate is decisive for mast cell activation after Fc epsilon receptor I triggering. *J. Exp. Med.* **190,** 1–8 (1999).

44. Jolly, P. S. *et al.* Transactivation of sphingosine-1-phosphate receptors by FcepsilonRI triggering is required for normal mast cell degranulation and chemotaxis. *J. Exp. Med.* **199,** 959–970 (2004).
45. Olivera, A. & Rivera, J. An emerging role for the lipid mediator sphingosine-1-phosphate in mast cell effector function and allergic disease. *Adv. Exp. Med. Biol.* **716,** 123–142 (2011).
46. Stokes, A. J., Shimoda, L. M., Koblan-Huberson, M., Adra, C. N. & Turner, H. A TRPV2-PKA signaling module for transduction of physical stimuli in mast cells. *J. Exp. Med.* **200,** 137–147 (2004).
47. Zhang, D. *et al.* Mast-cell degranulation induced by physical stimuli involves the activation of transient-receptor-potential channel TRPV2. *Physiol. Res.* **61,** 113–124 (2011).
48. Pan, S. *et al.* A monoselective sphingosine-1-phosphate receptor-1 agonist prevents allograft rejection in a stringent rat heart transplantation model. *Chem. Biol.* **13,** 1227–1234 (2006).
49. Matsushita, K., Morrell, C. N. & Lowenstein, C. J. Sphingosine 1-phosphate activates Weibel-Palade body exocytosis. *Proc. Natl Acad. Sci. USA* **101,** 11483–11487 (2004).
50. Florey, O. & Haskard, D. O. Sphingosine 1-phosphate enhances Fc gamma receptor-mediated neutrophil activation and recruitment under flow conditions. *J. Immunol.* **183,** 2330–2336 (2009).
51. Allende, M. L. *et al.* Sphingosine-1-phosphate lyase deficiency produces a pro-inflammatory response while impairing neutrophil trafficking. *J. Biol. Chem.* **286,** 7348–7358 (2010).
52. Zhao, Y. *et al.* Protection of LPS-induced murine acute lung injury by sphingosine-1-phosphate lyase suppression. *Am. J. Respir. Cell Mol. Biol.* **45,** 426–435 (2010).
53. Peng, X. *et al.* Protective effects of sphingosine 1-phosphate in murine endotoxin-induced inflammatory lung injury. *Am. J. Respir. Cell Mol. Biol.* **169,** 1245–1251 (2004).
54. Sawicka, E. *et al.* Inhibition of Th1- and Th2-mediated airway inflammation by the sphingosine 1-phosphate receptor agonist FTY720. *J. Immunol.* **171,** 6206–6214 (2003).
55. Salomone, S. & Waeber, C. Selectivity and specificity of sphingosine-1-phosphate receptor ligands: caveats and critical thinking in characterizing receptor-mediated effects. *Front. Pharmacol.* **2,** 9 (2011).
56. Nofer, J. R. *et al.* HDL induces NO-dependent vasorelaxation via the lysophospholipid receptor S1P(3). *J. Clin. Invest.* **113,** 569–581 (2004).
57. Theilmeier, G. *et al.* High-density lipoproteins and their constituent, sphingosine-1-phosphate, directly protect the heart against ischemia/reperfusion injury *in vivo* via the S1P(3) lysophospholipid receptor. *Circulation* **114,** 1403–1409 (2006).
58. Frenette, P. S. *et al.* Platelet-endothelial interactions in inflamed mesenteric venules. *Blood* **91,** 1318–1324 (1998).
59. Carvalho-Tavares, J. *et al.* A role for platelets and endothelial selectins in tumor necrosis factor-alpha-induced leukocyte recruitment in the brain microvasculature. *Circ. Res.* **87,** 1141–1148 (2000).
60. Uemura, T. *et al.* Biological properties of a specific Galpha q/11 inhibitor, YM-254890, on platelet functions and thrombus formation under high-shear stress. *Br. J. Pharmacol.* **148,** 61–69 (2006).
61. Niessen, F. *et al.* Dendritic cell PAR1-S1P3 signalling couples coagulation and inflammation. *Nature* **452,** 654–658 (2008).
62. Rosen, H., Gonzalez-Cabrera, P. J., Sanna, M. G. & Brown, S. Sphingosine 1-phosphate receptor signaling. *Annu. Rev. Biochem.* **78,** 743–768 (2009).
63. Cyster, J. G. & Schwab, S. R. Sphingosine-1-phosphate and lymphocyte egress from lymphoid organs. *Annu. Rev. Biochem.* **30,** 69–94 (2011).
64. Imeri, F. *et al.* Novel oxazolo-oxazole derivatives of FTY720 reduce endothelial cell permeability, immune cell chemotaxis and symptoms of experimental autoimmune encephalomyelitis in mice. *Neuropharmacology* **85,** 314–327 (2014).
65. Gossens, K. *et al.* Thymic progenitor homing and lymphocyte homeostasis are linked via S1P-controlled expression of thymic P-selectin/CCL25. *J. Exp. Med.* **206,** 761–778 (2009).
66. Choi, J. W. *et al.* FTY720 (fingolimod) efficacy in an animal model of multiple sclerosis requires astrocyte sphingosine 1-phosphate receptor 1 (S1P1) modulation. *Proc. Natl Acad. Sci. USA* **108,** 751–756 (2010).
67. Gothert, J. R. *et al.* Genetically tagging endothelial cells *in vivo*: bone marrow-derived cells do not contribute to tumor endothelium. *Blood* **104,** 1769–1777 (2004).
68. Jensen, B. M., Swindle, E. J., Iwaki, S. & Gilfillan, A. M. Generation, isolation, and maintenance of rodent mast cells and mast cell lines. *Curr. Protoc. Immunol.* Chapter 3, Unit 3 23 (2006).
69. Drew, E., Merkens, H., Chelliah, S., Doyonnas, R. & McNagny, K. M. CD34 is a specific marker of mature murine mast cells. *Exp. Hematol.* **30,** 1211–1218 (2002).
70. Sattler, K. J. E. *et al.* Sphingosine 1-phosphate levels in plasma and HDL are altered in coronary artery disease. *Basic Res. Cardiol.* **105,** 821–832 (2010).

Acknowledgements

We thank Susanne Bierschenk for her invaluable help in performing flow chamber experiments. We thank Klaus Seuwen (Novartis) for the kind provision of AUY 954. We are grateful to Franziska Röstel and Mareike Lipinski for lipid extractions and Christina-Maria Reimann for performing lipid analyses. This work was supported by the Deutsche Forschungsgemeinschaft to B.L. (LE940/4-2), M.S. (SP621/4-1), M.H.G. (GR 1943/2-2), B.L., G.H., V.P.P. (SFB656 project A6) and M.S. (SFB914 project B1). M.S. received support from the Deutsches Zentrum für Herz- und Kreislaufforschung. C.F.G.-d.-A., I.R., H.C.d.C.F.N. and M.S. have received funding from the European Community's Seventh Framework Programme [FP7-2007-2013] under grant agreement no. HEALTH-F4-2011-282095.

Author contributions

C.N., S.B., C.F.G.-d.-A., P.K., V.P.P., I.R., G.H., K.v.W.L. and H.K. performed research, collected data, analysed and interpreted data, performed statistical analysis, wrote the manuscript. M.H.G., H.C.d.C.F.N., J.G., G.H., B.L.-S. and S.O. contributed vital reagents or analytical tools and interpreted data. M.S. and B.L. designed research, analysed and interpreted data, and wrote the manuscript.

Additional information

Supplementary Information accompanies this paper at http://www.nature.com/naturecommunications

Competing financial interests: The authors declare no competing financial interests.

Reprints and permission information is available online at http://npg.nature.com/reprintsandpermissions/

How to cite this article: Nussbaum, C. *et al.* Sphingosine-1-phosphate receptor 3 promotes leukocyte rolling by mobilizing endothelial P-selectin. *Nat. Commun.* 6:6416 doi: 10.1038/ncomms7416 (2015).

JLB

Article

Neutrophil and endothelial adhesive function during human fetal ontogeny

Claudia Nussbaum, Anna Gloning,* Monika Pruenster,* David Frommhold,† Susanne Bierschenk,* Orsolya Genzel-Boroviczény,‡ Ulrich H. von Andrian,§ Elizabeth Quackenbush,‖ and Markus Sperandio*,1*

*Walter Brendel Centre of Experimental Medicine and ‡Division of Neonatology, Perinatal Center at the Department of Gynecology and Obstetrics, University Children's Hospital, Ludwig-Maximilians-Universität, Munich, Germany; †Department of Neonatology, University Children's Hospital, University of Heidelberg, Heidelberg, Germany; §Department of Microbiology and Immunobiology, Harvard Medical School, Boston, Massachusetts, USA; and ‖Agennix AG, Inc, Princeton, USA

RECEIVED SEPTEMBER 24, 2012; REVISED NOVEMBER 18, 2012; ACCEPTED NOVEMBER 23, 2012. DOI: 10.1189/jlb.0912468

ABSTRACT

Attenuation of the immune response contributes to the high rate of neonatal infections, particularly in premature infants. Whereas our knowledge of innate immune functions in mature neonates is growing, little is known about the ontogeny of neutrophil recruitment. We investigated neutrophils and ECs in the course of gestation with respect to rolling and adhesive functions. With the use of microflow chambers, we demonstrate that the neutrophil's ability to roll and adhere directly correlates with gestational age. These adhesion-related abilities are very rare in extremely premature infants (<30 weeks of gestation), which may correlate with our observation of markedly reduced expression of PSGL-1 and Mac-1 on neutrophils in preterm infants. In parallel, the capacity of HUVECs to mediate neutrophil adhesion under flow increases with gestational age. In addition, HUVECs from extremely premature infants exerting the lowest ability to recruit adult neutrophils show a diminished up-regulation of E-selectin and ICAM-1. Finally, by following neutrophil function postnatally, we show that maturation of PMN recruitment proceeds equivalently during extra- and intrauterine development. Thus, PMN recruitment and EC adhesion-related functions are ontogenetically regulated in the fetus, which might contribute significantly to the high risk of life-threatening infections in premature infants. *J. Leukoc. Biol.* 93: 175–184; 2013.

Introduction

Severe infections remain a leading cause of neonatal morbidity and mortality, despite advances in intensive care medicine and the early use of antibiotics. It is estimated that worldwide, over 1 million neonates die annually due to overwhelming infections [1]. The incidence of sepsis correlates inversely with the gestational age of the infants, and premature infants, in particular, show a unique susceptibility to (bacterial) pathogens with secondary sepsis rates ranging from 22% to 36% in very low birth-weight neonates and up to 62% in extremely premature infants [2–4]. In addition to extrinsic factors, such as invasive procedures and long hospital stays, an immaturity of the immune system is thought to account for the increased rate of neonatal infections [5].

During infection, PMNs play a crucial role in the early innate immune response [6]. The importance of these cells for host defense against invading microorganisms is underscored by the high risk of infections in patients with neutropenia or neutrophil disorders [7, 8]. This is particularly relevant for neonates, as it has been shown that they largely depend on the innate immune system for protection against sepsis, whereas the adaptive immune system initially has a minor role [9]. To fight pathogens, neutrophils are recruited from the vasculature into infected tissue in a multistep adhesion process involving a complex interplay of adhesion molecules with their respective ligands located on the neutrophil membrane and on ECs [10]. First, circulating PMNs are captured and begin to roll along the vessel wall through selectins (P-, E-, and L-selectin), binding to selectin-ligands, such as PSGL-1 [11, 12]. During rolling, neutrophils come in close contact with chemokines presented on inflamed endothelium, which bind to specific chemokine receptors on the neutrophil surface, leading to a conformational change and activation of neutrophil-expressed β-2 integrins (inside-out signaling). This results in firm neutrophil arrest, a prerequisite for subsequent transmigration of the cells into tissue [10]. At present, our detailed understanding of the PMN recruitment cascade is based primarily on studies performed on adult organisms [10]. It has long been known that there are distinct differences between neonates and adults in neutrophil adhesiveness and migratory behavior [13]. However, our knowledge about the ontogeny of neutrophil recruitment in

Abbreviations: EC=endothelial cell, FOV=field of view, h=human, Mac-1=macrophage-1 antigen, MFI=mean fluorescence intensity, PSGL-1=P-selectin glycoprotein ligand-1, VE=vascular endothelial, vWF=von Willebrand factor

1. Correspondence: Walter Brendel Centre of Experimental Medicine, Ludwig-Maximilians-Universität, Marchioninistr. 27, 81377 Munich, Germany. E-mail: markus.sperandio@med.uni-muenchen.de; Twitter: http://www.twitter.com/www.sfb914.de

the developing fetus remains incomplete. Animal experiments addressing this matter are scarce, have been performed primarily in nonmammalian organisms, but indicate an impaired response of the innate immune system during fetal development [14, 15]. These findings parallel the clinical observation of an inverse relationship between sepsis incidence and gestational age, with highest infection rates found in extremely premature infants. However, so far, it is still unclear whether PMN recruitment in human fetuses is subjected to a similar maturation process of the immune system during gestation and whether this maturation process can be accelerated following premature delivery.

In the present study, we investigated the recruitment of PMN from premature and mature human neonates. Our experiments reveal that the neutrophil's ability to roll, adhere, and express adhesion molecules increases significantly with gestational age. Intriguingly, the maturation of PMN recruitment during fetal development is not dependent on intrauterine factors, as comparisons of PMN function between premature infants with the same postconceptional but a different postnatal age demonstrated. In addition, we observed a corresponding reduced capacity of ECs from premature infants to up-regulate adhesion molecules and to induce PMN recruitment upon LPS stimulation, thus identifying another neonatal deficiency potentially contributing to the pathogenesis of severe infections in premature infants.

MATERIALS AND METHODS

Sample collection and study population

All neonates included in the study were delivered by Caesarean section. Umbilical cord blood and a piece of the umbilical cord were collected immediately after delivery. Exclusion criteria were maternal HIV infection, congenital malformations, or suspected syndromes, vaginal delivery, and familial immune diseases. Peripheral venous blood from infants and healthy adult volunteers was drawn by venipuncture. Standard blood collection tubes (S-Monovette, Sarstedt, Nümbrecht, Germany) containing trisodium citrate were used for anticoagulation of blood samples.

Based on their gestational age, as estimated by the date of the last menstrual period and by ultrasound measurements, infants were grouped into extremely premature infants (≤30 completed weeks of gestation), moderately premature infants (30+1–36+6 weeks of gestation), and mature neonates (>37 completed weeks of gestation). Because of small sample volumes, especially in the extremely premature infant group, we were unable to perform all measurements on each individual. The exact number of subjects for each experiment is given in the figure legends. We recorded baseline characteristics, including gender and birth weight; clinical data, such as antenatal steroid treatment; and the reason for prematurity or Caesarean section, as well as laboratory values (cord blood pH, differential blood-cell count, C-reactive protein).

Isolation of PMNs

As leukocyte and differential counts vary largely among different neonatal age groups, we isolated PMNs from the umbilical cord or peripheral venous blood for standardization of experimental conditions. Whole blood was layered onto a Ficoll density gradient (LSM 1077; PAA Laboratories GmbH, Coelbe, Germany) and centrifuged (1200 *g*, 20 min, room temperature). The resulting erythrocyte-granulocyte pellet was washed twice in Dulbecco's PBS (1×, without Ca^{2+} and Mg^{2+}; Invitrogen GmbH, Darmstadt, Germany) before lysis of erythrocytes by addition of hypotonic buffer (0.15 M NH_4Cl, 0.01 M $NaHCO_3^-$, 0.001 M EDTA, in Aqua ad injetabilia) for 7 min. The remaining granulocytes were washed twice, resuspended in 1 ml PBS, and counted in a Neubauer chamber using Turks solution (Merck, Darmstadt, Germany). By this method, we achieved 76% (premature infants) to 96% (adults) purity and >90% viability of cells. For some experiments, whole blood from adult donors was pretreated with bethamethasone (0.02 μg/ml; Celestan, Essex Pharma GmbH, Munich, Germany) for 1 h before isolation of PMN.

Isolation and culture of HUVECs

ECs were isolated from the umbilical cord vein using collagenase A (1 mg/ml; Roche Diagnostics GmbH, Mannheim, Germany), as reported previously [16]. The cells were resuspended in EC growth medium, supplemented with 10% FCS, basic fibroblast growth factor (1.0 ng/ml), EC growth supplement/heparin (0.004 ml/ml), endothelial growth factor (0.1 ng/ml), hydrocortisone (1.0 μg/ml), and phenol red (0.62 ng/ml; all PromoCell GmbH, Heidelberg, Germany) and 1% penicillin/streptomycin (10,000 U/10 mg/ml; PAA Laboratories GmbH), and grown in standard cell culture dishes. When confluent, cells were harvested using trypsin/EDTA (0.5 mg/0.22 mg/ml; PAA Laboratories GmbH) and cultured further in Medium 199 (Invitrogen GmbH) containing 10% FCS. For flow cytometry, cells of Passage II were collected by use of EDTA (5 mM; Merck) alone. For flow chamber assays, cells of Passage II were transferred into microflow chambers (μ-Slide VI ibiTreat; ibidi, Martinsried, Germany) and grown to confluence overnight. In some cases, freshly isolated HUVECs were incubated with betamethasone (0.02 μg/ml; Celestan, Essex Pharma GmbH) for 12 h and processed further as described above.

Flow chamber experiments

To analyze PMN recruitment, we used an in vitro flow chamber assay. For this purpose, glass capillaries (2×0.2 mm; VitroCom, Mountain Lakes, NJ, USA) were assembled into microflow chambers, as described previously [17]. To assess PMN rolling, the flow chambers were coated with rhP-selectin (CD62-P, 5 μg/ml; R&D Systems, Wiesbaden-Nordensteadt, Germany) or rhE-selectin (CD62-E, 5 μg/ml) in PBS with 0.1% BSA (PAA Laboratories GmbH). For adhesion studies, a combination of selectin (rhP-selectin 10 mg/ml or rhE-selectin 4 mg/ml), chemokine rhCXCL8 (IL-8, 10 μg/ml; R&D Systems), and integrin-ligand rhICAM-1 (CD54, 4 μg/ml; R&D Systems) was used. After overnight incubation, the flow chambers were blocked with 5% casein (from bovine milk; Sigma-Aldrich, Munich, Germany) in PBS for 2 h at room temperature and flushed with PBS. For negative controls, we used four approaches: chemokine or selectin omission, addition of EDTA to the cell suspension, and coating with PBS/0.1% BSA alone. Before the experiments, the isolated PMNs were resuspended in DMEM (low glucose without glutamine; Invitrogen GmbH), containing 1% BSA, $CaCl_2$ (1 mM), and $MgCl_2$ (1 mM), to a calculated concentration of 250,000 cells/ml (rolling assay) or 500,000 cells/ml (adhesion assay). The cell suspension was flushed through the flow chamber using a high-precision syringe pump (Harvard Apparatus, Holiston, MA, USA) at a flow rate of 0.115 ml/min, resulting in a shear stress of ~1 dyne/cm^2 [17].

In other experiments investigating the contribution of neonatal ECs to PMN recruitment, we stimulated HUVECs grown in ibidi flow chambers (3.8×4 mm, μ-Slide VI) with LPS (10 μg/ml, LPS from *Escherichia coli* 0111:B4; Sigma-Aldrich) for 4 h. After washing with HBSS (Pharmacy of the University Hospital Munich, Germany), the chambers were connected to a PE 50 tube (intramedic polyethylene tubing, inner diameter 0.58 mm; outer diameter 0.965 mm; Becton Dickinson, Franklin Lakes, NJ, USA) and perfused with PMNs from a healthy adult donor at a concentration of 250,000 cells/ml and a rate of 0.91 ml/min, resulting in a shear stress of ~1.6 dyne/cm^2 based on the manufacturer's description (ibidi Application Note #11; www.ibidi.com).

Microscopy and data analysis

The flow chamber studies were performed on an upright microscope (BX51; Olympus, Hamburg Germany) with a saline immersion objective (XLUMPlanFl, 20×, 0.95 NA) or on an inverse microscope (IM35, Nikon Fluor 20×, 0.75 NA; Zeiss MicroImaging GmbH, Munich, Germany) for

observation of ibidi chambers. Experiments were recorded for 10 min on a Super VHS recorder via a charge-coupled device camera (Model CF8/1; Kappa optronics GmbH, Germany) for later, off-line analysis. PMN rolling was quantified by counting the number of cells/FOV (740 mm×565 μm), moving at a velocity significantly lower than the center-line velocity for >30 s. Adherent PMNs were defined as cells that remained stationary for >30 s.

Flow cytometric analysis of adhesion molecule expression

Surface expression of adhesion molecules on PMNs and ECs was measured by flow cytometry. Isolated PMNs were incubated with primary mAb (all IgG1 mouse anti-human; BD PharMingen, Heidelberg, Germany) to LFA-1 (CD11a), Mac-1 (CD11b), PSGL-1 (CD162), or CXCR2 (CD182) for 45 min on ice. A PE-labeled goat anti-mouse antibody was used as a secondary antibody. Unstimulated and LPS-stimulated (4 h, 10 μg/ml) HUVECs of Passage II were stained with PE-labeled mAb (all IgG1 mouse anti-human; BD PharMingen) to E-selectin (CD62-E) or ICAM-1 (CD54) for 45 min on ice. For EC characterization, unstimulated HUVECs were treated with PE-labeled antibody to PECAM (CD31, IgG1; BD PharMingen) or with unlabeled primary antibody to vWf (IgG1; Dako, Eching, Germany) with PE-labeled goat anti-mouse secondary antibody. Measurements were performed on a FACSorter flow cytometer (Becton Dickinson) using the CellQuest Pro software (Becton Dickinson). The MFI for 10,000 cells/sample was obtained using log detection settings. All antibodies were normalized against isotype-matched controls.

Immunofluorescence staining

HUVECs from premature and mature neonates (for isolation procedure, see above) were grown to confluence in μ-Slides (ibidi) and fixed by addition of 3.7% paraformaldehyde (Applichem, Darmstadt, Germany) in PBS (Invitrogen GmbH) for 10 min at room temperature. After rinsing with PBS, cells were blocked with 1% BSA (PAA Laboratories GmbH) in PBS for 30 min at room temperature. Cells were incubated with primary monoclonal mouse anti-human VE-cadherin (CD144, IgG1; eBioscience, Frankfurt, Germany) for 2 h at room temperature, washed, and incubated with a secondary Alexa 546-labeled goat anti-mouse antibody (Invitrogen GmbH) for 2 h at room temperature. After repeated washing steps to remove unbound antibody, mounting medium (Permafluor; Beckman Coulter, Fullerton, CA, USA) was added to the channels, and VE-cadherin expression was detected by confocal laser-scanning microscopy (Leica TCS SP5; Leica Microsystems, Wetzlar, Germany) using a 40× oil immersion objective (HCX PLAPO CS 40×/1.25–0.75 oil) and Leica Application Suite software.

Statistical analysis

For multiple comparisons between groups, a Kruskal-Wallis ANOVA on ranks was used, followed by Student-Newman-Keuls or Dunn's post hoc test, as appropriate. To test for nonlinear correlation, Spearman's rank correlation coefficient was determined. A P value <0.05 was considered statistically significant. All statistical analyses were carried out with SigmaStat 3.5 (Systat Software GmbH, Germany). Data are presented as mean ± SEM.

Study approval

The study was approved by the local Medical Ethical Committee of the Ludwig-Maximilians-Universität (Project 249-08), and informed, written consent was obtained from the mothers of all participants during pregnancy prior to inclusion into the study.

RESULTS

Study population

From 10/2008 to 12/2009, a total of 58 newborns were included in this study. Infants were classified according to their gestational age into extremely premature infants (n=20), moderately premature infants (n=18), and mature neonates (n=19). Reasons for prematurity were placental insufficiency, premature labor and/or premature rupture of membranes, pre-eclampsia, HELLP syndrome, pathologic Doppler flow, suspected amnion infection, and twin pregnancy. Baseline characteristics and laboratory data of the patient groups are given in **Table 1**. As children were included consecutively, the gender distribution among the experimental groups shows some variation. As expected, premature neonates had a significantly lower birth weight than mature neonates. The white blood-cell count and the number of PMNs in whole blood, as well as the arterial pH value, also differed significantly among the groups.

Rolling and adhesion of neonatal PMNs in relation to gestational age

To assess whether gestational age influences PMN recruitment under dynamic conditions, we quantified rolling and adhesion of neutrophils obtained from umbilical cord blood of premature and mature infants in a microflow chamber system at a shear stress of ~1 dyne/cm^2, resembling a physiological shear stress found in postcapillary venules in vivo [18]. When looking at PMNs from adult healthy controls, we observed a continuous increase in the number of rolling cells in P-selectin (**Fig. 1A**)- and

TABLE 1. Patient Characteristics and Laboratory Values of Umbilical Cord Blood

Data	Extremely premature infants	Moderately premature infants	Mature neonates	P value (ANOVA)
Clinical	n = 20	n = 18	n = 19	
Gestational age (weeks)	27 3/7 ± 1 6/7	32 4/7 ± 1 5/7	38 4/7 ± 1 0/7	n.a.
Birth weight (g)	1043 ± 240	1825 ± 382	3378 ± 448	<0.001
Female/male	6/14	6/12	9/10	n.a.
Laboratory	n = 17	n = 15	n = 16	
WBC (G/l)	7.7 ± 4.9	7.5 ± 3.3	15.5 ± 6.9	<0.001
PMN (%)	31 ± 22	30 ± 12	50 ± 12	0.018
Hct (%)	40 ± 7	43 ± 6	47 ± 6	n.s.
Platelet count (G/l)	228 ± 95	217 ± 46	269 ± 35	n.s.
CrP (mg/dl)	<0.5	<0.5	<0.5	n.a.
Arterial pH	7.27 ± 0.09	7.35 ± 0.04	7.32 ± 0.05	0.029

Please note that laboratory data could not be obtained from each child as a result of small sample volume or sampling errors. Data are given as mean ± SEM. n.a., Not applicable; WBC, white blood-cell count; Hct, hematocrit; CrP, C-reactive protein.

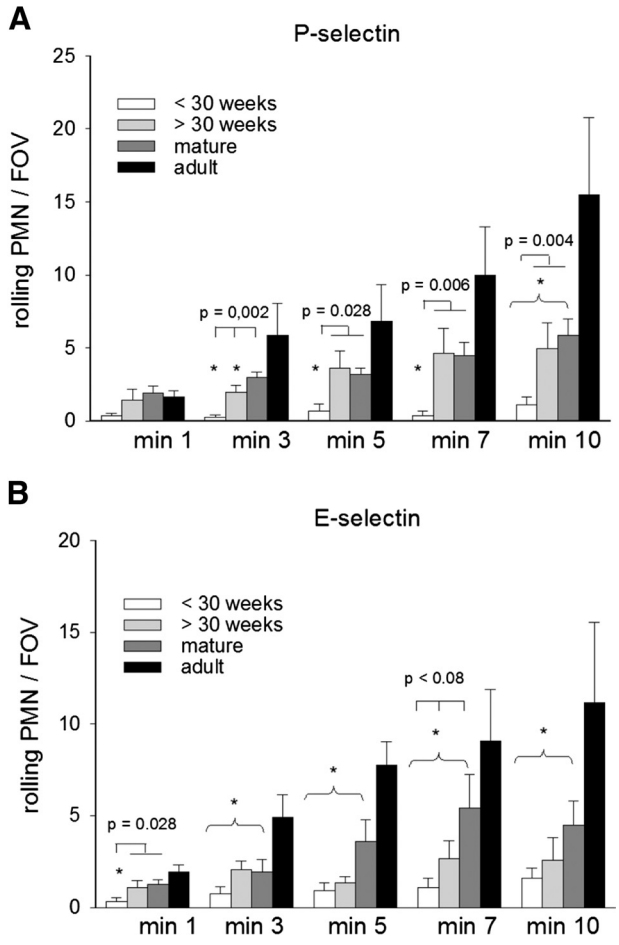

Figure 1. Rolling of neonatal and adult neutrophils under flow. PMNs, isolated from umbilical cord or peripheral venous blood (250×10^3/ml), were perfused through microflow chambers coated with (A) rhP-selectin (5 μg/ml) or (B) rhE-selectin (5 μg/ml) for 10 min at ~1 dyne/cm^2, and the number of rolling cells was quantified. Data are given as mean ± SEM (n=6/group). *Significance versus adult control; squared brackets indicate significance between experimental groups (P<0.05, ANOVA on ranks).

E-selectin (Fig. 1B)-coated flow chambers during the 10-min observation period. Compared with adult controls, the number of rolling PMNs was significantly lower in mature neonates and even further reduced in premature infants (Fig. 1A and B). Neutrophils from extremely premature infants showed almost no rolling on immobilized P- or E-selectin, suggesting that neutrophil rolling is developmentally regulated during fetal life.

Next, we studied PMN adhesion in flow chambers coated with a combination of P- or E-selectin, the CXCR2 chemokine IL-8, and the integrin ligand ICAM-1. We observed that the ability of neutrophils to adhere under conditions of flow strongly and significantly depends on gestational age. Whereas PMNs from extremely premature infants rarely showed adhesion (**Fig. 2A** and **B**), there were some adherent cells in the moderately premature infant group. A further increase in adhesion was seen when PMNs from mature neonates were perfused through the chambers. However, even mature neonates did not reach the levels seen in the adult control group (Fig. 2A and B). When plotting the number of adherent cells at 10 min against the gestational age of each individual, we found a highly significant correlation (Fig. 2C). To test whether PMN adhesion is mediated specifically by the immobilized molecules used in the experiment, we performed control microflow chamber experiments, where the selectin or the chemokine was omitted during coating, chambers were coated with PBS/BSA alone, or EDTA was added to the perfusion medium to eliminate divalent cations necessary for specific binding. We did not observe significant numbers of adherent cells from adult healthy donors in any of the control chambers (Fig. 2D), ruling out nonspecific PMN adhesion in our assay.

Recruitment of adult PMNs on HUVECs from premature and mature neonates

For the successful recruitment of PMNs in vivo, neutrophils need to interact with adhesion molecules expressed on ECs [10]. It has been shown that age-dependent variations in neutrophil recruitment to fetal porcine ECs exist, with a relative inability of ECs from midgestation fetuses to interact with neutrophils under conditions of flow [19]. We assessed whether ECs isolated from the umbilical cord of premature and mature infants are capable of supporting recruitment of PMNs isolated from adult healthy controls using the microflow chamber assay. As expected, we did not observe significant rolling or adhesion of adult PMNs on unstimulated HUVECs in any group (**Fig. 3A** and **B**). Upon EC stimulation with LPS for 4 h, PMNs started to roll and adhere on the HUVEC layer in all experimental groups. However, the extent of PMN rolling and adhesion differed significantly between the groups and depended on the gestational age of the neonates (Fig. 3C and D). After 10 min, the number of cells rolling on HUVECs from mature infants was nearly fivefold above the numbers found on HUVECs from extremely premature infants (Fig. 3A and C), and the number of adherent PMNs was nearly threefold higher (Fig. 3B and D).

Age-dependent expression of adhesion molecules on fetal PMNs and umbilical cord ECs

As a result of the age-dependent differences observed in PMN recruitment, we characterized the cells isolated from the umbilical vein of premature and mature neonates and quantified adhesion molecule expression by flow cytometry and confocal laser-scanning microscopy. Unstimulated cells expressed similar levels of CD31 and vWF, as well as VE-cadherin, demonstrating their endothelial nature (**Fig. 4A** and **B**). We then quantitated by flow cytometry the adhesion molecule expression on umbilical vein ECs from premature and mature neonates. ICAM-1 was expressed constitutively at low levels on untreated cells, whereas E- and P-selectin were not detected (Fig. 4C). After stimulation with LPS, expression of E-selectin increased significantly in all groups. However, the amount of up-regulation was lowest in extreme premature infants. Comparably, we found a significant LPS-stimulated up-regulation of ICAM-1 expression in term neonates, whereas ICAM-1 expression was less inducible by LPS in premature infants (Fig. 4C). In line with prior reports showing that LPS does not induce

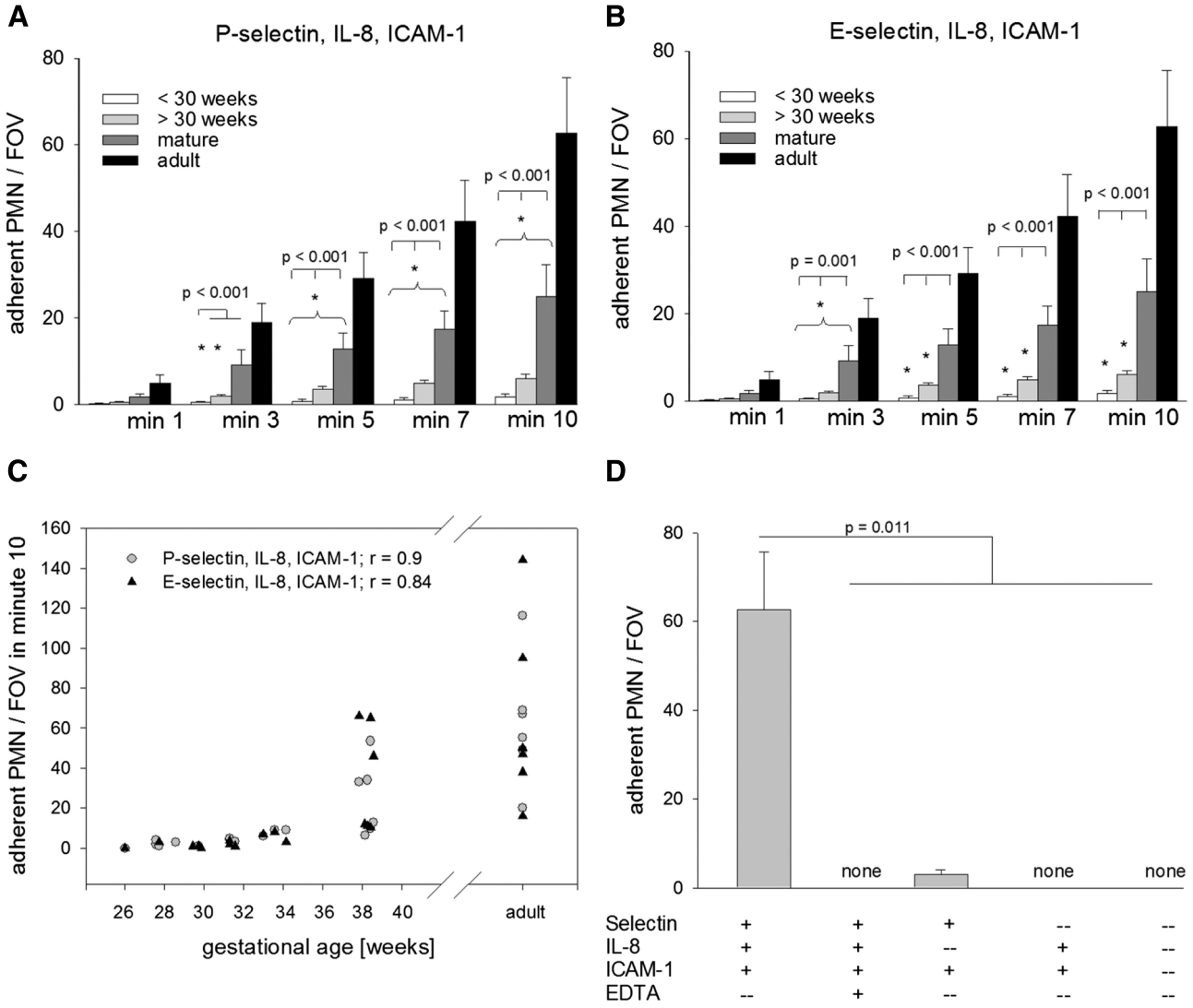

Figure 2. Adhesion of neonatal and adult neutrophils under flow. PMNs isolated from umbilical cord or peripheral venous blood (500×10^3/ml) were perfused through microflow chambers coated with (A) P-selectin (10 μg/ml), IL-8 (10 μg/ml), and ICAM-1 (4 μg/ml) or (B) E-selectin (4 μg/ml), IL-8 (10 μg/ml), and ICAM-1 (4 μg/ml) for 10 min at ~1 dyne/cm^2, and the number of adherent cells was quantified. Data are given as mean ± SEM (n=6/group). *Significance versus adult control; squared brackets indicate significance between experimental groups (P<0.05, ANOVA on ranks). (C) Correlation of the number of adherent cells in Minute 10 with the gestational age of the neonates (P<0.01, Spearman rank-order correlation). For comparison, adhesion of adult cells in Minute 10 is plotted. (D) For negative controls, different approaches were used: coating with PBS/BSA alone, omission of the selectin or the chemokine, and chelation of divalent cations by addition of EDTA (5 mM) to the perfusion medium. Adhesion of PMNs from adult healthy controls at Minute 10 is depicted (left bar in D is identical to black bar, min 10, in A; n=2–3/group).

P-selectin surface expression in HUVECs [20], we were not able to detect any P-selectin on LPS-stimulated HUVECs by means of flow cytometric analysis (not shown).

Next, we measured the surface expression of adhesion molecules relevant for rolling and adhesion on neonatal and adult neutrophils. For this purpose, PMNs were quantified for the selectin-ligand PSGL-1, the chemokine receptor CXCR2, and the β-2 integrins LFA-1 and Mac-1 using flow cytometry (Fig. 4D). Whereas expression levels of CXCR2 and LFA-1 were identical among our experimental groups, we found that PSGL-1 and Mac-1 surface expression was reduced significantly in extremely premature infants compared with adult controls. The expression of these molecules subsequently increased with advancing gestational age (Fig. 4D), suggesting that reduced expression of PSGL-1 and Mac-1 contributes to reduced neutrophil rolling and adhesion during fetal development.

Influence of antenatal steroid treatment on PMN and HUVEC functions

Acceleration of fetal lung maturation by betamethasone treatment of pregnant women with impending preterm delivery is nowadays standard clinical practice [21, 22]. In our patient cohort, 89% of extremely premature infants and 72% of moderately premature infants were exposed to antenatal maternal

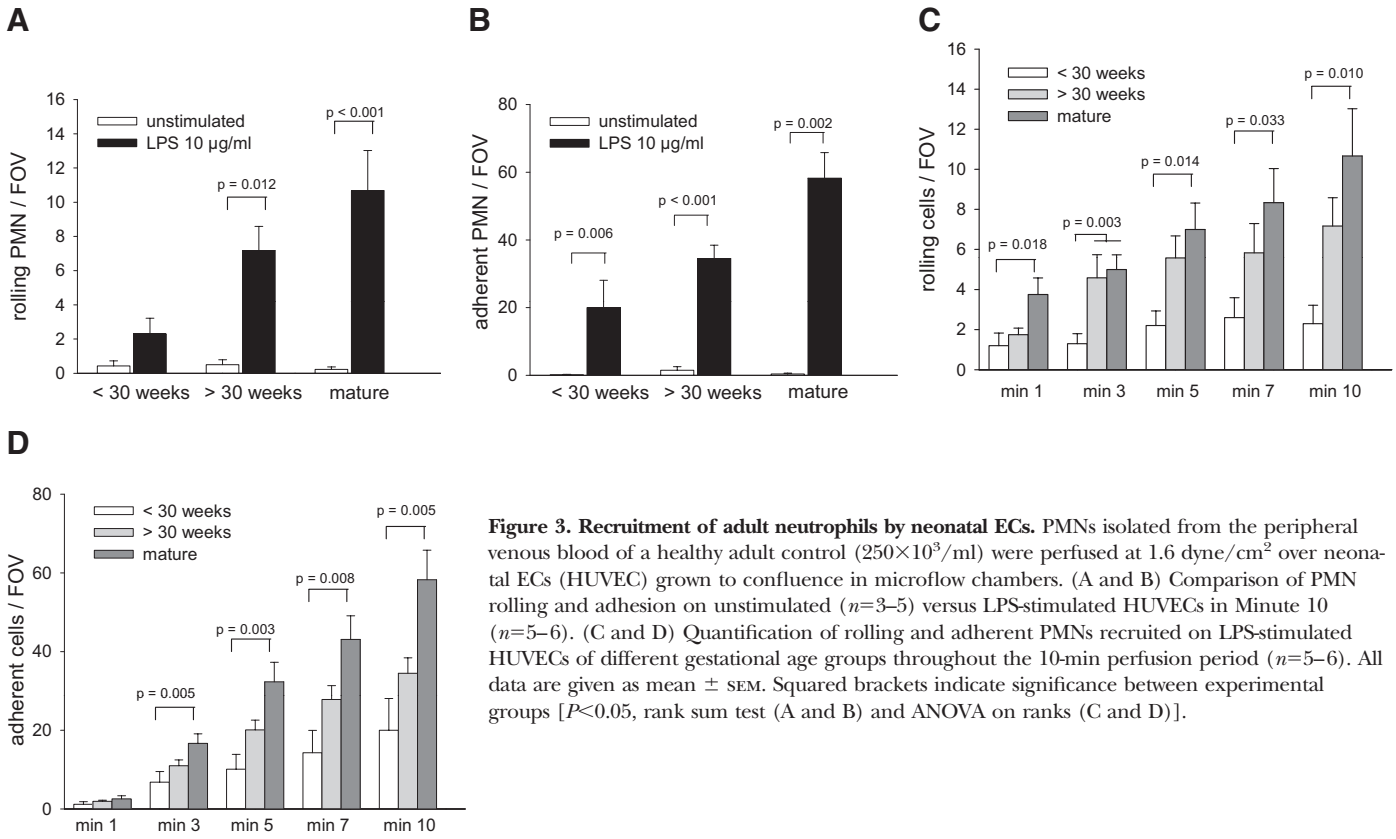

Figure 3. Recruitment of adult neutrophils by neonatal ECs. PMNs isolated from the peripheral venous blood of a healthy adult control (250×10^3/ml) were perfused at 1.6 dyne/cm^2 over neonatal ECs (HUVEC) grown to confluence in microflow chambers. (A and B) Comparison of PMN rolling and adhesion on unstimulated (n=3–5) versus LPS-stimulated HUVECs in Minute 10 (n=5–6). (C and D) Quantification of rolling and adherent PMNs recruited on LPS-stimulated HUVECs of different gestational age groups throughout the 10-min perfusion period (n=5–6). All data are given as mean ± SEM. Squared brackets indicate significance between experimental groups [P<0.05, rank sum test (A and B) and ANOVA on ranks (C and D)].

steroid treatment. To exclude the possibility that such exposure is responsible for the reduction of PMN recruitment seen in premature neonates, we performed microflow chamber experiments using adult donor PMNs that were pretreated (1 h) with betamethasone at a concentration found in the umbilical cord blood of neonates [23]. Adhesion of betamethasone-pretreated adult PMNs in flow chambers coated with P-selectin, IL-8, and ICAM-1 was similar to adhesion observed for untreated adult control PMNs (**Fig. 5A**). In addition, we incubated freshly isolated HUVECs with betamethasone (12 h) before seeding into flow chambers. HUVECs pretreated with betamethasone supported LPS-induced adhesion of adult PMNs to the same extent as HUVECs without prior betamethasone incubation (Fig. 5B). Furthermore, flow cytometric analysis of LPS-stimulated HUVECs (Passage II) demonstrated that the LPS-induced up-regulation of E-selectin and ICAM-1 was independent of prior betamethasone treatment (Fig. 5C), suggesting that betamethasone does not interfere with neutrophil recruitment in our setup.

Postnatal development of PMN recruitment

Recent reports indicated that neutrophils are subjected to a postnatal maturation process [24–26]. This prompted us to investigate the development of PMN recruitment postnatally and evaluate whether exposure of infants to extrauterine factors changes the development of PMN function when compared with the situation in utero. To address this, we compared adhesion of isolated neutrophils from premature infants born at <30 weeks of gestation directly after birth and 4–6 weeks later using P-selectin-, ICAM-1-, and IL-8-coated flow chambers. Compared with the adhesion observed for PMNs isolated directly after birth, PMN adhesion increased significantly with advancing postnatal age of the infants (**Fig. 6A**). However, this increase in adhesion (extrauterine development) was similar to the adhesion observed for PMNs obtained from umbilical cord blood of premature infants born >30 weeks of gestation (intrauterine development), which were matched for the same postconceptional age (Fig. 6B). These findings indicate that extrauterine factors do not seem to have a relevant influence on the development of neutrophil-adhesive capacity, implying that neutrophil maturation during development follows an intrinsic program rather than depending on postnatal factors.

DISCUSSION

The recruitment of neutrophils to sites of infection poses a key event in innate host defense against invading microorganisms. Whereas numerous studies investigating PMN functions in adult organisms have broadened the general understanding of this process, our knowledge of the developing innate immune system during gestation remains limited. In the present study, we analyzed PMN recruitment during human fetal development at different time-points of gestation.

Earlier reports have shown that neutrophil rolling and adhesion can be studied under defined conditions in microflow

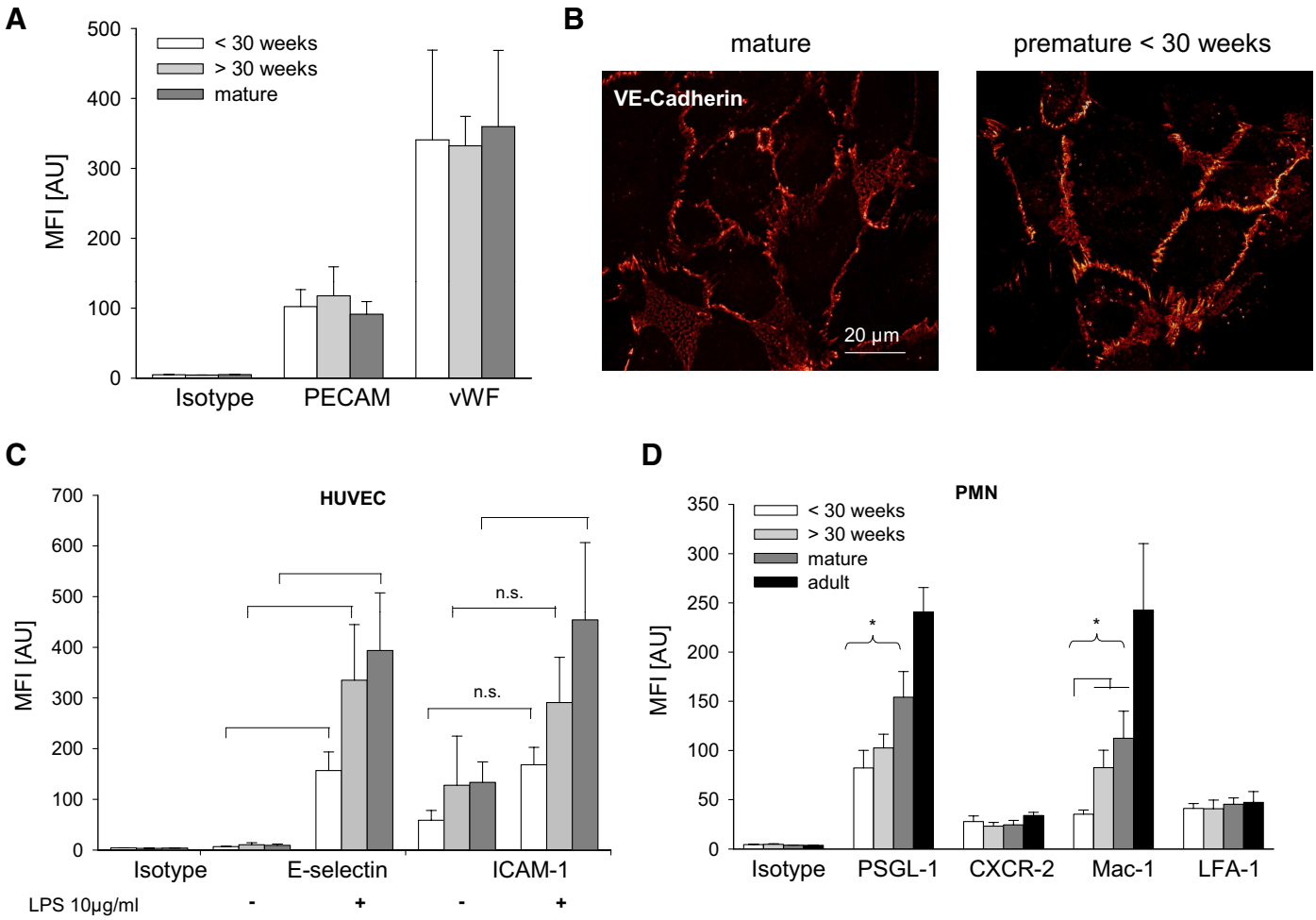

Figure 4. Expression of adhesion molecules on neutrophils and HUVECs. Cells isolated from the umbilical vein of premature and mature neonates were characterized as ECs by their expression of (A) PECAM (CD31) and vWF, as measured by flow cytometry, and (B) VE-cadherin (CD 144, Alexa 546), as seen in confocal laser-scanning microscopy (40× objective). Data are given as mean ± SEM (n=3–5/group). (C) Flow cytometric quantification of E-selectin and ICAM-1 surface expression on unstimulated (n=3) and LPS-stimulated HUVECs (n=6). (D) Flow cytometric quantification of PSGL-1, CXCR2, and Mac-1 (n=5–6) and LFA-1 (n=3–5) surface expression on isolated neonatal and adult PMNs. All data are given as mean ± SEM. *Significance versus adult control; squared brackets indicate significance between experimental groups (P<0.05, ANOVA on ranks).

chambers, guaranteeing reproducibility of experiments and comparability among different experimental groups [17]. With the use of this model, we demonstrate that recruitment of neutrophils under shear stress is almost absent in extremely premature infants. With advancing fetal development, the capability to sufficiently support rolling and adhesion of neutrophils increased gradually; however, even mature neonates did not reach the level of adult controls. This observation is in line with previous reports demonstrating decreased adhesion of human neonatal neutrophils under conditions of flow compared with adult neutrophils [27, 28]. Of importance, these earlier studies only included mature infants and did not take into account possible ontogenetic differences. Previous reports addressing neutrophil adhesion and migration in preterm infants demonstrated a reduction of PMN adhesion and chemotaxis compared with mature neonates or adults. Yet, the data are controversial in regard to age-dependent differences between premature and mature neonates [29–31] and have to be interpreted carefully, as experiments were performed under static conditions, altering adhesion and migration properties [32].

Here, we analyzed neutrophil rolling and adhesion under in vitro settings resembling venous blood flow. Capture and rolling of leukocytes in this setting are mediated by selectin–selectin ligand interactions. For mature neonates, it was described previously that neutrophil rolling on P- or E-selectin-presenting monolayers or on histamine- or IL-1-stimulated HUVECs, respectively, is impaired compared with adult controls [27, 33]. By analyzing neutrophils isolated from premature infants, we could expand those earlier findings and demonstrate that the ability of neutrophils to roll on immobilized P- or E-selectin is even reduced further in extremely premature neonates and increases progressively with increasing maturity of the infants. The severe reduction of capture and rolling events observed for extremely premature infants is very likely to contrib-

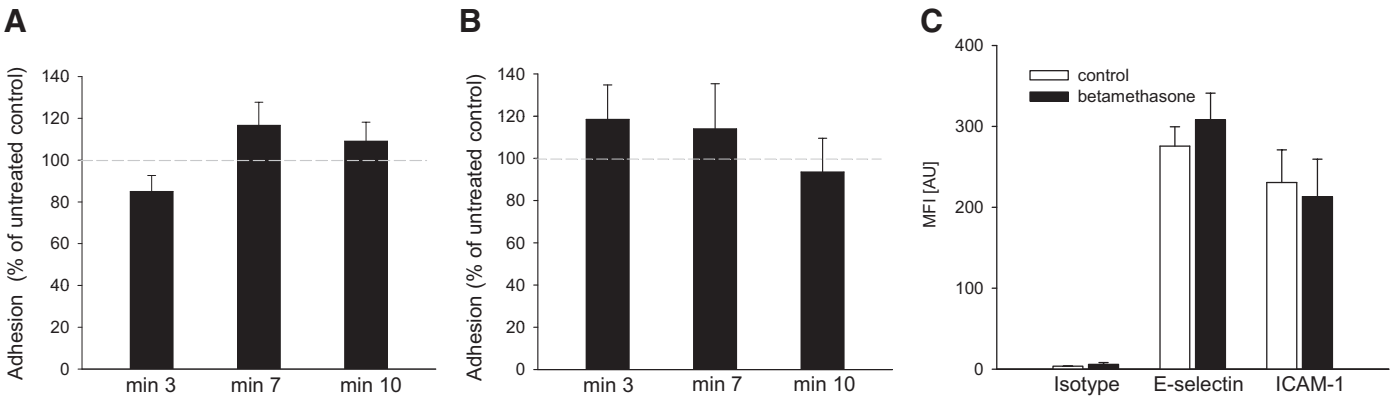

Figure 5. Influence of betamethasone treatment on experimental PMN recruitment and adhesion molecule expression. (A) Peripheral blood of adult controls was pretreated with betamethasone (0.02 μg/ml) for 1 h, and adhesion of isolated PMNs in flow chambers coated with P-selectin (10 μg/ml), IL-8 (10 μg/ml), and ICAM-1 (4 μg/ml) was compared with untreated control (=100%, dashed line; n=3/group). (B) Freshly isolated HUVEC from mature neonates (n=2) were pretreated with betamethasone (0.02 μg/ml), and LPS-stimulated recruitment of adult PMNs on HUVECs was compared with untreated control (=100%, dashed line; four chambers/group). (C) LPS-stimulated expression of adhesion molecules on HUVECs pretreated with betamethasone was measured by flow cytometry and compared with untreated control (n=3/group). All data are given as mean ± SEM.

ute to the very low amount of adhesion found in this age group, as capture and rolling are prerequisites for firm adhesion of cells to the endothelium [34].

In addition, quantitative and qualitative differences in neutrophil integrins and selectins are proposed to be responsible for the reduced recruitment of neonatal neutrophils compared with adults. This includes a decreased basal surface expression of L-selectin and a defective up-regulation of the β-2 integrin Mac-1 (CD11b/CD18) [27, 31, 35, 36]. Likewise, we observed a clear correlation of Mac-1 surface expression with advancing gestational age, possibly contributing to the observed correlation of PMN adhesion with gestational age. By contrast, LFA-1 was already expressed early during gestation and did not change with advancing maturation of the fetuses. Despite being reported consistently, the nature of this difference remains elusive [24, 31, 35]. It has been known for a long time that integrin expression is regulated differentially in a cell- and development-specific manner [37]. Whereas LFA-1 expression is controlled mainly through transcriptional activity, Mac-1 can also be mobilized from intracellular storage pools. In addition, CD18 and CD11a are widely expressed early during leukocyte differentiation, whereas CD11b expression is limited to the myeloid linage and occurs only at later time-points during myeloid cell differentiation. As LFA-1 and Mac-1 share the common β-subunit (CD18), it was suggested that a deficient production of the specific α-subunit (CD11b) may account for the reduced total cell content of Mac-1 observed in neonatal neutrophils [35]. This, in turn, may also explain the impaired basal Mac-1 expression on fetal and neonatal PMNs and its impaired up-regulation upon stimulation, described in earlier reports. In addition, it might also be possible that defective storage and/or mobilization from intracellular storage pools account for the decreased Mac-1 surface expression on fetal and neonatal neutrophils.

Furthermore, we were able to show that the expression of PSGL-1, the major selectin ligand on neutrophils, is also dependent on fetal maturity, as its expression increases during gestation. As suggested by Tcharmtchi et al. [38], reduced PSGL-1 expression may contribute to the diminished rolling capacity of neonatal neutrophils. However, the severity of impairment of fetal PMN recruitment observed in this study points toward other contributing factors. It is possible that our findings may also be related to a diminished response of neonatal neutrophils to chemokine stimulation [39]. Although we did not observe differences in the expression of the chemokine receptor CXCR2, which mediates intravascular neutrophil activation by the CXCL chemokine IL-8 [40], we cannot exclude the possible alterations in intracellular signaling pathways that may affect neutrophil activation. In this context, it has been reported that downstream signals involved in LPS-mediated neutrophil activation are attenuated in newborns [41].

As neutrophil recruitment also involves EC adhesive functions, we further analyzed the adhesive properties of neonatal ECs in the time course of gestation. Our findings clearly demonstrated that EC adhesion-related function depends on gestational age of the infants and is affected significantly in extremely premature infants, leading to reduced neutrophil recruitment as compared with mature infants. Our findings are supported by a comparable study investigating recruitment of adult neutrophils by fetal porcine ECs isolated at different time-points of gestation. This study revealed a similar age dependence of neutrophil-endothelial interactions with very little adhesion of neutrophils to early-gestation fetal EC [19]. This diminished interaction might, in part, be a result of alterations in the expression of inflammatory adhesion molecules on the EC. In this context, it has been reported that the expression of P-selectin on EC is reduced in premature human neonates compared with mature newborns and depends on the degree of maturity of the infants [42]. We now show that up-regulation of E-selectin and ICAM-1 upon stimulation with LPS is also reduced in ECs from premature neonates compared with mature infants. Steroids are known

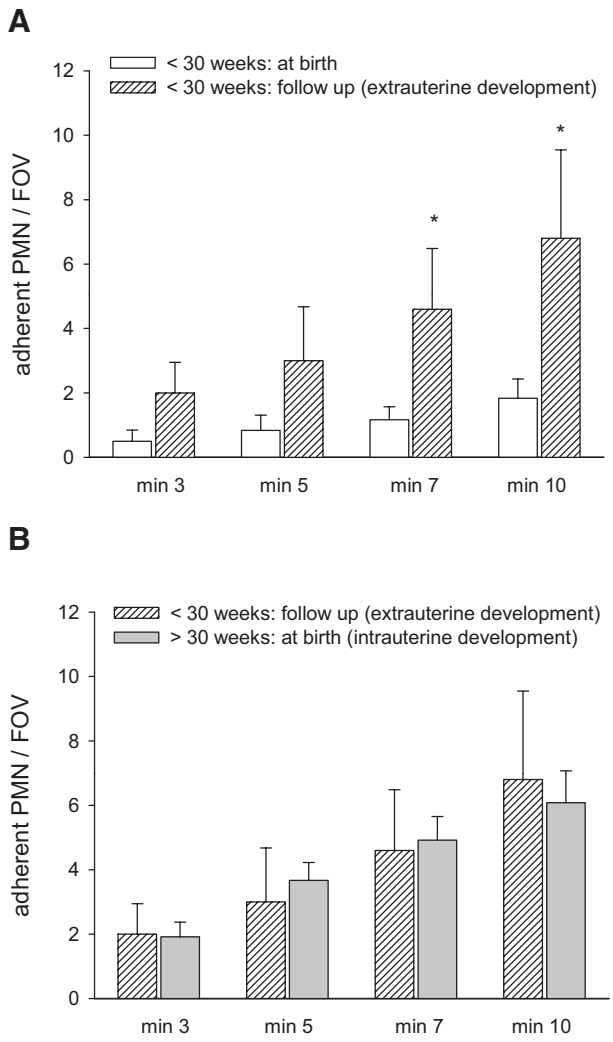

Figure 6. Postnatal maturation of PMN recruitment. Postnatal development of PMN adhesion in flow chambers coated with P-selectin (10 μg/ml), IL-8 (10 μg/ml), and ICAM-1 (4 μg/ml) was evaluated in the group of extreme premature infants (born <30 weeks of gestation) in a follow-up experiment, 4–6 weeks after birth, when the infants had reached a corrected postnatal age of >30 weeks of gestation ("extrauterine development"; hatched bars in (A) and (B)). Results were compared with (A) adhesion of PMN from those children at birth (white bars; data taken from Fig. 1) and (B) adhesion of PMN from moderate premature infants (>30 weeks of gestation) at birth ("intrauterine development"; gray bars; data taken from Fig. 1). Data are given as mean ± SEM (n=5–6). *Significance versus <30 weeks at birth (P<0.05, rank sum test).

to influence endothelial adhesion molecule expression [43, 44] and alter neonatal neutrophil function [45, 46]. Therefore, we performed separate experiments to analyze the impact of antenatal betamethasone treatment on neutrophils and ECs. In our experimental setting, pretreatment with betamethasone had no negative influence on neutrophil recruitment, thus supporting the concept of a true inherent immaturity of the innate immune response rather than a simple iatrogenic-induced effect.

The maturation of the PMN-recruitment process observed in the present study is likely to reflect a physiological adaptation to changing demands during fetal development [13]. As the intrauterine environment is usually sterile, the developing fetus does not need to mount a strong immune response. In contrast, a strong inflammatory reaction with production of TH_1-polarizing cytokines at the feto-maternal interface might even lead to the abortion of the fetus [47]. Toward the end of gestation, however, functional defenses against extrauterine pathogens become increasingly important. Interestingly, Zhao and coworkers [48] demonstrated recently in this context that newborn mice are capable of mounting a hyper-innate immune response compared with adult animals, resulting in what was termed "cytokine storm". All the more, we were surprised to find that the adhesive properties of fetal neutrophils in extreme premature newborns were not altered postnatally by exposure to extrauterine factors (i.e., bacterial colonization of the gut) but showed the same maturation as PMNs from infants that developed in utero, suggesting that intra- und extrauterine maturation of leukocyte recruitment are synchronized and regulated mostly by yet-unknown intrinsic factors that deserve future investigation.

Over the past decades, advances in the medical care of newborns have enabled the survival of ever-younger premature infants. This achievement is paid for with an increasing risk of severe infections, especially in extremely premature neonates. The successful prevention and treatment of neonatal infections are ongoing clinical challenges, demanding new therapeutic strategies. Further insight into the developmental regulation of fetal innate immune processes is crucial for a better understanding of the events taking place during neonatal infection. In conclusion, our experiments reveal that PMN recruitment in the fetus is subjected to a maturation process that involves neutrophil and EC functions. In this context, the inability of extremely premature neonates to sufficiently recruit PMNs is likely to contribute to their increased susceptibility to life-threatening infections. Future research is necessary and should be aimed at unraveling the precise mechanism governing the ontogeny of fetal and neonatal innate immune responses.

AUTHORSHIP

C.N. designed the project, performed and analyzed experiments, and wrote the manuscript. A.G. planned and performed experiments and analyzed data. M.P. performed flow cytometric experiments. S.B. performed flow chamber experiments. D.F., O.G-B., E.Q., and U.H.v.A. provided suggestions on the project and revised the manuscript. M.S. designed and supervised the project and wrote the manuscript.

ACKNOWLEDGMENTS

This work was supported by grants of the Friedrich-Baur-Stiftung (to C.N.), the B. Braun-Stiftung (to C.N.), and DFG Collaborative Research Center Grant 914 (SFB 914, Project B1) to M.S. We thank the teams of the Neonatal Intensive Care Unit and the Delivery Ward at the Department of Obstetrics and Gynecology, Ludwig-Maximilians-Universität (Munich,

Germany), for their help in recruiting patients. We thank Steffen Dietzel for assisting in confocal microscopy. Data presented in this study are part of the doctoral thesis of A.G.

REFERENCES

1. Lawn, J. E., Wilczynska-Ketende, K., Cousens, S. N. (2006) Estimating the causes of 4 million neonatal deaths in the year 2000. *Int. J. Epidemiol.* **35,** 706–718.
2. Fanaroff, A. A., Stoll, B. J., Wright, L. L., Carlo, W. A., Ehrenkranz, R. A., Stark, A. R., Bauer, C. R., Donovan, E. F., Korones, S. B., Laptook, A. R., Lemons, J. A., Oh, W., Papile, L. A., Shankaran, S., Stevenson, D. K., Tyson, J. E., Poole, W. K.NICHD Neonatal *Research Network* (2007) Trends in neonatal morbidity and mortality for very low birthweight infants. *Am. J. Obstet. Gynecol.* **196,** 147–148.
3. Genzel-Boroviczeny, O., MacWilliams, S., Von, P. M., Zoppelli, L. (2006) Mortality and major morbidity in premature infants less than 31 weeks gestational age in the decade after introduction of surfactant. *Acta Obstet. Gynecol. Scand.* **85,** 68–73.
4. Stoll, B. J., Hansen, N., Fanaroff, A. A., Wright, L. L., Carlo, W. A., Ehrenkranz, R. A., Lemons, J. A., Donovan, E. F., Stark, A. R., Tyson, J. E., Oh, W., Bauer, C. R., Korones, S. B., Shankaran, S., Laptook, A. R., Stevenson, D. K., Papile, L. A., Poole, W. K. (2002) Late-onset sepsis in very low birth weight neonates: the experience of the NICHD Neonatal Research Network. *Pediatrics* **110,** 285–291.
5. Levy, O. (2007) Innate immunity of the newborn: basic mechanisms and clinical correlates. *Nat. Rev. Immunol.* **7,** 379–390.
6. Burg, N. D., Pillinger, M. H. (2001) The neutrophil: function and regulation in innate and humoral immunity. *Clin. Immunol.* **99,** 7–17.
7. Valdez, J. M., Scheinberg, P., Young, N. S., Walsh, T. J. (2009) Infections in patients with aplastic anemia. *Semin. Hematol.* **46,** 269–276.
8. Dinauer, M. C. (2007) Disorders of neutrophil function: an overview. *Methods Mol.* Biol. **412,** 489–504.
9. Wynn, J. L., Scumpia, P. O., Winfield, R. D., Delano, M. J., Kelly-Scumpia, K., Barker, T., Ungaro, R., Levy, O., Moldawer, L. L. (2008) Defective innate immunity predisposes murine neonates to poor sepsis outcome but is reversed by TLR agonists. *Blood* **112,** 1750–1758.
10. Ley, K., Laudanna, C., Cybulsky, M. I., Nourshargh, S. (2007) Getting to the site of inflammation: the leukocyte adhesion cascade updated. *Nat. Rev. Immunol.* **7,** 678–689.
11. Sperandio, M., Smith, M. L., Forlow, S. B., Olson, T. S., Xia, L., McEver, R. P., Ley, K. (2003) P-selectin glycoprotein ligand-1 mediates L-selectin-dependent leukocyte rolling in venules. *J. Exp.* Med. **197,** 1355–1363.
12. Xia, L., Sperandio, M., Yago, T., McDaniel, J. M., Cummings, R. D., Pearson-White, S., Ley, K., McEver, R. P. (2002) P-selectin glycoprotein ligand-1-deficient mice have impaired leukocyte tethering to E-selectin under flow. *J. Clin. Invest.* **109,** 939–950.
13. Nussbaum, C., Sperandio, M. (2011) Innate immune cell recruitment in the fetus and neonate. *J. Reprod. Immunol.* **90,** 74–81.
14. Rouwet, E. V., Beuk, R. J., Heineman, E., Slaaf, D. W., oude Egbrink, M. G. (2000) Effect of repetitive asphyxia on leukocyte-vessel wall interactions in the developing chick intestine. *J. Pediatr. Surg.* **35,** 49–55.
15. Le Guyader, D., Redd, M. J., Colucci-Guyon, E., Murayama, E., Kissa, K., Briolat, V., Mordelet, E., Zapata, A., Shinomiya, H., Herbomel, P. (2008) Origins and unconventional behavior of neutrophils in developing zebrafish. *Blood* **111,** 132–141.
16. Jaffe, E. A., Nachman, R. L., Becker, C. G., Minick, C. R. (1973) Culture of human endothelial cells derived from umbilical veins. Identification by morphologic and immunologic criteria. *J. Clin. Invest.* **52,** 2745–2756.
17. Smith, M. L., Sperandio, M., Galkina, E. V., Ley, K. (2004) Autoperfused mouse flow chamber reveals synergistic neutrophil accumulation through P-selectin and E-selectin. *J. Leukoc. Biol.* **76,** 985–993.
18. Kim, M. B., Sarelius, I. H. (2003) Distributions of wall shear stress in venular convergences of mouse cremaster muscle. *Microcirculation* **10,** 167–178.
19. Naik-Mathuria, B., Gay, A. N., Zhu, X., Yu, L., Cass, D. L., Olutoye, O. O. (2007) Age-dependent recruitment of neutrophils by fetal endothelial cells: implications in scarless wound healing. *J. Pediatr. Surg.* **42,** 166–171.
20. Yao, L., Setiadi, H., Xia, L., Laszik, Z., Taylor, F. B., McEver, R. P. (1999) Divergent inducible expression of P-selectin and E-selectin in mice and primates. *Blood* **94,** 3820–3828.
21. Liggins, G. C., Howie, R. N. (1972) A controlled trial of antepartum glucocorticoid treatment for prevention of the respiratory distress syndrome in premature infants. *Pediatrics* **50,** 515–525.
22. Ballard, R. A., Ballard, P. L. (1976) Use of prenatal glucocorticoid therapy to prevent respiratory distress syndrome. A supporting view. *Am. J. Dis. Child* **130,** 982–987.
23. Ballard, P. L., Granberg, P., Ballard, R. A. (1975) Glucocorticoid levels in maternal and cord serum after prenatal betamethasone therapy to prevent respiratory distress syndrome. *J. Clin. Invest.* **56,** 1548–1554.
24. Storm, S. W., Mariscalco, M. M., Tosi, M. F. (2008) Postnatal maturation of total cell content and up-regulated surface expression of Mac-1 (CD11b/CD18) in polymorphonuclear leukocytes of human infants. *J. Leukoc. Biol.* **84,** 477–479.
25. Usmani, S. S., Schlessel, J. S., Sia, C. G., Kamran, S., Orner, S. D. (1991) Polymorphonuclear leukocyte function in the preterm neonate: effect of chronologic age. *Pediatrics* **87,** 675–679.
26. Eisenfeld, L., Krause, P. J., Herson, V., Savidakis, J., Bannon, P., Maderazo, E., Woronick, C., Giuliano, C., Banco, L. (1990) Longitudinal study of neutrophil adherence and motility. *J. Pediatr.* **117,** 926–929.
27. Mariscalco, M. M., Tcharmtchi, M. H., Smith, C. W. (1998) P-selectin support of neonatal neutrophil adherence under flow: contribution of L-selectin, LFA-1, and ligand(s) for P-selectin. *Blood* **91,** 4776–4785.
28. Anderson, D. C., Abbassi, O., Kishimoto, T. K., Koenig, J. M., McIntire, L. V., Smith, C. W. (1991) Diminished lectin-, epidermal growth factor-, complement binding domain-cell adhesion molecule-1 on neonatal neutrophils underlies their impaired CD18-independent adhesion to endothelial cells in vitro. *J. Immunol.* **146,** 3372–3379.
29. Carr, R., Pumford, D., Davies, J. M. (1992) Neutrophil chemotaxis and adhesion in preterm babies. *Arch. Dis. Child* **67,** 813–817.
30. Bektas, S., Goetze, B., Speer, C. P. (1990) Decreased adherence, chemotaxis and phagocytic activities of neutrophils from preterm neonates. *Acta Paediatr.* Scand. **79,** 1031–1038.
31. Anderson, D. C., Freeman, K. L., Heerdt, B., Hughes, B. J., Jack, R. M., Smith, C. W. (1987) Abnormal stimulated adherence of neonatal granulocytes: impaired induction of surface Mac-1 by chemotactic factors or secretagogues. *Blood* **70,** 740–750.
32. Zarbock, A., Ley, K. (2009) Neutrophil adhesion and activation under flow. *Microcirculation* **16,** 31–42.
33. Abbassi, O., Kishimoto, T. K., McIntire, L. V., Anderson, D. C., Smith, C. W. (1993) E-selectin supports neutrophil rolling in vitro under conditions of flow. *J. Clin. Invest.* **92,** 2719–2730.
34. Lawrence, M. B., Springer, T. A. (1991) Leukocytes roll on a selectin at physiologic flow rates: distinction from and prerequisite for adhesion through integrins. *Cell* **65,** 859–873.
35. McEvoy, L. T., Zakem-Cloud, H., Tosi, M. F. (1996) Total cell content of CR3 (CD11b/CD18) and LFA-1 (CD11a/CD18) in neonatal neutrophils: relationship to gestational age. *Blood* **87,** 3929–3933.
36. Henneke, P., Osmers, I., Bauer, K., Lamping, N., Versmold, H. T., Schumann, R. R. (2003) Impaired CD14-dependent and independent response of polymorphonuclear leukocytes in preterm infants. *J. Perinat. Med.* **31,** 176–183.
37. Miller, L. J., Schwarting, R., Springer, T. A. (1986) Regulated expression of the Mac-1, LFA-1, p150,95 glycoprotein family during leukocyte differentiation. *J. Immunol.* **137,** 2891–2900.
38. Tcharmtchi, M. H., Smith, C. W., Mariscalco, M. M. (2000) Neonatal neutrophil interaction with P-selectin: contribution of P-selectin glycoprotein ligand-1 and sialic acid. *J. Leukoc. Biol.* **67,** 73–80.
39. Fox, S. E., Lu, W., Maheshwari, A., Christensen, R. D., Calhoun, D. A. (2005) The effects and comparative differences of neutrophil specific chemokines on neutrophil chemotaxis of the neonate. *Cytokine* **29,** 135–140.
40. Stillie, R., Farooq, S. M., Gordon, J. R., Stadnyk, A. W. (2009) The functional significance behind expressing two IL-8 receptor types on PMN. *J. Leukoc. Biol.* **86,** 529–543.
41. Al-Hertani, W., Yan, S. R., Byers, D. M., Bortolussi, R. (2007) Human newborn polymorphonuclear neutrophils exhibit decreased levels of MyD88 and attenuated p38 phosphorylation in response to lipopolysaccharide. *Clin. Invest. Med.* **30,** E44–E53.
42. Lorant, D. E., Li, W. H., Tabatabaei, N., Garver, M. K., Albertine, K. H. (1999) P-selectin expression by endothelial cells is decreased in neonatal rats and human premature infants. *Blood* **94,** 600–609.
43. Cronstein, B. N., Kimmel, S. C., Levin, R. I., Martiniuk, F., Weissmann, G. (1992) A mechanism for the antiinflammatory effects of corticosteroids: the glucocorticoid receptor regulates leukocyte adhesion to endothelial cells and expression of endothelial-leukocyte adhesion molecule 1 and intercellular adhesion molecule 1. *Proc. Natl. Acad. Sci. USA* **89,** 9991–9995.
44. Aziz, K. E., Wakefield, D. (1996) Modulation of endothelial cell expression of ICAM-1, E-selectin, and VCAM-1 by β-estradiol, progesterone, and dexamethasone. *Cell. Immunol.* **167,** 79–85.
45. Fuenfer, M. M., Herson, V. C., Raye, J. R., Woronick, C. L., Eisenfeld, L., Ingardia, C. J., Block, C. F., Krause, P. J. (1987) The effect of betamethasone on neonatal neutrophil chemotaxis. *Pediatr. Res.* **22,** 150–153.
46. Jaarsma, A. S., Braaksma, M. A., Geven, W. B., Van Oeveren, W., Bambang-Oetomo, S. (2004) Antenatal glucocorticoids attenuate activation of the inflammatory reaction and clotting in preterm lambs. *Biol. Neonate* **85,** 82–89.
47. Makhseed, M., Raghupathy, R., Azizieh, F., Omu, A., Al-Shamali, E., Ashkanani, L. (2001) Th1 and Th2 cytokine profiles in recurrent aborters with successful pregnancy and with subsequent abortions. *Hum. Reprod.* **16,** 2219–2226.
48. Zhao, J., Kim, K. D., Yang, X., Auh, S., Fu, Y. X., Tang, H. (2008) Hyper innate responses in neonates lead to increased morbidity and mortality after infection. *Proc. Natl. Acad. Sci. USA* **105,** 7528–7533.

KEY WORDS:
leukocyte recruitment · rolling · adhesion · integrins · selectins

Maturation of Platelet Function During Murine Fetal Development In Vivo

Andreas Margraf,* Claudia Nussbaum,* Ina Rohwedder, Sarah Klapproth, Angela R.M. Kurz, Annamaria Florian, Volker Wiebking, Joachim Pircher, Monika Pruenster, Roland Immler, Steffen Dietzel, Ludmila Kremer, Friedemann Kiefer, Markus Moser, Andreas W. Flemmer, Elizabeth Quackenbush, Ulrich H. von Andrian, Markus Sperandio

Objective—Platelet function has been intensively studied in the adult organism. However, little is known about the function and hemostatic capacity of platelets in the developing fetus as suitable in vivo models are lacking.

Approach and Results—To examine fetal platelet function in vivo, we generated a fetal thrombosis model and investigated light/dye-induced thrombus formation by intravital microscopy throughout gestation. We observed that significantly less and unstable thrombi were formed at embryonic day (E) 13.5 compared with E17.5. Flow cytometry revealed significantly lower platelet counts in E13.5 versus E17.5 fetuses versus adult controls. In addition, fetal platelets demonstrated changed activation responses of surface adhesion molecules and reduced P-selectin content and mobilization. Interestingly, we also measured reduced levels of the integrin-activating proteins Kindlin-3, Talin-1, and Rap1 during fetal development. Consistently, fetal platelets demonstrated diminished spreading capacity compared with adults. Transfusion of adult platelets into the fetal circulation led to rapid platelet aggregate formation even in young fetuses. Yet, retrospective data analysis of a neonatal cohort demonstrated no correlation of platelet transfusion with closure of a persistent ductus arteriosus, a process reported to be platelet dependent.

Conclusions—Taken together, we demonstrate an ontogenetic regulation of platelet function in vivo with physiologically low platelet numbers and hyporeactivity early during fetal development shedding new light on hemostatic function during fetal life.

Visual Overview—An online visual overview is available for this article. **(*Arterioscler Thromb Vasc Biol*. 2017;37:1076-1086. DOI: 10.1161/ATVBAHA.116.308464.)**

Key Words: blood platelets ■ fetal development ■ hemostasis ■ intravital microscopy ■ microcirculation ■ thrombosis

Platelets control primary hemostasis by constantly scanning the vasculature for vessel injuries. At sites of vascular lesions, components of the subendothelial matrix are recognized by various platelet receptors, which initiate intracellular signaling events leading to numerous platelet responses such as shape change, degranulation, and activation of platelet integrins.[1–3]

Although platelet function has been extensively studied in the adult mammalian organism, little is known about platelet function in the developing fetus. In vitro studies reported hyporeactive platelets in human newborns when stimulated with physiological agonists.[4,5] However, similar responses were observed in platelets from newborns and adults once stimulated with agonists bypassing the platelet-activating surface receptors (calcium ionophore/phorbol esters). Interestingly, platelet activity and platelet counts were found to correlate with gestational age.[6–9] At the same time, when comparing platelets from human neonates and adults, an age-related lack of conformational change of the integrin GPIIb/IIIa (CD41/CD61, $\alpha_{2b}\beta_3$) was revealed.[10]

In strong contrast, shorter bleeding times and enhanced ristocetin-induced agglutination were observed in term infants compared with adults,[11] which was explained by higher levels and enhanced activity of plasmatic von Willebrand factor along with an increased hematocrit. In addition, a predominance of unusually large von Willebrand Factor multimers was reported in term neonates, which most likely results from decreased activity of von Willebrand Factor–cleaving protease.[12]

Taken together, these studies provide evidence for significant differences of the hemostatic system in neonates

Received on: September 16, 2016; final version accepted on: April 7, 2017.

From the Walter Brendel Centre of Experimental Medicine, Munich, Germany (A.M., C.N., I.R., S.K., A.R.M.K., A.F., J.P., M.P., R.I., S.D., M.S.); Division of Neonatology, Hauner Children's University Hospital and Perinatal Centre, Ludwig Maximilians University, Munich, Germany (C.N., A.F., V.W., A.W.F.); Medizinische Klinik und Poliklinik I, Klinikum der Ludwig Maximilians Universität, Munich, Germany (J.P.); Max Planck Institute for Molecular Biomedicine, Münster, Germany (L.K., F.K.); Max PIanck Institute of Biochemistry, Department of Molecular Medicine, Martinsried, Germany (M.M.); Roche Inc, New York, NY (E.Q.); and Department of Microbiology and Immunobiology, Harvard Medical School, Boston, MA (U.H.v.A.).

*These authors contributed equally to this article.

The online-only Data Supplement is available with this article at http://atvb.ahajournals.org/lookup/suppl/doi:10.1161/ATVBAHA.116.308464/-/DC1.

Correspondence to Markus Sperandio, MD, Walter Brendel Centre of Experimental Medicine, Biomedical Center Munich, Ludwig Maximilians University, Großhadernerstr. 9, 82152 Planegg, Germany. E-mail markus.sperandio@lmu.de

Nonstandard Abbreviations and Acronyms	
HSPDA	hemodynamically significant patent ductus arteriosus
PDA	patent ductus arteriosus

compared with adults and suggest an ontogenetic regulation of platelet function during fetal life.

To date, in vivo studies investigating platelet function and thrombus formation in the developing mouse fetus are lacking, likely because of the difficult access to the fetal circulation for microscopic studies and the challenging experimental conditions related to the small fetal size in mice.

Therefore, it was our aim to generate an intravital fetal thrombosis model in the mouse and study the dynamic processes of platelet adhesion and thrombus formation throughout fetal development in vivo. Using this model, we found low to absent thrombus formation in yolk sac microvessels and reduced thrombus stability at early developmental stages compared with near-term fetuses. Concomitantly, we observed low platelet numbers, diminished activation responses of platelet surface receptors, and reduced expression of platelet integrin-adaptor molecules in fetuses compared with adults, suggesting an ontogenetically controlled development of platelet function during fetal life.

Materials and Methods

Materials and Methods are available in the online-only Data Supplement.

Results

Model of In Vivo Thrombus Formation in the Murine Fetus

Using intravital epifluorescence and multiphoton microscopy, we set up a new phototoxic injury–induced thrombosis model in the living mouse fetus. This required microinjection of FITC (fluorescein isothiocyanate)-dextran into fetal yolk sac vessels leading to a local light/dye-induced microvascular injury (Movie I in the online-only Data Supplement).[13] Throughout the whole in vivo experiment, the fetus remained inside the yolk sac and attached to the placenta (Figure 1A through 1C). Using multiphoton laser-scanning microscopy, we also visualized the different vascular layers consisting of extraembryonic vessels of the yolk sac and intraembryonic vessels (Movie II in the online-only Data Supplement).

Impaired Thrombus Formation During Fetal Development

We first assessed platelet adhesion to the endothelium (onset). The percentage of vessels showing an onset of thrombus formation was significantly reduced in young fetuses (E13.5) compared with later developmental stages (E14.5–16.5; E17.5) with a mean onset rate of 17.7±9.5% (mean±SEM) compared with 65.6±8.5% and 75.0±16.4%, respectively (Figure 2A). In addition, initiation of thrombus formation was significantly delayed in young fetuses (Figure 2B), and primary vessel occlusion occurred only in 67% of E13.5 fetuses, whereas in older fetuses (E17.5), all vessels demonstrated a first occlusion (Figure 2C). Furthermore, thrombus growth and first vessel occlusion occurred significantly slower in E13.5 fetuses compared with older fetuses (Figure 2D).

Next, we addressed thrombus stability and found that re-establishment of flow in primarily occluded vessels (reflow phenomenon) appeared more frequently in younger compared with older fetuses (Movie III in the online-only Data Supplement). Intriguingly, E13.5 fetuses were not able to mount a first stable vessel occluding thrombus as reflow occurred in all of the primarily occluded vessels. In contrast, in E17.5 fetuses, reflow was only seen in 33.3% of primarily occluded vessels (Figure 2E). Moreover, time until reflow occurred was shorter in E13.5 compared with E14.5 to 16.5 and E17.5 fetuses (Figure 2F). Finally, we investigated final vessel occlusion defined as permanent occlusion without any further reflow phenomenon throughout 60 minutes of observation. E13.5 fetuses exhibited a significantly lower rate of final vessel occlusion compared with E17.5 fetuses (Figure 2G). In addition, time until final vessel occlusion was delayed in E13.5 fetuses compared with older fetuses (Figure 2H).

Microvascular and hemodynamic parameters for the in vivo experiments are provided in Table 1.

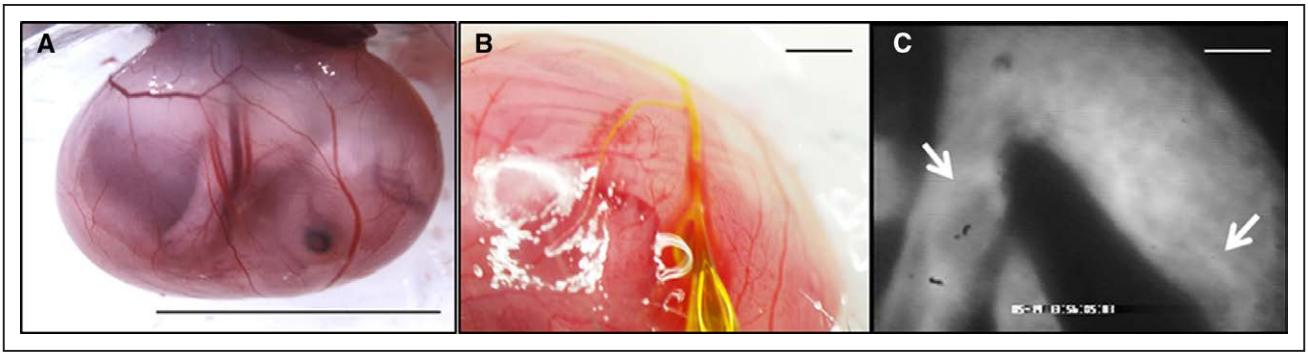

Figure 1. Model of in vivo thrombus formation in the murine fetus. **A**, To gain access to the yolk sac vasculature for microscopic studies, the fetus within the yolk sac is exteriorized from the uterus and placed in a modified Petri dish. The fetus remains attached to the placenta and thus the maternal circulation while protected inside the yolk sac (line=1 cm). **B**, Manually pulled and grinded microcapillaries are used to inject 10% fluorescein isothiocyanate (FITC)-dextran into fetal yolk sac vessels for later light/dye-induced thrombus formation (line=1 mm). **C**, Fluorescence microscopy of yolk sac vessels after injection of FITC-dextran (arrows show beginning thrombus formation, line=20 μm).

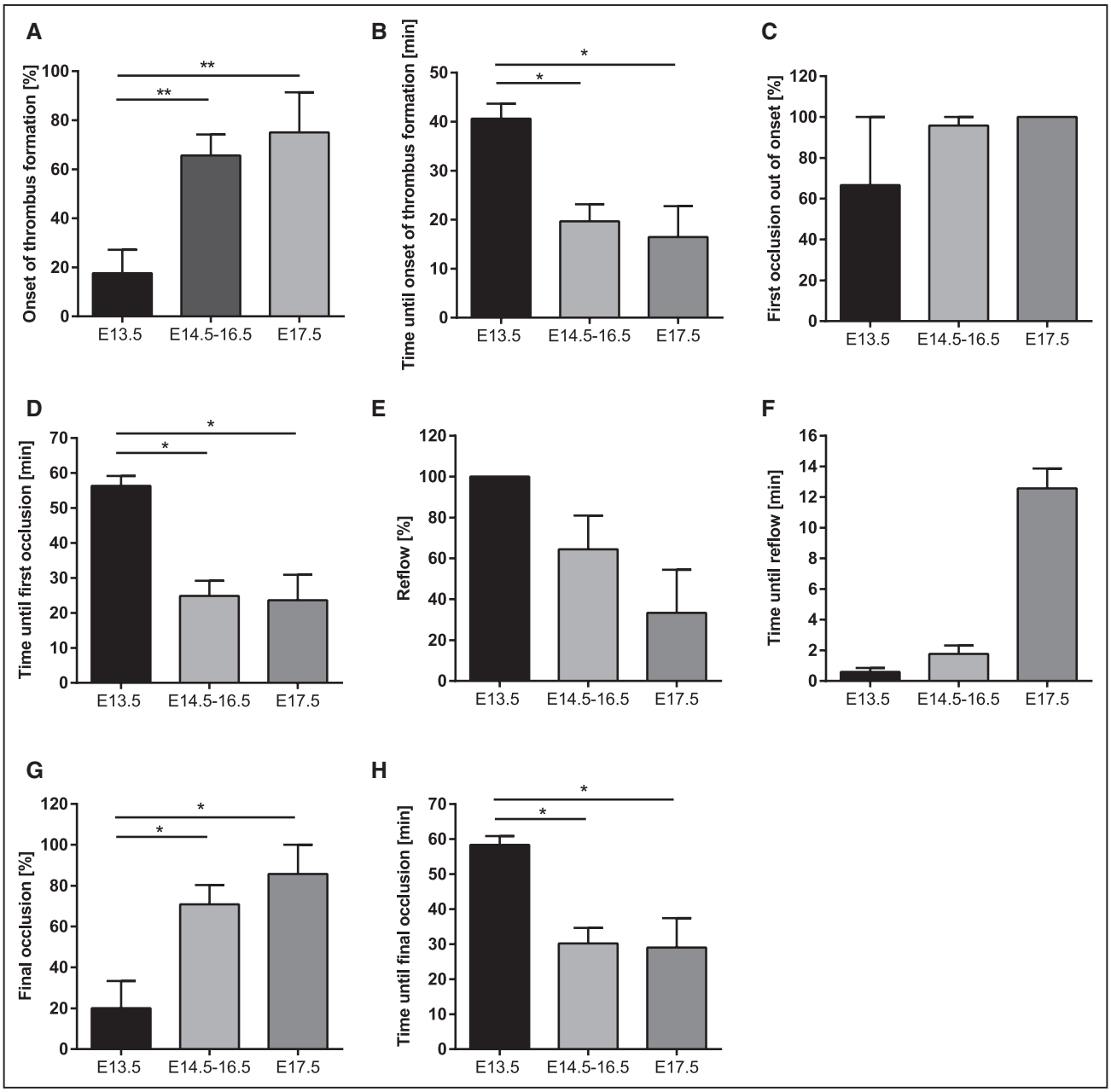

Figure 2. In vivo parameters of fetal platelet function and thrombus formation. Platelet adhesion, determined as onset of thrombus formation in E13.5 and older fetuses (**A** and **B**; n≥8 vessels per group). Rate of occurrence of first total vessel-occluding thrombi in fetal groups and time until first occlusion (**C** and **D**; n≥7 vessels). Re-establishment of flow and time until reflow in fetuses that exhibited a primary vessel occlusion (**E** and **F**; n≥2). Rate of final vessel-occluding thrombus formation without further reflow in the fetal groups and time until final vessel occlusion (**G** and **H**; n≥7). *P<0.05 and **P≤0.01. Data are presented as mean±SEM.

Significantly Diminished Platelet Counts and Altered Platelet Morphology in the Fetus

To determine reasons for reduced thrombus formation during fetal life, we analyzed platelet counts using flow cytometry. Fetal platelet counts were significantly reduced throughout development compared with adult values with lowest counts in the youngest fetuses (Figure 3A). Next, we studied platelet morphology using an Idexx hematology analyzer. Platelet distribution width, mean platelet volume, and platelet large cell ratio were found to be increased at early developmental (E13.5) compared with later time points (E17.5) and adult levels (Figure 3B through 3D), demonstrating that the existing low-numbered fetal platelets are significantly larger than adult control platelets. In addition, fetal erythrocyte counts were also found to depend on gestational age with significantly lower counts in E13.5 fetuses compared with adult controls (E13.5: 74±18×10^6/μL; E17.5: 239±30×10^6/μL; adult: 632±112×10^6/μL; P<0.001, data not shown).

Adhesion Molecule Expression on Platelets During Murine Fetal Development

Thrombus formation during primary hemostasis can be influenced not only by platelet numbers but also by expression of

Table 1. Microvascular and Hemodynamic Parameters of Intravital Microscopy Experiments

	Mother Animals, n	Fetuses, n	Vessels, n	Diameter, μm	Centerline Velocity, μm/s
E13.5	9	11	17	32±2	710±170
E14.5–16.5	12	14	32	31±1	780±90
E17.5	4	4	8	33±3	1740±740

Analysis of microvascular parameters showed no significant difference in vessel diameter and centerline velocity between the different groups.

adhesion molecules on platelets. Flow cytometric analysis of unstimulated platelets displayed lower surface levels of GPIb β and α (CD42c and b) in fetuses compared with adult mice (Figure 4A; Figures II through IV in the online-only Data Supplement). As expected,[14] we observed a decrease in GPIb surface expression after stimulation with thrombin (0.1 U/mL) in all groups. However, the decrease was more pronounced in fetal platelets leading to significantly lower stimulated levels of GPIb in fetal compared with adult platelets (Figure 4B; Figure II in the online-only Data Supplement). Next, we examined surface expression of GPIIb (CD41) on unstimulated platelets and found higher baseline values in young (E13.5) fetuses compared with adult controls (Figure 4C; Figures II through IV in the online-only Data Supplement). However, analysis of thrombin-stimulated platelets revealed that the shift toward a high-affinity conformation of GPIIb/IIIa (CD41/CD61) was significantly diminished in fetal platelets compared with adults, indicated as MFI-ratio relative to unstimulated baseline levels (Figure 4D; Figure II in the online-only Data Supplement). To exclude the possibility that the low response of fetal platelets toward thrombin is because of reduced thrombin receptor expression, Western blot analysis of platelet lysates was performed for protease-activated receptor 3 and 4 (PAR3 and PAR4). We found comparable PAR3 expression in E13.5, E17.5 fetuses and adult controls (Figure 4E, left), and even higher PAR4 levels in E13.5 fetuses compared with older fetuses and adults (Figure 4E, right). In addition, we repeated flow cytometric activation assays using ADP (10 μmol/L) as physiological weak agonist and calcium ionophore A23187 (3 μmol/L) as non-physiological agonist bypassing G-protein–coupled surface receptors. Although ADP elicited a mild activational upregulation of high-affinity GPIIb/IIIa in adult platelets, no such response was seen in fetal platelets. By contrast, after stimulation with calcium ionophore, we observed a clear increase in high-affinity GPIIb/IIIa even in platelets from E13.5 fetuses; however, levels were still significantly lower than that in adult controls (Figures III and IV in the online-only Data Supplement).

To better understand the reduced reactivity of fetal platelets, we next addressed integrin adaptor molecules Talin-1 and Kindlin-3 as well as small GTPase Rap1, which are essential for induction of the high-affinity conformation.[3,15,16] We found significantly lower levels of Kindlin-3, Talin-1, and Rap1 in fetal platelets (Figure 4F), which most likely contribute to impaired GPIIb/IIIa activation on platelets during fetal life.

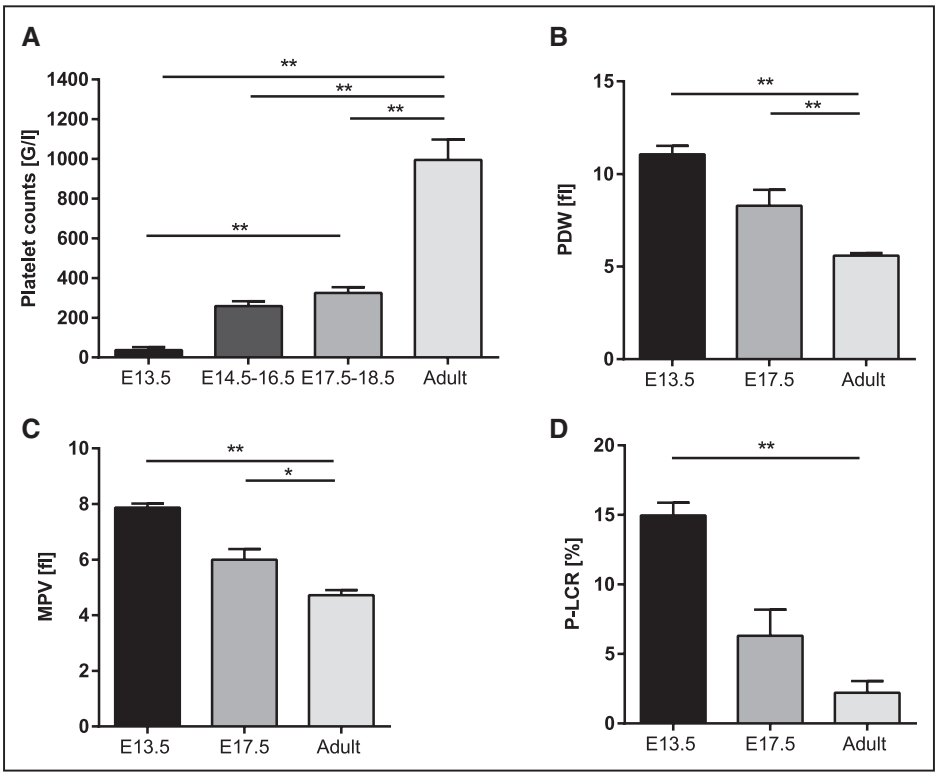

Figure 3. Platelet counts during fetal development. Flow cytometry was performed to investigate platelet counts in fetuses compared with adults (**A**; n≥5). In addition, platelet distribution width (PDW; **B**), mean platelet volume (MPV; **C**) and platelet large cell ratio (P-LRC; **D**) were determined using an Idexx hematology analyzer (n≥9). *P<0.05 and **P≤0.01. Data are presented as mean±SEM.

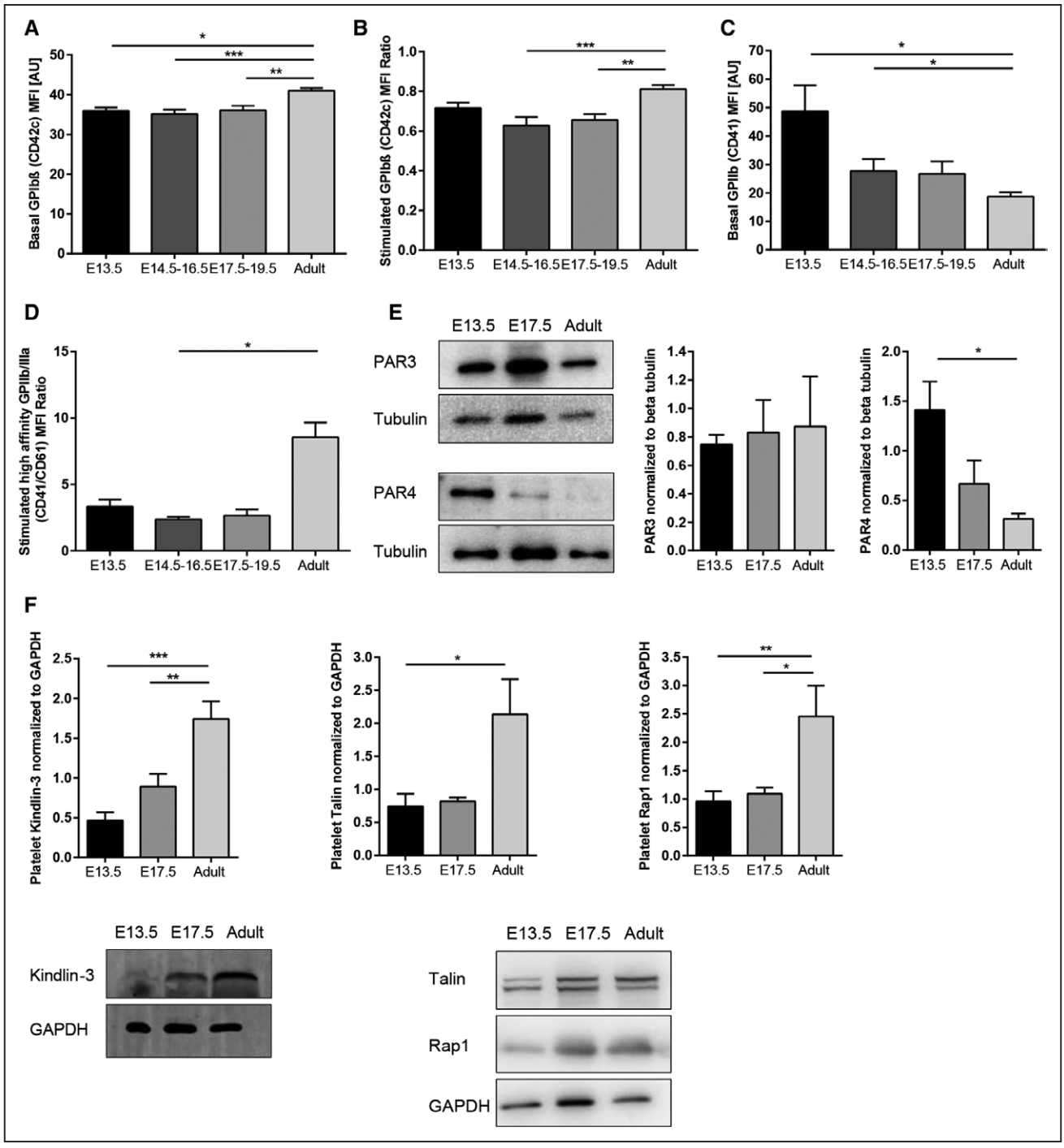

Figure 4. Expression levels of platelet surface receptors during fetal development. Flow cytometry was used to investigate platelet surface receptor expression on fetal and adult platelets. **A**, Basal and (**B**) thrombin-stimulated expression (relative to respective basal values) of GPIb β (CD42c). **C**, Baseline expression of GPIIb (CD41) and (**D**) change in expression of high-affinity GPIIb/IIIa (CD41/CD61) after thrombin stimulation (relative to respective basal values). Western blot analysis of platelet lysates for (**E**) levels of thrombin receptor protease-activated receptor (PAR)-3 and PAR4 and (**F**) integrin adaptor molecules Kindlin-3, Talin-1, and small GTPase Rap1 in fetal and adult platelets (n≥3 blots). *P<0.05, **P≤0.01, ***P≤0.001. Data are presented as mean±SEM.

Reduced Total P-Selectin Expression in Fetal Platelets

Thrombin-induced upregulation of P-selectin (CD62P) surface expression is prominent on adult platelets and used as a platelet activation marker.[17] Flow cytometry revealed that P-selectin surface expression on unstimulated platelets was low without significant difference between fetal and adult platelets (Figure 5A; Figures III and IV in the online-only Data Supplement). Intriguingly, upregulation of P-selectin surface expression following stimulation with thrombin and calcium ionophore was almost completely absent in fetal platelets (Figure 5B; Figure III and IV in the online-only Data

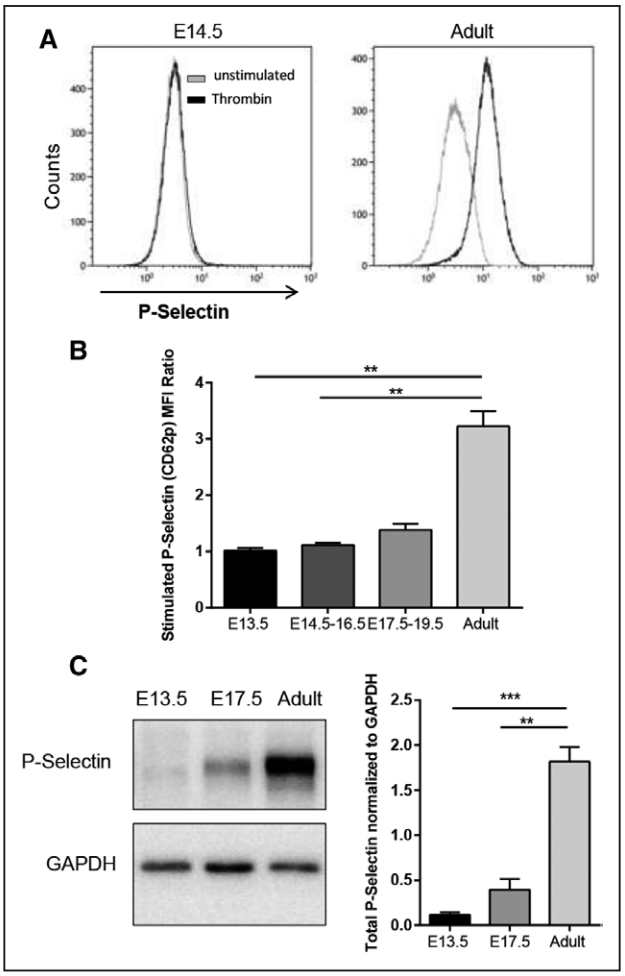

Figure 5. P-selectin levels of fetal platelets. Flow cytometry was used to measure P-selectin surface levels on unstimulated and thrombin-stimulated platelets. Representative flow cytometry measurements of E14.5 (**left**) and adult platelets (**right**) are shown (**A**). Upregulation of P-selectin surface levels after thrombin stimulation (relative to basal values) in fetal platelets compared with adults (**B**; n≥3). In addition, total P-selectin content of platelet lysates was measured by Western blot in fetuses compared with adults (**C**; n≥4). Images are representative for indicated n-number of blots. **P*<0.05 and ***P*≤0.01 (n≥3). Data are presented as mean±SEM.

Supplement). However, with advancing gestational age, a progressive increase in P-selectin upregulation could be observed. Yet, all fetal values still remained significantly below adult values (Figure 5B).

To investigate whether low P-selectin surface levels upon stimulation were because of decreased degranulation or diminished platelet P-selectin content, Western blot analysis of platelet lysates was performed. Our results revealed severely reduced total platelet P-selectin levels during fetal life with lowest content in the youngest fetuses (Figure 5C).

Reduced Spreading Capacity of Fetal Platelets

To analyze whether the observed differences in the levels of integrin-activating proteins and high-affinity GPIIb/IIIa surface expression on fetal platelets have functional consequences, we investigated platelet spreading on fibrinogen. Again, platelets from E13.5 fetuses were found to be

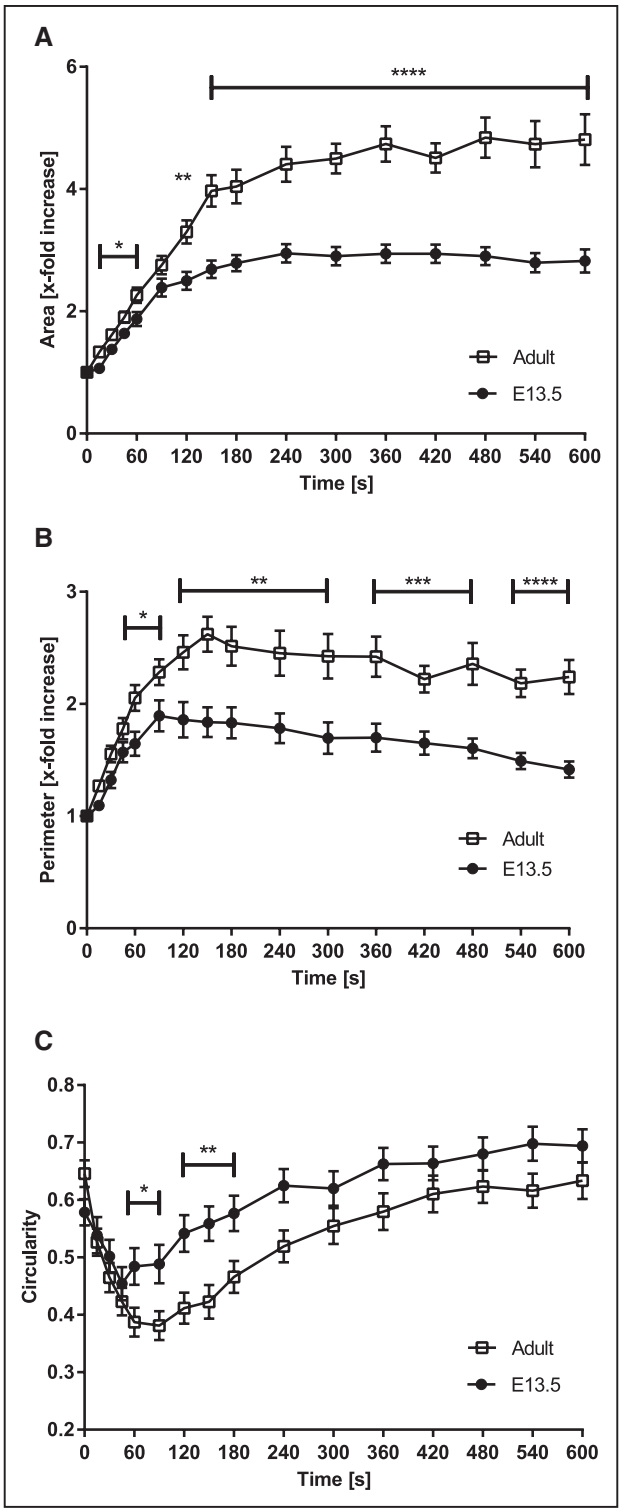

Figure 6. Platelet spreading on fibrinogen. Isolated platelets from E13.5 fetuses (n=5) and adult mice (n=5) were stimulated with 0.1 U/mL thrombin, and spreading of platelets in µ-slides coated with 1 mg/mL fibrinogen was recorded over 10 min. **A**, Change in platelet area relative to baseline (t0). **B**, Change in platelet perimeter relative to baseline (t0). **C**, Change in platelet circularity. A value of 1 indicates perfect circularity. **P*<0.05, ***P*<0.01, ****P*<0.001, and *****P*<0.0001. Data are presented as mean±SEM.

significantly larger at baseline compared with adult platelets (11.7±0.6 versus 6.2±0.3 μm² [mean±SEM], respectively; $P<0.001$). Therefore, changes in platelet area and perimeter were calculated as ratio relative to baseline. In line with the activation assays, platelets from E13.5 fetuses displayed a significantly reduced capability to spread on fibrinogen-coated surface after stimulation with thrombin compared with adult platelets (Figure 6A and 6B). Interestingly, spreading morphology between adult and fetal platelets also differed significantly. Although adult platelets showed normal stages of spreading including spindle-like forms and extrusion of long filopodia (decrease in circularity) followed by expansion of lamellipodia leading to the fully spread fried egg form (increase in circularity),[18] the majority of E13.5 platelets only formed short filopodia and spread in a circular fashion by primary expansion of lamellipodia (Figure 6C; Figure V in the online-only Data Supplement).

Transfusion of Adult Platelets Into E14.5 Fetuses Leads to Platelet Aggregate Formation But Does Not Promote Adhesion of Fetal Leukocytes

On the basis of our findings of a functional and numeric defect in the fetal platelet population, we wanted to assess how adult platelets behave in the fetal yolk sac circulation and whether they are able to form thrombi in E14.5 fetuses, indicating that reduced platelet interaction and thrombus formation are because of a platelet-intrinsic maturation defect. To this end, labeled platelets from adult donor animals were injected into yolk sac vessels of E14.5 fetuses (200 000 platelets/fetus). Rapid spontaneous platelet adhesion at multiple sites of the yolk sac vasculature could be noted together with platelet aggregate formation (Movie IV in the online-only Data Supplement). Interestingly, the forming thrombi exhibited a tendency to release emboli into the fetal circulation. By contrast, transfusion of age-matched E14.5 platelets into E14.5 fetuses (200 000 platelets/fetus) lead to platelet aggregate formation in only 33.3% of experiments compared with 100% after transfusion of adult platelets (n=3 per group). To exclude that the propensity of adult platelets to form spontaneous aggregates in the fetal circulation is merely because of platelet activation by the isolation and staining procedure, we investigated behavior of transfused adult platelets in mouse cremaster muscle vessels. In this setting, despite increasing the amount of transfused platelets to 40 million (≈ 3% to 5% of total platelet count), which equals roughly the concentration of platelets transfused into the fetal circulation, we did not observe any spontaneous platelet aggregation or thrombus formation (data not shown).

Apart from their role in primary hemostasis, platelets have been shown to be important regulators in inflammation and to facilitate leukocyte recruitment.[19,20] As we have recently demonstrated that fetal leukocytes at early developmental stages (<E15) are not able to adhere to the yolk sac vasculature in a model of traumatic inflammation,[21] we were interested whether transfusion of adult platelets is able to promote adhesion of fetal leukocytes.

For this purpose, isolated rhodamine 6G-labeled adult platelets were transfused into LysM-EGFP (enhanced green fluorescent protein) E14.5 fetuses displaying fluorescent neutrophils. Interestingly, despite rapid platelet adhesion, we did not observe interactions between adult platelets and fetal EGFP⁺ cells and saw no incorporation of EGFP⁺ leukocytes into the forming thrombus (Movies V and VI in the online-only Data Supplement).

Table 2. Clinical Parameters of Premature Infants With HSPDA and Indomethacin Therapy With or Without Platelet Transfusion

		No Platelet Transfusion		
	Platelet Transfusion	Thrombocytopenia	Normal Platelets	*P* Value
No. of patients, n	8	17	172	
Gestational age, wk, range	25 (22–27)	26 (23–30)	26 (23–32)	NS
Birth weight, g, range	598 (440–940)*	780 (320–1450)	822 (370–1480)	0.048
SGA, n (%)	2 (25)*	4 (24)*	9 (5)	0.004
Platelet count, G/L, SD	89.9±27.5*	101±22.6*	276.5±99.3	<0.0001
Hematocrit, %, SD	30±5†	39±7	36±6	0.011
Surgical ligation, n (%)	6 (75)*†	3 (17.6)	57 (33.1)	0.017
Death, n (%)	1 (12.5)	3 (17.6)*	4 (2.3)	0.004
Maternal diagnoses				
HELLP syndrome, %	0	12	4	NS
Preeclampsia, %	13	6	4	NS
Placental insufficiency, %	38*	6	6	0.005
Amnioninfection, %	25	12	16	NS

Platelet counts and hematocrit were obtained at the time PDA treatment was started. HSPDA indicates hemodynamically significant patent ductus arteriosus; HELLP, hemolysis, elevated liver enzymes, and low platelets; PDA, patent ductus arteriosus; and SGA, small for gestational age.

*Significance vs infants with normal platelet counts.

†Significance vs nontransfused thrombocytopenic infants.

Transfusion of Adult Platelets Into Thrombocytopenic Premature Infants Does Not Promote Pharmacological Closure of a Patent Ductus Arteriosus

It has been demonstrated that postnatal closure of a patent ductus arteriosus in term infants is associated with the formation of a stable thrombus and subsequent clot consolidation.[22] Preterm infants, however, frequently experience hemodynamically significant patent ductus arteriosus (HSPDA), and medical or surgical patent ductus arteriosus (PDA) closure is eventually needed to prevent organ failure or progressive heart failure.

On the basis of our finding of excessive in vivo aggregate formation after transfusion of adult platelets into fetuses, we became interested whether platelet transfusion impacts HSPDA closure in thrombocytopenic premature infants. To this end, we performed a retrospective analysis of 718 children born <1500 g and ≤32 weeks of gestation at the tertiary neonatal intensive care unit at the University Children's Hospital Munich (Table 2). A total of 197 infants (27.4%) developed a HSPDA requiring medical treatment with indomethacin and subsequent surgical ligation, if pharmacological treatment failed. Of those, 25 neonates (12.7%) exhibited thrombocytopenia (platelet count <150 G/L) and 8 infants (32% of thrombocytopenic infants) received at least one platelet transfusion at the time of HSPDA treatment. When focusing on the need for surgical closure of HSPDA and previous platelet transfusion, we found that surgical closure rate was significantly higher in infants transfused with adult platelets compared with nontransfused thrombocytopenic infants and infants with normal platelet counts (75% versus 17.6% and 33.1%, respectively; P=0.017; Table 2), suggesting that platelet transfusion does not demonstrate a beneficial effect on pharmacological closure of a hemodynamically relevant PDA in thrombocytopenic premature neonates. Finally, we analyzed mortality in our neonatal cohort and found a higher mortality in thrombocytopenic premature infants compared with infants with normal platelet counts. However, this was independent of platelet transfusions (Table 2).

Discussion

In the present study, we investigated in vivo thrombus formation at different developmental stages of the mouse fetus using a novel light/dye-induced fetal thrombosis model featuring an intact fetomaternal placental unit. Although light/dye-induced injury results in platelet adhesion and thrombus formation in cremaster muscle venules of adult mice within a few minutes,[23] we observed significantly decreased and delayed rates of functional thrombus formation in the developing fetus and a dependency on fetal maturation. Thus, our findings reveal an ontogenetic regulation of platelet function, impacting in vivo clot formation. This is in accordance with previous studies showing that bleeding time in human premature infants <33 weeks of gestation is about twice that of mature neonates.[24] Intriguingly, not only the clot-forming capacity seemed to depend on gestational age but also clot stability as evidenced by the reflow phenomenon. In this context, a recent study looking at clot formation in human neonates using rotational thromboelastometry found that clot firmness correlated with gestational age and was significantly reduced in premature newborns.[25]

To uncover reasons for reduced fetal in vivo thrombus formation, we investigated platelet counts and found strongly reduced platelet numbers in murine fetuses compared with adults and a correlation with gestational age. A multicenter study in >47 000 neonates reported lower platelet counts for premature infants <32 weeks of gestation compared with older ones.[26] In addition, as in murine fetuses, the platelet distribution width was found to be increased in preterm compared with term neonates.[27] Whether the changes in platelet indices are merely a result of the reduced platelet count[28] or possibly represent a mechanism to compensate for altered platelet function[29] deserves further investigation. In vivo experiments using antibodies to reduce murine platelet counts to numbers in the range we observed in the fetuses show that, depending on the model, counts as low as 25 G/L are sufficient to promote thrombus formation.[30] Thus, the reduced platelet count is likely to contribute to defective thrombus formation especially in the E13.5 fetuses but cannot fully explain our findings.

Our further in vitro analyses revealed altered integrin expression and a hyporeactive phenotype of fetal platelets. Different mechanisms have been discussed regarding the nature of platelet hyporeactivity in premature and mature infants, including impairment of calcium mobilization and altered intracellular signaling.[5,31] Our results support the concept that hyporesponsiveness of fetal platelets is multifaceted including altered signal transduction of surface receptors (which can be bypassed using calcium ionophore) but also an altered intracellular machinery necessary for integrin activation. In line with this notion, we were able to demonstrate that expression of Talin-1, Kindlin-3, and Rap1, which have been shown to be essential for inside-out mediated integrin activation and platelet function,[3,15,16] were significantly reduced in fetal platelets. It is plausible that these findings directly relate to the reduced capacity of fetal platelets to spread on fibrinogen and to stabilize forming thrombi in vivo, as both processes critically depend on GPIIb/IIIa integrin–mediated signaling (outside-in) upon substrate ligation.[32] The altered spreading morphology of fetal platelets with reduced filopodia formation is of interest with respect to thrombus stability, as filopodia enable binding to fibrin strands and other platelets to form a 3-dimensional thrombus.[33] In Wistar Furth rats, which display hereditary macrothrombocytopenia, a similar spreading pattern has been described and linked to the higher thrombus fragility found in these animals.[18]

Besides altered integrin expression and activation, we also found decreased P-selectin upregulation on fetal platelets. This is in accordance with recent findings in human neonates,[7,34] and likely related to the strongly reduced total P-selectin content we discovered in murine fetal platelets. P-selectin has been demonstrated to be instrumental in promoting platelet–leukocyte interactions.[20,35] Remarkably, in the fetal yolk sac, fetal leukocytes did not interact with fully mature transfused adult platelets (with presumably normal P-selectin expression). This might be because of reduced levels of PSGL-1, the major P-selectin ligand on

fetal leukocytes, as demonstrated earlier.[21,36] Although our findings elicit an important role of modulated platelet function and numbers, other factors are also likely to influence hemostasis during fetal development.[37] These include a lower erythrocyte count found in young fetuses, changes in the level and activity of plasmatic coagulation factors, and altered endothelial cell function. In addition, the release of second wave agonists such as ADP and thromboxane A2 has also been shown to be reduced in platelets from premature human neonates.[38] Because of the limited amount of blood, and the low platelet numbers in the murine fetus, it is at present not possible to perform reliable measurements of blood coagulation parameters and agonist release from murine fetal platelets.

The reduced capacity to form a stable clot, particularly during early fetal life, might be a protective factor against vascular thrombotic injury with its detrimental consequences for normal development. Studies in mice deficient in the transcription factor NF-E2 demonstrated a maturation arrest of megakaryocytes with loss of platelets. Yet, NF-E2–deficient embryos developed to term without major impairment, suggesting that strongly reduced platelet function and number do not necessarily impact fetal development in utero.[39] These results seem to conflict with studies demonstrating an essential role of platelets in lymph vessel development by interaction of platelet C-type lectin-like receptor with podoplanin on lymphatic endothelial cells.[40] However, the authors argue that for normal lymph vessel development, the presence of few platelets, which can still be found in NF-E2–deficient mice, is sufficient.

It is tempting to speculate that the maturation of fetal platelets during gestation reflects developmental differences in gene expression and function of hematopoietic stem cells as hematopoiesis moves from the yolk sac and aorta-gonad-mesonephros region to the fetal liver and finally the bone marrow. Megakaryopoiesis is differentially regulated during primitive (c-myb independent) and definitive hematopoiesis (c-myb dependent) with primitive megakaryocyte progenitors likely giving rise to the first megakaryocytes present in the yolk sac and large highly nucleated platelets found in the embryonic circulation by E10.5. Around that time, hematopoiesis moves to the fetal liver and by E12.5, the liver becomes the main hematopoietic niche for stem cell expansion and differentiation.[41,42] It is conceivable that early platelets derived from primitive progenitors exhibit distinct functional characteristics as compared with platelets from definitive progenitors. In E13.5 fetuses, both types of platelets likely are present concurrently, whereas the number of early primitive platelets should decrease with advancing gestation.

The ontogenetic regulation of platelet function becomes problematic in the setting of premature birth, where the fetus is suddenly exposed to the threats of extrauterine life. Indeed, one of the major complications in preterm infants is intraventricular hemorrhage and its incidence is inversely correlated with gestational age.[43] Thus, the otherwise physiological platelet hyporeactivity found in premature infants may, together with other factors, such as an immature vascular system and changing blood flow properties, contribute to the development of intraventricular hemorrhage. Furthermore, in a mouse study of PDA, it was suggested that platelets contribute to the closure of the ductus arteriosus following birth, and thrombocytopenia was proven to be a predictor for PDA in preterm infants.[22]

Based on our observation of platelet aggregate formation in fetuses following transfusion of adult platelets, we performed a retrospective data analysis investigating the impact of adult platelet transfusion on pharmacological PDA closure and mortality. Unexpectedly, we found that administration of adult platelets had no beneficial effects on PDA closure in thrombocytopenic premature infants treated with indomethacin. However, factors such as ductal size, treatment timing, differences in hematocrit and possibly coagulation parameters, and accompanying comorbidities may confound these results. Therefore, these findings need to be interpreted with caution and investigated by larger prospective studies. This is undermined by the existing conflicting clinical data on the role of platelets and ductal closure.[22,44,45] Interestingly, when looking for underlying maternal conditions affecting neonatal platelet counts, we observed a significantly higher rate of placental insufficiency in mothers from neonates requiring transfusion than in the other groups. Even though this observation does not allow concluding on a causal relationship because of the retrospective approach and the limited number of patients, we think that it is still noteworthy and deserves further evaluation. Finally, we observed similar overall mortality in transfused versus nontransfused thrombocytopenic premature infants. However, the decision for platelet transfusion should be considered carefully in view of possible adverse effects after transfusion of inadequately active platelets in neonates.[46] In this context, Ferrer-Marin et al[47] could elegantly show that adult platelets transfused into fetal blood in vitro exhibit an increased aggregatory and hemostatic performance compared with neonatal platelets pointing toward the existence of a developmental mismatch in platelet transfusion. In line with this notion, we observed rapid and spontaneous clot formation after transfusion of adult platelets into the fetal circulation, whereas transfusion of age-matched platelets did not result in thrombus formation. Furthermore, adult platelets transfused into the adult circulation did not exhibit any propensity to form spontaneous aggregates. These observations support the concept that the fetal plasma exerts some prothrombotic activity (eg, through increased levels and presence of ultralarge von Willebrand Factor),[11,12] possibly to compensate for reduced platelet numbers and function.

In summary, using a novel murine fetal thrombosis model, we demonstrate a developmental regulation of platelet function and thrombus formation. This involves platelet numbers and key molecules of platelet integrin signaling and surface receptors relevant for platelet adhesion and aggregation. Furthermore, we show that transfusion of adult platelets can override reduced clot-forming capacity in young fetuses. These findings do not only provide new valuable insights into the regulation of primary hemostasis during fetal life but also demand future clinical studies to further evaluate the benefits and risks of adult platelet transfusion in premature infants.

Acknowledgments

We thank Johannes Altstätter, Kristina Heinig, Nadine Schmidt, Susanne Bierschenk, Katharina Wachal, and Dennis Schock for help with animal care and technical support.

Sources of Funding

This study was supported by Deutsche Forschungsgemeinschaft SFB914 (Project B1 to M. Sperandio and A1 to M. Moser), associated Integrated Research Training Group of the SFB 914 (A. Margraf), scholarship program Förderung Forschung und Lehre FöFoLe (A. Margraf, C. Nussbaum, M. Sperandio), the student research scholarship grant of LMU (Lehre@LMU; A. Margraf), and the SFB 656 (F. Kiefer).

Disclosures

None.

References

1. Clemetson KJ. Platelets and primary haemostasis. *Thromb Res*. 2012;129:220–224. doi: 10.1016/j.thromres.2011.11.036.
2. Reed GL, Fitzgerald ML, Polgár J. Molecular mechanisms of platelet exocytosis: insights into the "secrete" life of thrombocytes. *Blood*. 2000;96:3334–3342.
3. Moser M, Nieswandt B, Ussar S, Pozgajova M, Fässler R. Kindlin-3 is essential for integrin activation and platelet aggregation. *Nat Med*. 2008;14:325–330. doi: 10.1038/nm1722.
4. Sola-Visner M. Platelets in the neonatal period: developmental differences in platelet production, function, and hemostasis and the potential impact of therapies. *Hematology Am Soc Hematol Educ Program*. 2012;2012:506–511. doi: 10.1182/asheducation-2012.1.506.
5. Israels SJ, Cheang T, Roberston C, McMillan-Ward EM, McNicol A. Impaired signal transduction in neonatal platelets. *Pediatr Res*. 1999;45(5 pt 1):687–691. doi: 10.1203/00006450-199905010-00014.
6. Levy-Shraga Y, Maayan-Metzger A, Lubetsky A, Shenkman B, Kuint J, Martinowitz U, Kenet G. Platelet function of newborns as tested by cone and plate(let) analyzer correlates with gestational age. *Acta Haematol*. 2006;115:152–156. doi: 10.1159/000090928.
7. Sitaru AG, Holzhauer S, Speer CP, Singer D, Obergfell A, Walter U, Grossmann R. Neonatal platelets from cord blood and peripheral blood. *Platelets*. 2005;16:203–210. doi: 10.1080/09537100400016862.
8. Patrick CH, Lazarchick J, Stubbs T, Pittard WB. Mean platelet volume and platelet distribution width in the neonate. *Am J Pediatr Hematol Oncol*. 1987;9:130–132.
9. Bednarek FJ, Bean S, Barnard MR, Frelinger AL, Michelson AD. The platelet hyporeactivity of extremely low birth weight neonates is age-dependent. *Thromb Res*. 2009;124:42–45. doi: 10.1016/j.thromres.2008.10.004.
10. Rajasekhar D, Barnard MR, Bednarek FJ, Michelson AD. Platelet hyporeactivity in very low birth weight neonates. *Thromb Haemost*. 1997;77:1002–1007.
11. Israels SJ, Rand ML, Michelson AD. Neonatal platelet function. *Semin Thromb Hemost*. 2003;29:363–372. doi: 10.1055/s-2003-42587.
12. Weinstein MJ, Blanchard R, Moake JL, Vosburgh E, Moise K. Fetal and neonatal von Willebrand factor (vWF) is unusually large and similar to the vWF in patients with thrombotic thrombocytopenic purpura. *Br J Haematol*. 1989;72:68–72.
13. Rumbaut RE, Slaff DW, Burns AR. Microvascular thrombosis models in venules and arterioles in vivo. *Microcirculation*. 2005;12:259–274. doi: 10.1080/10739680590925664.
14. Kovacsovics TJ, Hartwig JH. Thrombin-induced GPIb-IX centralization on the platelet surface requires actin assembly and myosin II activation. *Blood*. 1996;87:618–629.
15. Nieswandt B, Moser M, Pleines I, Varga-Szabo D, Monkley S, Critchley D, Fässler R. Loss of talin1 in platelets abrogates integrin activation, platelet aggregation, and thrombus formation in vitro and in vivo. *J Exp Med*. 2007;204:3113–3118. doi: 10.1084/jem.20071827.
16. Chrzanowska-Wodnicka M, Smyth SS, Schoenwaelder SM, Fischer TH, White GC 2nd. Rap1b is required for normal platelet function and hemostasis in mice. *J Clin Invest*. 2005;115:680–687. doi: 10.1172/JCI22973.
17. Stenberg PE, McEver RP, Shuman MA, Jacques YV, Bainton DF. A platelet alpha-granule membrane protein (GMP-140) is expressed on the plasma membrane after activation. *J Cell Biol*. 1985;101:880–886.
18. Stenberg PE, Barrie RJ, Pestina TI, Steward SA, Arnold JT, Murti AK, Hutson NK, Jackson CW. Prolonged bleeding time with defective platelet filopodia formation in the Wistar Furth rat. *Blood*. 1998;91:1599–1608.
19. Jenne CN, Kubes P. Platelets in inflammation and infection. *Platelets*. 2015;26:286–292. doi: 10.3109/09537104.2015.1010441.
20. Ed Rainger G, Chimen M, Harrison MJ, Yates CM, Harrison P, Watson SP, Lordkipanidze M, Nash GB. The role of platelets in the recruitment of leukocytes during vascular disease. *Platelets*. 2015;26:507–520.
21. Sperandio M, Quackenbush EJ, Sushkova N, et al. Ontogenetic regulation of leukocyte recruitment in mouse yolk sac vessels. *Blood*. 2013;121:e118–e128. doi: 10.1182/blood-2012-07-447144.
22. Echtler K, Stark K, Lorenz M, et al. Platelets contribute to postnatal occlusion of the ductus arteriosus. *Nat Med*. 2010;16:75–82. doi: 10.1038/nm.2060.
23. Rumbaut RE, Randhawa JK, Smith CW, Burns AR. Mouse cremaster venules are predisposed to light/dye-induced thrombosis independent of wall shear rate, CD18, ICAM-1, or P-selectin. *Microcirculation*. 2004;11:239–247. doi: 10.1080/10739680490425949.
24. Del Vecchio A, Latini G, Henry E, Christensen RD. Template bleeding times of 240 neonates born at 24 to 41 weeks gestation. *J Perinatol*. 2008;28:427–431. doi: 10.1038/jp.2008.10.
25. Strauss T, Levy-Shraga Y, Ravid B, Schushan-Eisen I, Maayan-Metzger A, Kuint J, Kenet G. Clot formation of neonates tested by thromboelastography correlates with gestational age. *Thromb Haemost*. 2010;103:344–350. doi: 10.1160/TH09-05-0282.
26. Wiedmeier SE, Henry E, Sola-Visner MC, Christensen RD. Platelet reference ranges for neonates, defined using data from over 47,000 patients in a multihospital healthcare system. *J Perinatol*. 2009;29:130–136. doi: 10.1038/jp.2008.141.
27. Wasiluk A, Osada J, Dabrowska M, Szczepański M, Jasinska E. Does prematurity affect platelet indices? *Adv Med Sci*. 2009;54:253–255. doi: 10.2478/v10039-009-0034-3.
28. Jackson SR, Carter JM. Platelet volume: laboratory measurement and clinical application. *Blood Rev*. 1993;7:104–113.
29. Thompson CB, Jakubowski JA, Quinn PG, Deykin D, Valeri CR. Platelet size as a determinant of platelet function. *J Lab Clin Med*. 1983;101:205–213.
30. Morowski M, Vögtle T, Kraft P, Kleinschnitz C, Stoll G, Nieswandt B. Only severe thrombocytopenia results in bleeding and defective thrombus formation in mice. *Blood*. 2013;121:4938–4947. doi: 10.1182/blood-2012-10-461459.
31. Gelman B, Setty BN, Chen D, Amin-Hanjani S, Stuart MJ. Impaired mobilization of intracellular calcium in neonatal platelets. *Pediatr Res*. 1996;39(4 pt 1):692–696. doi: 10.1203/00006450-199604000-00022.
32. Shattil SJ. Signaling through platelet integrin alpha IIb beta 3: inside-out, outside-in, and sideways. *Thromb Haemost*. 1999;82:318–325.
33. Hartwig JH, Bokoch GM, Carpenter CL, Janmey PA, Taylor LA, Toker A, Stossel TP. Thrombin receptor ligation and activated Rac uncap actin filament barbed ends through phosphoinositide synthesis in permeabilized human platelets. *Cell*. 1995;82:643–653.
34. Wasiluk A, Mantur M, Szczepański M, Kemona H, Baran E, Kemona-Chetnik I. The effect of gestational age on platelet surface expression of CD62P in preterm newborns. *Platelets*. 2008;19:236–238. doi: 10.1080/09537100701882046.
35. Schulz C, Schäfer A, Stolla M, Kerstan S, Lorenz M, von Brühl ML, Schiemann M, Bauersachs J, Gloe T, Busch DH, Gawaz M, Massberg S. Chemokine fractalkine mediates leukocyte recruitment to inflammatory endothelial cells in flowing whole blood: a critical role for P-selectin expressed on activated platelets. *Circulation*. 2007;116:764–773. doi: 10.1161/CIRCULATIONAHA.107.695189.
36. Nussbaum C, Gloning A, Pruenster M, Frommhold D, Bierschenk S, Genzel-Boroviczény O, von Andrian UH, Quackenbush E, Sperandio M. Neutrophil and endothelial adhesive function during human fetal ontogeny. *J Leukoc Biol*. 2013;93:175–184. doi: 10.1189/jlb.0912468.
37. Pearce WJ, Khorram O. Maturation and differentiation of the fetal vasculature. *Clin Obstet Gynecol*. 2013;56:537–548. doi: 10.1097/GRF.0b013e31829e5bc9.
38. Israels SJ, Odaibo FS, Robertson C, McMillan EM, McNicol A. Deficient thromboxane synthesis and response in platelets from premature infants. *Pediatr Res*. 1997;41:218–223. doi: 10.1203/00006450-199704001-01315.
39. Palumbo JS, Zogg M, Talmage KE, Degen JL, Weiler H, Isermann BH. Role of fibrinogen- and platelet-mediated hemostasis in mouse embryogenesis and reproduction. *J Thromb Haemost*. 2004;2:1368–1379. doi: 10.1111/j.1538-7836.2004.00788.x.

40. Bertozzi CC, Schmaier AA, Mericko P, et al. Platelets regulate lymphatic vascular development through CLEC-2-SLP-76 signaling. *Blood*. 2010;116:661–670. doi: 10.1182/blood-2010-02-270876.
41. Tober J, McGrath KE, Palis J. Primitive erythropoiesis and megakaryopoiesis in the yolk sac are independent of c-myb. *Blood*. 2008;111:2636–2639. doi: 10.1182/blood-2007-11-124685.
42. Mikkola HK, Orkin SH. The journey of developing hematopoietic stem cells. *Development*. 2006;133:3733–3744. doi: 10.1242/dev.02568.
43. Kuperman AA, Brenner B, Kenet G. Intraventricular hemorrhage in preterm infants and coagulation–ambivalent perspectives? *Thromb Res*. 2013;131 Suppl 1:S35–S38. doi: 10.1016/S0049-3848(13)70018-5.
44. Mitra S, Chan AK, Paes BA; Thrombosis and Hemostasis in Newborns (THIN) Group. The association of platelets with failed patent ductus arteriosus closure after a primary course of indomethacin or ibuprofen: a systematic review and meta-analysis. *J Matern Fetal Neonatal Med*. 2017;30:127–133. doi: 10.3109/14767058.2016.1163684.
45. Murphy DP, Lee HC, Payton KS, Powers RJ. Platelet count and associated morbidities in VLBW infants with pharmacologically treated patent ductus arteriosus. *J Matern Fetal Neonatal Med*. 2016;29:2045–2048. doi: 10.3109/14767058.2015.1076785.
46. Ferrer-Marin F, Stanworth S, Josephson C, Sola-Visner M. Distinct differences in platelet production and function between neonates and adults: implications for platelet transfusion practice. *Transfusion*. 2013;53:2814–2821; quiz 2813. doi: 10.1111/trf.12343.
47. Ferrer-Marin F, Chavda C, Lampa M, Michelson AD, Frelinger AL 3rd, Sola-Visner M. Effects of *in vitro* adult platelet transfusions on neonatal hemostasis. *J Thromb Haemost*. 2011;9:1020–1028. doi: 10.1111/j.1538-7836.2011.04233.x.

Highlights

- A novel murine fetal thrombosis model is introduced to study platelet function in vivo at different time points during fetal life.
- In vivo platelet adhesion, aggregation, and thrombus stability are ontogenetically regulated and severely reduced in mid-gestation murine fetuses.
- Besides reduced platelet counts, diminished activational responses and reduced integrin adaptor molecule levels contribute to the reduced fetal thrombus formation.

Supplemental Material

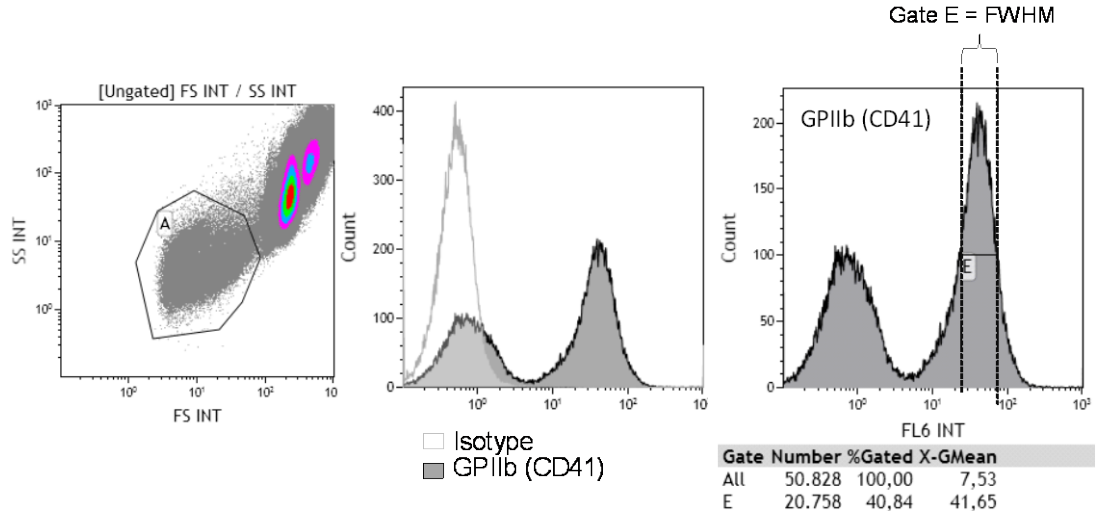

Supplemental Figure I): Gating strategy
Exemplary FACS histograms to demonstrate gating strategy in fetal samples with double fluorescence peak (E13.5). Note that the left peak is in the range of isotype control. To determine fluorescence values, the gate was set as "full width at half maximum intensity" (FWHM) of the right peak.

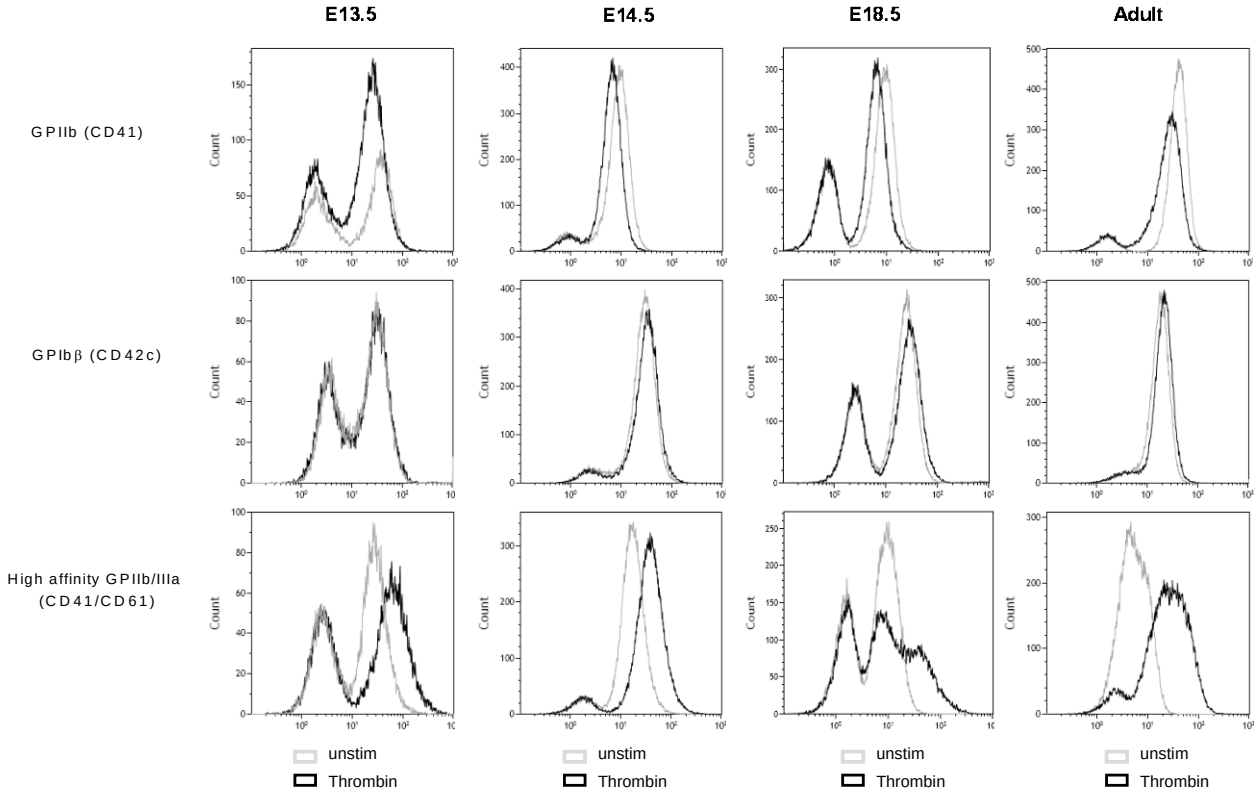

Supplemental Figure II): Representative FACS plots of basal and thrombin (0.1U/ml) stimulated surface receptor expression on fetal and adult platelets.

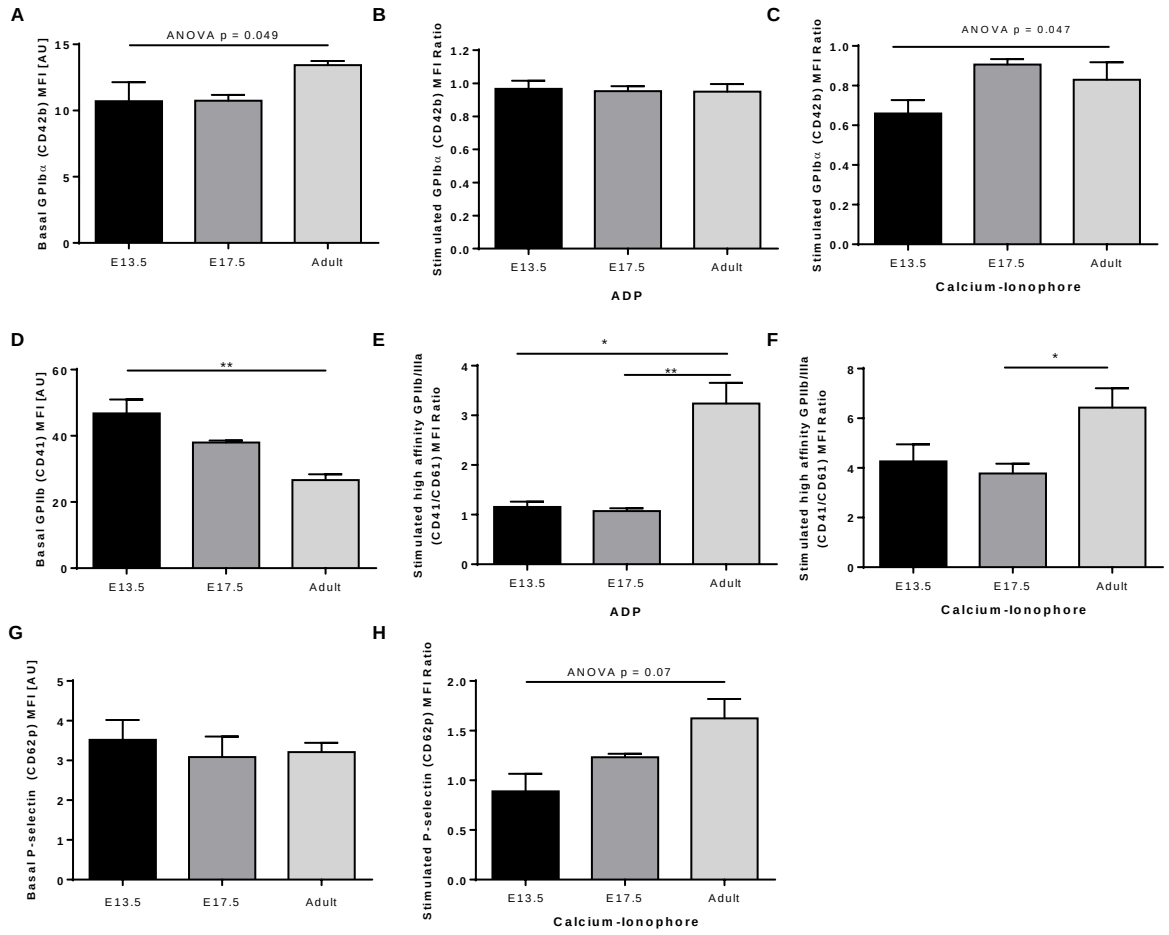

Supplemental Figure III): Expression levels of surface receptors during fetal development. A) Basal surface expression of GPIbα (CD42b) on fetal and adult platelets. (B) ADP- and (C) Calcium ionophore A23187-stimulated expression of GpIb alpha (relative to respective basal values). (D) Baseline expression of GpIIb (CD41) and change in expression of high affinity GpIIb/IIIa (CD41/61) following stimulation with (E) ADP- and (F) Calicum ionophore A23187 (relative to respective basal values). (G) Basal and (H) Calcium ionophore-stimulated change in P-selectin (CD62P) expression. Adult n = 6, E17.5 and E13.5 n = 5. *p<0.05, **p≤0.01, ***p≤0.001. Data are presented as mean + s.e.m.

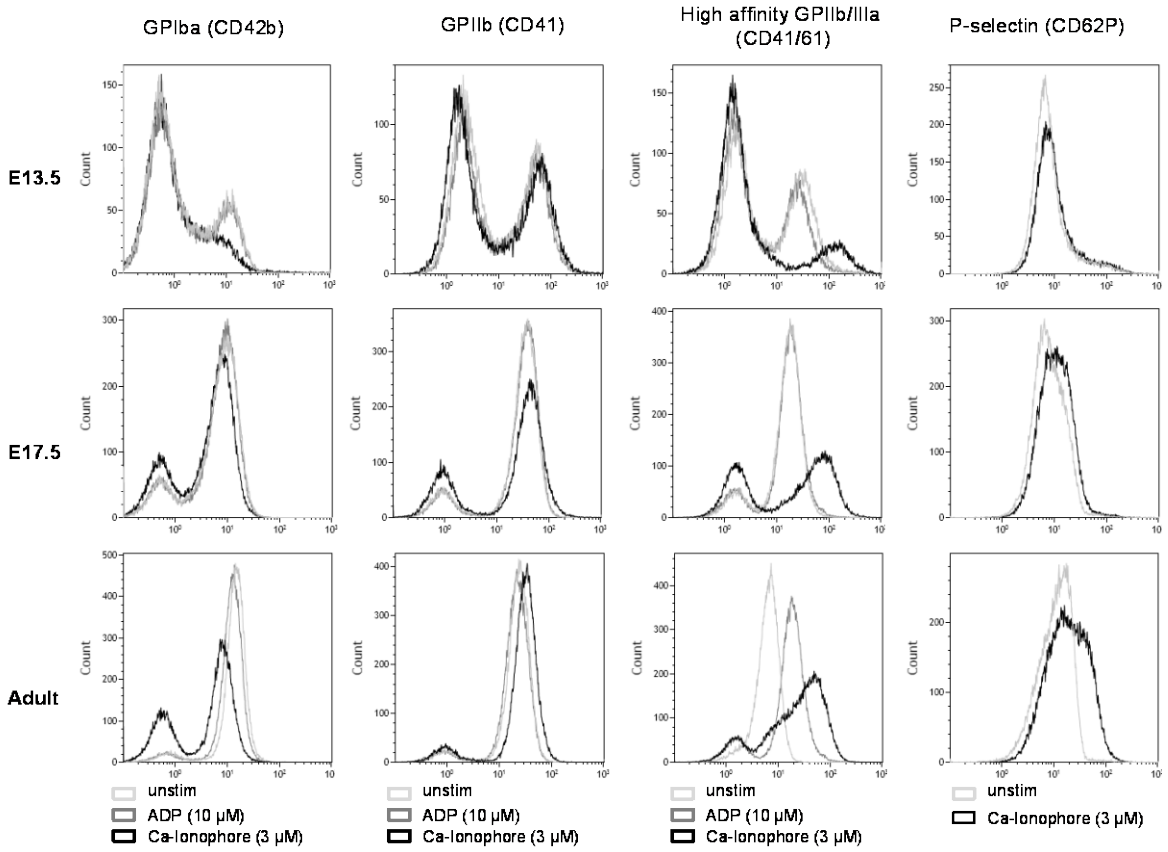

Supplemental Figure IV): Representative FACS plots of basal and stimulated surface receptor expression on fetal and adult platelets using different agonists as indicated.

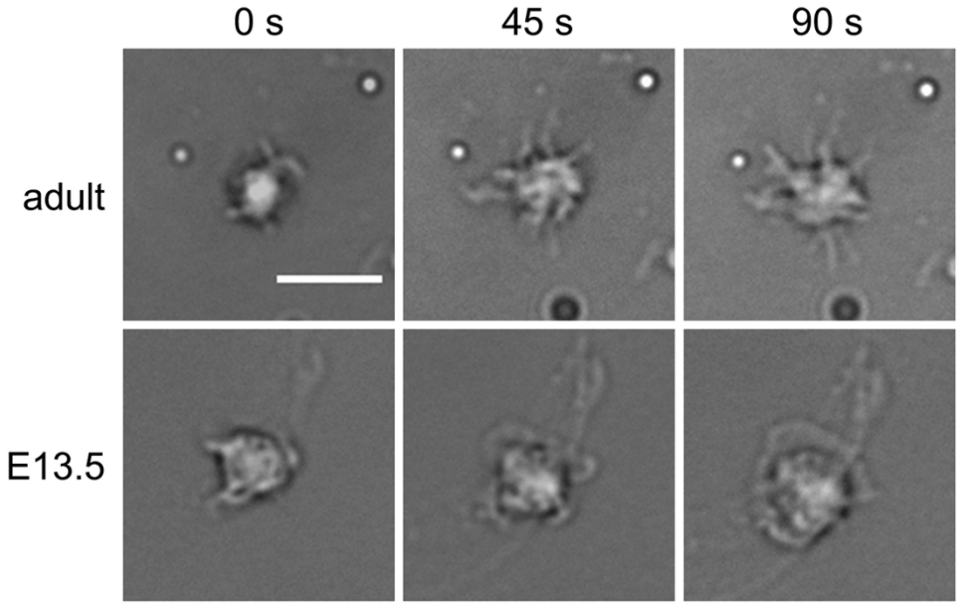

Supplemental Figure V): Representative images of spreading morphology of fetal (E13.5) and adult platelets on fibrinogen (Scale bar indicates 10 µm)

Movie legends:

Movie I: Exemplary video of light-dye induced thrombus formation in yolk sac vessels of an E15.5 fetus. Scale bar indicates 50 µm.

Movie II: 3D reconstruction of multiphoton image acquisition of fetal yolk sac (upper layer) and skin vessels (lower layer) following injection of FITC-dextran in an E15.5 fetus. Reconstruction was performed from an x-y-z image file, scale bar indicates 80 µm. Video is shown at 25 frames/s.

Movie III: Re-establishment of flow following primary vessel occlusion in E14.5 fetus. Note the primarily occluded vessel in the lower part of the image. Scale bar indicates 50 µm. Video is shown at 30 frames/s.

Movie IV: Complete vessel occluding thrombus formation following transfusion of adult labeled platelets into E14.5 fetus yolk sac. Rapid platelet accumulation, aggregate formation and thrombus growth can be noted. Embolization of thrombi consisting of labeled adult platelets can be seen at the beginning of the movie. Scale bar indicates 50 µm. Video is shown at 30 frames/s.

Movie V: Multiphoton recording of E14.5 LysM-EGFP fetus following transfusion of adult platelets (platelets green, leukocytes red). Adherent labeled adult platelets onto the yolk sac vessel wall can be seen. Passing leukocytes presenting as red lines within the blood flow do not interact with adult platelets. A migrating leukocyte can be noted in the upper left corner of the image. Scale bar indicates 40 µm at beginning of video, at maximum magnification scale bar indicates 20 µm. Video is shown at 30 frames/s.

Movie VI: Epifluorescence recording of E14.5 LysM-EGFP fetus following transfusion of adult platelets (platelets green, leukocytes red). Adherent labeled adult platelets with aggregate formation and embolization can be observed. Fast flowing red fetal leukocytes do not interact with activated platelets *in vivo.* Scale bar indicates 50 µm. Video is shown at 30 frames/s.

Material and Methods

Study Approval
All animal experiments were performed in accordance with Bavarian state regulations and approved by the responsible authorities at the Regierung von Oberbayern (Az.: 55.2-1-54-2531-69-07 and -122-12.). Retrospective clinical data analysis was approved by the local ethics committee (Az.: 219-16).

Antibodies and Chemicals
Thrombin from bovine plasma, Adenosine 5′-diphosphate sodium salt, Calcium ionophore A21387, rhodamine, 150 kD FITC-dextran, monoclonal mouse- anti-mouse antibody against β-tubulin (TUB2.1, Cat. No. T5201) and Talin (8d4, Cat. No. T3287) were from Sigma Aldrich (Taufkirchen, Germany). DyLight-488 and -649 labeled rat-anti-mouse antibodies against GPIbβ (CD42c, Cat. No. X488 and X649), FITC-labeled rat-anti-mouse antibody against GPIbα (CD42b, Clone Xia.H10, Cat. No. M041-1) and phycoerythrin (PE)-labeled rat-anti-mouse antibody against high affinity GpIIb/IIIa (CD41/CD61; clone Jon/A, Cat. No. M023-2) were acquired from Emfret Analytics (Eibelstadt, Germany). FITC-labeled monoclonal rat-anti-mouse antibodies against P-selectin (CD62P; clone RB40.34, Cat. No. 561923) and against GpIIb (CD41; clone MWReg30, Cat No. 553848) were obtained from BD Pharmingen (Franklin Lakes, NJ, USA). APC-labeled rat-anti-mouse antibody against GPIIb (CD41, clone MWReg30, Cat No. 133914) was from BioLegend (San Diego, CA, USA). FITC-labeled monoclonal mouse-anti-mouse/human antibody directed against murine PAR3 (8E8, Cat. No. sc-53819) was acquired from Santa Cruz (Santa Cruz, CA, USA). FITC-labeled polyclonal rabbit-anti-mouse/human/rat PAR4 was from Bioss (Woburn, MA, USA, Cat. No. bs-1196R-A488). Secondary anti-mouse and anti-rabbit horseradish-peroxidase antibodies were from Bio-Rad (Hercules, CA, USA). Polyclonal rabbit–anti-mouse P-selectin antibody was from Abcam (Cambridge, UK, Cat. No. ab59738). Immobilon HRP chemiluminescent substrate and polyclonal rabbit-anti-mouse antibody against Rap1 (Cat.No. 07-916) were from Merck Millipore (Darmstadt, Germany). Monoclonal mouse-anti-GAPDH (6C5, Cat. No. CB1001) was from Calbiochem (Merck Millipore). Polyclonal rabbit-anti-mouse Kindlin-3 antibody was prepared as described [1].

Experimental mice
Female C57/BL6 mice were obtained from Charles River Laboratories (Wilmington, MA, USA). For platelet leukocyte interaction studies, LysM-EGFP (enhanced green fluorescent protein) mice were used [2, 3] , which were kindly provided by Thomas Graf, Center for Genomic Regulation, Barcelona, Spain.

In vivo model to analyze thrombus formation in the mouse fetus
Fetuses from embryonic days E13.5 to E17.5 were analyzed. Preparation was performed as described[3]. Briefly, a pregnant mother animal was anesthetized (125 mg/kg ketamine, 25 mg/kg xylazine i.p.) and placed on a heating plate. The abdominal cavity was opened through a lateral incision. The right uterus horn was exteriorized and the myometrium carefully incised, leaving the yolk sac intact. Subsequently, one viable fetus inside the yolk sac, connected to the placenta, was exposed and placed in a modified petri-dish. To provoke thrombus formation by light/dye induced vascular injury [4], manually pulled and grinded glass micro-capillaries (GCI150TF-10, Clark Electromedical Instruments, Pangbourne Reading)

were used to inject FITC-dextran (10%; FD150S-1G) into a branch of the vitelline vein.
The preparation was then transferred to the microscope (Olympus BX51, Objective LUMPlan FI/IR 60x/0.90W, Olympus Hamburg, Germany) for intravital imaging. Image acquisition was performed using two CCD cameras (Kappa CF5 HS; Kappa Optronics GmbH, Gleichen and LaVision Imager ProX pco. 1600L, LaVision GmbH, Goettingen, Germany).
Additional imaging was performed using a multiphoton laser scanning microscopy setup (MPLSM), as described previously [5] (LaVision BioTec TrimScope, Hamamatsu H7422A-40 photomultipliers; Objective: Olympus XLUMPlan FI 20x, 0.95 W).
For transfusion experiments, isolated platelets were resuspended in modified Tyrodes-Hepes buffer, labeled with rhodamine 6G and injected (200,000 platelets/fetus) into fetal yolk sac vessels. Observations were performed using the MPLSM setup and the intravital microscopy setup using an additional 5x objective (ACHROSTIGMAT 5x/0.12) for acquisition of overview images. To investigate platelet leukocyte interactions, isolated adult rhodamine 6G labeled platelets were transfused into LysM-EGFP murine fetuses. Analysis and reconstruction of MPLSM image stacks was performed using IMARIS 7 (Bitplane) software. Color display of fluorescence signals in reconstructed MPLSM files was assigned arbitrarily with leukocytes encoded in red and platelets encoded in green.
For adult control transfusion experiments, the mouse cremaster muscle model was prepared as described previously [4], and isolated adult platelets were transfused via a carotis catheter.

Platelet and RBC counts
For measurement of platelet counts, adult blood samples (100 µl) were collected via cardiac puncture of the respective mother animal. Fetal blood samples were collected into 5 µl glass-capillaries (ETE005-0100; Bioanalytic, Freiburg, Germany) through lateral neck dissection and preparation of the subclavian vein of fetuses and subsequently analyzed by flow cytometry, using microbeads as a volumetric reference as described previously [6]. Briefly, blood samples were diluted 1:10 and labeled for 30 minutes with DyLight488-labeled GpIb antibody at 20 µg/ml. After staining, $1x10^5$ beads (SPHERO Rainbow Fluorescent Particles 5.26 µm, Spherotech, Lake Forest, IL, USA) in PBS were added and samples transferred to flow cytometric measurement. Platelets were distinguished by forward/sideward-scatter appearance and expression of GpIb. A total of 1000 beads were counted and platelet counts calculated based on collected volume and counted number of cells.
For determination of red blood cell (RBC) counts, whole blood was collected as described above and diluted 1:200 prior to counting in a modified Neubauer chamber.

Platelet activation assays
For platelet activation assays, adult blood samples were drawn from the inferior Vena cava of mother animals prior to preparation of the fetuses. Following general anesthesia, the abdomen was opened by laparotomy, the intestine and the uterus with the fetuses *in situ* were gently mobilized and 100 µl of whole blood collected. Further handling was according to fetal blood samples described below. For fetal samples, blood from all available fetuses of one mother animal (mean number of fetuses: E13.5: 7±1; E14.5-E16.5: 6.75±1,19; E17.5-E19.5: 4,33±1,45), was pooled by decapitation of fetuses in a petri dish containing 10 ml modified, calium- and magnesium-free Tyrode's-HEPES buffer with 10% (v/v) Heparin (20 U/ml) and

analyzed, as reported recently [7, 8]. Shortly, whole blood samples were washed twice with modified Tyrode's-HEPES buffer, before activation through administration of indicated platelet agonists (thrombin: 0.1 U/ml, ADP: 10 µM, calcium ionophore: 3 µM) and labeling with according antibodies for 15 minutes at room temperature in modified Tyrode's-HEPES buffer containing calcium and magnesium. Dilution of fetal and adult blood samples was based on the size of the blood pellet obtained after the first centrifugation. Samples were then analyzed by flow cytometry. Fetal samples often exhibited double peaks in the fluorescence histograms with the left peak being negative for typical platelet markers GPIb (CD42) and GPIIb (CD41). Thus, fluorescence intensity was determined as FWHM (full width at half maximum fluorescence intensity) of the right peak (Suppl. Figure I). Results are presented as median fluorescence intensity and fold time increase, by dividing the value of the stimulated sample by the unstimulated control sample.

Platelet isolation and labeling for transfusion experiments

Platelet isolation was performed as described previously with minor modifications [9]. Collection of blood from mother animals and fetuses was performed according to the platelet activation assays. Platelet-rich-plasma (PRP) was then obtained by low velocity centrifugation (180G). Thereafter, PRP was incubated with rhodamine (0.05%, 200 µL/ml)[10] in the presence of prostaglandin E2 (1 µg/mL) and then washed and isolated by centrifugation at 400 G for 5 minutes. Platelets were counted using an Idexx hematology analyser (Idexx Europe B.V., Hoofddorp, Netherlands) and resuspended in buffer containing calcium and magnesium. A total of 200.000 platelets were injected per animal. Injection was performed into a small side-branch of fetal yolk-sac microvessels. Afterwards, the preparation was turned and imaging was performed on the opposite site of the injection-site within the yolk-sac to avoid observation of mechanical injury.

Western blotting

Platelets were isolated as described above and platelet numbers were adjusted to equal levels for fetal and adult samples (100.000/µl). Isolated platelets were mixed with ice-cold protein extraction buffer to a final dilution of 50.000 platelets per µl and protein extracts stored at -80°C until usage. Protein concentrations were measured and adjusted using a pierce BCA assay (Thermo Fisher Scientific, Waltham, MA, USA). Samples were loaded on a 10% SDS-polyacrylamide gel and electro-blotted on PVDF membranes. After blocking in 5% BSA/TBS-T, blots were incubated overnight with following antibodies: polyclonal rabbit-anti-mouse P-selectin (1:1000), polyclonal rabbit-anti-mouse/human/rat PAR4 (1:1000), monoclonal mouse-anti-mouse/human PAR3 (1:500), mouse-anti-Talin (1:1000), polyclonal rabbit-anti-mouse Kindlin-3 (1:3000), polyclonal rabbit-anti-mouse Rap1 (1:1000), monoclonal mouse-anti-mouse beta-tubulin antibody (1:10000) and a mouse-anti-GAPDH (1:10000), respectively. A goat-anti-rabbit horseradish-peroxidase (HRP) conjugated antibody or a goat-anti-mouse HRP antibody was used as secondary antibody. Blots were washed, the HRP chemiluminescence substrate was added and images acquired. Acquired values were normalized to housekeeping proteins (GAPDH, beta-tubulin, alpha-tubulin), which were chosen according to the size of analyzed proteins.

Spreading experiments:

To investigate platelet spreading, µ-slides (ibidi µ-Slide VI 0.1, ibidi GmbH, Planegg/Martinsried, Germany) were coated with mouse fibrinogen (Innovative Research, Novi, MI, USA) at a concentration of 1 mg/ml overnight. After washing and

blocking for 1h with casein 5%, slides were transferred to the microscope (Zeiss, Axiovert 200, Objective Neofluar 63x/1.25 Oil; Jena, Germany). Platelets from pooled fetuses and from adult animals were isolated as described above. Counts were determined using an Idexx hematology analyzer.
Shortly before the experiment, platelets were resuspended in modified Tyrode's-HEPES buffer with calcium and magnesium at a concentration of 1 x 10^7/ml and stimulated with thrombin (0.1 U/ml). Recordings (FR 12/min) were started 2 minutes after injection of platelet suspension into the µ-slide. Platelet spreading was observed over a period of 10 minutes. Images were analyzed using Image J. Platelet area (μm^2) and perimeter [µm] are presented as ratio compared to baseline values. In addition platelet circularity (= 4π (a*rea/perimeter^2)) was calculated.* A circularity value of 1.0 indicates a perfect circle.[11]

Experimental data and statistical analysis
Statistical analysis of mouse experiments was performed using SigmaPlot Version 12.0 (Systat Software GmbH, Erkrath, Germany). For *in vivo* rate values, a Chi-square analysis was applied. To further distinguish subgroups in case of significance, pairwise z-test comparisons were performed. Time values were analyzed using the Kruskal-Wallis ANOVA on ranks with Dunn's posthoc test. Flow cytometry counts were analyzed using a One-way ANOVA. Fluorescence intensity and blood flow velocity were tested using the Kruskal-Wallis ANOVA on ranks with Dunn's posthoc test. Spreading data was compared with t-test for each time point. A *p*-value of ≤0.05 was considered significant.

Retrospective clinical data analysis
We conducted a retrospective neonatal intensive care database study between 11/2003 and 12/2013 of preterm infants born < than 1500g birth weight and ≤ 32 weeks gestational age at a tertiary NICU (Division of Neonatology, University Children's Hospital and Perinatal Center, Campus Grosshadern, Ludwig Maximilians University Munich, Germany). Data collection and statistical analysis were performed using Excel 2010 (Microsoft Corp., USA) and GraphPad Prism 5 (GraphPad Software Inc, USA). Numerical data was analyzed using a One-way ANOVA with Bonferroni posthoc test. Categorical data was analyzed using a Chi square test with subsequent Fisher's exact test for pairwise comparison. Thrombocytopenia was defined as a platelet count <150 G/l.

References

1. Ussar S, Wang HV, Linder S, Fassler R, Moser M. The kindlins: Subcellular localization and expression during murine development. *Experimental cell research*. 2006;312:3142-3151
2. Faust N, Varas F, Kelly LM, Heck S, Graf T. Insertion of enhanced green fluorescent protein into the lysozyme gene creates mice with green fluorescent granulocytes and macrophages. *Blood*. 2000;96:719-726
3. Sperandio M, Quackenbush EJ, Sushkova N, et al. Ontogenetic regulation of leukocyte recruitment in mouse yolk sac vessels. *Blood*. 2013;121:e118-128
4. Rumbaut RE, Randhawa JK, Smith CW, Burns AR. Mouse cremaster venules are predisposed to light/dye-induced thrombosis independent of wall shear rate, cd18, icam-1, or p-selectin. *Microcirculation*. 2004;11:239-247

5. Rehberg M, Krombach F, Pohl U, Dietzel S. Label-free 3d visualization of cellular and tissue structures in intact muscle with second and third harmonic generation microscopy. *PloS one*. 2011;6:e28237
6. Alugupalli KR, Michelson AD, Barnard MR, Leong JM. Serial determinations of platelet counts in mice by flow cytometry. *Thrombosis and haemostasis*. 2001;86:668-671
7. Moser M, Nieswandt B, Ussar S, Pozgajova M, Fassler R. Kindlin-3 is essential for integrin activation and platelet aggregation. *Nature medicine*. 2008;14:325-330
8. Bergmeier W, Schulte V, Brockhoff G, Bier U, Zirngibl H, Nieswandt B. Flow cytometric detection of activated mouse integrin alphaiibbeta3 with a novel monoclonal antibody. *Cytometry*. 2002;48:80-86
9. Pircher J, Fochler F, Czermak T, Mannell H, Kraemer BF, Wornle M, Sparatore A, Del Soldato P, Pohl U, Krotz F. Hydrogen sulfide-releasing aspirin derivative acs14 exerts strong antithrombotic effects in vitro and in vivo. *Arteriosclerosis, thrombosis, and vascular biology*. 2012;32:2884-2891
10. Massberg S, Enders G, Leiderer R, Eisenmenger S, Vestweber D, Krombach F, Messmer K. Platelet-endothelial cell interactions during ischemia/reperfusion: The role of p-selectin. *Blood*. 1998;92:507-515
11. Schindelin J, Arganda-Carreras I, Frise E, et al. Fiji: An open-source platform for biological-image analysis. *Nat Methods*. 2012;9:676-682

Early Microvascular Changes with Loss of the Glycocalyx in Children with Type 1 Diabetes

Claudia Nussbaum, MD[1], Ana Cavalcanti Fernandes Heringa, MD[1], Zuzana Mormanova, MD[1], Alexandra F. Puchwein-Schwepcke, MD[1], Susanne Bechtold-Dalla Pozza, MD[2], and Orsolya Genzel-Boroviczény, MD[1]

Objective To evaluate the microcirculation of children with type 1 diabetes mellitus who demonstrate no clinical signs of diabetic microangiopathy for the presence of microvascular alterations and glycocalyx perturbation.

Study design Images of sublingual vessels were obtained in 14 children with diabetes (ages 12.8 ± 2.8 years, diabetes duration 6.7 ± 4.3 years) and 14 control patients (ages 11.8 ± 2.8 years) by the use of sidestream dark field imaging and analyzed for total vessel density, vessel surface coverage, vessel diameter distribution, mean flow index, and glycocalyx thickness. Wilcoxon rank sum test and Pearson correlation were used for statistical analysis.

Results We observed profound microcirculatory changes in children with diabetes compared with control patients, with a significant reduction of glycocalyx thickness (0.38 μm vs 0.60 μm; $P = .013$), which was inversely correlated with blood glucose levels ($r = -0.55$; $P = .003$). Furthermore, the percentage of large vessels (>20 μm diameter) was significantly increased (11% vs 6%; $P = .023$) at the expense of capillaries (<10 μm diameter) with consequent increase in total vessel surface coverage (30% vs 26.0%; $P = .041$). No differences were seen in total vessel density and mean flow index.

Conclusions Microvascular alterations, including changes in microvessel distribution and loss of the glycocalyx, can be detected in children with type 1 diabetes mellitus before clinically apparent vascular complications. Our results disclose the glycocalyx as a possible monitoring measurement for earlier detection of diabetic microangiopathy and may provide a basis for new therapeutic strategies aiming at protection or restoration of the glycocalyx. *(J Pediatr 2014;164:584-9)*.

The long-term outcome of patients with type 1 diabetes mellitus (T1DM) is governed by the occurrence of vascular sequelae such as nephropathy, retinopathy, and cardiovascular disease, which are leading causes of morbidity and premature mortality.[1] The prevention and early identification of vascular complications are a central issue in the care of patients with diabetes.

The pathogenesis of vascular complications still remains incompletely understood; however, endothelial dysfunction (ED) is thought to play a central role in the development of diabetic microangiopathy and macroangiopathy.[2] There is some evidence that endothelial-dependent responses of the microvasculature and macrovasculature are impaired in children with T1DM when vascular complications are still subclinical.[3,4] These studies are supported by reports of increased markers of endothelial activation and perturbation such as intercellular adhesion molecule 1, E-selectin, and von Willebrand factor,[5] along with carotid intima-media thickening indicating beginning arteriosclerosis.[6,7]

The mechanisms leading to ED in diabetes mellitus are multifactorial.[8] Large clinical trials have underscored the causative role of hyperglycemia,[9,10] which contributes to ED by increasing production of reactive oxygen species and oxidative stress, activation of protein kinase C, and generation of vasoactive and proinflammatory substances. In recent years, the endothelial glycocalyx has emerged as an important target of hyperglycemia-induced vascular damage.[11] This complex layer of proteoglycans, glycoproteins, glycosaminoglycans, and attached plasma proteins covers the endoluminal vessel surface and has been recognized as a critical regulator of vascular integrity and endothelial function.[12] Acute and chronic elevation of blood glucose levels cause perturbation of the glycocalyx, leading to ED and increased microvascular permeability in vitro and in vivo.[13,14] Greater levels of hyaluronan, a major constituent of the endothelial glycocalyx, were found in the circulation of adults with diabetes, where they correlated with increased intima media thickness.[15] These data suggest that loss of the endothelial glycocalyx or alterations in the composition of the glycocalyx may present a common mechanism underlying the development

BP	Blood pressure
ED	Endothelial dysfunction
HbA1c	Glycosylated hemoglobin A1c
MFI	Mean flow index
SDF	Sidestream dark field
T1DM	Type 1 diabetes mellitus
TVD	Total vessel density

From the [1]Division of Neonatology IS; [2]Division of Endocrinology, Dr. von Hauner Children's Hospital, University Children's Hospital Munich, Munich, Germany

The authors declare no conflicts of interest.

 http://dx.doi.org/10.1016/j.jpeds.2013.11.016

of both microvascular and macrovacscular complications in diabetes. To date, it is not known whether such alterations of the glycocalyx occur in children with diabetes. Therefore, we assessed the microcirculation and the microvascular endothelial glycocalyx in children with T1DM and control patients.

Methods

Children with T1DM were recruited during their routine outpatient visits at the Dr. von Hauner Children's Hospital, University of Munich Medical Center. All patients had been diagnosed with T1DM for at least 1 year, and the diagnosis was made according to the current criteria of the American Diabetes Association: (1) symptoms of diabetes; (2) random plasma glucose or 2-hour plasma glucose during oral glucose tolerance testing of 200 mg/dL (11.1 mmol/L) or greater or fasting plasma glucose of 126 mg/dL (7 mmol/L) or greater; (3) detection of diabetes-specific autoantibodies; and (4) increased glycosylated hemoglobin A1c (HbA1c) levels. All patients were kept on daily subcutaneous insulin regimens. Two children were treated with L-thyroxin for autoimmune thyroiditis. One patient was suffering from paroxysmal seizures of unknown origin, and one patient had arterial prehypertension (blood pressure [BP] values ranging from the 90th to the 94th size-adjusted percentile). None of the children suffered from celiac disease.

Patients were screened routinely for the presence of microalbuminuria by measurement of the urinary albumin/creatinine ratio in first urine of the morning and for retinopathy by an annual mydriatic ophthalmoscopy examination performed from 11 years of age with ≥5 years of diabetes' duration, with none of the children demonstrating pathologic results. Pubertal status in patients with diabetes was documented twice a year, and there was no delay in pubertal development.

Age- and sex-matched control patients were recruited from the surgical outpatient clinic at the Dr. von Hauner Children's Hospital, University of Munich Medical Center where they presented for minor elective surgical procedures, including dermatologic, urologic, and orthopedic interventions. The presence of comorbidities likely to affect the (micro-) circulation in controls, such as hypertension, diabetes mellitus, acute infections, lead to the control patient's exclusion from the study. For all patients with TIDM and control patients, fasting plasma glucose levels, leukocyte count, and hematocrit were determined by the use of standard laboratory tests. Furthermore, the current HbA1c value of patients was measured, and the average HbA1c level during the preceding 2 years was retrieved from the patients' records. Level of HbA1c was measured by DCA 2000 Control (Bayer AG, Leverkusen, Germany), based on specific inhibition of latex immunoagglutination. Normal values of HbA1c as established in our laboratory range from 4.0% to 6.0%.

Blood was collected through peripheral venous puncture via the use of routine blood-collection tubes (S-Monovetten; Sarstedt, Nuembrecht, Germany), and samples were immediately transferred to the clinical laboratory for further processing. Written informed consent was obtained from at least one parent or legal guardian before the patient's inclusion in the study. The study was performed in accordance with the Declaration of Helsinki, and the study protocol was approved by the local ethics committee.

The sublingual microvasculature was visualized by use of the sidestream dark field (SDF) imaging technique as previously described.[16] Images (phase alternating line format, 1.35 μm/pixel) were recorded at a frame rate of 25 frames/s with a handheld video microscope (MicroScan; Microvision Medical, Amsterdam, The Netherlands) with a 5-fold objective connected to a computer and monitor via an analog-to-digital converter. The recordings were performed at the central area under the patient's tongue with patient lying on their back and took approximately 5-10 minutes. Care was taken to avoid movement artifacts and pressure on the tissue, as seen by increased background illumination attributable to greater reflection of light. To minimize measurement bias attributable to variability of the microvasculature within the sublingual area, at least 5 video sequences of 10 seconds' duration for each participant were obtained and stored digitally for later offline analysis. All recordings were performed by the same investigator to preclude interobserver variability.

Video sequences of the sublingual microcirculation underwent blinded offline analysis with the Automated Vascular Analysis software (AVA; Version 3.0, University of Amsterdam, Amsterdam, The Netherlands). Vessels were classified according to their diameter into small (<10 μm), medium (10-20 μm), and large (>20 μm). The following measures were calculated automatically: (1) total vessel density (TVD), defined as the total vessel length (mm) per image area (mm^2); (2) vessel diameter distribution, describing small, medium, and large vessels as percentage of total vessel length; and (3) vessel surface coverage, defined as the percentage of the total image area that is covered by vessel surface. Because the latter integrates both TVD and vessel diameter distribution, it is a sensitive measure of early, more subtle microcirculatory changes. Furthermore, blood flow velocity was assessed semiquantitatively according to the classification of Boerma. For this purpose, recordings of the sublingual microvasculature were divided into 4 quadrants, and a Boerma score was assigned to each quadrant depending on its predominant flow characteristics: no flow = 0, intermittent flow = 1, sluggish flow = 2, and continuous flow = 3. The mean flow index (MFI) was then calculated as average of the 4 quadrants.

Estimates of the endothelial glycocalyx dimension were obtained with a method that is based on the linear theory model as published by Nieuwdorp et al.[17] This method takes into account that flowing red blood cells are unable to compress or enter the intact glycocalyx and leukocytes traveling through a capillary are more rigid and cause compression of the glycocalyx. This allows the following red blood cells to get closer to the vessel wall, leading to a transient widening of the red blood cell column. By measuring the diameter of the red blood cell column before and after passage of the leukocytes (Δ vessel diameter), one can derive

an estimate of the local glycocalyx thickness by using the formula:

$$\text{glycocalyx thickness} = 1/2 * \Delta \text{ vessel diameter}$$

The method has been validated against measurements of the erythrocyte-endothelial gap as the gold standard showing good correlation ($r^2 = 0.973$) and high reproducibility.[17]

For our purposes, video sequences of the sublingual microvasculature were screened for spontaneous leukocyte passage through a capillary. The diameter of the red blood cell column was determined by use of the digital image processing software ImageJ (National Institutes of Health, Bethesda, Maryland). Before measurements were taken, the program was calibrated with a 1 mm/0.01-mm stage micrometer. To determine the red blood cell diameter, a perpendicular line was drawn though the according vessel and a light intensity profile plotted along the line before and directly after passage of the leukocyte. The diameter was defined as full width at one-half maximum of the corresponding light intensity profile. Only vessels with a diameter ranging from 3 to 7 μm were used for evaluation. The individual glycocalyx thickness was obtained by calculating the mean of at least 4 measurements in different vessels per child.

To determine interrater and intrarater reliability of our analyses, random SDF sequences of patients and controls were chosen for parallel assessment by 2 different raters as well as repeated assessment by the same rater at different time points.

Statistical Analyses

For pairwise comparison between experimental groups, a Wilcoxon rank sum test was performed. For univariate correlations between microvascular glycocalyx and other variables, as well as intrarater and interrater correlation Pearson correlation coefficient was determined. A $P < .05$ was considered statistically significant. All statistical analyses were carried out with SigmaStat 3.5 (Systat Software Company; GmbH, Erkrath, Germany). Data are presented as median (lower quartile-upper quartile).

Results

A total of 14 children with T1DM and 14 control patients were included in the study. Baseline characteristics of the 2 groups are provided in Table I. No significant differences between the groups were noted for age, sex, systolic and diastolic BP, body mass index, and hematocrit. As expected, blood glucose levels were significantly increased in children with diabetes compared with control patients. The median current HbA1c value in children with diabetes was increased above the normal range and did not differ significantly from the average HbA1c level during the preceding 2 years. Individual HbA1c values correlated significantly with the average HbA1c (r = 0.84, $P < .001$). The white blood cell count also was found to be significantly greater in patients with T1DM than control patients.

Table I. Patient characteristics and laboratory values

	Patients with T1DM	n	Control patients	n	*P* value rank sum test
Clinical data					
Age, y	13.6 [9.9-14.4]*	14	11.6 [9.7-14]	14	.382
Age at diagnose, y	6.5 [3.5-7.8]	14	n.a.		n.a.
Mean diabetes duration	6.3 [3.3-9.3]				
Male sex	8 of 14		7 of 14		n.a.
BMI, kg/m^2	20.4 [16.7-23.0]	14	16.5 [15.5-19.1]	11	.106
Systolic BP, mm Hg	112 [108-117]	14	111 [109-116]	13	.752
Diastolic BP, mm Hg	63 [58-67]	14	65 [61-72]	13	.679
Laboratory data					
Blood glucose, mg/dL	127 [93-165]	14	81 [75-95]	14	.004†
HbA1c, %	7.8 [7.2-8.4]	13	n.a.		n.a.
HbA1c, mmol/mol	61.8 [55.2-68.3]	13	n.a.		n.a.
HbA1c 2-year average, %	7.4 [7.0-8.0]	14	n.a.		n.a.
Hct, %	38.2 [36.9-41.2]	14	38.6 [36.7-39.9]	14	.504
WBC, g/L	6.9 [5.8-9.1]	14	5.9 [5.0-6.0]	14	.031†

BMI, body mass index; *Hct*, hematocrit; *n.a.*, not applicable; *WBC*, white blood cells.
*Values are given as median [lower quartile-upper quartile].
†Statistically significant.

The TVD of the sublingual vasculature and the MFI were found to be similar between children with diabetes and controls (TVD [mm/mm^2] patients with T1DM 20.9 [19.0-21.4] vs control patients 19.2 [18.2-20.6]; $P = .2$; patients with T1DM with a MFI score of 2.6 [2.5-2.8] vs control patients 2.9 [2.7-3.09]; $P = .08$). However, when the vessel diameter distribution was examined, the percentage of large vessels (>20 μm) was significantly increased in children with diabetes compared with control patients (patients with diabetes 11% [9%-13%] vs control patients 6% [3%-8%]; $P = .023$) at the expense of small vessels (Figure 1, A). This resulted in a significantly greater vessel surface coverage in the diabetic group compared with control patients (Figure 1, B).

Estimates of the microvascular glycocalyx thickness were obtained for capillaries of the sublingual vasculature. Compared with control patients, children with T1DM showed a significantly reduced glycocalyx thickness (0.38 μm [0.3-0.41 μm] vs control patients 0.60 μm [0.51-0.70 μm]; Figure 2, A). We did not observe differences in the glycocalyx dimensions between female and male patients (data not shown). Furthermore, a significant inverse correlation was noted between the microvascular glycocalyx dimension and acute serum glucose levels in children with diabetes and control patients (Figure 2, B). No significant correlation existed between glycocalyx thickness and HbA1c (r = 0.24, $P = .42$), body mass index (r = 0.31, $P = .14$), duration of diabetes (r = −0.196, $P = .50$), age at diagnosis (r = 0.197, $P = .50$), current age (r = −0.24, $P = .22$), and systolic (r = −0.34, P = .09) or diastolic BP (r = −0.18, $P = 0.38$).

Overall, SDF-based analysis of microcirculatory measurements and microvascular glycocalyx thickness in sublingual

vessels of patients and controls showed good interrater and intrarater correlation with correlation coefficients ranging between 0.74 and 0.99 (**Table II**; available at www.jpeds.com).

Discussion

We found a significant reduction of the microvascular endothelial glycocalyx thickness in children with diabetes by 36% compared with control patients. This finding is line with previous reports demonstrating a glycocalyx loss in sublingual capillaries by 18%-44% in adults with T1DM[18] and type 2 diabetes mellitus[19] compared with control patients. Our estimates of the glycocalyx in the control group are in accordance with measures obtained in healthy adults ranging from 0.58 to 0.9 μm in sublingual capillaries.[17,18]

Results from the Diabetes Control and Complication Trial and the Epidemiology of Diabetes Interventions and Complications Study confirm the importance of glycemic control in the prevention of vascular complications in patients with diabetes.[9,10] Here we found a significant inverse correlation of blood glucose levels and glycocalyx dimensions. Experimental data from animal models[20] and humans[14] demonstrate that elevation of blood glucose up to levels around 16-25 mmol/L (290-450 mg/dL) causes an acute loss of the glycocalyx along with an increase in circulating glycocalyx degradation products, suggesting glycocalyx shedding. This shedding may have severe consequences, because disruption of the glomerular endothelial glycocalyx was directly linked to the development of microalbuminuria as marker for diabetic nephropathy in adult patients.[18,21] Furthermore, circulating glycocalyx degradation products correlate significantly with the carotid intima media thickness in adults with T1DM, suggesting a possible association between glycocalyx damage and the development of arteriosclerosis.[15]

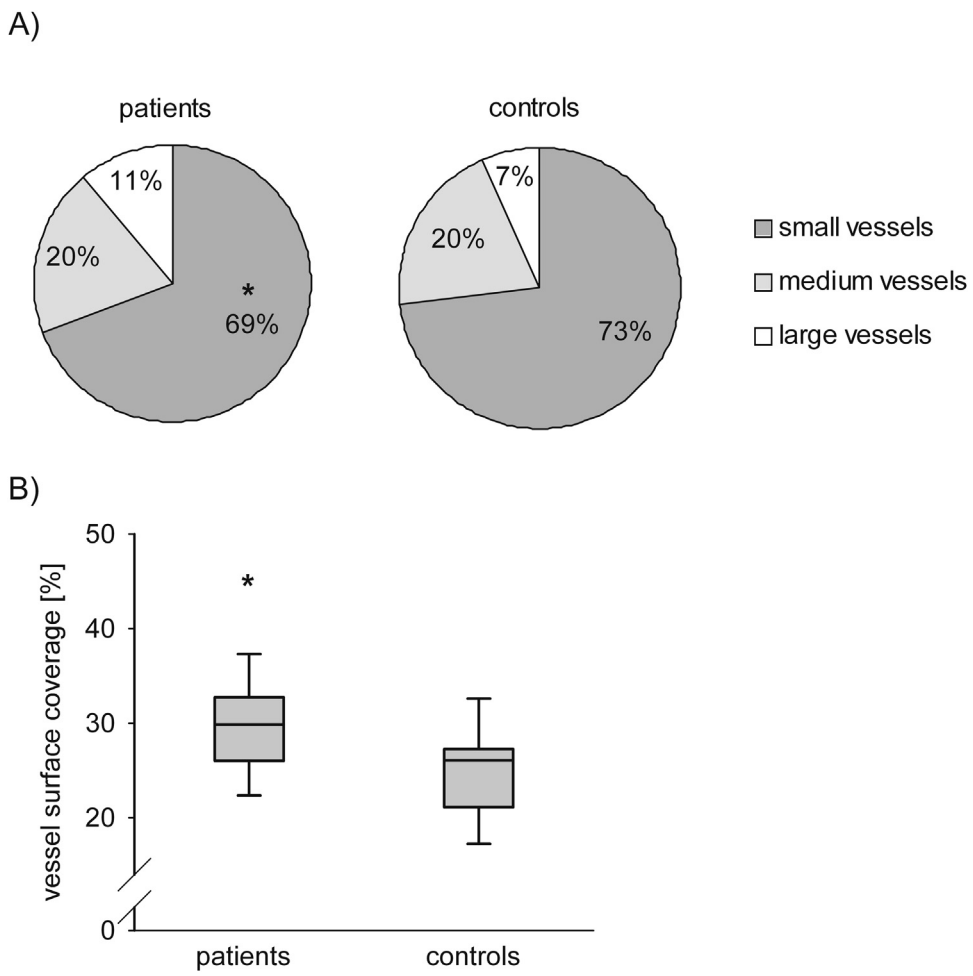

Figure 1. The sublingual microvasculature of children with T1DM (patients, n = 14) and control patients (n = 14) was visualized using SDF imaging (5-fold objective) and analyzed off-line with AVA 3.0 software (University of Amsterdam, The Netherlands). **A,** Vessel diameter distribution: *Percentage of large vessels in patients with T1DM vs control patients, P = .023, rank sum test. **B,** Vessel surface coverage: *Patients with T1DM vs control patients, P = .041, rank sum test. Data are depicted as median, lower/upper quartile, and min/max.

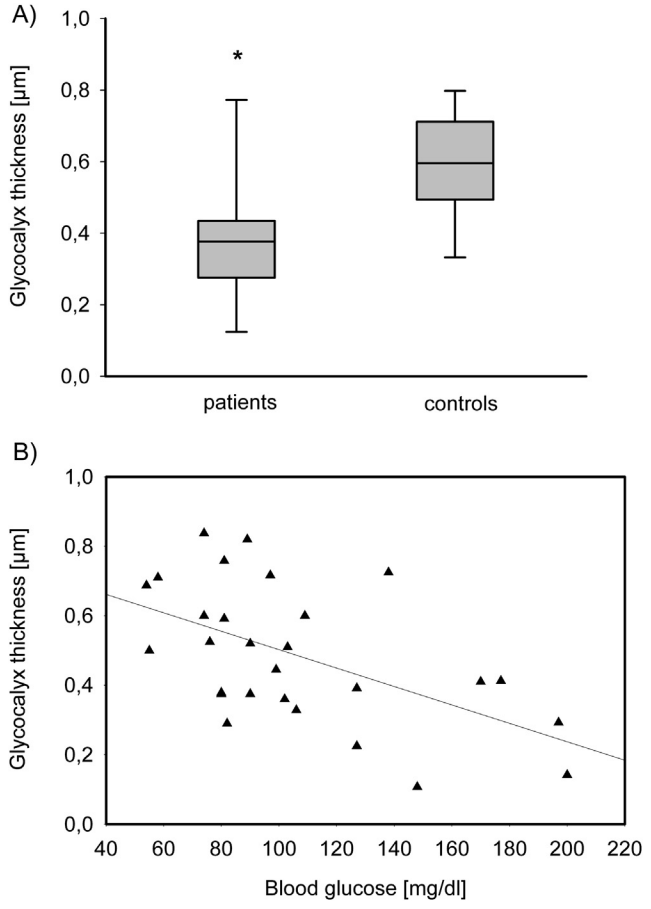

Figure 2. The dimension of the sublingual endothelial glycocalyx in children with T1DM (patients, n = 14) and control patients (n = 14) was indirectly calculated according to the formula: glycocalyx thickness = ½ * Δ vessel diameter, with Δ being the difference in vessel diameter before and after spontaneous leukocyte passage. **A,** Microvascular glycocalyx thickness: *Patients with T1DM vs control patients, $P = .013$, rank sum test. Data are depicted as median, lower/upper quartile, and min/max. **B,** Inverse correlation of glycocalyx thickness with acute blood glucose levels ($r = -0.55$, $P = .003$, Pearson correlation).

Because our investigations were limited to the sublingual microvasculature, we cannot say whether other vascular beds, such as the glomerular capillaries, are equally affected. However, it seems likely that our findings are not a local phenomenon but reflect a systemic condition because hyperglycemia should affect all vascular beds. This assumption is supported by previous studies demonstrating a parallel reduction of glycocalyx thickness in sublingual and retinal vessels in adults with type 2 diabetes mellitus[19] as well as a direct correlation of sublingual glycocalyx dimensions with estimates of the systemic glycocalyx volume.[18] Therefore, the microvascular glycocalyx in sublingual vessels might serve as surrogate monitoring measurement to detect subclinical systemic microangiopathy.

Glycocalyx dimensions did not correlate with HbA1c levels in our study. A possible explanation may be that the HbA1c provides information on average blood glucose levels and does not adequately express the amplitude of acute glucose fluctuations. These acute fluctuations were suggested to be a more potent inducer of oxidative stress than chronic hyperglycemia.[22] Increased oxidative stress is thought to be a central mechanism in the development of ED, and reactive oxygen species can directly disrupt the glycocalyx.[23] Interestingly, hyperglycemia and oxidative stress also trigger the production of advanced glycation end products, which exert potent proinflammatory activity. Elevated markers of inflammation such as C-reactive protein or interleukin-6 have been detected in children and adults with diabetes,[4,24] supporting the notion that diabetes represents a condition of chronic inflammation. This might explain the significantly greater white blood cell counts in children with diabetes compared with control patients.

We also observed changes in the diameter distribution of the sublingual microvasculature in children with diabetes with a significantly greater percentage of vessels >20 μm at the expense of capillaries. A similar pattern has been described by Algenstaedt et al,[25] who investigated the microvasculature in early-stage diabetic mice and found a shift in the diameter peak towards greater values with a significant reduction of capillaries compared with controls. In poorly controlled children with T1DM, a significantly larger diameter in the venous capillary trunk of the nailfold has been described.[26] These changes may have severe consequences as a reduction in the number of capillaries available for oxygen supply will ultimately result in tissue hypoxia.[27]

There are some limitations to our study. Because the offline analysis is still very time-consuming and not suitable for bedside analyses, only a relatively small number of patients with diabetes and control patients were included in the study limiting the generalizability of our results. Therefore, our findings need to be confirmed in larger cohort prospective clinical studies. Hopefully, this can be achieved in the future by the development of improved analysis systems, allowing a real-time assessment of the microcirculation as requirement for its application in the clinical setting. Furthermore, we cannot exclude that the microvascular alterations we observed in children with diabetes are only a transient phenomenon. Further research looking at the effect of intraindividual blood glucose variations in a longitudinal approach is necessary to dissect acute from chronic changes and to answer the question, whether these alterations are predictive for the development of vascular complications.

Our study does provide in vivo evidence that diabetes-associated changes of the microvasculature, which so far have only been described for adult patients, already occur in children with T1DM. These changes are known to precede vascular complications and are thought to contribute essentially to their development. Considering that none of the children with diabetes had signs of vasculopathy in the routine screening tests, including urine analysis and ophthalmoscopic examinations, our findings are of clinical interest, because they may help to

identify patients at greater risk of developing vascular complications at an earlier stage. Recognition of the glycocalyx as an early target of diabetes-induced damage may provide a basis for new therapeutic concepts aiming at restoration and protection of the glycocalyx to prevent vascular complications.[19,28] ■

Submitted for publication Jun 12, 2013; last revision received Oct 7, 2013; accepted Nov 7, 2013.

Reprint requests: Claudia Nussbaum, MD, Dr. von Hauner Children's Hospital, University of Munich Medical Center, Lindwurmstr. 4, 80337 Munich, Germany. E-mail: claudia.nussbaum@med.uni-muenchen.de

References

1. Daneman D. Type 1 diabetes. Lancet 2006;367:847-58.
2. Schalkwijk CG, Stehouwer CD. Vascular complications in diabetes mellitus: the role of endothelial dysfunction. Clin Sci (Lond) 2005;109:143-59.
3. Khan F, Elhadd TA, Greene SA, Belch JJ. Impaired skin microvascular function in children, adolescents, and young adults with type 1 diabetes. Diabetes Care 2000;23:215-20.
4. Babar GS, Zidan H, Widlansky ME, Das E, Hoffmann RG, Daoud M, et al. Impaired endothelial function in preadolescent children with type 1 diabetes. Diabetes Care 2011;34:681-5.
5. Elhadd TA, Kennedy G, Hill A, Mclaren M, Newton RW, Greene SA, et al. Abnormal markers of endothelial cell activation and oxidative stress in children, adolescents and young adults with type 1 diabetes with no clinical vascular disease. Diabetes Metab Res Rev 1999;15:405-11.
6. Jarvisalo MJ, Raitakari M, Toikka JO, Putto-Laurila A, Rontu R, Laine S, et al. Endothelial dysfunction and increased arterial intima-media thickness in children with type 1 diabetes. Circulation 2004;109:1750-5.
7. Dalla Pozza R, Netz H, Schwarz HP, Bechtold S. Subclinical atherosclerosis in diabetic children: results of a longitudinal study. Pediatr Diabetes 2010;11:129-33.
8. Hink U, Li H, Mollnau H, Oelze M, Matheis E, Hartmann M, et al. Mechanisms underlying endothelial dysfunction in diabetes mellitus. Circ Res 2001;88:E14-22.
9. Writing Team for the Diabetes Control and Complications Trial/Epidemiology of Diabetes Interventions and Complications Research Group. Sustained effect of intensive treatment of type 1 diabetes mellitus on development and progression of diabetic nephropathy: the Epidemiology of Diabetes Interventions and Complications (EDIC) study. JAMA 2003;290:2159-67.
10. The Diabetes Control and Complications Trial Research Group. The effect of intensive treatment of diabetes on the development and progression of long-term complications in insulin-dependent diabetes mellitus. The Diabetes Control and Complications Trial Research Group. N Engl J Med 1993;329:977-86.
11. Salmon AH, Satchell SC. Endothelial glycocalyx dysfunction in disease: albuminuria and altered microvascular permeability. J Pathol 2011;226:562-74.
12. Reitsma S, Slaaf DW, Vink H, van Zandvoort MA, oude Egbrink MG. The endothelial glycocalyx: composition, functions, and visualization. Pflugers Arch 2007;454:345-59.
13. Brower JB, Targovnik JH, Caplan MR, Massia SP. High glucose-mediated loss of cell surface heparan sulfate proteoglycan impairs the endothelial shear stress response. Cytoskeleton (Hoboken) 2010;67:135-41.
14. Nieuwdorp M, van Haeften TW, Gouverneur MC, Mooij HL, van Lieshout MH, Levi M, et al. Loss of endothelial glycocalyx during acute hyperglycemia coincides with endothelial dysfunction and coagulation activation in vivo. Diabetes 2006;55:480-6.
15. Nieuwdorp M, Holleman F, de GE, Vink H, Gort J, Kontush A, et al. Perturbation of hyaluronan metabolism predisposes patients with type 1 diabetes mellitus to atherosclerosis. Diabetologia 2007;50:1288-93.
16. Hiedl S, Schwepcke A, Weber F, Genzel-Boroviczeny O. Microcirculation in preterm infants: profound effects of patent ductus arteriosus. J Pediatr 2010;156:191-6.
17. Nieuwdorp M, Meuwese MC, Mooij HL, Ince C, Broekhuizen LN, Kastelein JJ, et al. Measuring endothelial glycocalyx dimensions in humans: a potential novel tool to monitor vascular vulnerability. J Appl Physiol 2008;104:845-52.
18. Nieuwdorp M, Mooij HL, Kroon J, Atasever B, Spaan JA, Ince C, et al. Endothelial glycocalyx damage coincides with microalbuminuria in type 1 diabetes. Diabetes 2006;55:1127-32.
19. Broekhuizen LN, Lemkes BA, Mooij HL, Meuwese MC, Verberne H, Holleman F, et al. Effect of sulodexide on endothelial glycocalyx and vascular permeability in patients with type 2 diabetes mellitus. Diabetologia 2010;53:2646-55.
20. Zuurbier CJ, Demirci C, Koeman A, Vink H, Ince C. Short-term hyperglycemia increases endothelial glycocalyx permeability and acutely decreases lineal density of capillaries with flowing red blood cells. J Appl Physiol 2005;99:1471-6.
21. Singh A, Friden V, Dasgupta I, Foster RR, Welsh GI, Tooke JE, et al. High glucose causes dysfunction of the human glomerular endothelial glycocalyx. Am J Physiol Renal Physiol 2011;300:F40-8.
22. Monnier L, Mas E, Ginet C, Michel F, Villon L, Cristol JP, et al. Activation of oxidative stress by acute glucose fluctuations compared with sustained chronic hyperglycemia in patients with type 2 diabetes. JAMA 2006;295:1681-7.
23. Brownlee M. Biochemistry and molecular cell biology of diabetic complications. Nature 2001;414:813-20.
24. Llaurado G, Ceperuelo-Mallafre V, Vilardell C, Simo R, Freixenet N, Vendrell J, et al. Arterial stiffness is increased in patients with type 1 diabetes without cardiovascular disease: a potential role of low-grade inflammation. Diabetes Care 2012;35:1083-9.
25. Algenstaedt P, Schaefer C, Biermann T, Hamann A, Schwarzloh B, Greten H, et al. Microvascular alterations in diabetic mice correlate with level of hyperglycemia. Diabetes 2003;52:542-9.
26. Koscielny J, Latza R, Wolf S, Kiesewetter H, Jung F. Early rheological and microcirculatory changes in children with type I diabetes mellitus. Clin Hemorheol Microcirc 1998;19:139-50.
27. Pittman RN. Oxygen transport and exchange in the microcirculation. Microcirculation 2005;12:59-70.
28. Gambaro G, Kinalska I, Oksa A, Pont'uch P, Hertlova M, Olsovsky J, et al. Oral sulodexide reduces albuminuria in microalbuminuric and macroalbuminuric type 1 and type 2 diabetic patients: the Di.N.A.S. randomized trial. J Am Soc Nephrol 2002;13:1615-25.

Table II. Intrarater and interrater correlation

Measurements	Patients with T1DM/control patients	Intrarater correlation (r)	*P*-value	Interrater correlation (r)	*P*-value
TVD	10/10	0.98	<.001	0.96	<.001
Vessel surface coverage	10/10	0.96	<.001	0.90	<.001
% small vessels	10/10	0.99	<.001	0.94	<.001
% medium vessels	10/10	0.96	<.001	0.94	<.001
% large vessels	10/10	0.99	<.001	0.92	<.001
Glycocalyx thickness	5/5	0.74	.015	0.78	.008

Perturbation of the microvascular glycocalyx and perfusion in infants after cardiopulmonary bypass

Claudia Nussbaum, MD,[a,b] Amelie Haberer, MD,[a] Anna Tiefenthaller,[a] Katarzyna Januszewska, MD,[c] Daniel Chappell, MD,[d] Florian Brettner, MD,[d] Peter Mayer, MD,[e] Robert Dalla Pozza, MD,[b] and Orsolya Genzel-Boroviczény, MD[a]

ABSTRACT

Objective: Perturbation of the endothelial glycocalyx is discussed in the pathogenesis of complications related to cardiopulmonary bypass. We evaluated the effects of cardiopulmonary bypass on the microcirculation and the microvascular endothelial glycocalyx of infants undergoing surgery for congenital cardiac defects.

Methods: The microcirculation was visualized at the ear conch using Sidestream dark field imaging before surgery (T0), after admission to the intensive care unit (T1), 24 hours postsurgery (T2), and 7 days postsurgery (T3). Glycocalyx thickness was assessed by measurement of the perfused boundary region. Microcirculatory parameters included total and perfused vessel density, vessel diameters, and microcirculatory flow index.

Results: A total of 40 infants undergoing cardiac surgery (36 with cardiopulmonary bypass, 4 without cardiopulmonary bypass) were examined. As controls, measurements before and after cardiac catheterization (n = 6) and before and after surgery for cleft palate (n = 9) were performed. After surgery with cardiopulmonary bypass, the perfused boundary region was significantly increased, indicating reduced glycocalyx thickness at T1 compared with preoperative values with a stepwise return to baseline by T3. In the control groups, no significant perfused boundary region changes were noted. Furthermore, after cardiopulmonary bypass, a transient, significant reduction of the microcirculatory flow index and the perfused vessel density was seen at T1. Similar changes were observed after cardiac surgery without cardiopulmonary bypass, but not in the other controls.

Conclusions: Our study reveals for the first time local perturbations of the endothelial glycocalyx and microvascular perfusion in infants after surgery with cardiopulmonary bypass. Microcirculatory monitoring might be a useful tool to evaluate interventions aiming at reduction of bypass-related complications. (J Thorac Cardiovasc Surg 2015;150:1474-81)

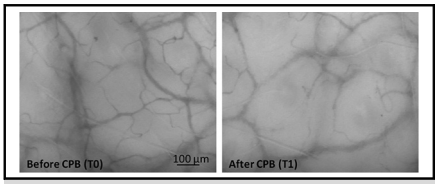

Reduced microvascular perfusion and glycocalyx perturbation after CPB in infants (T1).

Central Message

We show for the first time an acute perturbation of the microvascular glycocalyx and perfusion after cardiopulmonary bypass in infants.

Perspective

Glycocalyx shedding and disturbed microcirculatory perfusion are thought to contribute to complications after cardiopulmonary bypass. Monitoring of the microcirculation might be a useful tool to evaluate interventions aiming at the reduction of bypass-related complications.

See Editorial Commentary page 1482.

Supplemental material is available online.

The endothelial glycocalyx (EG) is increasingly recognized for its pivotal role in vascular homeostasis.[1] This fragile structure consisting of proteoglycans, glycoproteins, and glycosaminoglycans together with associated plasma proteins covers the lumen of the whole vasculature.[2] Because of its central position between the bloodstream and the endothelium, the EG is a frontline regulator of vascular functions, including shear stress response,

From the [a]Division of Neonatology, Campus Innenstadt, Dr von Hauner Children's University Hospital Munich, Munich, Germany; [b]Department of Pediatric Cardiology and Intensive Care Medicine, Dr von Hauner Children's University Hospital Munich, Munich, Germany; [c]Department of Cardiac Surgery, University of Münster, Albert-Schweitzer-Campus 1, Münster, Germany; [d]Department of Anesthesiology, University Hospital of Munich, Munich, Germany; and [e]Department of Oral and Maxillofacial Surgery, Ludwig-Maximilians-University Munich, Munich, Germany.

The study was supported by a research grant from the Deutsche Gesellschaft für Pädiatrische Kardiologie to C.N. None of the coauthors received any form of honorarium, grant, or other payment with respect to the present article.

Received for publication June 16, 2015; revisions received July 29, 2015; accepted for publication Aug 19, 2015; available ahead of print Sept 19, 2015.

Address for reprints: Claudia Nussbaum, MD, Dr von Hauner Children's University Hospital, Ludwig-Maximilians-University, Maistrasse 11, 80337 Munich, Germany (E-mail: claudia.nussbaum@med.uni-muenchen.de).

0022-5223/$36.00

http://dx.doi.org/10.1016/j.jtcvs.2015.08.050

Abbreviations and Acronyms

AC = aortic clamping
CLS = capillary leak syndrome
CPB = cardiopulmonary bypass
DHCA = deep hypothermic circulatory arrest
EG = endothelial glycocalyx
MFI = microcirculatory flow index
PBR = perfused boundary region
PVD = perfused vessel density
RBCW = red blood cell column width
S/T = subcutaneous-thoracic

anti-inflammatory, and anticoagulatory properties and regulation of vascular permeability.[2] Thus, shedding of the EG as observed during inflammation/sepsis, hyperglycemia, and ischemia/reperfusion leads to increased vascular permeability with edema formation, leukocyte recruitment, activation of the coagulation system, and endothelial dysfunction.[3-5]

In infants undergoing surgery with cardiopulmonary bypass (CPB) for congenital heart defects, many of these phenomena have been described, including generalized edema formation (capillary leak syndrome [CLS])[6] and a systemic inflammatory reaction with activation of the complement and coagulation system, platelets, endothelial cells, and leukocytes.[7,8] These observations suggest that damage to the EG may present an underlying mechanism in the pathogenesis of CPB-related complications. In line with this notion, Bruegger and colleagues[9] were recently able to demonstrate an increase in the circulating levels of glycocalyx components during cardiac surgery in children depending on the ischemic impact. These data provide the first indirect evidence for an acute degradation of the glycocalyx during CPB in children. However, the data are not conclusive on the condition of the EG on a local, microvascular level, and it remains unknown whether shedding is restricted to the ischemic organs or presents a global phenomenon.

Therefore, it was the aim of the present study to directly examine the effect of cardiac surgery with CPB on the microcirculation and the microvascular EG in infants with congenital heart defects and to correlate our findings with the postoperative clinical status.

PATIENTS AND METHODS

The study was performed in accordance with the Declaration of Helsinki and approved by the local ethics committee. Written informed consent was obtained from the parents before inclusion in the study. A total of 40 infants with congenital heart defects were recruited (Table E1 shows detailed diagnoses). For controls, we measured 6 infants before and after diagnostic cardiac catheterization and 9 infants before and after surgery for correction of a cleft palate (perfused boundary region [PBR] measurements only). None of the children were treated with anti-inflammatory medication or received catecholamines before surgery. Four children with congenital cardiac defect were kept on continuous prostaglandin E1 infusion.

For diagnosis of CLS in addition to noncardiac edema formation, pleural effusion, and ascites, the subcutaneous-thoracic (S/T) ratio was calculated from postoperative chest x-rays as described by Sonntag and colleagues[10] with a threshold of greater than 12.6%.

Cardiopulmonary Bypass Protocol

Depending on the cardiac defect, the following CPB protocols were applied:

1. CPB under heartbeating conditions (CPB, n = 11): On arterial and venous cannulation, CPB was established and surgery was continued without cardiac arrest in normothermia.
2. CPB with aortic clamping (AC) (CPB + AC, n = 17): CPB was started after arterial and bicaval venous cannulation. After aortic crossclamping, cardioplegic arrest was achieved by infusion of Bretschneider-histidine-tryptophan-ketoglutarate solution into the aortic root. During the ongoing CPB, the lungs and heart were exposed to ischemia while the children's core temperature was constantly kept at 28° to 32°C.
3. CPB with AC and deep hypothermic circulatory arrest (DHCA) (CPB + AC + DHCA, n = 8): CPB was started after cannulation with an arterial and a venous cannula placed in the right atrium, and cooling began. DHCA with whole body ischemia was initiated at a core temperature of 18°C. CPB was reinstated for rewarming.

All children received a systemic heparinization before CPB to keep the activating clotting time greater than 450 seconds. CPB was performed using nonpulsatile flow. All infants were weaned from CPB after gradual rewarming, and heparin was reversed by administration of protamine. Four children with congenital heart defect underwent open thoracic surgical procedures without the use of CPB.

Visualization and Recording of the Microvasculature

The skin microvasculature at the fossa triangularis of the ear was visualized using Sidestream dark field imaging.[5] Recordings were performed at 25 frames per second using a handheld video microscope (MicroScan, 5x/0.2; MicroVision Medical, Amsterdam, The Netherlands) providing a 325-fold magnification on screen (720 × 576 pixels). Care was taken to avoid motion artefacts and pressure on the tissue as identified by increased background illumination. The following time points were evaluated: T0 = the day before surgery, T1 = postsurgery/cardiac catheterization within 1 hour after transfer to the intensive care unit, T2 = 24 hours postsurgery, and T3 = 7 days postsurgery. At least 3 video sequences were recorded for each participant for later off-line analysis.

Measurement of the Endothelial Glycocalyx

The EG dimension was assessed with the GlycoCheck Measurement Software (GlycoCheck BV, Maastricht, The Netherlands).[11] The software automatically measures the red blood cell column width (RBCW) in at least 3000 vessel segments within a Sidestream dark field frame. On the basis of the distribution of the RBCW, the median RBCW is calculated, whereas the maximum RBCW is derived by linear regression analysis. The PBR, representing the outer part of the endothelial surface layer penetrable to erythrocytes, is defined as ½ * (maximum-median RBCW). When the glycocalyx is lost, red blood cells can move closer to the vessel wall leading to an increase in the maximum RBCW and thus in the PBR. Because measurements at T0, T2, and T3 were performed without anesthesia, we were able to obtain PBR values in only 25 of 40 children with congenital heart defect, because the program requires minimal motion during the recordings.

TABLE 1. Baseline characteristics of the experimental groups

	Cardiac surgery with CPB	Cardiac surgery without CPB	Cardiac catheterization	Cleft palate surgery	Statistics
No.	36	4	6	9	
Sex (male %)	56	25	67	44	
Age (mo)	8.9 (0.2-29)	9.0 (0.2-31)	15.4 (5.2-29)	5.2 (3.2-13.5)	$P = .19$
Weight (kg)	6.8 (2.9-14)	5.9 (3-11.3)	9.2 ± (4.8-12.8)	6.5 (5.1-8.5)	$P = .25$

CPB, Cardiopulmonary bypass.

Analysis of the Microcirculation

Video sequences were analyzed by a single rater blinded to the time point of recording, the surgical procedure, and the clinical status of the child using the Automated Vascular Analysis software (AVA 3.2, Amsterdam, The Netherlands).

The following parameters were calculated automatically: (1) total vessel density (mm/mm^2), (2) perfused vessel density (PVD) (mm/mm^2), and (3) diameter distribution: percentage of small (<10 μm), medium (10-20 μm), and large vessels (>20 μm). Blood flow was assessed semiquantitatively by assigning a microcirculatory flow index (MFI) according to the classification of Boerma and colleagues,[12] with 0 = no flow, 1 = intermittent flow, 2 = sluggish flow, 3 = continuous flow, and 4 = hyperdynamic flow.

Statistical Analysis

Data were analyzed using GraphPad Prism 5 (GraphPad Software Inc, La Jolla, Calif). Experimental data are presented as median, interquartile range, and minimum/maximum. Clinical data are presented as mean and range. For longitudinal comparison of data, a repeated-measures analysis of variance on ranks or a Wilcoxon signed-rank test was performed as appropriate. For comparison between 2 or more different experimental groups, a Wilcoxon rank-sum test or an analysis of variance on ranks was used. For correlation of 2 variables, a Pearson correlation was calculated.

RESULTS

Patient Characteristics

Demographic and procedural characteristics of the patient groups are shown in Tables 1 and 2. There were no significant differences in age or weight between the children undergoing cardiac surgery with CPB (in total) and the control groups; however, children were slightly older in the cardiac catheterization group and slightly younger in the cleft palate surgery group. As expected because of the underlying cardiac defect and thus the surgical procedure, we found significant differences among the CPB, CPB + AC, and CPB + AC + DHCA groups with respect to age, weight, and CPB and AC time with an inverse correlation between age and CPB duration ($r = -0.45$, $P = .005$).

Effect of Cardiac Surgery With Cardiopulmonary Bypass on the Microvascular Endothelial Glycocalyx

To evaluate the effect of surgery with CPB on the EG, the PBR was determined in the skin microvasculature. At baseline (T0), PBR values did not differ significantly among the experimental groups (Figure 1, *A* and *B*). Directly after surgery with CPB (T1), the PBR was significantly increased compared with T0, indicating an acute reduction of the glycocalyx dimension by approximately 0.2 μm with a stepwise return to almost baseline values at T3 (Figure 1, *A*). After cardiac catheterization or surgery without CPB, the PBR did not change significantly (Figure 1, *B*).

To evaluate whether the increase in PBR and thus the magnitude of EG damage depend on the ischemic impact during surgery, we analyzed the CPB and the CPB + AC groups at T1 separately. Because of the low number of successful PBR measurements (n = 3), the CPB + AC + DHCA group was not included in the subgroup analysis. Of note, the postoperative increase in the PBR was found to be identical in the CPB and CPB + AC groups, arguing for an ischemia/reperfusion-independent effect (Figure 1, *C*). In line with this observation, postoperative PBR values at T1 did not correlate with CPB duration ($r = 0.06$, $P = .78$). Of note, PBR at T1 was not related to the intraoperative and postoperative body temperatures ($r = 0.27$, $P = .34$ and $r = 0.18$, $P = .4$).

Effect of Cardiac Surgery With Cardiopulmonary Bypass on Parameters of the Microcirculation

At baseline, all groups showed comparable microcirculatory parameters (T0 in Figure 2, *A* and *B*). Although the total vessel density and the vessel diameter distribution remained unaffected in all groups (data not shown), we observed an acute reduction of the microvascular perfusion after cardiac surgery with CPB (T1), as seen by a significant decrease in the MFI and PVD, with a return to baseline values within 24 hours (Figure 2, *A*). In children undergoing cardiac

TABLE 2. Procedural characteristics

	CPB	CPB + AC	CPB + AC + DHCA	Statistics
No.	17	11	8	
Age (mo)	13.7 (1-29)	9.3 (2-24)	1.6 (0.2-7)	$P = .0053$
Weight (kg)	8.3 (4.3-14)	7.1 (4.1-12.7)	3.8 (2.9-6.3)	$P = .004$
CPB time (min)	42 (18-65)	82 (28-127)	136 (87-183)	$P < .001$
AC time (min)	NA	46 (9-73)	71 (45-91)	$P = .049$
DHCA time (min)	NA	NA	31 (15-56)	

CPB, Cardiopulmonary bypass; *AC*, aortic clamping; *DHCA*, deep hypothermic circulatory arrest; *NA*, not available.

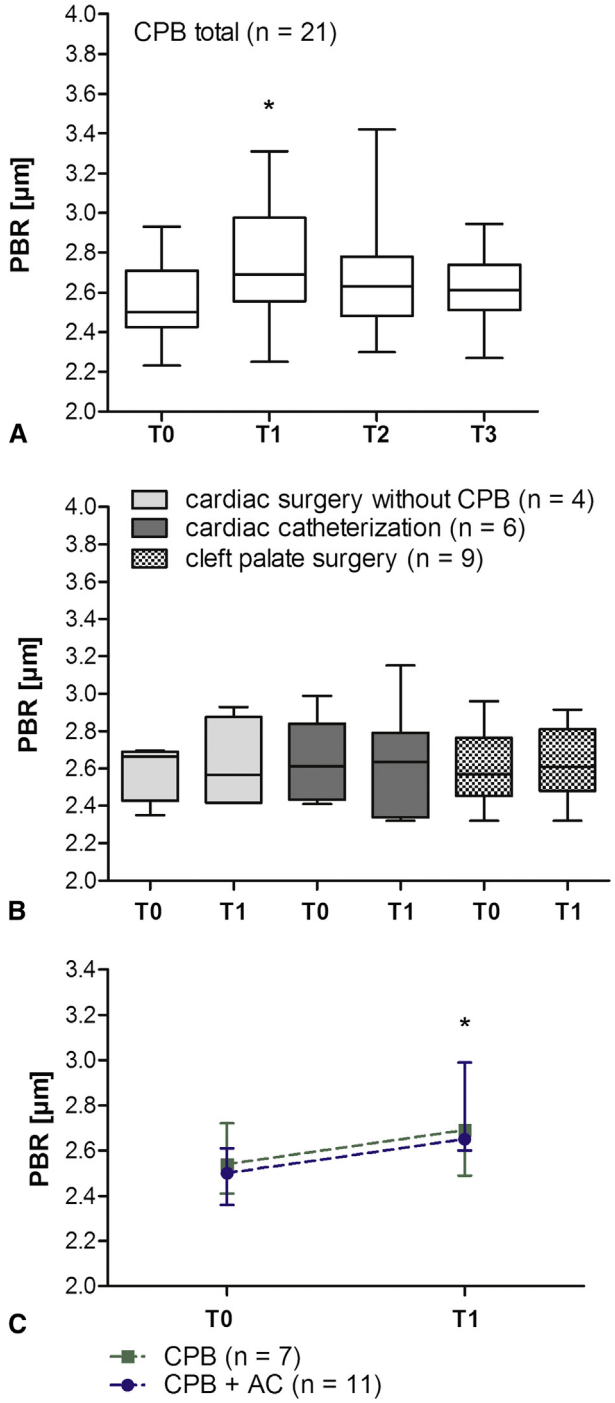

FIGURE 1. Evaluation of the EG by measurement of the PBR. Increases in the PBR indicate a reduction in the glycocalyx thickness. A, Cardiac surgery with CPB. B, Control groups. C, CPB subgroup analysis. *CPB*, Cardiopulmonary bypass; *PBR*, perfused boundary region; *T0*, Before surgery, *T1*, postsurgery after admission to the intensive care unit; *T2*, 24 hours postsurgery; *T3*, 7 days postsurgery; *AC*, aortic clamping. *$P < .05$ versus T0.

surgery without CPB, we observed a similar decrease in both parameters at T1, although values did not reach significance because of the small group size. In comparison, MFI and PVD after cardiac catheterization remained unchanged compared with baseline (Figure 2, *B*). Remarkably, when analyzing the change at T1 for the different CPB groups separately, we observed significant differences in the MFI and PVD depending on the ischemic impact, with the greatest reduction of the MFI at T1 compared with T0 in the CPB + AC + DHCA group (Figure 2, *C*). Although neither MFI nor PVD at T1 showed a correlation with intraoperative temperature, postoperative arterial blood pressure, or hematocrit (data not shown), we found a weak but significant inverse correlation of the MFI with CPB duration ($r = -0.39$, $P = .019$) and a direct correlation of the PVD with body temperature at T1 ($r = 0.43$, $P = .01$).

Relationship Between Changes in the Perfused Boundary Region and Microcirculatory Flow Index and the Postoperative Outcome

To see whether the outcome after surgery with CPB is related to the changes in the PBR and MFI, we analyzed the development of CLS, need of mechanical ventilation, and inotrope demand. In children with CPB, we found a significant increase in the S/T ratio on the first postoperative day (T2) compared with T0 (Figure 3, *A*) and a positive correlation with CPB duration ($r = 0.63$, $P = .0013$). However, only 4 children had an S/T ratio above the threshold defining CLS. Therefore, we were not able to stratify our experimental data by the development of CLS. Stratification by need for mechanical ventilation at T2 and inotrope demand at T1 revealed an interrelation with CPB duration (Figure 3, *B* and *C*), but no significant association with the postoperative PBR values or the MFI was seen at any time point (data not shown).

DISCUSSION

In the present study, we measured the PBR to assess the integrity of the EG in children undergoing cardiac surgery and CPB. This approach is based on the observation that erythrocytes cannot access the intact EG.[13] When the barrier properties of the EG are lost as the result of glycocalyx perturbation, the PBR increases.[14,15] After surgery with CPB, we observed an immediate significant increase in the PBR in skin microvessels, indicating an acute degradation of the microvascular glycocalyx. This finding is in line with previous studies in adults[4,16] and recently in children[9] reporting increased levels of circulating EG constituents after cardiac surgery with CPB. Although these studies provide indirect evidence for glycocalyx shedding, to our knowledge this is the first study demonstrating EG perturbation on a microvascular level after surgery with CPB in children. Of note, the postoperative increase in the PBR did not differ between infants receiving CPB with and without AC. This is in apparent contrast to the study by Bruegger and colleagues,[9] in which

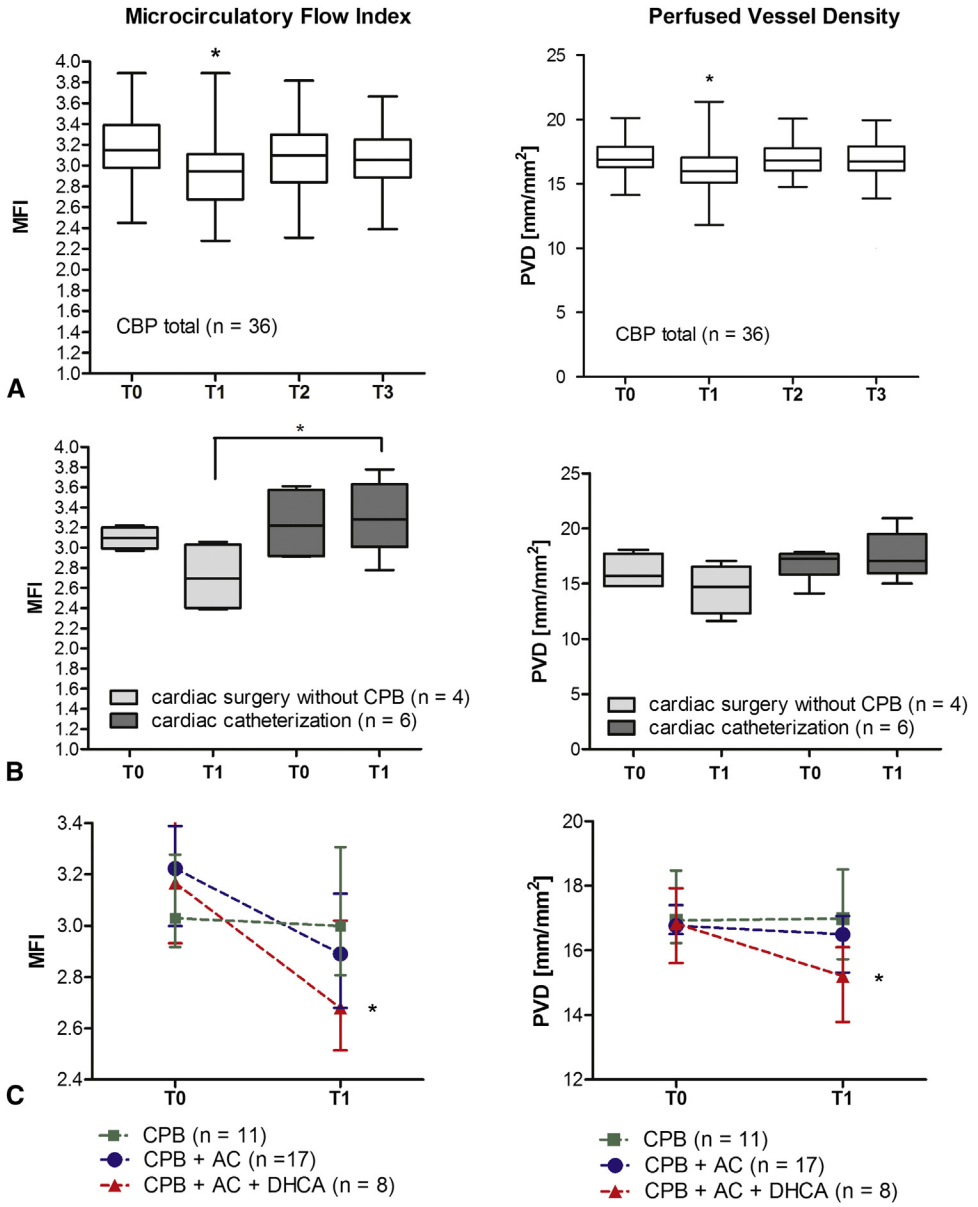

FIGURE 2. Quantification of the MFI (*left column*) and PVD (*right column*). A, Surgery with CPB. B, Control groups. C, CPB subgroup analysis. *MFI*, Microcirculatory flow index; *CPB*, cardiopulmonary bypass; *PVD*, perfused vessel density; *T0*, before surgery; *T1*, postsurgery after admission to the intensive care unit; *T2*, 24 hours postsurgery; *T3*, 7 days postsurgery; *AC*, aortic clamping; *DHCA*, deep hypothermic circulatory arrest. **P* < .05 versus T0.

the amount of shed EG constituents showed a clear correlation with the ischemic impact depending on the cardiac surgical procedure. However, while the EG constituents measured in the blood arise from the whole organism and thus may differ with the amount of organs subjected to ischemia/reperfusion, we performed our measurements at the ear, a site that was not exposed to ischemia in the CPB group or the CPB + AC group. Thus, EG shedding is not restricted to the vasculature of ischemic organs, but seems to be a general phenomenon after CPB. This raises the question why EG perturbation occurs despite the lack of ischemic stress. It seems plausible that other factors contribute to EG shedding, such as contact of the blood with foreign surfaces, altered blood flow, and manipulation of the large vessels during CPB.[17]

In addition, the surgical procedure itself may cause inflammation and EG shedding, as demonstrated in studies comparing coronary artery bypass surgery with and without CPB.[16,18,19] Because of the nature of the cardiac defects, almost all surgical procedures in infants require CPB. Therefore, it is impossible to compare the same surgery under on- and off-pump conditions to separate effects of

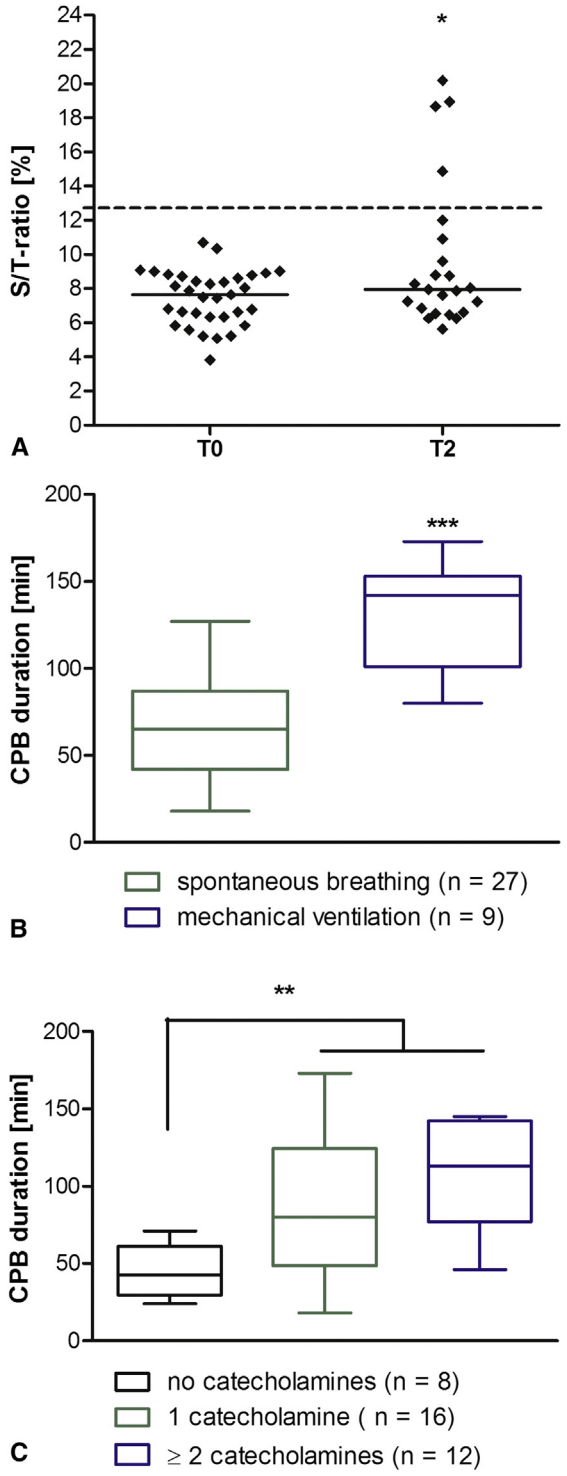

FIGURE 3. Measures of clinical outcome after CPB. A, Quantification of the S/T ratio from pre- and postoperative chest x-rays. An S/T ratio more than 12.6% indicates development of a CLS. B, Relationship between the need for mechanical ventilation at T2 and CPB duration. C, Relationship between the inotrope demand at T1 and CPB duration. *S/T*, Subcutaneous-thoracic; *T0*, before surgery; *T2*, 24 hours postsurgery; *CPB*, cardiopulmonary bypass. **P* < .05. ***P* < .01. ****P* < .001.

the surgery from those of the CPB. We were able to include data from 4 children undergoing minor open thoracic surgical procedures without CPB and did not find a significant change in the postoperative PBR compared with baseline. However, the limited group size and the different nature of the surgical procedures performed do not allow a final conclusion on the subject.

The second finding of this study was the transient perturbation of the microvascular perfusion after CPB, which was reversed 24 hours postsurgery. Although near-infrared spectroscopy is often used during pediatric cardiac surgery to monitor the cerebral oxygenation as an indirect measure of perfusion,[20] we are not aware of any study directly investigating the microcirculation. Previous studies in adults undergoing cardiac surgical procedures corroborate our results by demonstrating an acute reduction of the MFI and the proportion of perfused vessels in the sublingual microcirculation during surgery and after admission to the intensive care unit.[21,22] Of note, the CPB subgroup analysis revealed a clear dependence of the microcirculatory alterations on the ischemic stress during surgery. Accordingly, the postoperative MFI and PVD were lowest in the DHCA group, whereas both parameters remained stable in infants subjected to CPB under heartbeating conditions. This may be partially explained by differences in the body temperature, because we observed a weak although significant correlation of the PVD with postoperative temperature. However, because the MFI also varied significantly among CPB subgroups despite a missing correlation with body temperature, it is likely that other factors contribute to the perturbation of microvascular perfusion. Accordingly, distinct blood flow characteristics during surgery might significantly affect the microvascular perfusion. A pulsatile flow pattern remains in the CPB group under heartbeating conditions, whereas perfusion during AC is completely accomplished by the CPB with nonpulsatile flow. Studies comparing pulsatile versus nonpulsatile perfusion have demonstrated that the proportion of perfused vessels and the MFI were higher under pulsatile flow even after cessation of CPB.[23,24] The impact of different flow types on the microcirculation and the EG in particular should be systematically addressed in future studies, for example, by using small animal models of CPB.

We also observed a reduction in the microvascular perfusion after cardiac surgery without CPB. Possible explanations for the occurrence of microcirculatory disturbances in the absence of CPB may be the inflammatory response induced by the surgery itself, as well as blood flow disturbances during cardiac displacement.[25]

What are the clinical implications of our findings? The EG is thought to be an essential regulator of vascular permeability,[2] and degradation of the EG in animal models resulted in capillary leakage and tissue edema.[26,27]

Therefore, it is conceivable that EG shedding may promote the development of a CLS, which is characterized by generalized edema formation and organ dysfunction and contributes essentially to the morbidity and mortality of infants undergoing cardiac surgery with CPB.[6,7,28] In our patients, the rate of CLS was low overall despite the observed PBR changes. This does not necessarily rule out a causal role of EG disruption in CLS development. First, the PBR does not provide information on the total thickness of the glycocalyx. Thus, even if outer parts of the EG are shed, leading to an increase in the PBR, an inner layer may still exist and function as diffusion barrier.[29] Second, the PBR does not allow a conclusion on the composition of the EG. Studies using various enzymes to degrade the EG have demonstrated that different components of the EG contribute to permeability of the glycocalyx to a differing extent.[30] Thus, an increase in the PBR is not necessarily equivalent to an increase in permeability. Future studies should investigate whether PBR changes are more pronounced in infants with postoperative CLS compared with those without and, if so, define threshold values indicating a higher risk for CLS.

With respect to microcirculatory alteration, we and others have previously shown that a reduction in the functional small vessel density is an early predictor of sepsis in newborns,[31] and that heterogeneity of the microvascular perfusion correlated with organ dysfunction and adverse outcome in septic adults.[32] Similar findings were reported in patients with cardiogenic shock.[33] Of note, microcirculatory alterations were shown to be independent of the cardiac index and parameters of the macrocirculation.[21,22] In line with this notion, we did not find a correlation between the MFI or the PVD and systemic hemodynamic parameters, such as blood pressure or heart rate.

In view of the missing correlation with our postoperative outcome measures, the consequences of the transient decrease in the MFI and PVD after cardiac surgery are arguable. However, inotrope demand and duration of mechanical ventilation might not be the most suitable outcome measures for our methodology because they are subject to a variety of factors. In this context, the significant association of cardiac and extracardiac complications with adverse clinical outcome after pediatric cardiac surgery has recently been highlighted.[34] Thus, complications such as arrhythmias or a paralyzed diaphragm may cause higher inotrope demand and prolonged mechanical ventilation without necessarily affecting the microcirculation. Furthermore, the magnitude of microcirculatory alterations may differ between the skin and other vascular beds, such as pulmonary capillaries. Sidestream dark field imaging has recently been successfully used for intraoperative measurements of the liver microcirculation.[35] This may be an interesting future approach to directly compare the effect of CPB on the skin and lung/heart microcirculation.

Study Limitations

Our study has several limitations. First, because of the heterogeneity of the cardiac defects, we cannot exclude that conditions such as varying degrees of hypoxia or hemodynamic relevant shunts may have influenced our results. For example, a persistent ductus arteriosus may significantly alter functional vessel density.[36] Furthermore, we were able to obtain PBR values in only approximately 60% of patients with cardiac defects. Although this was true for all CPB subgroups, this may still have affected our results. Second, it remains unclear to what extent subgroup differences in age and weight, and factors related to the different surgical procedures may have influenced our findings. Finally, measurement results obtained at the ear may not be readily transferred to other organs. Yet, because investigations of the sublingual and rectal vasculature in adults undergoing CPB have generated similar results,[21,22,37] it seems likely that our findings are an expression of a generalized microcirculatory dysfunction.

CONCLUSIONS

Our study reveals local perturbations of the EG and perfusion at a microvascular level after surgery with CPB for congenital cardiac defects in infants. Microcirculatory monitoring might be a useful tool to evaluate interventions aimed at reducing bypass-related complications.

Conflict of Interest Statement

Authors have nothing to disclose with regard to commercial support.

The authors thank all the patients, parents, and medical staff for support.

References

1. Becker BF, Chappell D, Bruegger D, Annecke T, Jacob M. Therapeutic strategies targeting the endothelial glycocalyx: acute deficits, but great potential. *Cardiovasc Res*. 2010;87:300-10.
2. Pries AR, Secomb TW, Gaehtgens P. The endothelial surface layer. *Pflugers Arch*. 2000;440:653-66.
3. Schmidt EP, Yang Y, Janssen WJ, Gandjeva A, Perez MJ, Barthel L, et al. The pulmonary endothelial glycocalyx regulates neutrophil adhesion and lung injury during experimental sepsis. *Nat Med*. 2012;18:1217-23.
4. Rehm M, Bruegger D, Christ F, Conzen P, Thiel M, Jacob M, et al. Shedding of the endothelial glycocalyx in patients undergoing major vascular surgery with global and regional ischemia. *Circulation*. 2007;116:1896-906.
5. Nussbaum C, Cavalcanti Fernandes HA, Mormanova Z, Puchwein-Schwepcke AF, Bechtold-Dalla PS, Genzel-Boroviczeny O. Early microvascular changes with loss of the glycocalyx in children with type 1 diabetes. *J Pediatr*. 2013;164:584-9.
6. Kubicki R, Grohmann J, Siepe M, Benk C, Humburger F, Rensing-Ehl A, et al. Early prediction of capillary leak syndrome in infants after cardiopulmonary bypass. *Eur J Cardiothorac Surg*. 2013;44:275-81.
7. Stiller B, Sonntag J, Dahnert I, Alexi-Meskishvili V, Hetzer R, Fischer T, et al. Capillary leak syndrome in children who undergo cardiopulmonary bypass: clinical outcome in comparison with complement activation and C1 inhibitor. *Intensive Care Med*. 2001;27:193-200.
8. Ignjatovic V, Than J, Summerhayes R, Newall F, Horton S, Cochrane A, et al. The quantitative and qualitative responses of platelets in pediatric patients undergoing cardiopulmonary bypass surgery. *Pediatr Cardiol*. 2012;33:55-9.

9. Bruegger D, Brettner F, Rossberg I, Nussbaum C, Kowalski C, Januszewska K, et al. Acute degradation of the endothelial glycocalyx in infants undergoing cardiac surgical procedures. *Ann Thorac Surg*. 2015;99:926-31.
10. Sonntag J, Grunert U, Stover B, Obladen M. [The clinical relevance of subcutaneous-thoracic ratio in preterm newborns as a possibility for quantification of capillary leak syndrome]. *Z Geburtshilfe Neonatol*. 2003;207:208-12.
11. Lee DH, Dane MJ, van den Berg BM, Boels MG, van Teeffelen JW, de MR, et al. Deeper penetration of erythrocytes into the endothelial glycocalyx is associated with impaired microvascular perfusion. *PLoS One*. 2014;9:e96477.
12. Boerma EC, Mathura KR, van der Voort PH, Spronk PE, Ince C. Quantifying bedside-derived imaging of microcirculatory abnormalities in septic patients: a prospective validation study. *Crit Care*. 2005;9:R601-6.
13. Vink H, Duling BR. Identification of distinct luminal domains for macromolecules, erythrocytes, and leukocytes within mammalian capillaries. *Circ Res*. 1996;79:581-9.
14. Dane MJ, Khairoun M, Lee DH, van den Berg BM, Eskens BJ, Boels MG, et al. Association of kidney function with changes in the endothelial surface layer. *Clin J Am Soc Nephrol*. 2014;9:698-704.
15. Eskens BJ, Mooij HL, Cleutjens JP, Roos JM, Cobelens JE, Vink H, et al. Rapid insulin-mediated increase in microvascular glycocalyx accessibility in skeletal muscle may contribute to insulin-mediated glucose disposal in rats. *PLoS One*. 2013;8:e55399.
16. Bruegger D, Schwartz L, Chappell D, Jacob M, Rehm M, Vogeser M, et al. Release of atrial natriuretic peptide precedes shedding of the endothelial glycocalyx equally in patients undergoing on- and off-pump coronary artery bypass surgery. *Basic Res Cardiol*. 2011;106:1111-21.
17. Murphy GJ, Angelini GD. Side effects of cardiopulmonary bypass: what is the reality? *J Card Surg*. 2004;19:481-8.
18. Svennevig K, Hoel T, Thiara A, Kolset S, Castelheim A, Mollnes T, et al. Syndecan-1 plasma levels during coronary artery bypass surgery with and without cardiopulmonary bypass. *Perfusion*. 2008;23:165-71.
19. Bruegger D, Rehm M, Abicht J, Paul JO, Stoeckelhuber M, Pfirrmann M, et al. Shedding of the endothelial glycocalyx during cardiac surgery: on-pump versus off-pump coronary artery bypass graft surgery. *J Thorac Cardiovasc Surg*. 2009;138:1445-7.
20. Haydin S, Onan B, Onan IS, Ozturk E, Iyigun M, Yeniterzi M, et al. Cerebral perfusion during cardiopulmonary bypass in children: correlations between near-infrared spectroscopy, temperature, lactate, pump flow, and blood pressure. *Artif Organs*. 2013;37:87-91.
21. De Backer D, Dubois MJ, Schmartz D, Koch M, Ducart A, Barvais L, et al. Microcirculatory alterations in cardiac surgery: effects of cardiopulmonary bypass and anesthesia. *Ann Thorac Surg*. 2009;88:1396-403.
22. Koning NJ, Vonk AB, Meesters MI, Oomens T, Verkaik M, Jansen EK, et al. Microcirculatory perfusion is preserved during off-pump but not on-pump cardiac surgery. *J Cardiothorac Vasc Anesth*. 2014;28:336-41.
23. Koning NJ, Vonk AB, van Barneveld LJ, Beishuizen A, Atasever B, van den Brom CE, et al. Pulsatile flow during cardiopulmonary bypass preserves postoperative microcirculatory perfusion irrespective of systemic hemodynamics. *J Appl Physiol (1985)*. 2012;112:1727-34.
24. O'Neil MP, Fleming JC, Badhwar A, Guo LR. Pulsatile versus nonpulsatile flow during cardiopulmonary bypass: microcirculatory and systemic effects. *Ann Thorac Surg*. 2012;94:2046-53.
25. Atasever B, Boer C, Speekenbrink R, Seyffert J, Goedhart P, de MB, et al. Cardiac displacement during off-pump coronary artery bypass grafting surgery: effect on sublingual microcirculation and cerebral oxygenation. *Interact Cardiovasc Thorac Surg*. 2011;13:573-7.
26. Bruegger D, Rehm M, Jacob M, Chappell D, Stoeckelhuber M, Welsch U, et al. Exogenous nitric oxide requires an endothelial glycocalyx to prevent postischemic coronary vascular leak in guinea pig hearts. *Crit Care*. 2008;12:R73.
27. van den Berg BM, Vink H, Spaan JA. The endothelial glycocalyx protects against myocardial edema. *Circ Res*. 2003;92:592-4.
28. Seghaye MC, Grabitz RG, Duchateau J, Busse S, Dabritz S, Koch D, et al. Inflammatory reaction and capillary leak syndrome related to cardiopulmonary bypass in neonates undergoing cardiac operations. *J Thorac Cardiovasc Surg*. 1996;112:687-97.
29. Curry FE, Adamson RH. Endothelial glycocalyx: permeability barrier and mechanosensor. *Ann Biomed Eng*. 2012;40:828-39.
30. Gao L, Lipowsky HH. Composition of the endothelial glycocalyx and its relation to its thickness and diffusion of small solutes. *Microvasc Res*. 2010;80:394-401.
31. Weidlich K, Kroth J, Nussbaum C, Hiedl S, Bauer A, Christ F, et al. Changes in microcirculation as early markers for infection in preterm infants–an observational prospective study. *Pediatr Res*. 2009;66:461-5.
32. Trzeciak S, Dellinger RP, Parrillo JE, Guglielmi M, Bajaj J, Abate NL, et al. Early microcirculatory perfusion derangements in patients with severe sepsis and septic shock: relationship to hemodynamics, oxygen transport, and survival. *Ann Emerg Med*. 2007;49:88-98.
33. De BD, Creteur J, Dubois MJ, Sakr Y, Vincent JL. Microvascular alterations in patients with acute severe heart failure and cardiogenic shock. *Am Heart J*. 2004;147:91-9.
34. Agarwal HS, Wolfram KB, Saville BR, Donahue BS, Bichell DP. Postoperative complications and association with outcomes in pediatric cardiac surgery. *J Thorac Cardiovasc Surg*. 2014;148:609-16.
35. Nilsson J, Eriksson S, Blind PJ, Rissler P, Sturesson C. Microcirculation changes during liver resection–a clinical study. *Microvasc Res*. 2014;94:47-51.
36. Hiedl S, Schwepcke A, Weber F, Genzel-Boroviczeny O. Microcirculation in preterm infants: profound effects of patent ductus arteriosus. *J Pediatr*. 2010;156:191-6.
37. Kiessling AH, Reyher C, Philipp M, Beiras-Fernandez A, Moritz A. Real-time measurement of rectal mucosal microcirculation during cardiopulmonary bypass. *J Cardiothorac Vasc Anesth*. 2015;29:89-94.

Key Words: endothelial glycocalyx, microcirculation, cardiopulmonary bypass, infants, SDF, congenital cardiac defects

CHD

TABLE E1. Overview of cardiac diagnoses and surgical procedures

Patient	Cardiac diagnosis	Surgical procedure	Comment
01	TGA, CoA, ASD, VSD, PDA	Arterial switch operation, CoA resection, ASD/VSD closure, PDA ligation	
02	ASD, VSD, PDA	ASD/VSD closure, PDA ligation	
03	HLHS (s/p Norwood)	Bidirectional Glenn operation	
04	Double-chambered right ventricle, VSD	Resection of fibromuscular tissue, VSD closure	
05	VSD, Trisomy 21	VSD closure	
06	Criss-cross heart, TGA, PA, ASD, VSD (s/p Glenn)	Fontan operation	
07	IAA, VSD, ASD, PDA	Reconstruction of aortic arch, PDA ligation, PA banding	
08	TAPVR, ASD, PDA	Correction of TAPVR, ASD closure	
09	HRHS, ASD, VSD (s/p Glenn)	Fontan operation	
10	HLHS (s/p Glenn)	Fontan operation	
11	Heterotaxy, common inlet DORV, PS, APVR, ASD	Bidirectional Glenn operation	
12	Sinus venosus ASD	Sinus venosus ASD closure	
13	TOF	Complete correction of TOF	
14	Dextrocardia, TA, PS, ASD, VSD	Modified Blalock–Taussig shunt	Surgery without CPB
15	HLHS (s/p Fontan)	Glenn operation	
16	AVSD	AVSD closure	
17	HLHS (s/p Norwood)	Bidirectional Glenn operation	
18	DORV, hypoplastic LV, MA, LSVC	Atrioseptectomy, PA banding	
19	HLHS, CoA (s/p Fontan and CoA dilation), re-CoA	Stent implantation into aortic isthmus in hybrid technique	Surgery without CPB
20	DORV, ASD, VSD, LSVC	RVOT reconstruction, ASD/VSD closure	
21	AVSD, Trisomy 21	AVSD correction	
22	AVSD, Trisomy 21	AVSD correction	
23	HLHS (s/p Glenn)	Fontan operation	
24	HLHS (s/p Glenn)	Fontan operation	
25	HLHS (s/p Norwood)	Bidirectional Glenn operation	
26	DORV, ASD, VSD	RVOT reconstruction, ASD/VSD closure	
27	AVSD	AVSD correction	
28	IAA, VSD, ASD,	Reconstruction of aortic arch, ASD/VSD closure	
29	HRHS	Glenn operation	
30	VSD	VSD closure	
31	HLHS, ASD	Bilateral PA banding	Surgery without CPB
32	CoA	Resection of CoA, end-to-end anastomosis	Surgery without CPB
33	TGA, ASD, PDA	Arterial switch operation, ASD closure, PDA ligation	
34	TOF	Complete correction of TOF	
35	TA, ASD, VSD (s/p PA banding)	Glenn operation	
36	HLHS (s/p Glenn), Tricuspid insufficiency	Reconstruction of tricuspid valve	
37	PA, VSD (s/p modified Blalock-Taussig-Shunt)	Reconstruction of RVOT, VSD closure	
38	TGA, ASD, PDA	Arterial switch operation, ASD closure, PDA ligation	
39	HLHS (s/p Norwood)	Bidirectional Glenn operation	
40	HLHS	Norwood operation	

TGA, Transposition of the great arteries; *CoA*, coarctation of the aorta; *ASD*, atrial septal defect; *VSD*, ventricular septal defect; *PDA*, persistent ductus arteriosus; *HLHS/HRHS*, hypoplastic left/right heart syndrome; *s/p*, status post; *PA*, pulmonary artery; *IAA*, interrupted aortic arch; *TAPVR*, total anomalous pulmonary venous return; *DORV*, double outlet right ventricle; *PS*, pulmonary stenosis; *APVR*, anomalous pulmonary venous return; *TOF*, tetralogy of Fallot; *TA*, tricuspid atresia; *CPB*, cardiopulmonary bypass; *AVSD*, atrioventricular septal defect; *LV*, left ventricle; *MA*, mitral valve atresia; *LSVC*, left superior vena cava; *RVOT*, right ventricular outflow tract.

ANTIOXIDANTS & REDOX SIGNALING
Volume 18, Number 6, 2013

DOI: 10.1089/ars.2012.4783

Discoveries

FORUM REVIEW ARTICLE

Myeloperoxidase: A Leukocyte-Derived Protagonist of Inflammation and Cardiovascular Disease

Claudia Nussbaum,[1,*] Anna Klinke,[2,*] Matti Adam,[2] Stephan Baldus,[2] and Markus Sperandio[1]

Abstract

Significance: The heme-enzyme myeloperoxidase (MPO) is one of the major neutrophil bactericidal proteins and is stored in large amounts inside azurophilic granules of neutrophils. Upon cell activation, MPO is released and extracellular MPO has been detected in a wide range of acute and chronic inflammatory conditions. ***Recent Advances and Critical Issues:*** Apart from its role during infection, MPO has emerged as a critical modulator of inflammation throughout the last decade and is currently discussed in the initiation and propagation of cardiovascular diseases. MPO-derived oxidants (*e.g.,* hypochlorous acid) interfere with various cell functions and contribute to tissue injury. Recent data also suggest that MPO itself exerts proinflammatory properties independent of its catalytic activity. Despite advances in unraveling the complex action of MPO and MPO-derived oxidants, further research is warranted to determine the precise nature and biological role of MPO in inflammation. ***Future Directions:*** The identification of MPO as a central player in inflammation renders this enzyme an attractive prognostic biomarker and a potential target for therapeutic interventions. A better understanding of the (patho-) physiology of MPO is essential for the development of successful treatment strategies in acute and chronic inflammatory diseases. *Antioxid. Redox Signal*. 18, 692–713.

Introduction

The recruitment of leukocytes from the vasculature into the surrounding tissue is a hallmark of inflammation (131). Among the first cells to be recruited are polymorphonuclear neutrophils (PMN) (238). These cells are powerful members of the innate immune system and do not only have an impressive capacity to generate highly reactive oxidants, but also contain an armament of potent antimicrobial proteins that are stored in several specific intracellular granules. One of the major neutrophil effector proteins is the heme-enzyme myeloperoxidase (MPO), which is stored in large amounts inside azurophilic granules and released into the phagosome after phagocytic uptake of pathogens (109). Furthermore, MPO is also liberated upon cell activation and the extracellular MPO was detected in a broad spectrum of inflammatory diseases (224). Since its first description in 1941 by Agner (3), MPO has long been appreciated mainly for its role in the killing of phagocytosed bacteria and other pathogens (108). However, in light of the mostly subclinical phenotype of MPO deficiency, this concept was challenged and expanded by the increasing perception that MPO is functionally involved in the pathogenesis and regulation of various inflammatory conditions (154). Many of these conditions can be directly or indirectly linked to the enzymatic action of MPO. Yet, more recent data strongly suggest that MPO also exerts immunomodulatory functions that are independent of its catalytic properties (111, 121). This review is aimed at summarizing current concepts on the role of MPO in inflammation, with respect to basic mechanisms and selected clinical correlates, which will be a valuable addendum to previous reviews on this topic (11, 82, 109, 120, 154, 224). Figure 1 provides a schematic overview of the diverse effects of MPO on the various cell types in inflammation.

Characteristics of MPO

Origin and generation

The enzyme MPO belongs to the family of chordata heme peroxidases, a subgroup of the peroxidase–cyclooxygenase family (241). The generation and post-translational processing of MPO has been the subject of intensive research throughout the last decades as reviewed in (67, 78). Expression of MPO is restricted to the myeloid lineage of hematopoietic cells, where

[1]Walter Brendel Centre for Experimental Medicine, Ludwig-Maximilians-University Munich, Munich, Germany.
[2]Department of General and Interventional Cardiology, University Heart Center Hamburg, Cardiovascular Research Center, University Hospital Eppendorf, Hamburg, Germany.
*These two authors contributed equally to this work.

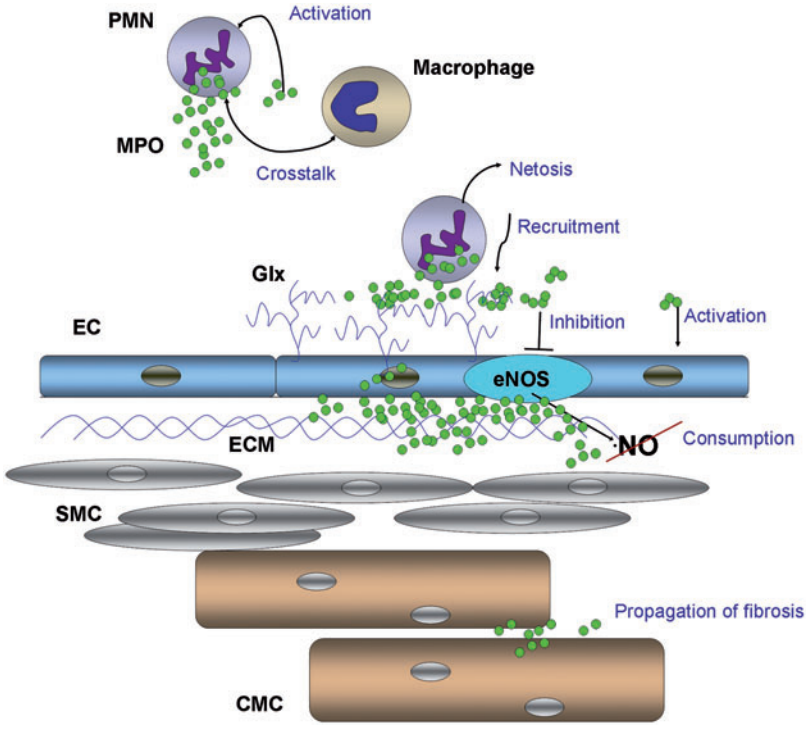

FIG. 1. Schematic overview of the diverse effects of MPO in inflammation. MPO modulates the activation state of PMN, macrophages, and ECs, participates in neutrophil extracellular trap formation and PMN recruitment, leads to the inhibition of eNOS, mediates $NO^{\bullet}$ consumption, alters ECM proteins, and contributes to the propagation of myocardial fibrosis. (To see this illustration in color, the reader is referred to the web version of this article at www.liebertpub.com/ars.) CMC, cardiomyocyte; EC, endothelial cell; ECM, extracellular matrix; eNOS, endothelial NO-synthase; Glx, glycocalyx; MPO, myeloperoxidase; $NO^{\bullet}$, nitric oxide; PMN, polymorphonuclear neutrophil; SMC, smooth muscle cell.

it is mainly found in PMN and in monocytes. MPO is actively synthesized at the promyelocytic stage, while its expression ceases with advancing cell differentiation (16, 214). The primary translation product, an 80-kDa protein (preproMPO), undergoes a complex series of post-translational modifications during its maturation process (67). These include (i) removal of a signal peptide and incorporation of high mannose oligosaccharide side chains to form apoproMPO (153, 155), (ii) insertion of a heme group yielding the catalytically active proMPO (12), and (iii) cleavage of the amino-terminal 125 amino acid propetide as well as a 6 amino acid sequence separating the heavy and the light chain of the final enzyme (5, 34). In mature neutrophils, MPO is stored in vast amounts inside peroxidase-positive granules also known as azurophilic granules, where it accounts for almost 7% of the total neutrophil dry mass equivalent to a concentration of nearly 10×10^{-6} μg/cell (190). Monocytes were shown to possess around one third of the MPO content found in neutrophils (27). Although MPO expression is usually lost during differentiation of monocytes into tissue macrophages (133), it can persist or be reinduced under certain circumstances as demonstrated in atherosclerosis (201, 209) and neurodegenerative diseases (39, 125). Moreover, MPO was demonstrated in astrocytes (136) and in neurons in the brain (37, 71). Notably, species differences must be taken into account when investigating the role of MPO in human biology. Avian neutrophils, for example, do not express MPO (172). This is especially relevant for differences between mice and humans, as murine knockout models are a common tool to investigate the involvement of MPO in distinct physiological and pathophysiological processes *in vivo*. The MPO content of murine neutrophils is only about 15% of human neutrophils (172). Furthermore, the MPO gene was found to be differentially expressed in mice and humans (142). These differences limit the transferability of data from animal studies and may explain some of the discrepancies found between mice and men reported later on in the review.

Structure

The three-dimensional structure of mature MPO consists of two identical protomers, which are covalently linked by a single disulfide bridge at Cys^{153} forming a 140-kDa homodimer (64, 244). Each half is made up of a heavy 58.5-kDa alpha chain (466 aa) and a light 14.5-kDa beta chain (108 aa) and contains a functional heme group and a calcium-binding site important for the correct interaction of both chains (26). The heavy chain includes five possible sites for N-linked glycosylation (Asn 157, 189, 225, 317, and 563), which were shown to be all occupied by high mannose type glycans in the human MPO (173, 220). Deglycosylation of MPO resulted in a significant reduction in the chlorinating activity as well as in low-density lipoprotein (LDL) oxidation and MPO-induced reactive oxygen species (ROS) production demonstrating the importance of glycosylation for the enzymatic function. Due to the large number of arginine and lysine residues, MPO is a strongly basic protein (IP > 10), and thus highly cationic at physiological pH (109).

The secondary structure of MPO is mostly alpha helical with the central heme-containing core being formed by four helices of the heavy chain and the carboxyl-terminal helix of the light chain. The remainder of the small chain spans around the surface of the molecule, while the heavy chain folds into four separate domains and one single open loop surrounding the central core (64, 244). A unique characteristic of MPO is its binding of the heme-group, which is a derivative of protoporphyrin IX (63, 210). The methyl groups of the A and C pyrrole rings are modified to allow formation of ester linkages with the protein residues Glu^{242} of the heavy and Asp^{94} of the light chain (113). In addition, a third link is found between the sulfur atom of Met^{243} and the β-carbon of the vinyl group on

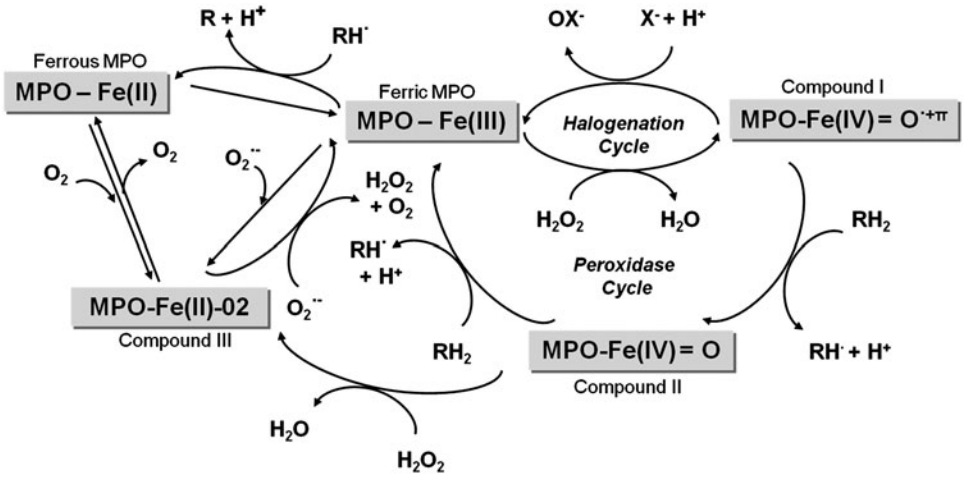

FIG. 2. Schematic overview of MPO's catalytic activity. Native ferric MPO reacts with H_2O_2 to form compound I, which can be reduced back to native MPO either by a two-electron transfer in the Halogenation Cycle generating highly reactive hypohalous acid or by two separate single-electron transfers in the Peroxidase Cycle *via* formation of the redox intermediate compound II. Two further redox states of MPO exist outside the catalytic cycles, namely, ferrous MPO, which is generated by the reaction of ferric MPO with reducing radicals formed in the peroxidase cycle, and compound III, a ferrous dioxy intermediate generated by reaction of ferrous MPO with dioxygen, ferric MPO with superoxide anion or compound II with H_2O_2. Compound III can act as superoxid dismutase reducing $O_2^{\bullet -}$ to H_2O_2 and O_2. H_2O_2, hydrogen peroxide; $O_2^{\bullet -}$, superoxide anion; O_2, dioxygen; OX^-, hypo (pseudo-)halous acid (*e.g.*, hypochlorous or hypobromous acid); $RH^{\bullet}$, substrate radical; RH_2, oxidizable substrate; X^-, (pseudo-) halide (*e.g.*, chloride, bromide).

the pyrrole ring A. This sulfonium–ion link seems to be responsible for the particular spectral properties of MPO leading to its characteristic green color (112).

Catalytic activity

The enzymatic activity profile of MPO is highly complex with a multitude of reactive intermediates and feasible substrates being identified throughout the last years. In view of the multitude of reaction partners of MPO described in the literature, one should bear in mind that not all reactions that are possible *in vitro* actually happen *in vivo* or are of biological relevance. The following section will provide a brief overview of the principal catalytic mechanism of MPO and some of its intermediates that play a role in modulating cellular functions described later on (for a comprehensive review the reader is also referred to (49, 67, 109).

The complete MPO system consists of the enzyme MPO, hydrogen peroxide (H_2O_2), generated during the respiratory burst by dismutation of superoxide anion ($O_2^{\bullet -}$), and oxidizable substrates (120). In general, MPO-catalyzed reactions can be divided into a so-called halogenation cycle and a peroxidase cycle (Fig. 2) (49). The primary reaction common to both cycles is the reduction of H_2O_2 to water by MPO in its native state containing ferric iron [MPO-Fe(III)]. This leads to the formation of a short-lived redox intermediate termed compound I, which contains an oxyferryl heme and a porphyrin π-cation radical (MPO-Fe(IV) = $O^{\bullet +\pi}$) (72, 140). In the halogenation cycle, ferric MPO is regenerated by reduction of compound I *via* a two-electron oxidation of halides (*e.g.*, chloride, bromide, and iodide) or pseudohalides (thiocyanate), resulting in the formation of their respective hypo(pseudo-)halous acid (43, 198, 222). The amount and kinetics of this reaction are dependent on the substrate availability and the local pH (25, 66, 198) and were shown to be significantly increased at acidic environment (89, 90, 243). Under physiological conditions, chloride and thiocyanate serve as the major substrates for compound I in the halogenation cycle resulting in the generation of the highly reactive intermediates, hypochlorous acid (HOCl) and hypothiocyanous acid (HOSCN) (222).

Host defense and MPO in the phagosome

The contribution of the MPO-H_2O_2-halide system to pathogen killing has been the subject of research for more than four decades and remains a matter of ongoing debate especially in the face of the mostly nonovert clinical phenotype of MPO-deficiency in humans (8, 108, 130, 162, 181, 237).

Despite evidence for a decreased killing activity of MPO-deficient neutrophils *in vitro* and a higher susceptibility of MPO knockout mice toward certain pathogens (9, 10), infectious complications in individuals displaying MPO deficiency are generally rare (119). This is in sharp contrast to subjects suffering from chronic granulomatous disease, where inactivity of the superoxide generating nicotinamide adenine dinucleotide phosphate (NADPH) oxidase of leukocytes leads to a markedly increased susceptibility for life-threatening infections (192). One possible explanation for this discrepancy may be the higher than normal levels of $O_2^{\bullet -}$ and H_2O_2 found in MPO-deficient human neutrophils (156, 180) together with an increased capacity for phagocytosis (200) and degranulation (55). However, these rather mild differences to native neutrophils have been doubted to compensate for the lack of MPO, in particular, as they have not been found in murine PMN. Furthermore, the generation of peroxynitrite from $O_2^{\bullet -}$ and $NO^{\bullet}$ has been suggested to be a backup mechanism of MPO-deficiency (77).

To elucidate the role of MPO for pathogen killing more profoundly, multiple efforts have been undertaken to disclose reactions taking place inside the phagosome: Upon invagination of a microbe, MPO is released into the phagosome up

to a concentration of about 1 m*M* (237). As MPO binds effectively to the microbial surface due to its cationic charge, it can generate oxidants in close proximity to the pathogen (109). The first direct proof of HOCl-production inside the phagosome upon ingestion of bacteria has been obtained by labeling the proteins of *Staphylococcus aureus* with [$^{13}C_6$] and identifying corresponding chlorinated isotopes after phagocytosis (41). Others had investigated the chlorination of fluorescein, which has been conjugated to microspheres before phagocytosis. Here, the authors estimated HOCl-production inside the phagosome to be sufficient for bacterial killing (94). Interestingly, no nitration of the phenolic structures of fluorescein took place even with high concentrations of nitrite. The yield of HOCl and the balance between MPO's chlorinating and peroxidase activity depends—among others—on chloride availability and pH, with acidic pH favoring chlorination (229). With the beginning of the respiratory burst, the oxidation of NADPH leads to acidification of the phagosomal cytoplasm, with a subsequent transient increase in pH due to dismutation of superoxide, which consumes H^+. Thereupon, several mechanisms occur, which level the acidity around pH 6 (77), an important determinant for HOCl production. In acidic pH, HOCl is then in equilibrium with molecular chlorine ($HOCl + Cl^- + H^+ \Leftrightarrow Cl_2 + H_2O$), which has been suggested to be the major agent of 3-chlorotyrosine (3-Cl-Tyr) synthesis (84). Using a kinetic model of reactions inside the phagosome, Winterbourn and coworkers calculated that HOCl is produced at a constant rate of 134 mmol/(l × min) (based on an estimated phagosome volume of 1.2 μl), even at neutral pH (237). While 1–5 μM HOCl has been shown to be rapidly lethal on *S. aureus* and *E. coli in vitro*, even 1 m*M* of HOCl had no lethal effects in the presence of granule proteins in phagosomal concentrations (176). Consequently, the importance of the MPO-H_2O_2-halide system for pathogen killing remained questionable. Investigations of the primary targets of MPO-driven oxidation in phagocytosing neutrophils revealed that, for the most part, proteins of the host cell were oxidized, whereas the ingested bacteria were hardly affected.

Based on these findings and on the observation that the bactericidal effect of H_2O_2 on cultured bacteria was found to be prevented in the presence of MPO, an alternative role for MPO was proposed, in which MPO acts as a catalase in the presence of high levels of H_2O_2 and protects microbicidal proteins against oxidative damage, thereby preserving their function (175, 176). This concept was recently challenged by Winterbourn *et al.* (237), who estimated the concentration of H_2O_2 inside the phagosome to be much lower than previously assumed and suggested that the catalase activity of MPO is minor in the presence of chloride. Furthermore, instead of protection against oxidative damage, MPO was shown to promote inactivation of microbicidal proteins and proteases present in neutrophils, such as neutrophil elastase (NE), cathepsin G, and lysozyme (87, 228, 230). In turn, activity of these proteins may be increased in MPO deficiency and could compensate for the loss of MPO (87), possibly contributing to the mild phenotype of MPO deficiency.

Extrabactericidal activity

In recent years, growing evidence supports a role of MPO and its intermediates in inflammatory events independent of its role in innate immune defense (88, 154). HOCl, as a highly potent oxidant, was shown to react avidly with a multitude of molecules, such as thiols and thioether groups, tyrosyl residues, amines and amides, sulfides, free fatty acids, and phenols (79, 234, 235). Biological targets of HOCl- and HOSCN-driven oxidation and chlorination include DNA (69), intracellular-signaling proteins (118, 146), heme proteins (135, 204), lipoproteins and cholesterol (22, 165, 233), plasma proteins (165, 166), glycoproteins (174), and many more. The reaction of HOCl with amino acid residues can cause changes in the tertiary structure of the target protein, and thereby influence its activity or processing. This leads to tissue damage by altering cell signaling, cell growth, protein expression, apoptosis, and other important cellular functions and has been linked to the pathogenesis of various inflammatory diseases (*e.g.*, atherosclerosis, COPD, malignancy as reviewed in (50, 82, 224). In this context, the formation of 3-Cl-Tyr or 3,5-dichlorotyrosine (3,5-diCl-Tyr) by HOCl or by chloramines, a long-lived redox intermediate generated by the reaction of HOCl with amines, is not only used as a classical marker of MPO activity, but also discussed for its contribution to the inflammatory process (44, 46, 99, 102).

As an alternative to the oxidation of halides, ferric MPO can be regenerated in the peroxidase cycle by oxidization of a large variety of organic and anorganic substrates, including aromatic amino acids, phenol- and indole derivatives, ascorbate, urate, and others (4, 139, 143, 197, 212, 240). First, compound I is reduced by a single-electron transfer to yield compound II [MPO-Fe(IV) = O], which has lost the porphyrin π-cation radical and is unable to react with halides (67). In a second single-electron transfer, compound II is further reduced to native ferric MPO. This second-rate limiting step can be enhanced by natural reductants, such as ascorbate and $O_2^{\bullet -}$, thereby regulating the balance between the peroxidase and the halogenation cycle (104, 140).

The consumption of nitric oxide ($NO^\bullet$), another substrate for MPO-driven oxidation, and the concomitant generation of reactive nitrogen intermediates has been shown to be of high relevance in human biology (1, 19, 42, 57). $NO^\bullet$ is oxidized either directly by compound I or—at physiological concentrations—more likely by reactive intermediates generated in the peroxidase cycle. In this context, reaction of nitric oxide with tyrosyl- and ascorbyl radicals was proposed to be the major mechanism leading to $NO^\bullet$ consumption (57). The reaction intermediate nitrosonium cation (NO^+) is rapidly hydrolyzed to nitrite (NO_2^-), which was detected in high concentrations in various tissues and fluids during inflammation (62, 215, 225). Furthermore, it was suggested that $NO^\bullet$ directly reacts with compound II and contributes to the turnover of MPO in the peroxidase cycle (1). However, $NO^\bullet$ (standard reduction potential $NO^+/NO^\bullet$: 1.22 V) is unlikely to reduce compound II (standard reduction potential compound II/ferric MPO 0.97 V), because its reduction potential is too high (65).

In the presence of MPO and H_2O_2, nitrite is further oxidized by compound I to generate nitrogen dioxide ($NO_2^\bullet$), a highly unstable radical that avidly promotes protein nitration and lipid peroxidation (58, 85, 188, 223, 225). This reaction takes place even in the presence of physiological concentrations of chloride and is favored at acidic pH (35, 186). Nitrotyrosine (NO_2-Tyr), one of the major products of NO_2^- driven oxidation has long been established as an inducer of oxidative stress and is increasingly recognized as a pathophysiological contributor to inflammation (171). Yet, it cannot be generalized

from these data that protein nitration takes place wherever $NO^{\bullet}$ and MPO are present *in vivo*. This is, for example, demonstrated by Hurst and coworkers, who were unable to detect any evidence for nitration reactions inside the phagosome (95).

Modulation and inactivation of MPO

Apart from the previously described forms of MPO, two further redox states exist, which do not participate actively in the halogenation or the peroxidase cycle, but are nonetheless important as their turnover critically regulates MPO catalytic activity (Fig. 2). These forms are ferrous MPO [MPO-Fe(II)], which is continuously formed inside the phagosome, and compound III [MPO-Fe(II)-02], a ferrous dioxy intermediate, which is generated through reaction of (i) ferric MPO with superoxide, (ii) ferrous MPO with oxygen or (iii) ferrous MPO with H_2O_2 *via* compound II (65, 92, 103). According to these reactions, the formation of compound III seems favorable in the presence of O_2, $O_2^{\bullet -}$ and H_2O_2 (92, 234, 237) and its presence was spectroscopically demonstrated inside activated neutrophils (236). The relative concentration of superoxide, oxygen, and H_2O_2 will thus modify the catalytic activity of MPO and determine the amount of reactive intermediates produced.

$O_2^{\bullet -}$, which is produced at a high rate during the respiratory burst inside the phagosome (237), rapidly reacts with ferric MPO to form inactive compound III (103). It was calculated that the majority of $O_2^{\bullet -}$ consumption in the phagosome happens through interaction with MPO (237). In turn, compound III can act as $O_2^{\bullet -}$ dismutase regenerating ferric MPO. However, at physiologically relevant pH values between 6.0 and 8.0 in the early phagosome (175), turnover of compound III is mainly sustained by its dissociation to ferrous MPO and oxygen rather than its conversion to ferric MPO (92) (Fig. 2). Superoxide can also serve as an alternative substrate for compound I and II, thereby influencing the turnover in the peroxidase cycle. In this context, $O_2^{\bullet -}$ was found to prevent the accumulation of compound II by accelerating the regeneration of ferric MPO, and thus maintaining production of HOCl (104).

H_2O_2 can modify MPO activity in several ways. Ferrous MPO is directly converted to compound II by excess H_2O_2. This allows MPO to re-enter the active catalytic cycle and restore chlorinating activity (65). On the other hand, H_2O_2 can compete with other substrates as an electron donor for compound I and II. However, these reactions seem unfavored inside the phagosome (237). The affinity of MPO toward H_2O_2 is altered by binding of small molecules to the heme iron of MPO. These molecules include $NO^{\bullet}$, NO_2^-, hydrocyanic acid (HCN) (1, 138), and carbon monoxide, as recently demonstrated (150). Binding of these molecules leads to the formation of a stable low-spin complex, which lacks the free position of the hexacoordinated heme iron essential for H_2O_2 ligation. Variations in local pH and availability of competing substrates further determine the extent of these interactions and make it difficult to conclude on their *in vivo* relevance. The effect of $NO^{\bullet}$ binding to MPO *in vitro* was shown to be concentration dependent with low amounts of $NO^{\bullet}$ enhancing peroxidation of substrate, whereas high amounts have an irreversible inhibitory effect through formation of the respective low-spin six coordinate Fe(III)-nitrosyl complex (1). This could become relevant under inflammatory conditions, where high local concentrations of $NO^{\bullet}$ may be present (225), though the *in vivo* significance of this inhibitory mechanism remains unclear.

Similarly, SCN^- was shown to function as both, substrate or inhibitor of MPO (205). As suggested by Abu-Soud and colleagues, this involves two distinct binding sites (169). At lower concentrations ($< 60\ \mu M$), SCN^- binds to a distal cavity of compound I (substrate site) and is readily converted to hypothiocyanate. At higher concentrations, SCN^- additionally occupies a proximal helix site, leading to formation of an inactive Fe(III)-SCN complex. This can considerably restrict H_2O_2 access *in vitro*, however, it is not established whether formation of such a complex takes place at normal SCN^- plasma levels *in vivo*. Moreover, $OSCN^-$ formed by oxidation of SCN^- in the halogenation cycle can limit the activity of MPO by promoting accumulation of compound II (221).

Trapping of MPO as compound II is the inhibitory mechanism of many endogenous and exogenous compounds as demonstrated for nonsteroidal anti-inflammatory drugs (158), nitroxides (170), indole, and tryptamine derivatives (93). These compounds can be readily oxidized by compound I, but are a poor substrate for compound II, thereby halting the peroxidase cycle and limiting the availability of active MPO. However, due to the presence of natural reductants, such as ascorbate, urate, and $O_2^{\bullet -}$, the effect of these reversible inhibitors *in vivo* is limited.

Finally, a number of so-called suicide substrates have been identified, which irreversibly inhibit MPO activity by promoting heme destruction. These include, for example, the hydrazide isoniazid, 4-aminobenzoic acid hydrazide (4-ABAH), and the thyreostatic drug propylthiouracil (36, 226). Just recently, 2-thioxanthines were also shown to effectively suppress HOCl generation *in vitro* and *in vivo* by irreversible inhibition of MPO (211).

Modulation of Leukocyte Functions

Leukocyte recruitment

One of the central mechanisms in inflammation is the recruitment of leukocytes from the vasculature into the surrounding tissue. This process follows a well-defined cascade of events and is orchestrated by a complex interplay of adhesion molecules, cell surface receptors, and chemokines (131). The initial capture and rolling of circulating leukocytes along the inflamed endothelium are mediated by selectins (P- E- and L-selectin) interacting with carbohydrate determinants on selectin ligands, mainly P-selectin glycoprotein-ligand 1 (199). During rolling, the cells are activated by endothelial-bound chemokines leading to a conformational change of leukocyte β2-integrins (lymphocyte function-associated antigen-1 [LFA-1] and macrophage-1 antigen [Mac-1]). Integrin activation enables their binding to endothelial adhesion molecules of the immunoglobulin superfamily (*e.g.,* intercellular cell adhesion molecule [ICAM]-1 and ICAM-2), which mediates firm arrest of the cell on the vessel wall in preparation for subsequent transmigration (242).

Increasing evidence demonstrates a role of MPO-derived oxidants in leukocyte recruitment (Figs. 3 and 4). Stimulation of neutrophils with H_2O_2 or monochloramine (NH_2Cl) chloramines resulted in upregulation of β2-integrins on neutrophils and enhanced leukocyte recruitment *in vivo* (203). HOSCN, one of the major products of physiological MPO activity, is a potent inducer of E-selectin and ICAM-1

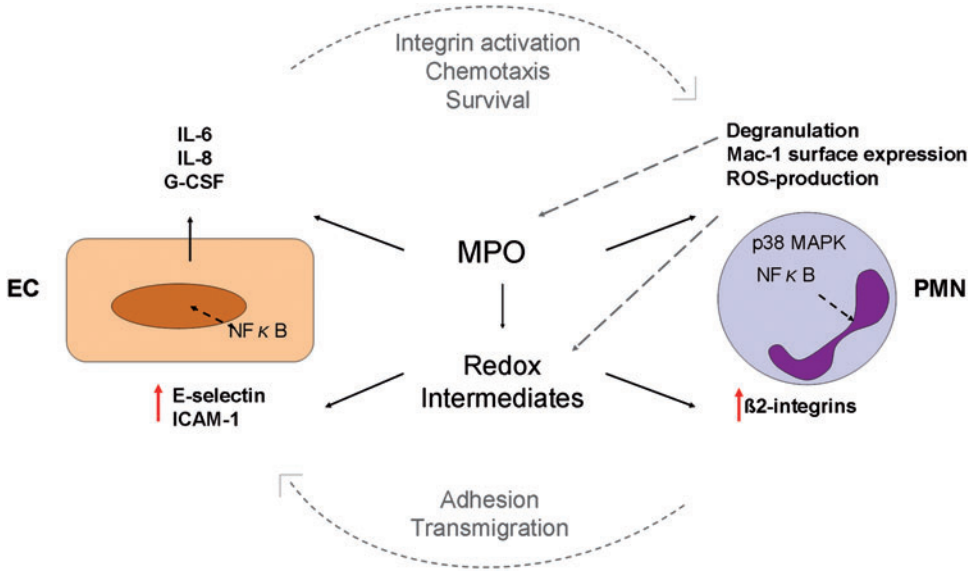

FIG. 3. Effect of extracellular MPO and MPO-derived oxidants on PMN and ECs. Binding of MPO to PMN leads to the activation of intracellular- signaling cascades with nuclear translocation of NFκB resulting in increased ROS production, degranulation, and upregulation of Mac-1 surface expression. In EC, MPO stimulates the production of proinflammatory cytokines and chemokines, such as IL-6, IL-8, and G-CSF. MPO-derived redox intermediates trigger the expression of adhesion molecules on PMN and EC, thereby promoting PMN recruitment. (To see this illustration in color, the reader is referred to the web version of this article at www.liebertpub.com/ars.) G-CSF, granulocyte colony-stimulating factor; ICAM-1, intercellular cell adhesion molecule-1; IL, interleukin; Mac-1, macrophage-1 antigen; MAPK, mitogen-activated protein-kinase; NFκB, nuclear factor kappa-light-chain-enhancer of activated B-cells; ROS, reactive oxygen species.

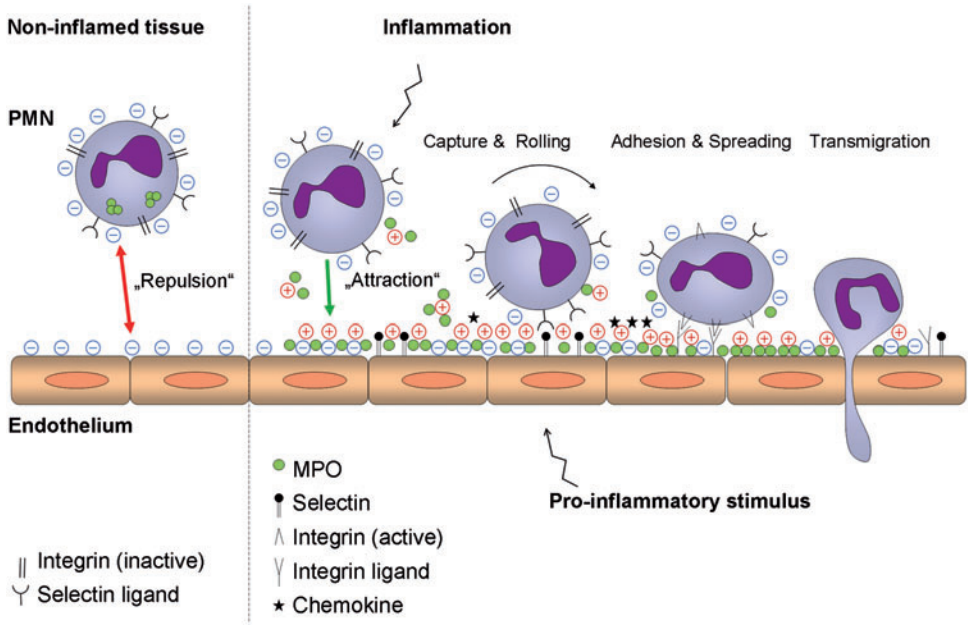

FIG. 4. The leukocyte recruitment cascade: possible effects of MPO. In noninflamed tissue, electrostatic repulsion between the negatively charged glycocalyx of PMN and the vessel wall prevents the interactions of circulating cells with the endothelium. Upon proinflammatory stimulation, highly cationic MPO is released from PMN and binds rapidly to the endothelial glycocalyx leading to a reduction of the negative surface charge. This allows for electrostatic attraction of PMN to the endothelium and facilitates receptor–ligand interactions between PMN and ECs, which mediate rolling and adhesion, and finally transmigration of the cells into the surrounding tissue. MPO further promotes leukocyte recruitment by triggering the expression of adhesion molecules and the secretion of proinflammatory cytokines and chemokines as depicted in Figure 3. (To see this illustration in color, the reader is referred to the web version of this article at www.liebertpub.com/ars.)

expression in the human umbilical vein endothelial cell (EC) by a pathway involving nuclear factor kappa-light-chain-enhancer of activated B-cells (NFκB). This does not only lead to increased adhesion of neutrophils to the endothelial lining, but also to leukocyte recruitment after intraperitoneal injection of HOSCN *in vivo* (231). Furthermore, downstream targets of MPO-derived oxidants, such as HOCl-modified lipids, can exert proadhesive effects by upregulating the expression of adhesion molecules (52, 217). Another possible mechanism by which MPO might indirectly enhance leukocyte adhesion is *via* consumption of $NO^{\bullet}$, which is known to exert anti-adhesive properties (24, 116).

In addition, leukocytes were shown to directly adhere to immobilized MPO in a Mac-1-dependent fashion (96). Surprisingly, this property of MPO seems to be independent of its enzymatic activity as catalase treatment did not alter cell adhesion. In support of this concept, it was demonstrated that inactive MPO is more effective than catalytically active MPO in stimulating ECs to produce ROS, interleukin (IL)-6 and IL-8 (128). Increased production of IL-8, a major chemokine involved in neutrophil activation and migration *in vivo*, could thus promote leukocyte recruitment. The nature of the difference between active and inactive MPO remains unclear, however, as it was proposed that MPO is rapidly inactivated upon extracellular release (107), this finding could be of high physiological relevance. MPO is also capable of directly activating neutrophils in an autocrine or paracrine fashion independent of its oxidative properties, but dependent on leukocyte β2-integrin Mac-1 (121). Extracellular MPO was shown to bind to circulating neutrophils and to colocalize with Mac-1 surface expression triggering NADPH oxidase activity, nuclear translocation of NFκB, degranulation, and upregulation of CD11b surface expression (121). These effects could be blocked by treatment with a blocking antibody against Mac-1, but not by inhibition of MPO with 4-ABAH. The *in vivo* relevance of these observations was recently confirmed by a study demonstrating a proadhesive effect of catalytically active as well as inactive MPO in different models of inflammation (111). Intriguingly, a charge-dependent mechanism seems to be involved in directing neutrophil recruitment and migratory behavior. Extracellular MPO as a highly cationic protein avidly binds to the endothelium and could thereby promote cell adhesion *via* an electrostatic interaction (Fig. 4). A similar effect on leukocyte recruitment has been described for other highly cationic proteins, such as azurocidin or proteinase 3, which are released by activated neutrophils (48, 194, 196). Interestingly, an involvement of the β2 integrin Mac-1 is also discussed for those proteins, similar to MPO. However, further studies are warranted (i) to explore the contribution of physical forces for interactions of MPO with leukocytes (and other cells) and (ii) the role of specific adhesion molecules, such as Mac-1, in this process. Taken together, these data support a role of MPO in regulating leukocyte recruitment *in vivo*. This notion is supported by several reports on reduced leukocyte recruitment observed in MPO-deficient animals in different models of neutrophil-dependent inflammation (74, 111, 141).

Apoptosis and resolution of inflammation

Apoptosis of neutrophils and effective clearance by phagocytic uptake into macrophages are essential steps in the resolution of inflammation (53, 100). This complex process is highly regulated and disturbances may lead to chronic inflammation and increased tissue injury. Research on the role of MPO in regulating apoptosis of neutrophils and other leukocyte subsets has yielded ambiguous results.

ROS and the MPO-H_2O_2-halide system were shown to induce apoptosis involving different pathways (98, 134, 151, 247). H_2O_2 and NH_2Cl, as a downstream effector of HOCl-driven chlorination, exert proapoptotic effects in neutrophils and Jurkat cells through activation of cJun N-terminal kinase (JNK) and inhibition of NFκB (98, 163). The higher rate of apoptosis was associated with increased caspase cleavage and contributed to resolution of inflammation in a model of experimental antigen-induced arthritis (134). Caspase activation is also triggered by HOCl-modified lipoproteins leading to apoptosis of monocytes/macrophages and T-cells *in vitro* (61, 178, 227), and HOCl-modified LDL was found to colocalize with MPO and CD3-positive T-cells in human placental tissue (178). HOSCN also induces apoptosis *in vitro* and was shown to be more effective than HOCl or hypobromous acid (HOBr), likely due to a more selective targeting of thiol groups in the mitochondrial membrane with subsequent cytosolic release of cytochrome *c* (132).

In contrast to the aforementioned studies, incubation of isolated neutrophils with purified MPO reduced cytochrome *c* release and caspase-3 activation and delayed spontaneous apoptosis *in vitro* in a concentration-dependent manner (59). As previously observed for the proadhesive properties of MPO, this effect was not inhibited by blocking MPO catalytic activity with 4-ABAH, but was found to involve Mac-1 integrins and ERK1/2 activation. The anti-apoptotic effect of extracellular MPO translated into a prolonged inflammatory reaction *in vivo* in a model of acute lung injury (59). It remains unclear whether the anti-apoptotic effect of MPO is mediated by direct interaction with neutrophils or possibly *via* secondary molecules. In this regard, inactive MPO was shown to trigger the release of cytokines with known antiapoptotic action, such as granulocyte colony-stimulating factor and IL-6 (124, 128). The MPO-induced delay of apoptosis could be overcome by treatment with 15-epi-lipoxin A4, which possesses anti-inflammatory properties and contributes to resolution of inflammation (60). Interestingly, MPO-deficient mice were shown to produce a lower amount of anti-inflammatory lipid metabolites, but more pro-inflammatory leukotrienes compared to wild-type (WT) mice following intraperitoneal injection of endotoxin (115).

Neutrophil macrophage cross talk

The functional interplay between different subsets of leukocytes is a critical determinant for the course of inflammation. Following the initial recruitment of neutrophils, monocytes enter the inflamed tissue and make contact with multiple secretion products of activated neutrophils. Several studies support the concept, that neutrophil cationic proteins, including MPO, are involved in modulating monocyte/macrophage function (Fig. 5) (70, 124, 195). Earlier studies by Lefkowitz and coworkers using exogenous MPO at physiological levels to stimulate resident peritoneal macrophages, demonstrated an increased production of tumor necrosis factor-alpha (TNF-α) and other proinflammatory

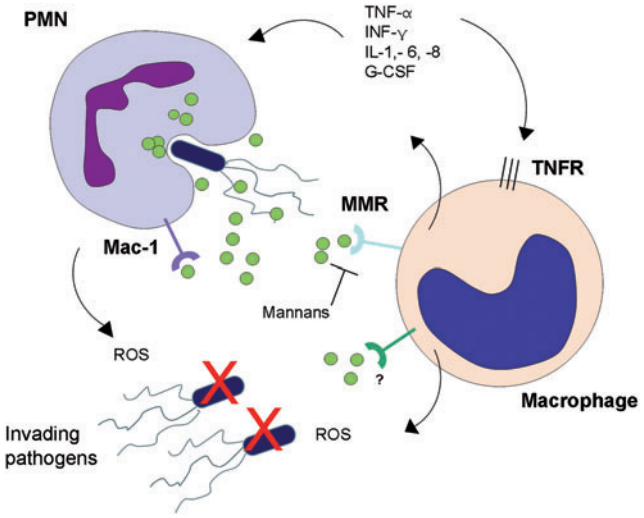

FIG. 5. Role of MPO in neutrophil–macrophage cross talk. During pathogen elimination, MPO is released from phagocytosing neutrophils and interacts with nearby PMN and macrophages. Binding of MPO to the MMR leads to an increased production of cytokines and chemokines, which in turn can activate neutrophils, macrophages, and other immune cells in an auto- and paracrine fashion. In addition, MPO can directly activate neutrophils *via* interaction with the β2-integrin Mac-1. These interactions lead to enhanced ROS production by PMN and macrophages and support pathogen killing. (To see this illustration in color, the reader is referred to the web version of this article at www.liebertpub.com/ars.) INF, interferon; MMR, macrophage mannose receptor; TNF, tumor necrosis factor; TNFR, TNF-receptor.

cytokines *in vitro* as well as increased serum levels of TNF-α and interferon-γ following intravenous injection of MPO (127). Exposure to MPO also enhanced phagocytosis and killing of *E. coli* and *Candida albicans* by macrophages through increased production of ROS (68, 126, 129). The *in vivo* relevance of these findings is underscored by the observation that intra-articular injection of MPO triggered a flare of experimental arthritis induced by streptococcal wall fragments (68, 123). These effects were also seen with catalytically inactive MPO, and attributed to a direct interaction of MPO with the mannose receptor on macrophages. Indeed, blocking of the mannose receptor with mannans abrogated the symptoms (joint swelling, erythema) induced by MPO injection. However, also other receptors or pathways must exist, as MPO-mediated respiratory burst and production of TNF-α and IL-1 by alveolar macrophages *in vitro* was unaffected by coadministration of mannan (70). A possible candidate might be the β 2 integrin Mac-1, which is involved in the interaction of MPO with neutrophils (59, 121) and was shown to mediate effects of other neutrophil proteins on monocytes (195).

The activation of macrophages (and ECs) by active and inactivated MPO at sites of neutrophil accumulation with release of strong proinflammatory cytokines, such as TNF-α and chemotactic proteins (*e.g.*, IL-8), may induce further leukocyte recruitment and contribute to the perpetuation of inflammation.

Neutrophil extracellular trap formation

Besides the classical mode of pathogen elimination by phagocytic uptake, a novel defensive strategy of neutrophils termed neutrophil extracellular trap (NET) formation has been identified by Brinkmann *et al.* (30). Upon activation by cytokines or by direct pathogen encounter, neutrophils undergo cytoplasmic and nuclear changes, the intracellular architecture is lost, and DNA fibers are expelled that contain granular proteins and histones. Several studies have demonstrated NET formation during infection *in vitro* and *in vivo* (30, 45) and it has been postulated that within NETs, MPO in concert with other granular proteins might help to trap and kill bacteria and fungi due to its highly cationic charge (31). Interestingly, NETs are also present in sterile inflammation and seem to contribute to autoimmune and autoinflammatory disease (73, 101).

The mechanisms leading to NET formation are still incompletely understood. However, recent studies provide evidence for a critical role of ROS and MPO during this process (144, 164, 219). During NET formation, intracellular MPO has been localized to the decondensed nucleus and after disintegration of the plasma membrane, MPO is erupted and found within DNA fibers (164, 219). Coincubation of isolated nuclei from neutrophils with MPO and NE *in vitro* demonstrated a dose-dependent increase of NE-induced nuclear decondensation by MPO. This effect could not be blocked by addition of 4-ABAH suggesting a mechanism independent of MPO's enzymatic activity. The importance of MPO for NET formation is emphasized by the observation that individuals with a complete MPO deficiency seem to be unable to generate NETs upon stimulation of neutrophils with phorbol myristate acetate or pathogens (144). Whether this is of biological significance for infection control *in vivo* needs further clarification as MPO-deficient neutrophils inhibited *C. albicans* growth as efficiently as healthy neutrophils. In constrast, excessive NET formation as demonstrated in influenza pneumonitis and cystic fibrosis might have deleterious effects by enhancing tissue damage (137, 152). Furthermore, extracellular MPO within NETs might serve as autoantigen, thereby contributing to the pathogenesis of antineutrophil cytoplasmic antibody-associated inflammatory diseases (76, 101).

MPO-Dependent Modulation of ECs and Vascular Function

EC binding and transcytosis of MPO

The pivotal role of MPO in vascular disease has called for the investigation of the enzyme's dissemination within the vasculature once it is released from activated neutrophils. The high affinity of MPO to negatively charged structures, which is due to MPO's cationic charge at physiological pH, predestines the enzyme to bind to the endothelial surface layer. This layer is termed "glycocalyx" and carries strong anionic charges arising from proteoglycans with linear polysaccharide chains composed of sulfated and carboxylated disaccharides (110). In fact, MPO binds to the vascular endothelium, which has first been reported in renal arteries of the rat: Upon infusion, MPO was observed to adhere to the glomerular capillary wall, which led to acute glomerular injury following application of H_2O_2 (97). Further investigations revealed that the favored binding partner of MPO is the perlecan-

constituent heparansulfate glycosaminoglycan (GAG), which is the main component of the endothelial glycocalyx (17, 110). Several studies confirmed the intense binding of MPO to the EC in culture (21, 47), in *ex vivo* (17) and *in vivo* studies (111, 141). Noteworthy, the affinity to heparansulfate appears to reach even beyond electrostatic interactions, as the binding to chondroitinsulfate-GAGs, which are negatively charged as well, is less pronounced (17). In cell culture experiments and in humans, MPO was found to be released from the EC surface by the application of heparin—most probable due to a competing binding of heparin and heparansulfate-GAGs to MPO (20, 47). Resulting from the abundant binding of MPO to the glycocalyx, its overall negative surface charge has been observed to be reduced, which might entail extensive consequences on endothelial functions (111).

Importantly, MPO does not only bind to the luminal surface of ECs, but is also transported through ECs to the basolateral membrane (17). In cultured bovine aortic ECs, MPO was taken up by the cells, and subsequently accumulated at the basolateral side, where it colocalized with the matrix protein fibronectin. Here, MPO remained catalytically active and in the presence of nitrite promoted the nitration of matrix protein tyrosine residues. The transcytosis has been suggested to rely on caveolae, with an electrostatic interaction between MPO and albumin promoting the uptake of the enzyme to the vesicles (213). Another study described the EC surface molecule cytokeratin 1 to serve as a receptor for MPO and to facilitate its internalization (15). Further studies may be necessary to fully elucidate the subcellular mediators of MPO's fate within the EC.

Endothelial dysfunction

Dysfunction of the endothelium comprises impaired barrier and vasomotor function and imbalanced release of pro- and anti-inflammatory and -coagulatory factors. A reduced bioavailability of $NO^{\bullet}$, which is an important regulator of endothelial homeostasis, is recognized as a key factor of endothelial dysfunction. The impact of MPO on endothelial function and the cardiovascular system is summarized in Figure 6. The accumulation of MPO in the subendothelial space forces a tight contact of the enzyme with endothelium-derived $NO^{\bullet}$. As described above, $NO^{\bullet}$ was identified to serve as a substrate for the one-electron reactions of the peroxidase compounds I and II. Thus, MPO was assumed to serve as a catalytic sink for $NO^{\bullet}$ (1). Further investigations revealed that under physiological conditions $NO^{\bullet}$, apart from directly reacting with compounds I and II, was oxidized by radical intermediates of small molecule substrates of MPO, such as ascorbate or tyrosine (57). This MPO-dependent oxidative consumption of the important vasodilating molecule resulted in impaired acetylcholine-induced relaxation of rat and mouse aortic and tracheal segments (57). Apart from that, MPO was proposed to attenuate vasodilation *via* HOCl-mediated oxidation of L-arginine (245, 246). Moreover, reactive nitrogen species such as those generated by MPO have been identified to lead to uncoupling of N $NO^{\bullet-}$ synthases, which results in superoxide production instead of the formation of $NO^{\bullet}$ (250). The impact of MPO on vasomotor functions has recently been confirmed in a porcine model disclosing systemic MPO application to decrease myocardial blood flow, to reduce myocardial perfusion, and to increase

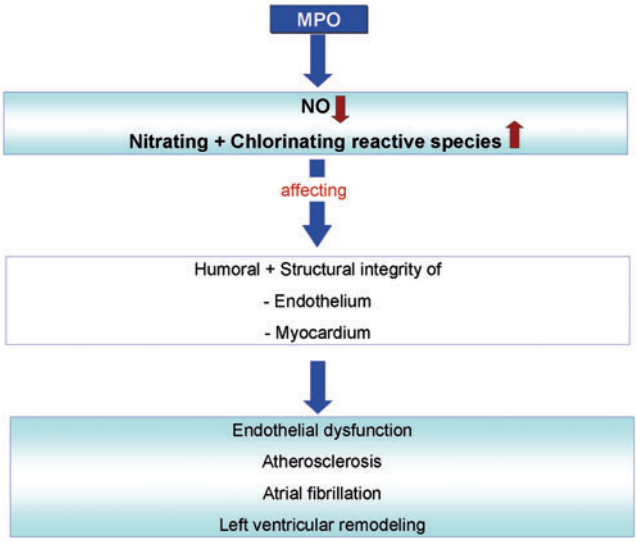

FIG. 6. Schematic overview of MPO's impact on the cardiovascular system. Decreased $NO^{\bullet}$-bioavailability and increased production of chlorinating and nitrating reactive species impair endothelial and myocardial humoral and structural integrity, which contributes to the initiation and propagation of cardiovascular disease. (To see this illustration in color, the reader is referred to the web version of this article at www.liebertpub.com/ars.)

pulmonary vascular resistance (182). In patients, a significant inverse correlation of MPO plasma levels with the relaxation of blood vessels has been described (182). Furthermore, in patients undergoing coronary angiography, endothelium-bound MPO was released by heparin application, which caused an improvement of flow-mediated dilation (FMD) (20). Further, corroborating the role of MPO in endothelial dysfunction, microvascular function inversely correlated with MPO plasma levels in patients with coronary artery disease (CAD). In these patients, vessel recanalization upon myocardial infarction increased the concentration of circulating MPO with enhanced $NO^{\bullet}$ consumption assessed in their plasma *ex vivo* (19).

Modification of LDL and high density lipoprotein by MPO

Atherosclerosis is the principal cause of CAD. The oxidation of lipoproteins, in particular of LDL, is a pivotal mechanism in atherogenesis (216). Therefore, the inflammatory pathways driving oxidative modifications of LDL have been extensively studied. To date, an increasing body of evidence reveals that MPO importantly contributes to the oxidation of LDL. Lysine residues of apolipoprotein B-100—the predominant protein of LDL—have been found to be oxidized by HOCl, which resulted in increased uptake of the modified LDL by macrophages (81). Likewise, the nitrated form of LDL (NO_2-LDL) generated by the MPO-H_2O_2-nitrite-system appeared to be avidly taken up by macrophages and promoted the formation of foam cells (85, 168). Analysis of human atherosclerotic aortic tissue disclosed the enrichment of LDL containing 3-Cl-Tyr (80, 83) as well as 3-NO_2Tyr (122, 168). Noteworthy, apart from LDL, also the high-density lipoprotein (HDL) has been identified as a target of

MPO-dependent modifications. While intact HDL exhibits antioxidant, anti-inflammatory, and antithrombotic properties, it can be converted to a dysfunctional form by MPO (161). In analogy to observations regarding LDL, 3-Cl-Tyr and 3-nitrotyrosine (3-NO_2-Tyr) were found to be enriched in HDL from atherosclerotic intima (22, 167), with the degree of chlorinated and nitrated tyrosine residues within apolipoprotein A1 (the major protein component of HDL) correlating with the prevalence of cardiovascular disease (CVD). Several studies regarding MPO-modified HDL revealed the loss of its ability to promote cholesterol efflux from macrophages (23, 217, 249).

Unexpectedly, in LDL receptor-deficient mice receiving a high-fat, high-cholesterol diet, the extent of atherosclerotic lesions increased in a subgroup transplanted with bone marrow from MPO-deficient mice (28). Yet, different pathomechanisms for the development of murine and human atherosclerosis were suggested, due to the fact that in MPO-deficient mice ($Mpo^{-/-}$) as well as in WT mice, MPO and 3-Cl-Tyr were undetectable in aortic lesions. This observation emphasizes that one has to be aware of species differences limiting a categorical translation of findings from rodents to man as mentioned before.

Nevertheless, accumulated data advocate a role of MPO in the transition of atherosclerotic plaques to a vulnerable state (160), which is further strengthened by observations of increased MPO release from PMN, in particular, within the coronary circulation in patients with unstable angina (33). Taken together, MPO emerges as a likely modulator of lipoprotein function and a critical participant in atherogenesis and the initiation and propagation of CVD (Fig. 7A).

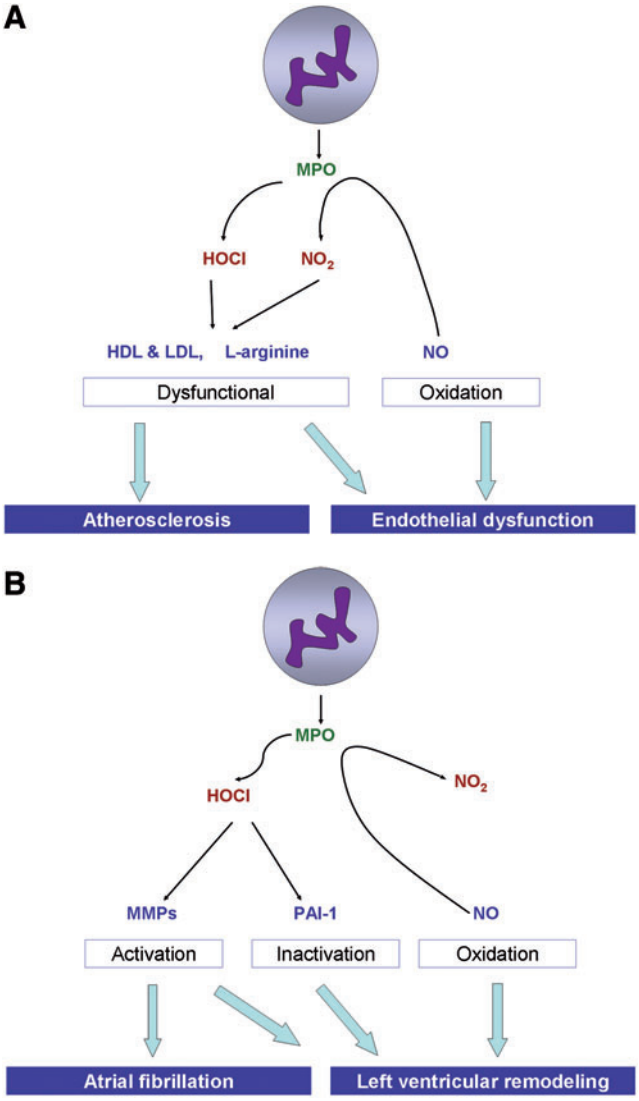

FIG. 7. Contribution of MPO to cardiovascular and myocardial dysfunction. (A) MPO-generated HOCl and nitrating species like NO_2 convert LDL and HDL into a proatherogenic form. Chlorination of L-arginine by HOCl and oxidation of $NO^{\bullet}$ lead to endothelial dysfunction. **(B)** HOCl induces the activation of MMPs, which contributes to the propagation of myocardial fibrosis. Fibrosis of atrial tissue promotes atrial fibrillation, whereas ventricular fibrosis nurtures adverse left ventricular remodeling. Further contributing mechanisms of left ventricular remodeling are oxidative consumption of $NO^{\bullet}$ and the activation of PAI-1 by HOCl. (To see this illustration in color, the reader is referred to the web version of this article at www.liebertpub.com/ars.) HDL, high-density lipoprotein; HOCl, hypochlorous acid; LDL, low-density lipoprotein; NO_2, nitrogen dioxide; PAI-1, plasminogen activator inhibitor-1.

MPO-Dependent Modulation of Myocardial Function

Atrial fibrillation

Besides MPO's impact on vascular homeostasis, the enzyme also modulates myocardial integrity (Fig. 7B). It has been shown recently, that MPO does not only accumulate in plasma of patients with paroxysmal atrial fibrillation, but is also mechanistically linked to the pathogenesis of this disease (183). Besides electrical triggers, atrial fibrosis with augmented turnover and deposition of collagen and other extracellular matrix (ECM) proteins has emerged as a principal prerequisite of the perpetuation of the disease (75, 105). Importantly, MPO-derived hypochlorite is known to activate matrix metalloproteinase (MMP)-7 by oxidation of a critical cysteine residue in the active site (232). MMPs comprise a group of proteases responsible for the degradation of ECM proteins, which can result in augmented turnover of ECM and release of bioactive fragments and growth factors (51, 149) and is considered a profibrotic event. In a murine model of angiotensin II induced MPO release from PMN, MPO has been proven to promote the activation of MMP-2 and -9 (183). This resulted in increased atrial fibrosis and significantly enhanced the vulnerability to atrial fibrillation, whereas $Mpo^{-/-}$ mice exhibited no significant increase in atrial fibrosis and fibrillation probability. Of note, the mass spectrometric and immunohistochemical analysis of atrial tissue revealed enhanced formation of NO_2-Tyr and 3-Cl-Tyr in angiotensin II-treated WT mice as compared to $Mpo^{-/-}$ mice, which was accompanied by an inhomogeneity of electrical conduction. Likewise, in a canine model of sterile pericarditis, MPO deposition in the atria was found to correlate with an inhomogeneity of electrical conduction (91). These findings support the notion that MPO is critically involved in the pathogenesis of atrial arrhythmias and evolves as a potential target in this disease.

Left ventricular remodeling

Whereas left ventricular (LV) remodeling is a physiological adaptive process of regulating LV function and shape, multiple research efforts predominantly focus on its pathophysiological role implicating myocardial infarction or hypertension (202). Inflammation has emerged as a key player in adverse LV remodeling resulting in a dysfunctional, failing heart (218). In particular, ischemic cardiomyopathy is promoted by the recruitment and activation of leukocytes (13). The fact that MPO implicates leukocyte recruitment, endothelial dysfunction, and fibrosis, advocates for a role of MPO in adverse LV remodeling (Fig. 7B). In fact, a murine model of acute myocardial infarction revealed preservation of LV function in $Mpo^{-/-}$ animals (14), which arose from reduced leukocyte infiltration, diminished collagen deposition, and attenuated plasmin activity in the myocardium of $Mpo^{-/-}$ mice.

Clinical implications

Increasing lines of evidence point toward an important role of MPO in modulating leukocyte and EC function affecting vascular and myocardial integrity. Whether these, in part, proatherogenic mechanisms described so far translate into a clinical phenotype, however, remains a matter of debate.

MPO as a biomarker in CVD

Clinical studies report increased levels of circulating MPO in patients with overt CAD compared to healthy controls (157, 248). Zhang *et al.* (248) could initially reveal that patients in the highest MPO quartile of leukocyte MPO had an adjusted risk with an odds ratio of 11.9 (95% CI, 5.5–25.5) for the presence of CAD. Furthermore, MPO plasma levels are associated with the clinical outcome in patients suffering from CAD in terms of long-term cardiovascular mortality, severity of CVD, and *de novo* myocardial infarction (38, 86, 147). In a cohort of 885 patients undergoing coronary angiography, baseline-MPO plasma levels independently predicted long-term cardiovascular mortality and correlated with the severity of CVD.

Remarkably, MPO plasma levels were particularly informative in patients with acute states of the disease. In patients presenting with a new onset of chest pain or in the setting of acute coronary syndromes, MPO is significantly elevated compared to controls and even provides prognostic information about adverse cardiovascular events (18, 29, 38, 147, 148, 179, 187, 191). In these patients, MPO identifies individuals at a high risk for adverse cardiac events, including mortality, in particular, in those in whom markers of myocardial necrosis–such as troponins–are initially negative (18, 147, 187). MPO plasma concentrations may even increase more rapidly than troponins, and therefore indicate patients at high risk at an earlier time point (193).

Notably, MPO does not only suggest to predict an adverse outcome and future risk of CAD-progression in patients with acute or stable coronary disease, but also in apparently healthy subjects and after exclusion of CAD (145). Wong *et al.* revealed that MPO levels correlated with the extent of deposition of coronary artery calcium assessed by computed tomography in asymptomatic adults (239).

The fact that high MPO levels are prognostic for the development of CVD in healthy subjects raises the question, if MPO deficiency in humans would be vasculature-protective *per se*, assuming that MPO deficiency should be highly advantageous for one's health.

Unfortunately, studies ultimately proving this notion are lacking so far. However, Kutter *et al.* followed 92 MPO-deficient individuals and appropriate control subjects (117) and disclosed that the number of subjects with cardiovascular problems, including myocardial infarction and coronary atheroma was significantly lower among the MPO-deficient individuals. Furthermore, the observation that nicotine-driven activation of leukocytes did not alter FMD in patients with low MPO expression, respectively, strongly suggests that MPO absence could be critical in regulation of endothelial function *in vivo* as mentioned above (182). Further studies would be valuable to elucidate the dimension of connections between MPO-dependent proinflammatory mechanisms and a clinical phenotype.

MPO as a biomarker in heart failure

In analogy to experimental studies investigating MPO's role in ischemic heart failure (HF) (13, 14), MPO levels were found to be associated with the development of HF after myocardial infarction in patients with a Hazard Ratio of 1.55 (95% CI 1.14–2.11) (191). Furthermore, in patients with diagnosed HF, MPO plasma levels were increased in comparison to healthy controls. Even after adjustment for age and BNP levels, there remained a strong association of MPO plasma levels with the prevalence of HF (OR 27.7, 95% CI 3.6–371.1) (206).

In patients with a stable chronic systolic HF, MPO levels were associated with increasing diastolic dysfunction, indicating an effect of MPO on the impairment of compliance and filling of the failing heart. This was even aggravated in patients with severe systolic HF (EF < 20%). Furthermore, in this cohort, increasing plasma MPO levels were predictive for mortality and cardiac transplantation (208). Rudolph *et al.* showed, that elevation of MPO-plasma levels in HF patients is irrespective of etiology of HF and even proved a correlation of systolic parameters with MPO levels (MPO-LVEF-correlation Spearmans rho 0.3, $p < 0.01$) (184). Furthermore, MPO was an independent predictor of 1-year mortality in these patients with an adjusted HR of 1.52 (95% CI 1.03–2.24) (177).

As seen for the development of CAD, MPO was observed to predict an increased risk of developing HF even in healthy subjects in cohorts of over 3500 patients during long-term follow-up (7.2 ± 2.3 years) (207) and to significantly increase the diagnostic value of BNP for detecting LV systolic dysfunction (159).

Limitations

In contrast to the above-mentioned studies, others could not confirm prognostic information provided by MPO in predicting cardiovascular events (HR 1.26, 95% CI 1.00–1.59, $p = 0.052$) (191), in particular, after adjustment for other biomarkers like troponins. Chang *et al.* (40) observed a significant, but overall weak adjusted risk for MACE in patients following myocardial infarction (1.003 [95% CI 1.002–1.005]). Other studies found no incremental benefit of circulating MPO for diagnosis of CAD (114) in patients with chest pain (56) or after myocardial infarction (32). Of note, all of the above-named studies were performed using the first

Table 1. Overview of Clinical Studies Investigating the Relationship of Myeloperoxidase and Coronary Artery Disease

	Inclusion criteria and number of patients	*Study design*	*Sample type*	*Duration of follow-up*	*End point*	*Result*
Meuwese *et al.* (145)	1138 healthy subjects	Longitudinal	Serum	8 years	CAD	Adjusted odds ratio 1.36 (95% CI 1.07–1.73) for 4th *vs.* 1st MPO-quartile
Wong *et al.* (239)	1302 asymptomatic subjects	Longitudinal	EDTA plasma	Average of 3.8 years	Death, AMI, revascularization, stroke	Adjusted hazard ratio1.9 (95% CI 1.0–3.6) for MPO above median levels
Ndrepepa *et al.* (157)	874 patients with CAD *vs.* 194 controls	Cross-sectional	EDTA plasma		CAD	Independent odds ratio 2.08 (95% CI 1.54–2.81) for 75 μg/L increase in MPO concentration
Zhang *et al.* (248)	158 patients with CAD *vs.* 175 controls	Cross-sectional	Leukocytes from isolated EDTA-blood		CAD	Adjusted odds ratio of 11.9 (95% CI 5.5–25.5) for 4th *vs.* 1st MPO-quartile
Heslop *et al.* (86)	Suspected CAD, 885 patients	Longitudinal	EDTA plasma	>13 years	Cardiovascular mortality	Adjusted hazard ratio 1.96 (95% CI 1.15–3.37) for 3rd *vs* 1st tertile of MPO
Kubala *et al.* (114)	Suspected CAD, 557 patients	Cross-sectional	EDTA plasma		CAD	No difference in MPO-plasma levels in CAD *vs.* non-CAD patients
Apple *et al.* (6)	Suspected ACS, 400 patients	Longitudinal	EDTA plasma	6 months	AMI, cardiac death, revascularization	Adjusted hazard ratio 2.7 (95% CI 2.4–6.4) for MPO above cut point (633 p*M*) at 30 days Adjusted hazard ratio 2.4 (95% CI 1.3–4.6) for MPO above cut point (633 p*M*) at 6 months
Baldus *et al.* (18)	ACS,1090 patients	Longitudinal	Serum	6 months	Death, nonfatal MI	Adjusted hazard ratio 2.25 (95% CI 1.32–3.82) for MPO above cut point (350 μg/L) at 30 days
Brennan *et al.* (29)	Chest pain, 604 patients	Longitudinal	Plasma	6 months	Death, AMI, or revascularization	Unadjusted odds ratio 4.7 (95% CI 2.8–7.7) for 4th *vs.* 1st MPO-quartile at 30 days Unadjusted odds ratio 4.7 (95% CI 2.9–7.7) for 4th *vs.* 1st MPO-quartile at 6 months

(*continued*)

Table 1. (Continued)

	Inclusion criteria and number of patients	*Study design*	*Sample type*	*Duration of follow-up*	*End point*	*Result*
Brugger-Andersen *et al.* (32)	AMI, 298 patients	Longitudinal	Citrate plasma	45 months	Cardiac death, AMI, revascularization	Adjusted hazard ratio 1.04 (95% CI 0.59–1.86) for 4th *vs.* 1st MPO-quartile
Chang *et al.* (40)	STEMI, 136 patients	Longitudinal	EDTA plasma	30 days	Death, shock, re-infarction, revascularization	Adjusted odds ratio 1.003 (95% CI 1.002–1.005) for above cut point MPO-levels
Dominguez-Rodriguez *et al.* (54)	STEMI and cardiogenic shock, 38 patients	Longitudinal	Serum	During hospital stay	Death	Adjusted odds ratio 3.9 (95% CI 1,8–7.5) for MPO (continuous)
Eggers *et al.* (56)	Chest pain, 380 patients	Longitudinal	EDTA plasma	6 months	Death, AMI	Adjusted hazard ratio 1.1 (95% CI 0.8–1.5) for) for 1 SD of ln(MPO)
Khan *et al.* (106)	STEMI, 384 patients	Longitudinal	EDTA plasma	Minimum 30 days	Death or AMI	Adjusted hazard ratio 6.91 (95% CI 1.79 *vs.* 26.73) for log(MPO) above *vs.* below median
Morrow *et al.* (148)	Non-ST-elevation ACS, 1524patients	Longitudinal	Citrate plasma	30 days	Nonfatal AMI or ACS	Adjusted odds ratio 2.10 (95% CI 1.36–3.23) for MPO above median
Roman *et al.* (179)	ACS, 130 patients	Longitudinal	EDTA plasma	During hospital stay	Mortality, revascularization, recurrent angina, HF, arrhythmia	Adjusted odds ratio of 3.8 (95% CI 1.2–12) for above median MPO levels
Sawicki 2011(187)	Suspected ACS, 300 patients	Cross-sectional	EDTA plasma		AMI	Area under ROC curve for MPO >527 p*M*: 0.906 (95% CI 0.87–0.934)
Cavusoglu *et al.* (38)	ACS, 193 men	Longitudinal	Plasma	2 years	AMI	Adjusted odds ratio 1.60 (95% CI 1.09–2.36) for 1 SD of log(MPO)
Mocatta *et al.* (147)	AMI, 512 patients	Longitudinal	EDTA plasma	5 years	Mortality	Adjusted risk ratio 1.8 (95% CI 1.1–3.1) for above median MPO levels
Scirica *et al.* (191)	Non-ST-elevation ACS, 4352 patients	Longitudinal	EDTA plasma	Median 348 days	HF	Adjusted hazard ratio of 1.14 (95% CI 1.14–2.11) for above cut point MPO levels (670 p*M*)

Extent of gray shading indicates the extent of CAD in study patients.

ACS, acute coronary syndrome; AMI, acute myocardial infarction; CAD, coronary artery disease; EDTA, ethylene-diamine-tetra-acetic acid; HF, heart failure; MPO, myeloperoxidase; STEMI, ST-segment elevation myocardial infarction.

generation, nonsensitive tests to detect troponins. Further large-scale studies are necessary to assess the adjunct diagnostic and prognostic value of MPO in the presence of the current sensitive troponin assays.

Another important limitation for assessing the clinical utility of MPO as a biomarker in CVD is a lack of standardized measurement methods for MPO. In fact, a large variety of assays has been introduced (7). Moreover, one has to consider that leukocyte activation with the release of MPO into the circulation is an unspecific event, as neutrophil and macrophage activation is not limited to cardiovascular events. Also, several drugs interfere with MPO plasma levels, including heparins, which increase circulating MPO (20), and bivalirudin, which promotes binding of the enzyme toward the vascular compartment (185).

Finally, the prognostic value of increased plasma MPO levels does not necessarily prove the involvement of MPO itself, but may only reflect increased neutrophil activation. However, in the synopsis of the lacking correlation of MPO with leukocyte count, the adjustment for other inflammatory markers in clinical studies, the *in vivo* data from $Mpo^{-/-}$ animals after myocardial infarction (237), and the *in vitro* data described above, a direct role of MPO in the pathogenesis of CVD is likely.

Taken together, MPO evolves as a biomarker for risk stratification in initiation and progression of CVD (Table 1). Due to MPO's pathophysiological role associated with plaque instability and vascular inflammation, its diagnostic value adds additional information to the biomarkers routinely used. Noting the relationship between MPO and HF, the pathophysiological role of MPO extends from vascular event to cardiac plasticity. However, there are still issues to be solved, including low MPO-specificity, divergent measurement methods, and therapeutic relevance of MPO-derived diagnoses (6, 189).

Outlook

Since MPO's first description 70 years ago, the enzyme's potent bactericidal properties and its heterogeneous role beyond innate immunity have been extensively characterized. Not only the ability of MPO to catalyze the generation of reactive oxygen and nitrogen intermediates, but also its extracatalytic properties modulate the activation state of PMN, macrophages, and ECs. This calls for further experimental studies to ultimately establish MPO's diagnostic and therapeutic potential in inflammation and CVD.

References

1. Abu-Soud HM and Hazen SL. Nitric oxide modulates the catalytic activity of myeloperoxidase. *J Biol Chem* 275: 5425–5430, 2000.
2. Abu-Soud HM and Hazen SL. Interrogation of heme pocket environment of mammalian peroxidases with diatomic ligands. *Biochemistry* 40: 10747–10755, 2001.
3. Agner K. Verdoperoxidase: a ferment isolated from neutrophils. *Acta Physiol Scand* 2, Suppl 8: 1–62, 1941.
4. Allegra M, Furtmuller PG, Jantschko W, Zederbauer M, Tesoriere L, Livrea MA, and Obinger C. Mechanism of interaction of betanin and indicaxanthin with human myeloperoxidase and hypochlorous acid. *Biochem Biophys Res Commun* 332: 837–844, 2005.
5. Andersson E, Hellman L, Gullberg U, and Olsson I. The role of the propeptide for processing and sorting of human myeloperoxidase. *J Biol Chem* 273: 4747–4753, 1998.
6. Apple FS, Smith SW, Pearce LA, Schulz KM, Ler R, and Murakami MM. Myeloperoxidase improves risk stratification in patients with ischemia and normal cardiac troponin I concentrations. *Clin Chem* 57: 603–608, 2011.
7. Apple FS, Wu AH, Mair J, Ravkilde J, Panteghini M, Tate J, Pagani F, Christenson RH, Mockel M, Danne O, and Jaffe AS. Future biomarkers for detection of ischemia and risk stratification in acute coronary syndrome. *Clin Chem* 51: 810–824, 2005.
8. Aratani Y, Kura F, Watanabe H, Akagawa H, Takano Y, Suzuki K, Dinauer MC, Maeda N, and Koyama H. Critical role of myeloperoxidase and nicotinamide adenine dinucleotide phosphate-oxidase in high-burden systemic infection of mice with *Candida albicans*. *J Infect Dis* 185: 1833–1837, 2002.
9. Aratani Y, Kura F, Watanabe H, Akagawa H, Takano Y, Suzuki K, Dinauer MC, Maeda N, and Koyama H. Relative contributions of myeloperoxidase and NADPH-oxidase to the early host defense against pulmonary infections with *Candida albicans* and Aspergillus fumigatus. *Med Mycol* 40: 557–563, 2002.
10. Aratani Y, Kura F, Watanabe H, Akagawa H, Takano Y, Suzuki K, Dinauer MC, Maeda N, and Koyama H. *In vivo* role of myeloperoxidase for the host defense. *Jpn J Infect Dis* 57: S15, 2004.
11. Arnhold J and Flemmig J. Human myeloperoxidase in innate and acquired immunity. *Arch Biochem Biophys* 500: 92–106, 2010.
12. Arnljots K and Olsson I. Myeloperoxidase precursors incorporate heme. *J Biol Chem* 262: 10430–10433, 1987.
13. Arslan F, de Kleijn DP, and Pasterkamp G. Innate immune signaling in cardiac ischemia. *Nat Rev Cardiol* 8: 292–300, 2011.
14. Askari AT, Brennan ML, Zhou X, Drinko J, Morehead A, Thomas JD, Topol EJ, Hazen SL, and Penn MS. Myeloperoxidase and plasminogen activator inhibitor 1 play a central role in ventricular remodeling after myocardial infarction. *J Exp Med* 197: 615–624, 2003.
15. Astern JM, Pendergraft WF, III, Falk RJ, Jennette JC, Schmaier AH, Mahdi F, and Preston GA. Myeloperoxidase interacts with endothelial cell-surface cytokeratin 1 and modulates bradykinin production by the plasma Kallikrein-Kinin system. *Am J Pathol* 171: 349–360, 2007.
16. Austin GE, Zhao WG, Adjiri A, and Lu JP. Control of myeloperoxidase gene expression in developing myeloid cells. *Leuk Res* 20: 817–820, 1996.
17. Baldus S, Eiserich JP, Mani A, Castro L, Figueroa M, Chumley P, Ma W, Tousson A, White CR, Bullard DC, Brennan ML, Lusis AJ, Moore KP, and Freeman BA. Endothelial transcytosis of myeloperoxidase confers specificity to vascular ECM proteins as targets of tyrosine nitration. *J Clin Invest* 108: 1759–1770, 2001.
18. Baldus S, Heeschen C, Meinertz T, Zeiher AM, Eiserich JP, Munzel T, Simoons ML, and Hamm CW. Myeloperoxidase serum levels predict risk in patients with acute coronary syndromes. *Circulation* 108: 1440–1445, 2003.
19. Baldus S, Heitzer T, Eiserich JP, Lau D, Mollnau H, Ortak M, Petri S, Goldmann B, Duchstein HJ, Berger J, Helmchen U, Freeman BA, Meinertz T, and Munzel T. Myeloperoxidase enhances nitric oxide catabolism during myocardial

ischemia and reperfusion. *Free Radic Biol Med* 37: 902–911, 2004.
20. Baldus S, Rudolph V, Roiss M, Ito WD, Rudolph TK, Eiserich JP, Sydow K, Lau D, Szocs K, Klinke A, Kubala L, Berglund L, Schrepfer S, Deuse T, Haddad M, Risius T, Klemm H, Reichenspurner HC, Meinertz T, and Heitzer T. Heparins increase endothelial nitric oxide bioavailability by liberating vessel-immobilized myeloperoxidase. *Circulation* 113: 1871–1878, 2006.
21. Ballieux BE, Zondervan KT, Kievit P, Hagen EC, van Es LA, van der Woude FJ, and Daha MR. Binding of proteinase 3 and myeloperoxidase to endothelial cells: ANCA-mediated endothelial damage through ADCC? *Clin Exp Immunol* 97: 52–60, 1994.
22. Bergt C, Pennathur S, Fu X, Byun J, O'Brien K, McDonald TO, Singh P, Anantharamaiah GM, Chait A, Brunzell J, Geary RL, Oram JF, and Heinecke JW. The myeloperoxidase product hypochlorous acid oxidizes HDL in the human artery wall and impairs ABCA1-dependent cholesterol transport. *Proc Natl Acad Sci U S A* 101: 13032–13037, 2004.
23. Bergt C, Reicher H, Malle E, and Sattler W. Hypochlorite modification of high density lipoprotein: effects on cholesterol efflux from J774 macrophages. *FEBS Lett* 452: 295–300, 1999.
24. Biffl WL, Moore EE, Moore FA, and Barnett C. Nitric oxide reduces endothelial expression of intercellular adhesion molecule (ICAM)-1. *J Surg Res* 63: 328–332, 1996.
25. Bolscher BG and Wever R. A kinetic study of the reaction between human myeloperoxidase, hydroperoxides and cyanide. Inhibition by chloride and thiocyanate. *Biochim Biophys Acta* 788: 1–10, 1984.
26. Booth KS, Kimura S, Lee HC, Ikeda-Saito M, and Caughey WS. Bovine myeloperoxidase and lactoperoxidase each contain a high affinity site for calcium. *Biochem Biophys Res Commun* 160: 897–902, 1989.
27. Bos A, Wever R, and Roos D. Characterization and quantification of the peroxidase in human monocytes. *Biochim Biophys Acta* 525: 37–44, 1978.
28. Brennan ML, Anderson MM, Shih DM, Qu XD, Wang X, Mehta AC, Lim LL, Shi W, Hazen SL, Jacob JS, Crowley JR, Heinecke JW, and Lusis AJ. Increased atherosclerosis in myeloperoxidase-deficient mice. *J Clin Invest* 107: 419–430, 2001.
29. Brennan ML, Penn MS, Van LF, Nambi V, Shishehbor MH, Aviles RJ, Goormastic M, Pepoy ML, McErlean ES, Topol EJ, Nissen SE, and Hazen SL. Prognostic value of myeloperoxidase in patients with chest pain. *N Engl J Med* 349: 1595–1604, 2003.
30. Brinkmann V, Reichard U, Goosmann C, Fauler B, Uhlemann Y, Weiss DS, Weinrauch Y, and Zychlinsky A. Neutrophil extracellular traps kill bacteria. *Science* 303: 1532–1535, 2004.
31. Brinkmann V and Zychlinsky A. Beneficial suicide: why neutrophils die to make NETs. *Nat Rev Microbiol* 5: 577–582, 2007.
32. Brugger-Andersen T, Aarsetoy H, Grundt H, Staines H, and Nilsen DW. The long-term prognostic value of multiple biomarkers following a myocardial infarction. *Thromb Res* 123: 60–66, 2008.
33. Buffon A, Biasucci LM, Liuzzo G, D'Onofrio G, Crea F, and Maseri A. Widespread coronary inflammation in unstable angina. *N Engl J Med* 347: 5–12, 2002.
34. Bulow E, Nauseef WM, Goedken M, McCormick S, Calafat J, Gullberg U, and Olsson I. Sorting for storage in myeloid cells of nonmyeloid proteins and chimeras with the propeptide of myeloperoxidase precursor. *J Leukoc Biol* 71: 279–288, 2002.
35. Burner U, Furtmuller PG, Kettle AJ, Koppenol WH, and Obinger C. Mechanism of reaction of myeloperoxidase with nitrite. *J Biol Chem* 275: 20597–20601, 2000.
36. Burner U, Obinger C, Paumann M, Furtmuller PG, and Kettle AJ. Transient and steady-state kinetics of the oxidation of substituted benzoic acid hydrazides by myeloperoxidase. *J Biol Chem* 274: 9494–9502, 1999.
37. Campuzano O, Castillo-Ruiz MM, Acarin L, Gonzalez B, and Castellano B. Decreased myeloperoxidase expressing cells in the aged rat brain after excitotoxic damage. *Exp Gerontol* 46: 723–730, 2011.
38. Cavusoglu E, Ruwende C, Eng C, Chopra V, Yanamadala S, Clark LT, Pinsky DJ, and Marmur JD. Usefulness of baseline plasma myeloperoxidase levels as an independent predictor of myocardial infarction at two years in patients presenting with acute coronary syndrome. *Am J Cardiol* 99: 1364–1368, 2007.
39. Chang CY, Song MJ, Jeon SB, Yoon HJ, Lee DK, Kim IH, Suk K, Choi DK, and Park EJ. Dual functionality of myeloperoxidase in rotenone-exposed brain-resident immune cells. *Am J Pathol* 179: 964–979, 2011.
40. Chang LT, Chua S, Sheu JJ, Wu CJ, Yeh KH, Yang CH, and Yip HK. Level and prognostic value of serum myeloperoxidase in patients with acute myocardial infarction undergoing primary percutaneous coronary intervention. *Circ J* 73: 726–731, 2009.
41. Chapman AL, Hampton MB, Senthilmohan R, Winterbourn CC, and Kettle AJ. Chlorination of bacterial and neutrophil proteins during phagocytosis and killing of *Staphylococcus aureus*. *J Biol Chem* 277: 9757–9762, 2002.
42. Chapman AL, Morrissey BM, Vasu VT, Juarez MM, Houghton JS, Li CS, Cross CE, and Eiserich JP. Myeloperoxidase-dependent oxidative metabolism of nitric oxide in the cystic fibrosis airway. *J Cyst Fibros* 9: 84–92, 2010.
43. Chapman AL, Skaff O, Senthilmohan R, Kettle AJ, and Davies MJ. Hypobromous acid and bromamine production by neutrophils and modulation by superoxide. *Biochem J* 417: 773–781, 2009.
44. Chen J, Fu X, Wang Y, Ling M, McMullen B, Kulman J, Chung DW, and Lopez JA. Oxidative modification of von Willebrand factor by neutrophil oxidants inhibits its cleavage by ADAMTS13. *Blood* 115: 706–712, 2010.
45. Clark SR, Ma AC, Tavener SA, McDonald B, Goodarzi Z, Kelly MM, Patel KD, Chakrabarti S, McAvoy E, Sinclair GD, Keys EM, len-Vercoe E, Devinney R, Doig CJ, Green FH, and Kubes P. Platelet TLR4 activates neutrophil extracellular traps to ensnare bacteria in septic blood. *Nat Med* 13: 463–469, 2007.
46. Curtis MP, Hicks AJ, and Neidigh JW. Kinetics of 3-chlorotyrosine formation and loss due to hypochlorous acid and chloramines. *Chem Res Toxicol* 24: 418–428, 2011.
47. Daphna EM, Michaela S, Eynat P, Irit A, and Rimon S. Association of myeloperoxidase with heparin: oxidative inactivation of proteins on the surface of endothelial cells by the bound enzyme. *Mol Cell Biochem* 183: 55–61, 1998.
48. David A, Kacher Y, Specks U, and Aviram I. Interaction of proteinase 3 with CD11b/CD18 (beta2 integrin) on the cell membrane of human neutrophils. *J Leukoc Biol* 74: 551–557, 2003.
49. Davies MJ. Myeloperoxidase-derived oxidation: mechanisms of biological damage and its prevention. *J Clin Biochem Nutr* 48: 8–19, 2011.

50. Davies MJ, Hawkins CL, Pattison DI, and Rees MD. Mammalian heme peroxidases: from molecular mechanisms to health implications. *Antioxid Redox Signal* 10: 1199–1234, 2008.
51. de Jong S, van Veen TA, van Rijen HV, and de Bakker JM. Fibrosis and cardiac arrhythmias. *J Cardiovasc Pharmacol* 57: 630–638, 2011.
52. Dever GJ, Benson R, Wainwright CL, Kennedy S, and Spickett CM. Phospholipid chlorohydrin induces leukocyte adhesion to ApoE-/- mouse arteries via upregulation of P-selectin. *Free Radic Biol Med* 44: 452–463, 2008.
53. Devitt A and Marshall LJ. The innate immune system and the clearance of apoptotic cells. *J Leukoc Biol* 90: 447–457, 2011.
54. Dominguez-Rodriguez A, Samimi-Fard S, Abreu-Gonzalez P, Garcia-Gonzalez MJ, and Kaski JC. Prognostic value of admission myeloperoxidase levels in patients with ST-segment elevation myocardial infarction and cardiogenic shock. *Am J Cardiol* 101: 1537–1540, 2008.
55. Dri P, Cramer R, Menegazzi R, and Patriarca P. Increased degranulation of human myeloperoxidase-deficient polymorphonuclear leucocytes. *Br J Haematol* 59: 115–125, 1985.
56. Eggers KM, Dellborg M, Johnston N, Oldgren J, Swahn E, Venge P, and Lindahl B. Myeloperoxidase is not useful for the early assessment of patients with chest pain. *Clin Biochem* 43: 240–245, 2010.
57. Eiserich JP, Baldus S, Brennan ML, Ma W, Zhang C, Tousson A, Castro L, Lusis AJ, Nauseef WM, White CR, and Freeman BA. Myeloperoxidase, a leukocyte-derived vascular NO oxidase. *Science* 296: 2391–2394, 2002.
58. Eiserich JP, Hristova M, Cross CE, Jones AD, Freeman BA, Halliwell B, and Van der Vliet A. Formation of nitric oxide-derived inflammatory oxidants by myeloperoxidase in neutrophils. *Nature* 391: 393–397, 1998.
59. El Kebir D, Jozsef L, Pan W, and Filep JG. Myeloperoxidase delays neutrophil apoptosis through CD11b/CD18 integrins and prolongs inflammation. *Circ Res* 103: 352–359, 2008.
60. El Kebir D, Jozsef L, Pan W, Wang L, Petasis NA, Serhan CN, and Filep JG. 15-epi-lipoxin A4 inhibits myeloperoxidase signaling and enhances resolution of acute lung injury. *Am J Respir Crit Care Med* 180: 311–319, 2009.
61. Ermak N, Lacour B, Drueke TB, and Vicca S. Role of reactive oxygen species and Bax in oxidized low density lipoprotein-induced apoptosis of human monocytes. *Atherosclerosis* 200: 247–256, 2008.
62. Farrell AJ, Blake DR, Palmer RM, and Moncada S. Increased concentrations of nitrite in synovial fluid and serum samples suggest increased nitric oxide synthesis in rheumatic diseases. *Ann Rheum Dis* 51: 1219–1222, 1992.
63. Fenna R, Zeng J, and Davey C. Structure of the green heme in myeloperoxidase. *Arch Biochem Biophys* 316: 653–656, 1995.
64. Fiedler TJ, Davey CA, and Fenna RE. X-ray crystal structure and characterization of halide-binding sites of human myeloperoxidase at 1.8 A resolution. *J Biol Chem* 275: 11964–11971, 2000.
65. Furtmuller PG, Arnhold J, Jantschko W, Pichler H, and Obinger C. Redox properties of the couples compound I/compound II and compound II/native enzyme of human myeloperoxidase. *Biochem Biophys Res Commun* 301: 551–557, 2003.
66. Furtmuller PG, Jantschko W, Zederbauer M, Jakopitsch C, Arnhold J, and Obinger C. Kinetics of interconversion of redox intermediates of lactoperoxidase, eosinophil peroxidase and myeloperoxidase. *Jpn J Infect Dis* 57: S30–S31, 2004.
67. Furtmuller PG, Zederbauer M, Jantschko W, Helm J, Bogner M, Jakopitsch C, and Obinger C. Active site structure and catalytic mechanisms of human peroxidases. *Arch Biochem Biophys* 445: 199–213, 2006.
68. Gelderman MP, Stuart R, Vigerust D, Fuhrmann S, Lefkowitz DL, Allen RC, Lefkowitz SS, and Graham S. Perpetuation of inflammation associated with experimental arthritis: the role of macrophage activation by neutrophilic myeloperoxidase. *Mediators Inflamm* 7: 381–389, 1998.
69. Gomez-Mejiba SE, Zhai Z, Gimenez MS, Ashby MT, Chilakapati J, Kitchin K, Mason RP, and Ramirez DC. Myeloperoxidase-induced genomic DNA-centered radicals. *J Biol Chem* 285: 20062–20071, 2010.
70. Grattendick K, Stuart R, Roberts E, Lincoln J, Lefkowitz SS, Bollen A, Moguilevsky N, Friedman H, and Lefkowitz DL. Alveolar macrophage activation by myeloperoxidase: a model for exacerbation of lung inflammation. *Am J Respir Cell Mol Biol* 26: 716–722, 2002.
71. Green PS, Mendez AJ, Jacob JS, Crowley JR, Growdon W, Hyman BT, and Heinecke JW. Neuronal expression of myeloperoxidase is increased in Alzheimer's disease. *J Neurochem* 90: 724–733, 2004.
72. Gumiero A, Metcalfe CL, Pearson AR, Raven EL, and Moody PC. Nature of the ferryl heme in compounds I and II. *J Biol Chem* 286: 1260–1268, 2011.
73. Gupta AK, Hasler P, Holzgreve W, Gebhardt S, and Hahn S. Induction of neutrophil extracellular DNA lattices by placental microparticles and IL-8 and their presence in preeclampsia. *Hum Immunol* 66: 1146–1154, 2005.
74. Haegens A, Heeringa P, van Suylen RJ, Steele C, Aratani Y, O'Donoghue RJ, Mutsaers SE, Mossman BT, Wouters EF, and Vernooy JH. Myeloperoxidase deficiency attenuates lipopolysaccharide-induced acute lung inflammation and subsequent cytokine and chemokine production. *J Immunol* 182: 7990–7996, 2009.
75. Hagiwara N. Inflammation and atrial fibrillation. *Circ J* 74: 246–247, 2010.
76. Hakkim A, Furnrohr BG, Amann K, Laube B, Abu AU, Brinkmann V, Herrmann M, Voll RE, and Zychlinsky A. Impairment of neutrophil extracellular trap degradation is associated with lupus nephritis. *Proc Natl Acad Sci U S A* 107: 9813–9818, 2010.
77. Hampton MB, Kettle AJ, and Winterbourn CC. Inside the neutrophil phagosome: oxidants, myeloperoxidase, and bacterial killing. *Blood* 92: 3007–3017, 1998.
78. Hansson M, Olsson I, and Nauseef WM. Biosynthesis, processing, and sorting of human myeloperoxidase. *Arch Biochem Biophys* 445: 214–224, 2006.
79. Hawkins CL, Pattison DI, and Davies MJ. Hypochlorite-induced oxidation of amino acids, peptides and proteins. *Amino Acids* 25: 259–274, 2003.
80. Hazell LJ, Arnold L, Flowers D, Waeg G, Malle E, and Stocker R. Presence of hypochlorite-modified proteins in human atherosclerotic lesions. *J Clin Invest* 97: 1535–1544, 1996.
81. Hazell LJ and Stocker R. Oxidation of low-density lipoprotein with hypochlorite causes transformation of the lipoprotein into a high-uptake form for macrophages. *Biochem J* 290 (Pt 1): 165–172, 1993.
82. Hazen SL. Neutrophils, hypercholesterolemia, and atherogenesis. *Circulation* 122: 1786–1788, 2010.

83. Hazen SL and Heinecke JW. 3-Chlorotyrosine, a specific marker of myeloperoxidase-catalyzed oxidation, is markedly elevated in low density lipoprotein isolated from human atherosclerotic intima. *J Clin Invest* 99: 2075–2081, 1997.
84. Hazen SL, Hsu FF, Mueller DM, Crowley JR, and Heinecke JW. Human neutrophils employ chlorine gas as an oxidant during phagocytosis. *J Clin Invest* 98: 1283–1289, 1996.
85. Hazen SL, Zhang R, Shen Z, Wu W, Podrez EA, MacPherson JC, Schmitt D, Mitra SN, Mukhopadhyay C, Chen Y, Cohen PA, Hoff HF, and Abu-Soud HM. Formation of nitric oxide-derived oxidants by myeloperoxidase in monocytes: pathways for monocyte-mediated protein nitration and lipid peroxidation *in vivo*. *Circ Res* 85: 950–958, 1999.
86. Heslop CL, Frohlich JJ, and Hill JS. Myeloperoxidase and C-reactive protein have combined utility for long-term prediction of cardiovascular mortality after coronary angiography. *J Am Coll Cardiol* 55: 1102–1109, 2010.
87. Hirche TO, Gaut JP, Heinecke JW, and Belaaouaj A. Myeloperoxidase plays critical roles in killing *Klebsiella pneumoniae* and inactivating neutrophil elastase: effects on host defense. *J Immunol* 174: 1557–1565, 2005.
88. Hoy A, Leininger-Muller B, Kutter D, Siest G, and Visvikis S. Growing significance of myeloperoxidase in non-infectious diseases. *Clin Chem Lab Med* 40: 2–8, 2002.
89. Ikeda-Saito M. Spectroscopic, ligand binding, and enzymatic properties of the spleen green hemeprotein. A comparison with myeloperoxidase. *J Biol Chem* 260: 11688–11696, 1985.
90. Ikeda-Saito M, Lee HC, Adachi K, Eck HS, Prince RC, Booth KS, Caughey WS, and Kimura S. Demonstration that spleen green hemeprotein is identical to granulocyte myeloperoxidase. *J Biol Chem* 264: 4559–4563, 1989.
91. Ishii Y, Schuessler RB, Gaynor SL, Yamada K, Fu AS, Boineau JP, and Damiano RJ, Jr. Inflammation of atrium after cardiac surgery is associated with inhomogeneity of atrial conduction and atrial fibrillation. *Circulation* 111: 2881–2888, 2005.
92. Jantschko W, Furtmuller PG, Zederbauer M, Jakopitsch C, and Obinger C. Kinetics of oxygen binding to ferrous myeloperoxidase. *Arch Biochem Biophys* 426: 91–97, 2004.
93. Jantschko W, Furtmuller PG, Zederbauer M, Neugschwandtner K, Lehner I, Jakopitsch C, Arnhold J, and Obinger C. Exploitation of the unusual thermodynamic properties of human myeloperoxidase in inhibitor design. *Biochem Pharmacol* 69: 1149–1157, 2005.
94. Jiang Q, Griffin DA, Barofsky DF, and Hurst JK. Intraphagosomal chlorination dynamics and yields determined using unique fluorescent bacterial mimics. *Chem Res Toxicol* 10: 1080–1089, 1997.
95. Jiang Q and Hurst JK. Relative chlorinating, nitrating, and oxidizing capabilities of neutrophils determined with phagocytosable probes. *J Biol Chem* 272: 32767–32772, 1997.
96. Johansson MW, Patarroyo M, Oberg F, Siegbahn A, and Nilsson K. Myeloperoxidase mediates cell adhesion via the alpha(m)beta(2) integrin (mac-1, cd11b/cd18). *J Cell Sci* 110: 1133–1139, 1997.
97. Johnson RJ, Guggenheim SJ, Klebanoff SJ, Ochi RF, Wass A, Baker P, Schulze M, and Couser WG. Morphologic correlates of glomerular oxidant injury induced by the myeloperoxidase-hydrogen peroxide-halide system of the neutrophil. *Lab Invest* 58: 294–301, 1988.
98. Kanayama A and Miyamoto Y. Apoptosis triggered by phagocytosis-related oxidative stress through FLIPS down-regulation and JNK activation. *J Leukoc Biol* 82: 1344–1352, 2007.
99. Kang JI, Jr. and Neidigh JW. Hypochlorous acid damages histone proteins forming 3-chlorotyrosine and 3,5-dichlorotyrosine. *Chem Res Toxicol* 21: 1028–1038, 2008.
100. Kennedy AD and Deleo FR. Neutrophil apoptosis and the resolution of infection. *Immunol Res* 43: 25–61, 2009.
101. Kessenbrock K, Krumbholz M, Schonermarck U, Back W, Gross WL, Werb Z, Grone HJ, Brinkmann V, and Jenne DE. Netting neutrophils in autoimmune small-vessel vasculitis. *Nat Med* 15: 623–625, 2009.
102. Kettle AJ. Neutrophils convert tyrosyl residues in albumin to chlorotyrosine. *FEBS Lett* 379: 103–106, 1996.
103. Kettle AJ, Anderson RF, Hampton MB, and Winterbourn CC. Reactions of superoxide with myeloperoxidase. *Biochemistry* 46: 4888–4897, 2007.
104. Kettle AJ and Winterbourn CC. Superoxide modulates the activity of myeloperoxidase and optimizes the production of hypochlorous acid. *Biochem J* 252: 529–536, 1988.
105. Khan IA. Atrial fibrillation: interaction between the trigger and the substrate. *Int J Cardiol* 87: 301–302, 2003.
106. Khan SQ, Kelly D, Quinn P, Davies JE, and Ng LL. Myeloperoxidase aids prognostication together with N-terminal pro-B-type natriuretic peptide in high-risk patients with acute ST elevation myocardial infarction. *Heart* 93: 826–831, 2007.
107. King CC, Jefferson MM, and Thomas EL. Secretion and inactivation of myeloperoxidase by isolated neutrophils. *J Leukoc Biol* 61: 293–302, 1997.
108. Klebanoff SJ. Myeloperoxidase: contribution to the microbicidal activity of intact leukocytes. *Science* 169: 1095–1097, 1970.
109. Klebanoff SJ. Myeloperoxidase: friend and foe. *J Leukoc Biol* 77: 598–625, 2005.
110. Klebanoff SJ, Kinsella MG, and Wight TN. Degradation of endothelial cell matrix heparan sulfate proteoglycan by elastase and the myeloperoxidase-H_2O_2-chloride system. *Am J Pathol* 143: 907–917, 1993.
111. Klinke A, Nussbaum C, Kubala L, Friedrichs K, Rudolph TK, Rudolph V, Paust HJ, Schroder C, Benten D, Lau D, Szocs K, Furtmuller PG, Heeringa P, Sydow K, Duchstein HJ, Ehmke H, Schumacher U, Meinertz T, Sperandio M, and Baldus S. Myeloperoxidase attracts neutrophils by physical forces. *Blood* 117: 1350–1358, 2011.
112. Kooter IM, Koehler BP, Moguilevsky N, Bollen A, Wever R, and Johnson MK. The Met243 sulfonium ion linkage is responsible for the anomalous magnetic circular dichroism and optical spectral properties of myeloperoxidase. *J Biol Inorg Chem* 4: 684–691, 1999.
113. Kooter IM, Moguilevsky N, Bollen A, Sijtsema NM, Otto C, Dekker HL, and Wever R. Characterization of the Asp94 and Glu242 mutants in myeloperoxidase, the residues linking the heme group via ester bonds. *Eur J Biochem* 264: 211–217, 1999.
114. Kubala L, Lu G, Baldus S, Berglund L, and Eiserich JP. Plasma levels of myeloperoxidase are not elevated in patients with stable coronary artery disease. *Clin Chim Acta* 394: 59–62, 2008.
115. Kubala L, Schmelzer KR, Klinke A, Kolarova H, Baldus S, Hammock BD, and Eiserich JP. Modulation of arachidonic and linoleic acid metabolites in myeloperoxidase-deficient mice during acute inflammation. *Free Radic Biol Med* 48: 1311–1320, 2010.
116. Kubes P, Sihota E, and Hickey MJ. Endogenous but not exogenous nitric oxide decreases TNF-alpha- induced leukocyte rolling. *Am J Physiol* 36: G 628–G 635, 1997.

117. Kutter D, Devaquet P, Vanderstocken G, Paulus JM, Marchal V, and Gothot A. Consequences of total and subtotal myeloperoxidase deficiency: risk or benefit? *Acta Haematol* 104: 10–15, 2000.
118. Lane AE, Tan JT, Hawkins CL, Heather AK, and Davies MJ. The myeloperoxidase-derived oxidant HOSCN inhibits protein tyrosine phosphatases and modulates cell signalling via the mitogen-activated protein kinase (MAPK) pathway in macrophages. *Biochem J* 430: 161–169, 2010.
119. Lanza F. Clinical manifestation of myeloperoxidase deficiency. *J Mol Med (Berl)* 76: 676–681, 1998.
120. Lau D and Baldus S. Myeloperoxidase and its contributory role in inflammatory vascular disease. *Pharmacol Ther* 111: 16–26, 2006.
121. Lau D, Mollnau H, Eiserich JP, Freeman BA, Daiber A, Gehling UM, Brummer J, Rudolph V, Munzel T, Heitzer T, Meinertz T, and Baldus S. Myeloperoxidase mediates neutrophil activation by association with CD11b/CD18 integrins. *Proc Natl Acad Sci U S A* 102: 431–436, 2005.
122. Leeuwenburgh C, Hardy MM, Hazen SL, Wagner P, Ohishi S, Steinbrecher UP, and Heinecke JW. Reactive nitrogen intermediates promote low density lipoprotein oxidation in human atherosclerotic intima. *J Biol Chem* 272: 1433–1436, 1997.
123. Lefkowitz DL, Gelderman MP, Fuhrmann SR, Graham S, Starnes JD, III, Lefkowitz SS, Bollen A, and Moguilevsky N. Neutrophilic myeloperoxidase-macrophage interactions perpetuate chronic inflammation associated with experimental arthritis. *Clin Immunol* 91: 145–155, 1999.
124. Lefkowitz DL and Lefkowitz SS. Macrophage-neutrophil interaction: a paradigm for chronic inflammation revisited. *Immunol Cell Biol* 79: 502–506, 2001.
125. Lefkowitz DL and Lefkowitz SS. Microglia and myeloperoxidase: a deadly partnership in neurodegenerative disease. *Free Radic Biol Med* 45: 726–731, 2008.
126. Lefkowitz DL, Lincoln JA, Lefkowitz SS, Bollen A, and Moguilevsky N. Enhancement of macrophage-mediated bactericidal activity by macrophage-mannose receptor-ligand interaction. *Immunol Cell Biol* 75: 136–141, 1997.
127. Lefkowitz DL, Mills K, Morgan D, and Lefkowitz SS. Macrophage activation and immunomodulation by myeloperoxidase. *Proc Soc Exp Biol Med* 199: 204–210, 1992.
128. Lefkowitz DL, Roberts E, Grattendick K, Schwab C, Stuart R, Lincoln J, Allen RC, Moguilevsky N, Bollen A, and Lefkowitz SS. The endothelium and cytokine secretion: the role of peroxidases as immunoregulators. *Cell Immunol* 202: 23–30, 2000.
129. Lefkowitz SS, Gelderman MP, Lefkowitz DL, Moguilevsky N, and Bollen A. Phagocytosis and intracellular killing of *Candida albicans* by macrophages exposed to myeloperoxidase. *J Infect Dis* 173: 1202–1207, 1996.
130. Lehrer RI, Hanifin J, and Cline MJ. Defective bactericidal activity in myeloperoxidase-deficient human neutrophils. *Nature* 223: 78–79, 1969.
131. Ley K, Laudanna C, Cybulsky MI, and Nourshargh S. Getting to the site of inflammation: the leukocyte adhesion cascade updated. *Nat Rev Immunol* 7: 678–689, 2007.
132. Lloyd MM, van Reyk DM, Davies MJ, and Hawkins CL. Hypothiocyanous acid is a more potent inducer of apoptosis and protein thiol depletion in murine macrophage cells than hypochlorous acid or hypobromous acid. *Biochem J* 414: 271–280, 2008.
133. Locksley RM, Nelson CS, Fankhauser JE, and Klebanoff SJ. Loss of granule myeloperoxidase during *in vitro* culture of human monocytes correlates with decay in antiprotozoa activity. *Am J Trop Med Hyg* 36: 541–548, 1987.
134. Lopes F, Coelho FM, Costa VV, Vieira EL, Sousa LP, Silva TA, Vieira LQ, Teixeira MM, and Pinho V. Resolution of neutrophilic inflammation by H_2O_2 in antigen-induced arthritis. *Arthritis Rheum* 63: 2651–2660, 2011.
135. Maitra D, Banerjee J, Shaeib F, Souza CE, and Abu-Soud HM. Melatonin can mediate its vascular protective effect by modulating free iron level by inhibiting hypochlorous acid-mediated hemoprotein heme destruction. *Hypertension* 57: e22, 2011.
136. Maki RA, Tyurin VA, Lyon RC, Hamilton RL, DeKosky ST, Kagan VE, and Reynolds WF. Aberrant expression of myeloperoxidase in astrocytes promotes phospholipid oxidation and memory deficits in a mouse model of Alzheimer disease. *J Biol Chem* 284: 3158–3169, 2009.
137. Manzenreiter R, Kienberger F, Marcos V, Schilcher K, Krautgartner WD, Obermayer A, Huml M, Stoiber W, Hector A, Griese M, Hannig M, Studnicka M, Vitkov L, and Hartl D. Ultrastructural characterization of cystic fibrosis sputum using atomic force and scanning electron microscopy. *J Cyst Fibros* 11: 84–92, 2012.
138. Marquez LA and Dunford HB. Cyanide binding to canine myeloperoxidase. *Biochem Cell Biol* 67: 187–191, 1989.
139. Marquez LA and Dunford HB. Kinetics of oxidation of tyrosine and dityrosine by myeloperoxidase compounds I and II. Implications for lipoprotein peroxidation studies. *J Biol Chem* 270: 30434–30440, 1995.
140. Marquez LA, Huang JT, and Dunford HB. Spectral and kinetic studies on the formation of myeloperoxidase compounds I and II: roles of hydrogen peroxide and superoxide. *Biochemistry* 33: 1447–1454, 1994.
141. Matthijsen RA, Huugen D, Hoebers NT, de VB, Peutz-Kootstra CJ, Aratani Y, Daha MR, Tervaert JW, Buurman WA, and Heeringa P. Myeloperoxidase is critically involved in the induction of organ damage after renal ischemia reperfusion. *Am J Pathol* 171: 1743–1752, 2007.
142. McMillen TS, Heinecke JW, and LeBoeuf RC. Expression of human myeloperoxidase by macrophages promotes atherosclerosis in mice. *Circulation* 111: 2798–2804, 2005.
143. Meotti FC, Jameson GN, Turner R, Harwood DT, Stockwell S, Rees MD, Thomas SR, and Kettle AJ. Urate as a physiological substrate for myeloperoxidase: implications for hyperuricemia and inflammation. *J Biol Chem* 286: 12901–12911, 2011.
144. Metzler KD, Fuchs TA, Nauseef WM, Reumaux D, Roesler J, Schulze I, Wahn V, Papayannopoulos V, and Zychlinsky A. Myeloperoxidase is required for neutrophil extracellular trap formation: implications for innate immunity. *Blood* 117: 953–959, 2011.
145. Meuwese MC, Stroes ES, Hazen SL, van Miert JN, Kuivenhoven JA, Schaub RG, Wareham NJ, Luben R, Kastelein JJ, Khaw KT, and Boekholdt SM. Serum myeloperoxidase levels are associated with the future risk of coronary artery disease in apparently healthy individuals: the EPIC-Norfolk Prospective Population Study. *J Am Coll Cardiol* 50: 159–165, 2007.
146. Midwinter RG, Vissers MC, and Winterbourn CC. Hypochlorous acid stimulation of the mitogen-activated protein kinase pathway enhances cell survival. *Arch Biochem Biophys* 394: 13–20, 2001.
147. Mocatta TJ, Pilbrow AP, Cameron VA, Senthilmohan R, Frampton CM, Richards AM, and Winterbourn CC. Plasma concentrations of myeloperoxidase predict mortal-

ity after myocardial infarction. *J Am Coll Cardiol* 49: 1993–2000, 2007.
148. Morrow DA, Sabatine MS, Brennan ML, de Lemos JA, Murphy SA, Ruff CT, Rifai N, Cannon CP, and Hazen SL. Concurrent evaluation of novel cardiac biomarkers in acute coronary syndrome: myeloperoxidase and soluble CD40 ligand and the risk of recurrent ischaemic events in TACTICS-TIMI 18. *Eur Heart J* 29: 1096–1102, 2008.
149. Mott JD and Werb Z. Regulation of matrix biology by matrix metalloproteinases. *Curr Opin Cell Biol* 16: 558–564, 2004.
150. Murphy EJ, Marechal A, Segal AW, and Rich PR. CO binding and ligand discrimination in human myeloperoxidase. *Biochemistry* 49: 2150–2158, 2010.
151. Nakazato T, Sagawa M, Yamato K, Xian M, Yamamoto T, Suematsu M, Ikeda Y, and Kizaki M. Myeloperoxidase is a key regulator of oxidative stress mediated apoptosis in myeloid leukemic cells. *Clin Cancer Res* 13: 5436–5445, 2007.
152. Narasaraju T, Yang E, Samy RP, Ng HH, Poh WP, Liew AA, Phoon MC, van RN, and Chow VT. Excessive neutrophils and neutrophil extracellular traps contribute to acute lung injury of influenza pneumonitis. *Am J Pathol* 179: 199–210, 2011.
153. Nauseef WM. Insights into myeloperoxidase biosynthesis from its inherited deficiency. *J Mol Med (Berl)* 76: 661–668, 1998.
154. Nauseef WM. Contributions of myeloperoxidase to proinflammatory events: more than an antimicrobial system. *Int J Hematol* 74: 125–133, 2001.
155. Nauseef WM, Cogley M, and McCormick S. Effect of the R569W missense mutation on the biosynthesis of myeloperoxidase. *J Biol Chem* 271: 9546–9549, 1996.
156. Nauseef WM, Root RK, Newman SL, and Malech HL. Inhibition of zymosan activation of human neutrophil oxidative metabolism by a mouse monoclonal antibody. *Blood* 62: 635, 1983.
157. Ndrepepa G, Braun S, Mehilli J, von BN, Schomig A, and Kastrati A. Myeloperoxidase level in patients with stable coronary artery disease and acute coronary syndromes. *Eur J Clin Invest* 38: 90–96, 2008.
158. Neve J, Parij N, and Moguilevsky N. Inhibition of the myeloperoxidase chlorinating activity by non-steroidal anti-inflammatory drugs investigated with a human recombinant enzyme. *Eur J Pharmacol* 417: 37–43, 2001.
159. Ng LL, Pathik B, Loke IW, Squire IB, and Davies JE. Myeloperoxidase and C-reactive protein augment the specificity of B-type natriuretic peptide in community screening for systolic heart failure. *Am Heart J* 152: 94–101, 2006.
160. Nicholls SJ, Cutri B, Worthley SG, Kee P, Rye KA, Bao S, and Barter PJ. Impact of short-term administration of high-density lipoproteins and atorvastatin on atherosclerosis in rabbits. *Arterioscler Thromb Vasc Biol* 25: 2416–2421, 2005.
161. Nicholls SJ, Zheng L, and Hazen SL. Formation of dysfunctional high-density lipoprotein by myeloperoxidase. *Trends Cardiovasc Med* 15: 212–219, 2005.
162. Odell EW and Segal AW. The bactericidal effects of the respiratory burst and the myeloperoxidase system isolated in neutrophil cytoplasts. *Biochim Biophys Acta* 971: 266–274, 1988.
163. Ogino T, Ozaki M, Hosako M, Omori M, Okada S, and Matsukawa A. Activation of c-Jun N-terminal kinase is essential for oxidative stress-induced Jurkat cell apoptosis by monochloramine. *Leuk Res* 33: 151–158, 2009.
164. Papayannopoulos V, Metzler KD, Hakkim A, and Zychlinsky A. Neutrophil elastase and myeloperoxidase regulate the formation of neutrophil extracellular traps. *J Cell Biol* 191: 677–691, 2010.
165. Pattison DI, Hawkins CL, and Davies MJ. Hypochlorous acid-mediated oxidation of lipid components and antioxidants present in low-density lipoproteins: absolute rate constants, product analysis, and computational modeling. *Chem Res Toxicol* 16: 439–449, 2003.
166. Pattison DI, Hawkins CL, and Davies MJ. What are the plasma targets of the oxidant hypochlorous acid? A kinetic modeling approach. *Chem Res Toxicol* 22: 807–817, 2009.
167. Pennathur S, Bergt C, Shao B, Byun J, Kassim SY, Singh P, Green PS, McDonald TO, Brunzell J, Chait A, Oram JF, O'Brien K, Geary RL, and Heinecke JW. Human atherosclerotic intima and blood of patients with established coronary artery disease contain high density lipoprotein damaged by reactive nitrogen species. *J Biol Chem* 279: 42977–42983, 2004.
168. Podrez EA, Schmitt D, Hoff HF, and Hazen SL. Myeloperoxidase-generated reactive nitrogen species convert LDL into an atherogenic form *in vitro*. *J Clin Invest* 103: 1547–1560, 1999.
169. Proteasa G, Tahboub YR, Galijasevic S, Raushel FM, and Abu-Soud HM. Kinetic evidence supports the existence of two halide binding sites that have a distinct impact on the heme iron microenvironment in myeloperoxidase. *Biochemistry* 46: 398–405, 2007.
170. Queiroz RF, Vaz SM, and Augusto O. Inhibition of the chlorinating activity of myeloperoxidase by tempol: revisiting the kinetics and mechanisms. *Biochem J* 439: 423–431, 2011.
171. Radi R. Nitric oxide, oxidants, and protein tyrosine nitration. *Proc Natl Acad Sci U S A* 101: 4003–4008, 2004.
172. Rausch PG and Moore TG. Granule enzymes of polymorphonuclear neutrophils: a phylogenetic comparison. *Blood* 46: 913–919, 1975.
173. Ravnsborg T, Houen G, and Hojrup P. The glycosylation of myeloperoxidase. *Biochim Biophys Acta* 1804: 2046–2053, 2010.
174. Rees MD, Whitelock JM, Malle E, Chuang CY, Iozzo RV, Nilasaroya A, and Davies MJ. Myeloperoxidase-derived oxidants selectively disrupt the protein core of the heparan sulfate proteoglycan perlecan. *Matrix Biol* 29: 63–73, 2010.
175. Reeves EP, Lu H, Jacobs HL, Messina CG, Bolsover S, Gabella G, Potma EO, Warley A, Roes J, and Segal AW. Killing activity of neutrophils is mediated through activation of proteases by K+ flux. *Nature* 416: 291–297, 2002.
176. Reeves EP, Nagl M, Godovac-Zimmermann J, and Segal AW. Reassessment of the microbicidal activity of reactive oxygen species and hypochlorous acid with reference to the phagocytic vacuole of the neutrophil granulocyte. *J Med Microbiol* 52: 643–651, 2003.
177. Reichlin T, Socrates T, Egli P, Potocki M, Breidthardt T, Arenja N, Meissner J, Noveanu M, Reiter M, Twerenbold R, Schaub N, Buser A, and Mueller C. Use of myeloperoxidase for risk stratification in acute heart failure. *Clin Chem* 56: 944–951, 2010.
178. Resch U, Semlitsch M, Hammer A, Susani-Etzerodt H, Walczak H, Sattler W, and Malle E. Hypochlorite-modified low-density lipoprotein induces the apoptotic machinery in Jurkat T-cell lines. *Biochem Biophys Res Commun* 410: 895–900, 2011.
179. Roman RM, Camargo PV, Borges FK, Rossini AP, and Polanczyk CA. Prognostic value of myeloperoxidase in coronary artery disease: comparison of unstable and stable angina patients. *Coron Artery Dis* 21: 129–136, 2010.

180. Rosen H and Klebanoff SJ. Chemiluminescence and superoxide production by myeloperoxidase-deficient leukocytes. *J Clin Invest* 58: 50–60, 1976.
181. Rosen H, Klebanoff SJ, Wang Y, Brot N, Heinecke JW, and Fu X. Methionine oxidation contributes to bacterial killing by the myeloperoxidase system of neutrophils. *Proc Natl Acad Sci U S A* 106: 18686–18691, 2009.
182. Rudolph TK, Wipper S, Reiter B, Rudolph V, Coym A, Detter C, Lau D, Klinke A, Friedrichs K, Rau T, Pekarova M, Russ D, Knoll K, Kolk M, Schroeder B, Wegscheider K, Andresen H, Schwedhelm E, Boeger R, Ehmke H, and Baldus S. Myeloperoxidase deficiency preserves vasomotor function in humans. *Eur Heart J* 33: 1625–1634, 2011.
183. Rudolph V, Andrie RP, Rudolph TK, Friedrichs K, Klinke A, Hirsch-Hoffmann B, Schwoerer AP, Lau D, Fu X, Klingel K, Sydow K, Didie M, Seniuk A, von Leitner EC, Szoecs K, Schrickel JW, Treede H, Wenzel U, Lewalter T, Nickenig G, Zimmermann WH, Meinertz T, Boger RH, Reichenspurner H, Freeman BA, Eschenhagen T, Ehmke H, Hazen SL, Willems S, and Baldus S. Myeloperoxidase acts as a profibrotic mediator of atrial fibrillation. *Nat Med* 16: 470–474, 2010.
184. Rudolph V, Rudolph TK, Hennings JC, Blankenberg S, Schnabel R, Steven D, Haddad M, Knittel K, Wende S, Wenzel J, Munzel T, Heitzer T, Meinertz T, Hubner C, and Baldus S. Activation of polymorphonuclear neutrophils in patients with impaired left ventricular function. *Free Radic Biol Med* 43: 1189–1196, 2007.
185. Rudolph V, Rudolph TK, Schopfer FJ, Bonacci G, Lau D, Szocs K, Klinke A, Meinertz T, Freeman BA, and Baldus S. Bivalirudin decreases NO bioavailability by vascular immobilization of myeloperoxidase. *J Pharmacol Exp Ther* 327: 324–331, 2008.
186. Sampson JB, Ye Y, Rosen H, and Beckman JS. Myeloperoxidase and horseradish peroxidase catalyze tyrosine nitration in proteins from nitrite and hydrogen peroxide. *Arch Biochem Biophys* 356: 207–213, 1998.
187. Sawicki M, Sypniewska G, Kozinski M, Gruszka M, Krintus M, Obonska K, Pilaczynska-Cemel M, and Kubica J. Diagnostic efficacy of myeloperoxidase for the detection of acute coronary syndromes. *Eur J Clin Invest* 41: 667–671, 2011.
188. Schewe T and Sies H. Myeloperoxidase-induced lipid peroxidation of LDL in the presence of nitrite. Protection by cocoa flavanols. *Biofactors* 24: 49–58, 2005.
189. Schindhelm RK and van der Zwan LP. Myeloperoxidase as a diagnostic and prognostic marker in cardiology: beware of pre-analytical factors that may influence results. *Int J Lab Hematol* 33: 332, 2011.
190. Schultz J and Kaminker K. Myeloperoxidase of the leucocyte of normal human blood. I. Content and localization. *Arch Biochem Biophys* 96: 465–467, 1962.
191. Scirica BM, Sabatine MS, Jarolim P, Murphy SA, de Lemos JL, Braunwald E, and Morrow DA. Assessment of multiple cardiac biomarkers in non-ST-segment elevation acute coronary syndromes: observations from the MERLIN-TIMI 36 trial. *Eur Heart J* 32: 697–705, 2011.
192. Segal AW. The electron transport chain of the microbicidal oxidase of phagocytic cells and its involvement in the molecular pathology of chronic granulomatous disease. *J Clin Invest* 83: 1785–1793, 1989.
193. Sinning C, Schnabel R, Peacock WF, and Blankenberg S. Up-and-coming markers: myeloperoxidase, a novel biomarker test for heart failure and acute coronary syndrome application? *Congest Heart Fail* 14: 46–48, 2008.
194. Soehnlein O, Lindbom L, and Weber C. Mechanisms underlying neutrophil-mediated monocyte recruitment. *Blood* 114: 4613–4623, 2009.
195. Soehnlein O, Weber C, and Lindbom L. Neutrophil granule proteins tune monocytic cell function. *Trends Immunol* 30: 538–546, 2009.
196. Soehnlein O, Xie X, Ulbrich H, Kenne E, Rotzius P, Flodgaard H, Eriksson EE, and Lindbom L. Neutrophil-derived heparin-binding protein (HBP/CAP37) deposited on endothelium enhances monocyte arrest under flow conditions. *J Immunol* 174: 6399–6405, 2005.
197. Spalteholz H, Furtmuller PG, Jakopitsch C, Obinger C, Schewe T, Sies H, and Arnhold J. Kinetic evidence for rapid oxidation of (-)-epicatechin by human myeloperoxidase. *Biochem Biophys Res Commun* 371: 810–813, 2008.
198. Spalteholz H, Panasenko OM, and Arnhold J. Formation of reactive halide species by myeloperoxidase and eosinophil peroxidase. *Arch Biochem Biophys* 445: 225–234, 2006.
199. Sperandio M. Selectins and glycosyltransferases in leukocyte rolling *in vivo*. *FEBS J* 273: 4377–4389, 2006.
200. Stendahl O, Coble BI, Dahlgren C, Hed J, and Molin L. Myeloperoxidase modulates the phagocytic activity of polymorphonuclear neutrophil leukocytes. Studies with cells from a myeloperoxidase-deficient patient. *J Clin Invest* 73: 366–373, 1984.
201. Sugiyama S, Okada Y, Sukhova GK, Virmani R, Heinecke JW, and Libby P. Macrophage myeloperoxidase regulation by granulocyte macrophage colony-stimulating factor in human atherosclerosis and implications in acute coronary syndromes. *Am J Pathol* 158: 879–891, 2001.
202. Sutton MG and Sharpe N. Left ventricular remodeling after myocardial infarction: pathophysiology and therapy. *Circulation* 101: 2981–2988, 2000.
203. Suzuki M, Asako H, Kubes P, Jennings S, Grisham MB, and Granger DN. Neutrophil-derived oxidants promote leukocyte adherence in postcapillary venules. *Microvasc Res* 42: 125–138, 1991.
204. Szuchman-Sapir AJ, Pattison DI, Davies MJ, and Witting PK. Site-specific hypochlorous acid-induced oxidation of recombinant human myoglobin affects specific amino acid residues and the rate of cytochrome b5-mediated heme reduction. *Free Radic Biol Med* 48: 35–46, 2010.
205. Tahboub YR, Galijasevic S, Diamond MP, and Abu-Soud HM. Thiocyanate modulates the catalytic activity of mammalian peroxidases. *J Biol Chem* 280: 26129–26136, 2005.
206. Tang WH, Brennan ML, Philip K, Tong W, Mann S, Van LF, and Hazen SL. Plasma myeloperoxidase levels in patients with chronic heart failure. *Am J Cardiol* 98: 796–799, 2006.
207. Tang WH, Katz R, Brennan ML, Aviles RJ, Tracy RP, Psaty BM, and Hazen SL. Usefulness of myeloperoxidase levels in healthy elderly subjects to predict risk of developing heart failure. *Am J Cardiol* 103: 1269–1274, 2009.
208. Tang WH, Tong W, Troughton RW, Martin MG, Shrestha K, Borowski A, Jasper S, Hazen SL, and Klein AL. Prognostic value and echocardiographic determinants of plasma myeloperoxidase levels in chronic heart failure. *J Am Coll Cardiol* 49: 2364–2370, 2007.
209. Tavora FR, Ripple M, Li L, and Burke AP. Monocytes and neutrophils expressing myeloperoxidase occur in fibrous caps and thrombi in unstable coronary plaques. *BMC Cardiovasc Disord* 9: 27, 2009.
210. Taylor KL, Strobel F, Yue KT, Ram P, Pohl J, Woods AS, and Kinkade JM, Jr. Isolation and identification of a protoheme IX

derivative released during autolytic cleavage of human myeloperoxidase. *Arch Biochem Biophys* 316: 635–642, 1995.
211. Tiden AK, Sjogren T, Svensson M, Bernlind A, Senthilmohan R, Auchere F, Norman H, Markgren PO, Gustavsson S, Schmidt S, Lundquist S, Forbes LV, Magon NJ, Paton LN, Jameson GN, Eriksson H, and Kettle AJ. 2-Thioxanthines are mechanism-based inactivators of myeloperoxidase that block oxidative stress during inflammation. *J Biol Chem* 286: 37578–37589, 2011.
212. Tien M. Myeloperoxidase-catalyzed oxidation of tyrosine. *Arch Biochem Biophys* 367: 61–66, 1999.
213. Tiruppathi C, Naqvi T, Wu Y, Vogel SM, Minshall RD, and Malik AB. Albumin mediates the transcytosis of myeloperoxidase by means of caveolae in endothelial cells. *Proc Natl Acad Sci U S A* 101: 7699–7704, 2004.
214. Tobler A, Miller CW, Johnson KR, Selsted ME, Rovera G, and Koeffler HP. Regulation of gene expression of myeloperoxidase during myeloid differentiation. *J Cell Physiol* 136: 215–225, 1988.
215. Torre D, Ferrario G, Speranza F, Orani A, Fiori GP, and Zeroli C. Serum concentrations of nitrite in patients with HIV-1 infection. *J Clin Pathol* 49: 574–576, 1996.
216. Tsimikas S and Miller YI. Oxidative modification of lipoproteins: mechanisms, role in inflammation and potential clinical applications in cardiovascular disease. *Curr Pharm Des* 17: 27–37, 2011.
217. Undurti A, Huang Y, Lupica JA, Smith JD, DiDonato JA, and Hazen SL. Modification of high density lipoprotein by myeloperoxidase generates a pro-inflammatory particle. *J Biol Chem* 284: 30825–30835, 2009.
218. Ungvari Z, Gupte SA, Recchia FA, Batkai S, and Pacher P. Role of oxidative-nitrosative stress and downstream pathways in various forms of cardiomyopathy and heart failure. *Curr Vasc Pharmacol* 3: 221–229, 2005.
219. Urban CF, Ermert D, Schmid M, bu-Abed U, Goosmann C, Nacken W, Brinkmann V, Jungblut PR, and Zychlinsky A. Neutrophil extracellular traps contain calprotectin, a cytosolic protein complex involved in host defense against *Candida albicans*. *PLoS Pathog* 5: e1000639, 2009.
220. Van AP, Slomianny MC, Boudjeltia KZ, Delporte C, Faid V, Calay D, Rousseau A, Moguilevsky N, Raes M, Vanhamme L, Furtmuller PG, Obinger C, Vanhaeverbeek M, Neve J, and Michalski JC. Glycosylation pattern of mature dimeric leukocyte and recombinant monomeric myeloperoxidase: glycosylation is required for optimal enzymatic activity. *J Biol Chem* 285: 16351–16359, 2010.
221. van Dalen CJ and Kettle AJ. Substrates and products of eosinophil peroxidase. *Biochem J* 358: 233–239, 2001.
222. van Dalen CJ, Whitehouse MW, Winterbourn CC, and Kettle AJ. Thiocyanate and chloride as competing substrates for myeloperoxidase. *Biochem J* 327 (Pt 2): 487–492, 1997.
223. van Dalen CJ, Winterbourn CC, Senthilmohan R, and Kettle AJ. Nitrite as a substrate and inhibitor of myeloperoxidase. Implications for nitration and hypochlorous acid production at sites of inflammation. *J Biol Chem* 275: 11638–11644, 2000.
224. Van der Veen BS, de Winther MP, Heeringa P, Augusto O, Chen JW, Davies M, Ma XL, Malle E, Pignatelli P, and Rudolph T. Myeloperoxidase: molecular mechanisms of action and their relevance to human health and disease. *Antioxid Redox Signal* 11: 2899–2937, 2009.
225. Van der Vliet A, Eiserich JP, Halliwell B, and Cross CE. Formation of reactive nitrogen species during peroxidase-catalyzed oxidation of nitrite. A potential additional mechanism of nitric oxide-dependent toxicity. *J Biol Chem* 272: 7617–7625, 1997.
226. van Zyl JM, Basson K, Uebel RA, and van der Walt BJ. Isoniazid-mediated irreversible inhibition of the myeloperoxidase antimicrobial system of the human neutrophil and the effect of thyronines. *Biochem Pharmacol* 38: 2363–2373, 1989.
227. Vicca S, Massy ZA, Hennequin C, Rihane D, Drueke TB, and Lacour B. Apoptotic pathways involved in U937 cells exposed to LDL oxidized by hypochlorous acid. *Free Radic Biol Med* 35: 603–615, 2003.
228. Vissers MC and Winterbourn CC. Myeloperoxidase-dependent oxidative inactivation of neutrophil neutral proteinases and microbicidal enzymes. *Biochem J* 245: 277–280, 1987.
229. Vlasova II, Arnhold J, Osipov AN, and Panasenko OM. pH-dependent regulation of myeloperoxidase activity. *Biochemistry (Mosc)* 71: 667–677, 2006.
230. Voetman AA, Weening RS, Hamers MN, Meerhof LJ, Bot AA, and Roos D. Phagocytosing human neutrophils inactivate their own granular enzymes. *J Clin Invest* 67: 1541–1549, 1981.
231. Wang JG, Mahmud SA, Nguyen J, and Slungaard A. Thiocyanate-dependent induction of endothelial cell adhesion molecule expression by phagocyte peroxidases: a novel HOSCN-specific oxidant mechanism to amplify inflammation. *J Immunol* 177: 8714–8722, 2006.
232. Wang Y, Rosen H, Madtes DK, Shao B, Martin TR, Heinecke JW, and Fu X. Myeloperoxidase inactivates TIMP-1 by oxidizing its N-terminal cysteine residue: an oxidative mechanism for regulating proteolysis during inflammation. *J Biol Chem* 282: 31826–31834, 2007.
233. Whitman SC, Hazen SL, Miller DB, Hegele RA, Heinecke JW, and Huff MW. Modification of type III VLDL, their remnants, and VLDL from ApoE-knockout mice by p-hydroxyphenylacetaldehyde, a product of myeloperoxidase activity, causes marked cholesteryl ester accumulation in macrophages. *Arterioscler Thromb Vasc Biol* 19: 1238–1249, 1999.
234. Winterbourn CC. Comparative reactivities of various biological compounds with myeloperoxidase-hydrogen peroxide-chloride, and similarity of the oxidant to hypochlorite. *Biochim Biophys Acta* 840: 204–210, 1985.
235. Winterbourn CC. Biological reactivity and biomarkers of the neutrophil oxidant, hypochlorous acid. *Toxicology* 181–182: 223–227, 2002.
236. Winterbourn CC, Garcia RC, and Segal AW. Production of the superoxide adduct of myeloperoxidase (compound III) by stimulated human neutrophils and its reactivity with hydrogen peroxide and chloride. *Biochem J* 228: 583–592, 1985.
237. Winterbourn CC, Hampton MB, Livesey JH, and Kettle AJ. Modeling the reactions of superoxide and myeloperoxidase in the neutrophil phagosome: implications for microbial killing. *J Biol Chem* 281: 39860–39869, 2006.
238. Witko-Sarsat V, Rieu P, Descamps-Latscha B, Lesavre P, and Halbwachs-Mecarelli L. Neutrophils: molecules, functions and pathophysiological aspects. *Lab Invest* 80: 617–653, 2000.
239. Wong ND, Gransar H, Narula J, Shaw L, Moon JH, Miranda-Peats R, Rozanski A, Hayes SW, Thomson LE, Friedman JD, and Berman DS. Myeloperoxidase, subclinical atherosclerosis, and cardiovascular disease events. *JACC Cardiovasc Imaging* 2: 1093–1099, 2009.
240. Ximenes VF, Maghzal GJ, Turner R, Kato Y, Winterbourn CC, and Kettle AJ. Serotonin as a physiological substrate for myeloperoxidase and its superoxide-dependent oxidation to cytotoxic tryptamine-4,5-dione. *Biochem J* 425: 285–293, 2010.

241. Zamocky M, Jakopitsch C, Furtmuller PG, Dunand C, and Obinger C. The peroxidase-cyclooxygenase superfamily: reconstructed evolution of critical enzymes of the innate immune system. *Proteins* 72: 589–605, 2008.
242. Zarbock A and Ley K. Neutrophil adhesion and activation under flow. *Microcirculation* 16: 31–42, 2009.
243. Zederbauer M, Jantschko W, Neugschwandtner K, Jakopitsch C, Moguilevsky N, Obinger C, and Furtmuller PG. Role of the covalent glutamic acid 242-heme linkage in the formation and reactivity of redox intermediates of human myeloperoxidase. *Biochemistry* 44: 6482–6491, 2005.
244. Zeng J and Fenna RE. X-ray crystal structure of canine myeloperoxidase at 3 A resolution. *J Mol Biol* 226: 185–207, 1992.
245. Zhang C, Patel R, Eiserich JP, Zhou F, Kelpke S, Ma W, Parks DA, Darley-Usmar V, and White CR. Endothelial dysfunction is induced by proinflammatory oxidant hypochlorous acid. *Am J Physiol Heart Circ Physiol* 281: H1469-H1475, 2001.
246. Zhang C, Reiter C, Eiserich JP, Boersma B, Parks DA, Beckman JS, Barnes S, Kirk M, Baldus S, Darley-Usmar VM, and White CR. L-arginine chlorination products inhibit endothelial nitric oxide production. *J Biol Chem* 276: 27159–27165, 2001.
247. Zhang L, Jiang H, Gao X, Zou Y, Liu M, Liang Y, Yu Y, Zhu W, Chen H, and Ge J. Heat shock transcription factor-1 inhibits H_2O_2-induced apoptosis via down-regulation of reactive oxygen species in cardiac myocytes. *Mol Cell Biochem* 347: 21–28, 2011.
248. Zhang R, Brennan ML, Fu X, Aviles RJ, Pearce GL, Penn MS, Topol EJ, Sprecher DL, and Hazen SL. Association between myeloperoxidase levels and risk of coronary artery disease. *JAMA* 286: 2136–2142, 2001.
249. Zheng L, Nukuna B, Brennan ML, Sun M, Goormastic M, Settle M, Schmitt D, Fu X, Thomson L, Fox PL, Ischiropoulos H, Smith JD, Kinter M, and Hazen SL. Apolipoprotein A-I is a selective target for myeloperoxidase-catalyzed oxidation and functional impairment in subjects with cardiovascular disease. *J Clin Invest* 114: 529–541, 2004.
250. Zou MH, Shi C, and Cohen RA. Oxidation of the zinc-thiolate complex and uncoupling of endothelial nitric oxide synthase by peroxynitrite. *J Clin Invest* 109: 817–826, 2002.

Address correspondence to:
Dr. Claudia Nussbaum
Walter Brendel Center for Experimental Medicine
Ludwig-Maximilians-Universität
Marchioninistr. 15
81377 Munich
Germany

E-mail: claudia.nussbaum@med.uni-muenchen.de

Dr. Anna Klinke
Department of General and Interventional Cardiology
University Heart Center Hamburg
Cardiovascular Research Center
University Hospital Eppendorf
Martinistr. 52
20246 Hamburg
Germany

E-mail: aklinke@uke.de

Date of first submission to ARS Central, June 29, 2012; date of acceptance, July 24, 2012.

Abbreviations Used

3-Cl-Tyr = 3-chlorotyrosine
3-NO_2-Tyr = 3-nitrotyrosine
3,5-diCl-Tyr = 3,5-dichlorotyrosine
4-ABAH = 4-aminobenzoic acid hydrazide
ACS = acute coronary syndrome
AMI = acute myocardial infarction
CAD = coronary artery disease
Cl_2 = chlorine
Cl^- = chloride
CVD = cardiovascular disease
EC = endothelial cell
ECM = extracellular matrix
EDTA = ethylene-diamine-tetra-acetic acid;
eNOS = endothelial NO-synthase
ERK1/2 = extracellular signal-regulated kinase 1/2
FMD = flow-mediated dilation
GAG = glycosaminoglycan
G-CSF = granulocyte colony-stimulating factor
Glx = glycocalyx
H_2O_2 = hydrogen peroxide
HDL = high-density lipoprotein
HF = heart failure
HOBr = hypobromous acid
HOCl = hypochlorous acid
HOSCN = hypothiocyanous acid
ICAM = intercellular cell adhesion molecule
IL = interleukin
IP = isoelectric point
JNK = cJun N-terminal kinase
LDL = low-density lipoprotein
LFA-1 = lymphocyte function-associated antigen-1
LV = left ventricular
Mac-1 = macrophage-1 antigen
MAPK = mitogen-activated protein kinase
MIP-2 = macrophage inflammatory protein-1
MMP = matrix metalloproteinase
MMR = macrophage mannose receptor
MPA = microscopic polyangitis
MPO = myeloperoxidase
NADPH = nicotinamide adenine dinucleotide phosphate
NE = neutrophil elastase
NET = neutrophil extracellular trap
NFκB = nuclear factor kappa-light-chain-enhancer of activated B-cells
NH_2Cl = monochloramine
$NO^\bullet$ = nitric oxide
NO^+ = nitrosonium cation
$NO_2^\bullet$ = nitrogen dioxide
NO_2^- = nitrite
O_2 = molecular oxygen
$O_2^{\bullet-}$ = superoxide radical
$OSCN^-$ = hypothiocyanite
PAI-1 = plasminogen activator inhibitor-1
PMN = polymorphonuclear neutrophil
ROS = reactive oxygen species
SCN^- = thiocyanate
SMC = smooth muscle cell
STEMI = ST-segment elevation myocardial infarction
TNFR = TNF-receptor
TNF-α = tumor necrosis factor-alpha
WT = wild type

Journal of Reproductive Immunology 90 (2011) 74–81

Contents lists available at ScienceDirect

Journal of Reproductive Immunology

journal homepage: www.elsevier.com/locate/jreprimm

Innate immune cell recruitment in the fetus and neonate

Claudia Nussbaum, Markus Sperandio*

Walter-Brendel-Center of Experimental Medicine, Ludwig-Maximilians-Universität, Marchioninistr. 27, 81377 Munich, Germany

ARTICLE INFO

Article history:
Received 7 January 2011
Received in revised form 26 January 2011
Accepted 27 January 2011

Keywords:
Neonate
Fetus
Leukocyte recruitment
Adhesion
Selectins
Integrins

ABSTRACT

Recruitment of innate immune cells from the vasculature into infected tissue is a key event in primary host defense against invading pathogens. This highly regulated process requires a functional interplay of specialized adhesion molecules and involves a series of steps leading from rolling of leukocytes along the endothelium to firm adhesion and finally transmigration. In the developing fetus, innate immune functions are ontogenetically regulated and show increasing maturation throughout gestation. Developmental differences in the innate immune response leave the neonate and especially the premature newborn at high risk of severe infections. Understanding the ontogeny of immune functions in the fetus and newborn is therefore essential for the prevention and treatment of neonatal infections. In this review, an overview will be given of the developmental aspects of innate immune cell recruitment including a discussion of controversial findings and open questions.

1. Introduction

During intrauterine development, the fetal immune system is adapted to the special requirements of pregnancy (Szekeres-Bartho, 2002). This intricately regulated system is challenged when an infant is born prematurely leaving the newborn at high risk of infection, which is still a leading cause of neonatal morbidity and mortality (Lawn et al., 2010). The incidence of neonatal sepsis correlates inversely with gestational age and reaches levels as high as 58% in very low birth weight infants (Stoll et al., 2010). This inverse relationship reflects physiological changes in the fetal immune system during gestation. As the intrauterine environment is usually sterile, there is no obvious need for an adult-like immune response in the growing fetus. However, towards the end of gestation a functioning protection against the pending threats of extra-uterine pathogens becomes increasingly important. At birth, the neonatal adaptive immune system is still relatively naïve with respect to foreign antigens and the neonate relies to a large extent on the innate immune system for control and prevention of infection (Wynn et al., 2008; Levy, 2007). Understanding the development of innate immune functions is therefore essential for our understanding of the pathophysiology of neonatal infections. In this review, the authors aim to summarize current concepts of the fetal and neonatal innate immune response focusing on the essential steps and elements of innate immune cell recruitment. Where applicable, reference is made to ontogenetic differences in relation to gestational age. Although a functional interplay between the innate and the adaptive immune system already exists in neonates, aspects of the neonatal adaptive immune system will not be covered as this would reach beyond the scope of this article.

2. Immune cell recruitment

One of the central mechanisms in the cellular immune response against invading pathogens is the recruitment of leukocytes from the vasculature into infected or inflamed tissue. The recruitment process follows a well-defined cascade of events orchestrated by a complex interplay of adhesion molecules, cell surface receptors and chemokines

* Corresponding author. Tel.: +49 89 2180 76505; fax: +49 89 2189 76503.
E-mail address: markus.sperandio@med.uni-muenchen.de (M. Sperandio).

0165-0378/$ – see front matter © 2011 Elsevier Ireland Ltd. All rights reserved.
doi:10.1016/j.jri.2011.01.022

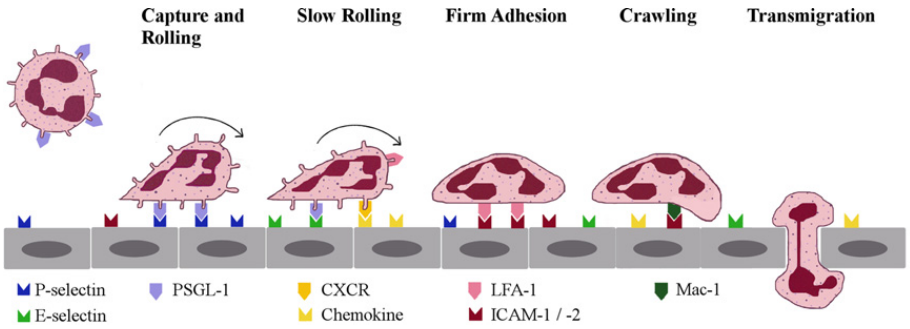

Fig. 1. Schematic overview of the leukocyte recruitment cascade using the example of a neutrophil leaving a postcapillary venule. Capture and rolling are mediated by interaction of selectins with PSGL-1 on the neutrophil surface. During rolling, the neutrophil is activated by chemokines presented on inflamed endothelium leading to firm adhesion through binding of neutrophil integrins (LFA-1 and Mac-1) to endothelial adhesion molecules (e.g., ICAM-1 and -2). Upon firm adhesion, the neutrophil spreads and begins to crawl along the endothelial lining in search of an appropriate site for transmigration.

as depicted in Fig. 1 (Ley et al., 2007). The initial capture of circulating leukocytes and the subsequent rolling of the cells along the endothelium are mediated by selectins interacting with carbohydrate determinants on selectin ligands (Sperandio, 2006). During rolling, the cells slow down and get into intimate contact with endothelial bound chemokines, which, in concert with selectin-induced signals (Kuwano et al., 2010), lead to the activation of leukocyte integrins (inside out signaling). Activation of integrins allows their binding to endothelial adhesion molecules leading to the arrest of the cell on the vessel wall (Zarbock and Ley, 2008). Additional integrin-dependent signaling (outside-in signaling) further strengthens the adhesion process and induces leukocyte spreading. Thereafter, leukocytes start to crawl along the endothelial surface in search of an appropriate exit point in order to leave the vessel and transmigrate into the surrounding tissue (Phillipson et al., 2006). Within the tissue, cell migration is directed through gradients of chemokines and other chemoattractants such as bacterial proteins and leukotrienes (Stephens et al., 2008). Of note, the adhesive interactions mediated by selectins and integrins are not unique to leukocyte recruitment, but reflect a pattern critically involved in other "recruitment processes" such as blastocyst implantation (Karsten and Kruse, 2008).

The importance of an effective leukocyte recruitment for immune defense is emphasized by the clinical picture of leukocyte adhesion deficiency (LAD) types I-III (Etzioni, 2009). This disease entity is characterized by an impairment of leukocyte recruitment due to genetic mutations affecting the function of leukocyte-expressed adhesion-relevant molecules. Patients with LAD I-III commonly suffer from recurrent bacterial infections that may lead to death early in childhood.

In the early immune response towards invading pathogens, polymorphonuclear neutrophils (PMN) are considered key effectors of innate host defense as they are first recruited into infected tissue (Kantari et al., 2008). Thus, the majority of studies exploring developmental aspects of rolling, adhesion and migration of innate immune cells in the fetus and neonate have concentrated on neutrophils. To date, information on the recruitment of other cell types of innate immunity, such as monocytes, dendritic cells and natural killer cells, is very limited or lacking. In the following, the most important findings of these studies, as summarized in Tables 1 and 2, will be outlined and discussed.

3. Developmental aspects of selectin-dependent rolling

Rolling interactions between neutrophils (and other leukocyte subsets) and the endothelium require selectin–selectin ligand interactions. Of the three known selectins, P-selectin (CD62P) and E-selectin (CD62E) are upregulated on inflamed endothelial cells, while L-selectin (CD62L) is constitutively expressed on leukocytes and shed after cell activation (Sperandio, 2006). The major selectin ligand on leukocytes is P-selectin glycoprotein ligand-1 (PSGL-1, CD162), binding to all members of the selectin family (Sperandio, 2006). While the initial capture (primary tethering) of circulating leukocytes under conditions of flow is mainly mediated by P-selectin, L-selectin can mediate endothelial-independent rolling interactions by binding to PSGL-1 expressed on already adherent leukocytes (secondary tethering). Selectin binding further induces intracellular signaling events that contribute to the transition from rolling to firm adhesion (Kuwano et al., 2010).

Many investigators have looked at L-selectin expression on neonatal neutrophils and reported reduced basal levels in mature neonates compared with adult controls (Moriguchi et al., 2006; Koenig et al., 1996; Fortenberry et al., 1994; Anderson et al., 1991) with a further reduction in the first 72 h of life (Kim et al., 2003). In addition, the capability to shed L-selectin from the cell surface upon stimulation is impaired. Interestingly, the extent of shedding that could be induced, varied with the stimulus employed (Moriguchi et al., 2006; Koenig et al., 1996). In fetuses, L-selectin is present on neutrophils as early as 21 weeks of gestation (Strunk et al., 2004; Rebuck et al., 1995; Smith and Tabsh, 1993), but there are controversies as to the relative amount of L-selectin expression and -shedding compared with mature neonates and adults. While Strunk et al. found a further reduction of basal L-selectin expression on neutrophils from fetuses compared with mature neonates and adults (Strunk et al., 2004) and Rebuck and colleagues report significantly lower L-selectin shedding in premature infants (Rebuck et al., 1995), Smith and co-workers detected comparable L-selectin levels and

Table 1
Quantitative differences in adhesion molecule expression during fetal development.

	Cell type/tissue investigated	Fetus/premature neonates	Mature neonates	Correlation with gestational age
L-selectin	PMN	↓ (Strunk et al., 2004; Rebuck et al., 1995) ↔ (Smith and Tabsh, 1993)	↓ (Moriguchi et al., 2006; Mariscalco et al., 1998; Koenig et al., 1996; Fortenberry et al., 1994)	+ (Strunk et al., 2004; Buhrer et al., 1995)
	Monocytes		↔ (Torok et al., 1993) ↓ On CD14-dim subpopulation (Murphy and Reen, 1996)	
P-selectin	Endothelial cells	↓ On rat mesenteric venules and HUVEC (Lorant et al., 1999) ↓ On porcine EC (Olutoye et al., 2005)	↓ On rat mesenteric venules (Lorant et al., 1999)	+ (Lorant et al., 1999) + In skin from 11 to 16 weeks (Davies et al., 1996)
E-selectin	Small intestine and skin	Little or no constitutive expression before 16 weeks, upregulation upon stimulation (Davies et al., 1996; Dogan et al., 1995)		
PSGL-1	PMN		↓ (Tcharmtchi et al., 2000)	
LFA-1	PMN	↑ (Bikoue et al., 1997) ↔ (Rebuck et al., 1995) ↓ Premature <35 weeks (McEvoy et al., 1996)	↔ (Storm et al., 2008; Anderson et al., 1987)	
	Monocytes	↑ (Bikoue et al., 1997)	↓ Upregulation (Torok et al., 1993)	
Mac-1	PMN	↔ Basal expression (Bikoue et al., 1997)	↔ Basal expression, ↓ upregulation (Moriguchi et al., 2006; Kim et al., 2003; Fortenberry et al., 1994; Anderson et al., 1987)	+ (McEvoy et al., 1996)
		↓ Basal expression (Strunk et al., 2004)	↑ Basal expression, ↔ upregulation (Rebuck et al., 1995; Mariscalco et al., 1998)	+ With postnatal age (Storm et al., 2008)
		↑ Basal expression, ↔ upregulation (Rebuck et al., 1995) ↓ Total content (McEvoy et al., 1996)	↓ Total content (McEvoy et al., 1996)	
	Monocytes	↔ Basal expression (Bikoue et al., 1997)	↓ Upregulation (Torok et al., 1993)	
ICAM-1	Small intestine and skin	Expression at 11 weeks (Davies et al., 1996; Dogan et al., 1995)		+ In skin from 11 to 16 weeks' gestation (Davies et al., 1996)
VCAM-1	Small intestine and skin	Expression in intestine at 11 weeks (Dogan et al., 1995) Little expression in skin at 16 weeks (Davies et al., 1996)		

↓ = reduced vs. higher gestational age or adult; ↑ = increased vs. higher gestational age or adult; ↔ = equal to higher gestational age or adult; PMN = polymorphonuclear neutrophils. + = correlates positively with gestational age.

shedding in premature neonates and adults (Smith and Tabsh, 1993). Likely, these differences are due to methodological variations in the studies such as differences in sample handling and in measurement techniques (e.g., measurement of the percentage of positive cells vs. measurement of mean fluorescence intensities). With respect to ontogenetic alterations of L-selectin levels on neutrophils as well as soluble L-selectin in plasma, a positive correlation with gestational age was demonstrated (Strunk et al., 2004; Buhrer et al., 1995). Concerning the L-selectin expression on other innate immune cells, limited data are available for neonatal monocytes. Torok and colleagues found no differences in L-selectin levels and shedding when comparing monocytes from mature infants with those from adults (Torok et al., 1993). However, differences may exist for different monocyte subpopulations (Murphy and Reen, 1996).

Both P-selectin and E-selectin can be detected on human fetal endothelial cells early in gestation (Davies et al., 1996; Dogan et al., 1995). However, the expression pattern depends on the organ examined. While endothelial cells in the skin of human fetuses show increasing staining for P-selectin from 11 to 16 weeks' gestation, hardly any P-selectin is present in fetal mesenteric vessels before

Table 2
Functional differences in the leukocyte recruitment process during fetal development.

	Cell type investigated	Fetus/premature neonates	Mature neonates	Correlation with gestational age
Rolling	PMN		↓ (Mariscalco et al., 1998; Tcharmtchi et al., 2000; Abbassi et al., 1993) ↔ In vivo (Mariscalco et al., 2002)	
Adhesion	PMN	↓ (Bektas et al., 1990) ↑ Unstimulated, ↓ stimulated (Carr et al., 1992)	↓ (Anderson et al., 1987, 1990, 1991)	+ With postnatal age (Eisenfeld et al., 1990)
	Monocytes		↔ (Roth and Polin, 1992)	
	Endothelial cells (porcine)	↓ Reduced adhesion of adult PMN on fetal EC (Olutoye et al., 2005; Naik-Mathuria et al., 2007)		+ (Naik-Mathuria et al., 2007)
Transmigration	PMN		↓ (Mariscalco et al., 2002; Anderson et al., 1990, 1991)	
Chemotaxis	PMN	↓ (Usmani et al., 1991; Bektas et al., 1990)	↓ (Weinberger et al., 2001; Fox et al., 2005; Merry et al., 1996; Eisenfeld et al., 1990)	+ (Usmani et al., 1991; Bektas et al., 1990)
	Monocytes		↓ (Marodi et al., 1980)	

↓ = reduced vs. higher gestational age or adult; ↑ = increased vs. higher gestational age or adult; ↔ = equal to higher gestational age or adult; EC = endothelial cells. + = correlates positively with gestational age.

27 gestational weeks (Lorant et al., 1999). E-selectin is not constitutively expressed, but can be induced in the fetal intestine by pro-inflammatory stimulation (Dogan et al., 1995). In the mesentery as well as in human umbilical vein endothelial cells (HUVEC), P-selectin expression increases throughout gestation, with significantly higher levels in term neonates compared with mid-gestation fetuses. Studies in rat pups demonstrated that even in mature neonates, the amount of P-selectin on postcapillary mesenteric venules is still reduced compared with adult animals (Lorant et al., 1999).

Despite the large number of studies covering developmental aspects of selectin expression, only a few have investigated functional leukocyte rolling. Mariscalco and co-workers compared rolling of neutrophils from mature neonates and adults on stimulated HUVEC and P-selectin expressing CHO cells (Mariscalco et al., 1998). Under conditions of flow, a significantly lower fraction of neonatal neutrophils exhibited rolling behavior compared with adults and the rolling interactions of neonatal cells were less resistant to increasing shear. These findings seem at least in part to be related to a reduction of surface L-selectin on neonatal neutrophils. There are also differences in the PSGL-1 expression between mature neonatal and adult neutrophils that might contribute to the lower number of neonatal neutrophils being captured on P-selectin-presenting CHO cells (Tcharmtchi et al., 2000). Likewise, rolling of neutrophils from mature neonates on E-selectin expressing cell monolayers is reduced compared with adult neutrophils (Abbassi et al., 1993). Interestingly, performing intravital microscopy of mesenteric venules in newborn rabbits, Mariscalco and co-workers observed normal rolling flux fractions compared with adult animals, suggesting that there might be overlapping or compensatory mechanisms supporting rolling in neonates in vivo (Mariscalco et al., 2002). Of note, we are not aware of any report investigating rolling behavior of human fetal neutrophils during fetal development. Interestingly, it was shown in fetal pigs that P-selectin expression on porcine endothelial cells at mid-gestation is reduced, possibly underlying their diminished capability to recruit adult neutrophils compared with adult porcine endothelial cells (Olutoye et al., 2005).

Taken together, all these reports suggest a developmentally regulated maturation process regarding selectin-dependent leukocyte rolling in the fetus, although a direct in vivo proof through appropriate fetal animal models and human dynamic in vitro models is still lacking.

4. Developmental aspects of integrin-dependent adhesion

The transition from rolling to firm adhesion requires activation and binding of leukocyte-expressed integrins to endothelial adhesion molecules (Zarbock and Ley, 2008). On neutrophils, the major integrins involved in this process are the β_2 integrins LFA-1 ($\alpha L\beta 2$, CD11a/CD18) and Mac-1 ($\alpha M\beta 2$, CD11b/CD18), whereas monocytes also adhere through the $\beta 1$ integrin VLA-4 ($\alpha 4\beta 1$, CD49d/CD29). The respective counter-receptors expressed on inflamed endothelial cells with demonstrated in vivo relevance belong to the immunoglobulin superfamily of adhesion molecules and include ICAM-1 (CD54), ICAM-2 (CD102), VCAM-1 (CD106) and RAGE (Frommhold et al., 2010; Ley et al., 2007). ICAM-1, VCAM-1 and RAGE are present in the early stages of fetal development. Comparable to selectin

expression, organ-specific differences exist concerning the time course of appearance. Constitutive expression of both ICAM-1 and VCAM-1 was shown in the human fetal small intestine at 11 weeks' gestation, which could be further increased by pro-inflammatory stimuli (Lorant et al., 1999; Dogan et al., 1995). In contrast, in the fetal skin ICAM-1 expression increases from 11 to 16 weeks, while VCAM-1 is only weakly present on a very limited number of endothelial cells at 16 weeks (Davies et al., 1996).

Human neonatal neutrophils have been extensively studied with respect to developmental differences in β_2 integrin expression (Moriguchi et al., 2006; Strunk et al., 2004; Kim et al., 2003; Bikoue et al., 1997; McEvoy et al., 1996). The majority of these studies found no age-related differences in basal and stimulated LFA-1 surface expression down to a gestational age of 18 weeks. In contrast, the upregulation of Mac-1 on the neutrophil surface upon chemotactic stimulation is severely diminished in mid-gestation fetuses approaching levels found in patients with LAD-1 (McEvoy et al., 1996), but increases with advancing gestational age. Interestingly, neutrophils from mature neonates still have lower Mac-1 levels than adults. Furthermore, Storm et al. were able to demonstrate that the total cell content, as well as the up-regulated surface expression of Mac-1, continues to rise after birth and correlates with postnatal age reaching adult levels by 11 months (Storm et al., 2008). In contrast to these studies, some reports show a higher resting Mac-1 expression in the fetus compared with adults and a normal increase after stimulation (Mariscalco et al., 1998; Rebuck et al., 1995). The authors claim that the observed differences between neonatal and adult neutrophils in earlier studies are related to a differing reaction of neonatal cells towards the isolation procedure used. However, many of the aforementioned studies have investigated Mac-1 expression on whole blood neutrophils and still found the described developmental differences.

Fetal and adult monocytes express β_2 integrins at equal basal levels (Bikoue et al., 1997). But similar to neutrophils, the stimulated upregulation of Mac-1 on monocytes is dependent on gestational age (Torok et al., 1993). To our knowledge, there are no data available on the ontogeny of VLA-4 expression on fetal monocytes.

The lower surface expression of Mac-1 on neonatal neutrophils has been directly linked to a reduced adhesive capacity of the cells (Anderson et al., 1987, 1990). Using different chemotactic stimuli, the authors demonstrated that neutrophil adhesion to HUVEC- and ICAM-1-coated cover slips is significantly impaired in mature neonates compared with adults. Blockade of Mac-1 reduced adhesion of adult neutrophils to neonatal levels, while this treatment had no effect on adhesion of neonatal cells. Interestingly, LFA-1-dependent adhesion was not affected in newborns. Additional work by Anderson and colleagues showed that CD18-independent adhesion was also impaired in mature neonates. This was mainly attributed to the lower expression of L-selectin on neonatal neutrophils (Anderson et al., 1991).

At present, the data on developmental aspects of leukocyte adhesion are sparse and results are conflicting. While Bektas et al. found a severe reduction in neutrophil adhesion in preterm neonates compared with mature infants (Bektas et al., 1990), Carr et al. observed equal adhesive properties between both groups with hyperadherence of unstimulated neonatal neutrophils compared with adults, but defective upregulation of adhesion upon chemotactic stimulation (Carr et al., 1992). Taking into account that adhesion was studied under non-physiological conditions using static assays and artificial substrates, the results of these studies have to be interpreted with caution. Neither of the studies looked at adhesive capacity with respect to different gestational ages. For the immediate postnatal period, adhesion of neonatal neutrophils increases with postnatal age, which is in accordance with the observed postnatal upregulation (maturation) of surface-expressed Mac-1 (Eisenfeld et al., 1990). The adhesion properties of monocytes seem to be independent of gestational age, although the current evidence is too limited to allow a general statement (Roth and Polin, 1992).

5. Developmental aspects of transendothelial migration and chemotaxis

Once a leukocyte has adhered to the vessel wall, inside-out signals transduced by integrin-binding to its ligand lead to spreading and crawling of the cell along the endothelial lining before it transmigrates into the surrounding tissue (Ley et al., 2007). In order to reach the site of microbial invasion, extravasated leukocytes follow gradients of chemoattractants, which are either directly derived from the pathogen (e.g., fMLP) or produced by the host itself (chemokines, leukotrienes, etc.). These chemotactic gradients are sensed through specialized G-protein coupled receptors that induce a series of intracellular signaling cascades leading to cytoskeletal rearrangement, adhesion molecule clustering, and cell polarization (Stephens et al., 2008).

The perception of intraluminal crawling, a mostly Mac-1-dependent process that is molecularly distinct from adhesion, is relatively new (Frommhold et al., 2010; Phillipson et al., 2006) and has not been investigated in the fetus or neonate.

Transmigration of leukocytes through the endothelial layer can occur either paracellularly or transcellularly (Ley et al., 2007). This complex process is still not fully understood and involves a multitude of adhesion molecules, many of which have not been looked at under developmental aspects. Of the known endothelial adhesion molecules involved in transmigration, platelet endothelial cell adhesion molecule 1 (PECAM-1, CD31) was found to be stably expressed at early stages of development (Lorant et al., 1999).

Transendothelial migration has been directly explored in vivo in newborn rabbits (Mariscalco et al., 2002) and in vitro using isolated human neutrophils from mature neonates under static and dynamic conditions (Anderson et al., 1990, 1991). In these studies, a significantly lower number of neonatal neutrophils transmigrated compared with adult cells. As seen with adhesion, transmigration of adult neutrophils through a HUVEC monolayer in vitro is significantly reduced by blocking either Mac-1 or L-selectin, while in neonatal samples no further reduction

is achieved, suggesting that quantitative and/or qualitative differences in these adhesion molecules contribute to the reduced transmigration phenotype in newborns. In addition, chemotaxis is impaired in neonatal neutrophils and monocytes compared with the respective cells in adults (Fox et al., 2005; Marodi et al., 1980) and correlates with gestational age (Usmani et al., 1991; Bektas et al., 1990), whereas random migration is largely unaffected. While neutrophils from mid-gestation fetuses show severely diminished chemotactic movements, mature neonates reach the levels of adults by the age of one week (Eisenfeld et al., 1990). Several factors might contribute to the low chemotactic potential of neonatal neutrophils. These include developmental differences in chemoattractant-induced intracellular signaling pathways such as NF-κB activation (Weinberger et al., 2001), defective cytoskeletal rearrangements (Merry et al., 1996) and a higher prevalence of unresponsive neutrophil subpopulations (Krause et al., 1989). In addition, immature neutrophil precursors, which are present in a higher proportion in the peripheral blood of neonates born prematurely, were shown to be more rigid than mature neutrophils, thereby further hindering transendothelial cell migration in these infants (Linderkamp et al., 1998). These developmental differences between fetuses, newborns and adults in combination with the altered rolling and adhesive capacity described before are likely to account for the overall reduced recruitment of leukocytes observed in neonate animal models in vivo (Lorant et al., 1999; Fortenberry et al., 1994).

6. Impact of extrinsic factors on neonatal leukocyte recruitment

Besides developmental factors governing leukocyte recruitment in the fetus and newborn, many extrinsic factors have an influence on the recruitment process. In industrialized countries, virtually all infants born before 32 complete weeks' gestation are exposed to antenatal steroids for induction of lung maturation. Steroids are known to reduce the endothelial expression of adhesion molecules, which is important for cell rolling and adhesion, including E-selectin, ICAM-1, and VCAM-1 (Aziz and Wakefield, 1996). Furthermore, betamethasone treatment inhibits chemotaxis of neonatal neutrophils (Fuenfer et al., 1987). A similar effect on the chemotactic activity of neutrophils was indirectly shown for magnesium sulfate, which is commonly used for tocolysis in preterm labor (Mehta and Petrova, 2006). Neutrophils from premature infants whose mothers had received magnesium sulfate before birth exhibited significantly less chemotactic movement than those from infants not exposed to magnesium and the functional activity of the cells correlated directly with maternal serum magnesium levels.

The mode of delivery may be another factor that has an impact on leukocyte recruitment processes. The comparison of newborns delivered vaginally vs. newborns delivered by caesarean section before onset of labor demonstrated that labor-induced stress leads to the upregulation of Mac-1 and the IL-8 receptor CXCR1 on neonatal neutrophils (Gessler and Dahinden, 2003) and enhances neutrophil adhesion (Kinoshita et al., 1991) and chemotaxis (Yektaei-Karin et al., 2007). In contrast, during sepsis the chemotactic response of fetal and neonatal cells deteriorates (Merry et al., 1996).

Since multiple of these factors may be present when examining the function of fetal and neonatal immune cells, it is difficult and challenging to distinguish whether observed differences are due to extrinsic influences or intrinsic developmental effects.

7. Concluding considerations and future prospects

Although many aspects of the neonatal innate immune response have been shown to be reduced compared with adults, it would be incorrect to state that the innate immune function in neonates is generally defective. The differences observed between neonates and adults rather reflect physiological alterations in the course of development. This is best seen when looking at the neonatal inflammatory response. It was initially believed that the inflammatory response in the developing fetus and neonate is generally depressed due to the low production of Th_1-polarizing cytokines (e.g., TNF-α and INFγ) by stimulated monocytes and antigen-presenting cells (Levy, 2007). However, Zhao and co-workers have shown that under certain circumstances neonates are capable of mounting an inflammatory response that exceeds those of adults, resulting in what was termed a "cytokine storm" (Zhao et al., 2008). Although this presumed hyper innate response of neonates needs to be put into perspective by the rather weak reaction of adult controls towards intraperitoneal LPS injection (and other TLR agonists), this study still demonstrates that newborns may be less restricted in their immune function than previously thought.

It is now understood that the innate immune response shows a propensity towards Th_2-polarizing cytokines during fetal development, i.e., certain cytokines such as IL-6, IL-10, and IL-23 are produced at even higher levels than in adults (Belderbos et al., 2009; Kollmann et al., 2009). From a developmental point of view this bias in cytokine production is reasonable and needs to be seen in the context of the special immunological demands of pregnancy. It is well known that elevated circulating levels of Th_1-polarizing cytokines at the feto-maternal interface are associated with a higher rate of abortion of the fetus (Makhseed et al., 2001). Thus, the Th_2-polarization in the fetus may be seen as the result of a general effort to suppress possibly harmful Th_1 reactions during pregnancy by preferential production of Th_1 antagonistic mediators in the placenta such as IL-4, progesterone, and PGE_2 (Szekeres-Bartho et al., 1996; Hilkens et al., 1995). However, in the setting of premature birth, this bias renders the newborn more susceptible to severe infections.

Another lesson learned from many of the studies quoted in this review is that the function of innate immune cells is largely context-dependent and varies with the exact subtype of immune cells examined, the stimulus used, and the methods employed. Thus, neonatal monocytes in whole blood behave in a very distinct manner compared with isolated cells, and engagement of different Toll-like receptors (TLR) results in different or even opposing cytokine patterns (Kollmann et al., 2009). Likewise, we observed

TLR-dependent variations in the ability of neonatal neutrophils to form so-called neutrophil extracellular traps (NETs) – a defensive mechanism by which neutrophils contribute to the extracellular elimination of pathogens (Marcos et al., 2009). While TLR-2- and TLR-4-mediated NET formation was significantly delayed in neonates compared with adults, no differences were observed after stimulation of TLR-5, -8, and -9. These variations, in combination with the many extrinsic influence factors, make it very difficult to draw a concise picture of the innate immune response in the fetus and neonate.

In addition, it becomes obvious why many of the immune-modulatory interventions explored so far (e.g., treatment with colony-stimulating factors such as G-CSF or intravenous immunoglobulin infusions) have been of limited success in clinical practise (Wynn et al., 2009). Further insights into the ontogenetic regulation of fetal innate immune processes and the events taking place during infection are crucial for the development of new therapeutic approaches to treating life-threatening infections in the newborn. Promising experimental results were achieved by Wynn et al. using different TLR agonists to prime innate immune cells in a neonatal murine model of polymicrobial sepsis (Wynn et al., 2008). In this study, pre-treatment with a TLR-4 (LPS) agonist or a TLR-7/8 agonist (resiquimod) lowered sepsis mortality by 25% or 40%, respectively, compared with controls. The primed animals exhibited an enhanced, but shortened inflammatory response with increased recruitment of neutrophils, improved production of reactive oxygen species and phagocytosis and reduced bacteremia. For a successful translation of such therapeutic concepts into the clinic, a better understanding of the interplay between different subsets of innate immune cells, as well as the communication between innate and adaptive immunity, is necessary. Therefore, future research is warranted and should be aimed at optimizing functional studies to closer resemble fetal and neonatal physiology, for example, by use of more homogeneous immunological systems. In this context, the development of appropriate fetal in vivo models (e.g., in the mouse) is of great interest as they may have the potential to become an invaluable tool in unraveling the exact molecular processes of leukocyte recruitment during fetal development.

References

Abbassi, O., Kishimoto, T.K., McIntire, L.V., Anderson, D.C., Smith, C.W., 1993. E-selectin supports neutrophil rolling in vitro under conditions of flow. J. Clin. Invest. 92, 2719–2730.

Anderson, D.C., Freeman, K.L., Heerdt, B., Hughes, B.J., Jack, R.M., Smith, C.W., 1987. Abnormal stimulated adherence of neonatal granulocytes: impaired induction of surface Mac-1 by chemotactic factors or secretagogues. Blood 70, 740–750.

Anderson, D.C., Rothlein, R., Marlin, S.D., Krater, S.S., Smith, C.W., 1990. Impaired transendothelial migration by neonatal neutrophils: abnormalities of Mac-1 (CD11b/CD18)-dependent adherence reactions. Blood 76, 2613–2621.

Anderson, D.C., Abbassi, O., Kishimoto, T.K., Koenig, J.M., McIntire, L.V., Smith, C.W., 1991. Diminished lectin-, epidermal growth factor-, complement binding domain-cell adhesion molecule-1 on neonatal neutrophils underlies their impaired CD18-independent adhesion to endothelial cells in vitro. J. Immunol. 146, 3372–3379.

Aziz, K.E., Wakefield, D., 1996. Modulation of endothelial cell expression of ICAM-1, E-selectin, and VCAM-1 by beta-estradiol, progesterone, and dexamethasone. Cell Immunol. 167, 79–85.

Bektas, S., Goetze, B., Speer, C.P., 1990. Decreased adherence, chemotaxis and phagocytic activities of neutrophils from preterm neonates. Acta Paediatr. Scand. 79, 1031–1038.

Belderbos, M.E., van Bleek, G.M., Levy, O., Blanken, M.O., Houben, M.L., Schuijff, L., et al., 2009. Skewed pattern of Toll-like receptor 4-mediated cytokine production in human neonatal blood: low LPS-induced IL-12p70 and high IL-10 persist throughout the first month of life. Clin. Immunol. 133, 228–237.

Bikoue, A., D'Ercole, C., George, F., Dameche, L., Mutin, M., Sampol, J., 1997. Quantitative analysis of leukocyte membrane antigen expression on human fetal and cord blood: normal values and changes during development. Clin. Immunol. Immunopathol. 84, 56–64.

Buhrer, C., Stibenz, D., Graulich, J., Gernhold, U., Butcher, E.C., Dudenhausen, J.W., et al., 1995. Soluble L-selectin (sCD62L) umbilical cord plasma levels increase with gestational age. Pediatr. Res. 38, 336–341.

Carr, R., Pumford, D., Davies, J.M., 1992. Neutrophil chemotaxis and adhesion in preterm babies. Arch. Dis. Child 67, 813–817.

Davies, J.R., Dyson, M., Mustafa, Y., Compton, F., Perry, M.E., 1996. The ontogeny of adhesion molecules expressed on the vascular endothelium of the developing human skin. J. Anat. 189 (Pt 2), 373–382.

Dogan, A., MacDonald, T.T., Spencer, J., 1995. Expression of cell adhesion molecules in the fetal gut. Adv. Exp. Med. Biol. 371A, 141–143.

Eisenfeld, L., Krause, P.J., Herson, V., Savidakis, J., Bannon, P., Maderazo, E., et al., 1990. Longitudinal study of neutrophil adherence and motility. J. Pediatr. 117, 926–929.

Etzioni, A., 2009. Genetic etiologies of leukocyte adhesion defects. Curr. Opin. Immunol. 21, 481–486.

Fortenberry, J.D., Marolda, J.R., Anderson, D.C., Smith, C.W., Mariscalco, M.M., 1994. CD18-dependent and L-selectin-dependent neutrophil emigration is diminished in neonatal rabbits. Blood 84, 889–897.

Fox, S.E., Lu, W., Maheshwari, A., Christensen, R.D., Calhoun, D.A., 2005. The effects and comparative differences of neutrophil specific chemokines on neutrophil chemotaxis of the neonate. Cytokine 29, 135–140.

Frommhold, D., Kamphues, A., Hepper, I., Pruenster, M., Lukic, I.K., Socher, I., et al., 2010. RAGE and ICAM-1 cooperate in mediating leukocyte recruitment during acute inflammation in vivo. Blood 116, 841–849.

Fuenfer, M.M., Herson, V.C., Raye, J.R., Woronick, C.L., Eisenfeld, L., Ingardia, C.J., et al., 1987. The effect of betamethasone on neonatal neutrophil chemotaxis. Pediatr. Res. 22, 150–153.

Gessler, P., Dahinden, C., 2003. Increased respiratory burst and increased expression of complement receptor-3 (CD11b/CD18) and of IL-8 receptor-A in neutrophil granulocytes from newborns after vaginal delivery. Biol. Neonate 83, 107–112.

Hilkens, C.M., Vermeulen, H., van Neerven, R.J., Snijdewint, F.G., Wierenga, E.A., Kapsenberg, M.L., 1995. Differential modulation of T helper type 1 (Th1) and T helper type 2 (Th2) cytokine secretion by prostaglandin E2 critically depends on interleukin-2. Eur. J. Immunol. 25, 59–63.

Kantari, C., Pederzoli-Ribeil, M., Witko-Sarsat, V., 2008. The role of neutrophils and monocytes in innate immunity. Contrib. Microbiol. 15, 118–146.

Karsten, C.M., Kruse, A., 2008. The role of vascular addressins in implantations sites during successful and failing mouse pregnancies. Immunol. Invest. 37, 449–466.

Kim, S.K., Keeney, S.E., Alpard, S.K., Schmalstieg, F.C., 2003. Comparison of L-selectin and CD11b on neutrophils of adults and neonates during the first month of life. Pediatr. Res. 53, 132–136.

Kinoshita, Y., Masuda, K., Kobayashi, Y., 1991. Adherence of cord blood neutrophils: effect of mode of delivery. J. Pediatr. 118, 115–117.

Koenig, J.M., Simon, J., Anderson, D.C., Smith, E., Smith, C.W., 1996. Diminished soluble and total cellular L-selectin in cord blood is associated with its impaired shedding from activated neutrophils. Pediatr. Res. 39, 616–621.

Kollmann, T.R., Crabtree, J., Rein-Weston, A., Blimkie, D., Thommai, F., Wang, X.Y., et al., 2009. Neonatal innate TLR-mediated responses are distinct from those of adults. J. Immunol. 183, 7150–7160.

Krause, P.J., Kreutzer, D.L., Eisenfeld, L., Herson, V.C., Weisman, S., Bannon, P., et al., 1989. Characterization of nonmotile neutrophil subpopulations in neonates and adults. Pediatr. Res. 25, 519–524.

Kuwano, Y., Spelten, O., Zhang, H., Ley, K., Zarbock, A., 2010. Rolling on E- or P-selectin induces the extended but not high-affinity conformation of LFA-1 in neutrophils. Blood 116, 617–624.

Lawn, J.E., Kerber, K., Enweronu-Laryea, C., Cousens, S., 2010. 3.6 million neonatal deaths – what is progressing and what is not? Semin. Perinatol. 34, 371–386.

Levy, O., 2007. Innate immunity of the newborn: basic mechanisms and clinical correlates. Nat. Rev. Immunol. 7, 379–390.

Ley, K., Laudanna, C., Cybulsky, M.I., Nourshargh, S., 2007. Getting to the site of inflammation: the leukocyte adhesion cascade updated. Nat. Rev. Immunol. 7, 678–689.

Linderkamp, O., Ruef, P., Brenner, B., Gulbins, E., Lang, F., 1998. Passive deformability of mature, immature, and active neutrophils in healthy and septicemic neonates. Pediatr. Res. 44, 946–950.

Lorant, D.E., Li, W.H., Tabatabaei, N., Garver, M.K., Albertine, K.H., 1999. P-selectin expression by endothelial cells is decreased in neonatal rats and human premature infants. Blood 94, 600–609.

Makhseed, M., Raghupathy, R., Azizieh, F., Omu, A., Al-Shamali, E., Ashkanani, L., 2001. Th1 and Th2 cytokine profiles in recurrent aborters with successful pregnancy and with subsequent abortions. Hum. Reprod. 16, 2219–2226.

Marcos, V., Nussbaum, C., Vitkov, L., Hector, A., Wiedenbauer, E.M., Roos, D., et al., 2009. Delayed but functional neutrophil extracellular trap formation in neonates. Blood 114, 4908–4911.

Mariscalco, M.M., Tcharmtchi, M.H., Smith, C.W., 1998. P-selectin support of neonatal neutrophil adherence under flow – contribution of L-selectin, LFA-1, and ligand(s) for P-selectin. Blood 91, 4776–4785.

Mariscalco, M.M., Vergara, W., Mei, J., Smith, E.O., Smith, C.W., 2002. Mechanisms of decreased leukocyte localization in the developing host. Am. J. Physiol. Heart Circ. Physiol. 282, H636–H644.

Marodi, L., Csorba, S., Nagy, B., 1980. Chemotactic and random movement of human newborn monocytes. Eur. J. Pediatr. 135, 73–75.

McEvoy, L.T., Zakem-Cloud, H., Tosi, M.F., 1996. Total cell content of CR3 (CD11b/CD18) and LFA-1 (CD11a/CD18) in neonatal neutrophils: relationship to gestational age. Blood 87, 3929–3933.

Mehta, R., Petrova, A., 2006. Intrapartum magnesium sulfate exposure attenuates neutrophil function in preterm neonates. Biol. Neonate 89, 99–103.

Merry, C., Puri, P., Reen, D.J., 1996. Defective neutrophil actin polymerisation and chemotaxis in stressed newborns. J. Pediatr. Surg. 31, 481–485.

Moriguchi, N., Yamamoto, S., Isokawa, S., Andou, A., Miyata, H., 2006. Granulocyte functions and changes in ability with age in newborns; Report no. 2, activation of granulocyte functions by cytokines. Pediatr. Int. 48, 22–28.

Murphy, F.J., Reen, D.J., 1996. Differential expression of function-related antigens on newborn and adult monocyte subpopulations. Immunology 89, 587–591.

Naik-Mathuria, B., Gay, A.N., Zhu, X., Yu, L., Cass, D.L., Olutoye, O.O., 2007. Age-dependent recruitment of neutrophils by fetal endothelial cells: implications in scarless wound healing. J. Pediatr. Surg. 42, 166–171.

Olutoye, O.O., Zhu, X., Cass, D.L., Smith, C.W., 2005. Neutrophil recruitment by fetal porcine endothelial cells: implications in scarless fetal wound healing. Pediatr. Res. 58, 1290–1294.

Phillipson, M., Heit, B., Colarusso, P., Liu, L., Ballantyne, C.M., Kubes, P., 2006. Intraluminal crawling of neutrophils to emigration sites: a molecularly distinct process from adhesion in the recruitment cascade. J. Exp. Med. 203, 2569–2575.

Rebuck, N., Gibson, A., Finn, A., 1995. Neutrophil adhesion molecules in term and premature infants: normal or enhanced leucocyte integrins but defective L-selectin expression and shedding. Clin. Exp. Immunol. 101, 183–189.

Roth, P., Polin, R.A., 1992. Adherence of human newborn infants' monocytes to matrix-bound fibronectin. J. Pediatr. 121, 285–288.

Smith, J.B., Tabsh, K.M., 1993. Fetal neutrophils and eosinophils express normal levels of L-selectin. Pediatr. Res. 34, 253–257.

Sperandio, M., 2006. Selectins and glycosyltransferases in leukocyte rolling in vivo. FEBS J. 273, 4377–4389.

Stephens, L., Milne, L., Hawkins, P., 2008. Moving towards a better understanding of chemotaxis. Curr. Biol. 18, R485–R494.

Stoll, B.J., Hansen, N.I., Bell, E.F., Shankaran, S., Laptook, A.R., Walsh, M.C., et al., 2010. Neonatal outcomes of extremely preterm infants from the NICHD Neonatal Research Network. Pediatrics 126, 443–456.

Storm, S.W., Mariscalco, M.M., Tosi, M.F., 2008. Postnatal maturation of total cell content and up-regulated surface expression of Mac-1 (CD11b/CD18) in polymorphonuclear leukocytes of human infants. J. Leukoc. Biol. 84, 477–479.

Strunk, T., Temming, P., Gembruch, U., Reiss, I., Bucsky, P., Schultz, C., 2004. Differential maturation of the innate immune response in human fetuses. Pediatr. Res. 56, 219–226.

Szekeres-Bartho, J., 2002. Immunological relationship between the mother and the fetus. Int. Rev. Immunol. 21, 471–495.

Szekeres-Bartho, J., Faust, Z., Varga, P., Szereday, L., Kelemen, K., 1996. The immunological pregnancy protective effect of progesterone is manifested via controlling cytokine production. Am. J. Reprod. Immunol. 35, 348–351.

Tcharmtchi, M.H., Smith, C.W., Mariscalco, M.M., 2000. Neonatal neutrophil interaction with P-selectin: contribution of P-selectin glycoprotein ligand-1 and sialic acid. J. Leukoc. Biol. 67, 73–80.

Torok, C., Lundahl, J., Hed, J., Lagercrantz, H., 1993. Diversity in regulation of adhesion molecules (Mac-1 and L-selectin) in monocytes and neutrophils from neonates and adults. Arch. Dis. Child. 68, 561–565.

Usmani, S.S., Schlessel, J.S., Sia, C.G., Kamran, S., Orner, S.D., 1991. Polymorphonuclear leukocyte function in the preterm neonate: effect of chronologic age. Pediatrics 87, 675–679.

Weinberger, B., Laskin, D.L., Mariano, T.M., Sunil, V.R., DeCoste, C.J., Heck, D.E., et al., 2001. Mechanisms underlying reduced responsiveness of neonatal neutrophils to distinct chemoattractants. J. Leukoc. Biol. 70, 969–976.

Wynn, J.L., Scumpia, P.O., Winfield, R.D., Delano, M.J., Kelly-Scumpia, K., Barker, T., et al., 2008. Defective innate immunity predisposes murine neonates to poor sepsis outcome but is reversed by TLR agonists. Blood 112, 1750–1758.

Wynn, J.L., Neu, J., Moldawer, L.L., Levy, O., 2009. Potential of immunomodulatory agents for prevention and treatment of neonatal sepsis. J. Perinatol. 29, 79–88.

Yektaei-Karin, E., Moshfegh, A., Lundahl, J., Berggren, V., Hansson, L.O., Marchini, G., 2007. The stress of birth enhances in vitro spontaneous and IL-8-induced neutrophil chemotaxis in the human newborn. Pediatr. Allergy Immunol. 18, 643–651.

Zarbock, A., Ley, K., 2008. Mechanisms and consequences of neutrophil interaction with the endothelium. Am. J. Pathol. 172, 1–7.

Zhao, J., Kim, K.D., Yang, X., Auh, S., Fu, Y.X., Tang, H., 2008. Hyper innate responses in neonates lead to increased morbidity and mortality after infection. Proc. Natl. Acad. Sci. U. S. A. 105, 7528–7533.